



U.S. Department
of Transportation
**Federal Highway
Administration**

MAY 1997

OFFICE OF ENGINEERING
OFFICE OF TECHNOLOGY APPLICATIONS
400 SEVENTH STREET, SW
WASHINGTON, DC 20590

GEOTECHNICAL ENGINEERING CIRCULAR No. 3

DESIGN GUIDANCE: GEOTECHNICAL EARTHQUAKE ENGINEERING FOR HIGHWAYS

VOLUME II - DESIGN EXAMPLES

No. 3 • GEOTECHNICAL ENGINEERING CIRCULAR No. 3 • GEOTECHNICAL

ENGINEERING CIRCULAR No. 3 • GEOTECHNICAL ENGINEERING CIRCULAR

No. 3 • GEOTECHNICAL ENGINEERING CIRCULAR No. 3 • GEOTECHNICAL

ENGINEERING CIRCULAR No. 3 • GEOTECHNICAL ENGINEERING CIRCULAR

No. 3 • GEOTECHNICAL ENGINEERING CIRCULAR No. 3 • GEOTECHNICAL

ENGINEERING CIRCULAR No. 3 • GEOTECHNICAL ENGINEERING CIRCULAR

No. 3 • GEOTECHNICAL ENGINEERING CIRCULAR No. 3 • GEOTECHNICAL

ENGINEERING CIRCULAR No. 3 • GEOTECHNICAL ENGINEERING CIRCULAR

No. 3 • GEOTECHNICAL ENGINEERING CIRCULAR No. 3 • GEOTECHNICAL

ENGINEERING CIRCULAR No. 3 • GEOTECHNICAL ENGINEERING CIRCULAR

No. 3 • GEOTECHNICAL ENGINEERING CIRCULAR No. 3 • GEOTECHNICAL

ENGINEERING CIRCULAR No. 3 • GEOTECHNICAL ENGINEERING CIRCULAR

No. 3 • GEOTECHNICAL ENGINEERING CIRCULAR No. 3 • GEOTECHNICAL

ENGINEERING CIRCULAR No. 3 • GEOTECHNICAL ENGINEERING CIRCULAR

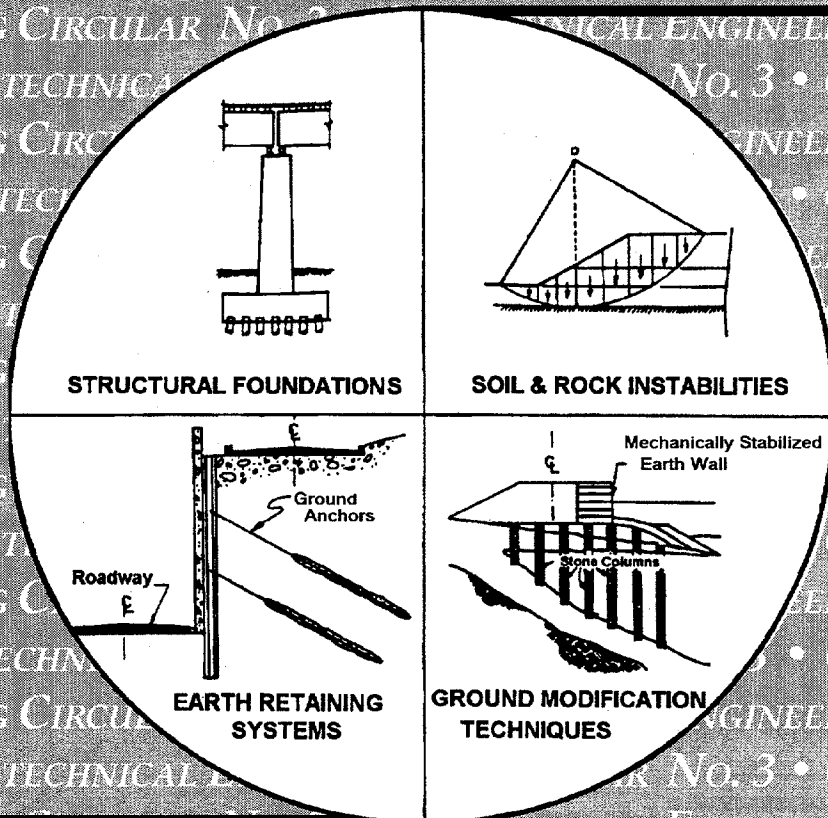
No. 3 • GEOTECHNICAL ENGINEERING CIRCULAR No. 3 • GEOTECHNICAL

ENGINEERING CIRCULAR No. 3 • GEOTECHNICAL ENGINEERING CIRCULAR

No. 3 • GEOTECHNICAL ENGINEERING CIRCULAR No. 3 • GEOTECHNICAL

ENGINEERING CIRCULAR No. 3 • GEOTECHNICAL ENGINEERING CIRCULAR

No. 3 • GEOTECHNICAL ENGINEERING CIRCULAR No. 3 • GEOTECHNICAL



ENGINEERING CIRCULAR No. 3 • GEOTECHNICAL ENGINEERING CIRCULAR

No. 3 • GEOTECHNICAL ENGINEERING CIRCULAR No. 3 • GEOTECHNICAL

ENGINEERING CIRCULAR No. 3 • GEOTECHNICAL ENGINEERING CIRCULAR

No. 3 • GEOTECHNICAL ENGINEERING CIRCULAR No. 3 • GEOTECHNICAL

The FHWA Geotechnical Engineering Circulars are a series of comprehensive and practical manuals that provide state-of-the-practice methods and techniques to assist the highway engineer in the design and construction of highway facilities. No other agency or group has assembled such a complete set of manuals for geotechnical engineering. The manuals are modeled after the well-respected set of hydraulic engineering circulars and hydraulic design series, and they are expected to become a mainstay of geotechnical engineering practice worldwide.

The published circulars in this series are the following:

Geotechnical Engineering Circular No. 1 - Dynamic Compaction FHWA-SA-95-037
Geotechnical Engineering Circular No. 2 - Earth Retaining Systems FHWA-SA-96-038
Geotechnical Engineering Circular No. 3 - Design Guidance: Geotechnical Earthquake
Engineering for Highways, Volume I - Design Principles FHWA-SA-97-076 and
Volume II - Design Examples FHWA-SA-97-077

Geotechnical Engineering Circulars are currently being developed in the following areas:

Ground Anchor Structures
Soil and Rock Properties

Technical Report Documentation Page

1. Report No. FHWA-SA-97-077		2. Government Accession No.		3. Recipient's Catalog No.	
4. Title and Subtitle Geotechnical Engineering Circular # 3 Design Guidance: Geotechnical Earthquake Engineering for Highways, Volume II- Design Examples				4. Report Date May 1997	
				6. Performing Organization Code:	
7. Author(s) E. Kavazanjian, Jr., N. Matasović, T. Hadj-Hamou, and P.J. Sabatini				8. Performing Organization Report No.	
9. Performing Organization Name and Address GeoSyntec Consultants 2100 Main Street, Suite 150 Huntington Beach, CA 92648				10. Work Unit No.(TRAIS)	
				11. Contract or Grant No. DTFH61-94-C-00099	
12. Sponsoring Agency Name and Address Office of Technology Application Office of Engineering/Bridge Division Federal Highway Administration 400 Seventh Street, S.W. Washington, D.C. 20590				13. Type of Report and Period Covered	
				14. Sponsoring Agency Code	
15. Supplementary Notes Contracting Officer's Technical Representative (COTR) FHWA Technical Consultant				Chien-Tan Chang, HTA-22 Richard S. Cheney, HNG-31	
16. Abstract This document presents a series of five design examples illustrating the principles and methods of geotechnical earthquake engineering and seismic design for highway facilities. These principles and methods are described in a companion volume entitled, "Geotechnical Engineering Circular No. 3, Design Guidance: Geotechnical Earthquake engineering for highways, Volume I - Design Principles." The examples presented in this volume cover a wide range of problems encountered in geotechnical earthquake engineering practice. The design examples presented in this document include:					
<ul style="list-style-type: none"> • seismic design of a shallow bridge foundation; • seismic design of a driven pile bridge foundation; • seismic design of a gravity retaining wall based on results of a detailed seismic hazard analysis; • seismic slope stability analysis of a cut slope in soft rock; and • liquefaction potential analysis. 					
17. Key Words Geotechnical earthquake engineering, soil dynamics, engineering seismology, engineering geology			18. Distribution Statement No restrictions. This document is available to the public from the National Technical Information Service, Springfield, Virginia 22161.		
19. Security Classif. (of this report) Unclassified		20. Security Classif. (of this page) Unclassified		21. No. of Pages	22. Price

DISCLAIMER

The information in this document has been funded wholly or in part by the U.S. Department of Transportation, Federal Highway Administration (FHWA) under Contract No. DTFH61-94-C-00099 to GeoSyntec Consultants. The document has been subjected to the Department's peer and administrative review, and it has been approved for publication as a FHWA document. Mention of trade names or commercial products does not constitute endorsement or recommendation for use by either the authors or FHWA.

CONTENTS

<u>Example</u>	<u>Page</u>
INTRODUCTION	1
1. SEISMIC ANALYSIS OF A SHALLOW BRIDGE FOUNDATION	3
1.1 Introduction	3
1.1.1 Description of the Project	3
1.1.2 Source Materials Required	3
1.2 Site Geology	3
1.3 Geotechnical Exploration	6
1.4 Design of Shallow Foundation	8
1.5 Seismic Settlement and Liquefaction Potential	9
1.6 Calculations	9
1.7 Summary and Conclusions	28
2. SEISMIC DESIGN OF A DEEP FOUNDATION SYSTEM	29
2.1 Introduction	29
2.1.1 Description of the Project	29
2.1.2 Source Materials Required	29
2.2 Geotechnical Exploration	32
2.3 Design of Pile Foundations	32
2.4 Calculations	36
2.5 Summary and Conclusions	52
3. SEISMIC DESIGN OF A RETAINING WALL	53
3.1 Introduction	53
3.1.1 Description of the Project	53
3.1.2 Source Materials Required	53
3.2 Geologic and Seismic Setting	54
3.3 Geotechnical Investigation	54
3.4 Seismic Hazard Analysis	57
3.4.1 Introduction	57
3.4.2 Peak Horizontal Ground Acceleration	57
3.4.3 Earthquake Magnitude	60
3.4.4 Representative Acceleration Time Histories	60
3.5 Seismic Response Analysis	63
3.6 Design of the Wall	66

TABLE OF CONTENTS (continued)

<u>Example</u>	<u>Page No.</u>
3.7 Calculations	67
3.8 Summary and Conclusions	82
4. SLOPE STABILITY ANALYSIS	83
4.1 Introduction	83
4.1.1 Description of the Project	83
4.1.2 Source Materials Required	83
4.2 Site Geology	85
4.3 Geotechnical Exploration	85
4.3.1 General	85
4.3.2 Geotechnical Properties	85
4.3.2.1 Intact Rock	85
4.3.2.2 Bedding Plane/Claystone and Siltstone Seam Material	87
4.4 Deterministic Seismic Hazard Analysis	87
4.5 Slope Stability Analysis	87
4.5.1 Design Criteria	87
4.5.2 Stability Analyses	90
4.6 Results	90
4.7 Remedial Solution	95
4.8 Summary and Conclusions	100
5. LIQUEFACTION POTENTIAL ANALYSIS	101
5.1 Introduction	101
5.1.1 Description of the Project	101
5.1.2 Source Materials Required	101
5.2 Geological Setting	102
5.2.1 Regional Setting	102
5.2.2 Local Geology	102
5.3 Seismic Design Criteria	102
5.4 Probabilistic Seismic Hazard Analysis	104
5.5 Geotechnical Information	104
5.6 Design of the Embankment	108
5.6.1 Design Considerations	108
5.6.2 Seismic Slope Stability	113
5.6.3 Liquefaction Potential	113
5.6.4 Evaluation of the Consequences of Liquefaction	119

TABLE OF CONTENTS (continued)

<u>Example</u>	<u>Page No.</u>
5.7 Site Response Analyses	120
5.8 Calculations	129
5.9 Summary and Conclusions	159
REFERENCES	161

TABLES

<u>Number</u>	<u>Page</u>
1. Brief description of volume II examples.	2
2. Summary of soil properties.	6
3. Geometry of bridge foundations.	8
4. Coefficients of stiffness matrix.	9
5. Dynamic loading characteristics.	36
6. Peak horizontal acceleration and velocity values.	66
7. Summary of design earthquake parameters.	107
8. Main characteristics of candidate CLE accelerograms.	124
9. Main characteristics of candidate OLE accelerograms.	125
10. Liquefaction potential in the free-field.	133
11. Liquefaction potential under the centerline of the embankment.	137
12. Liquefaction potential under the toe of the embankment.	142

FIGURES

<u>Number</u>		<u>Page</u>
1.	Cross section of proposed bridge and soil stratigraphy.	4
2.	Location of Example 1 test borings.	5
3.	Corrected SPT results for Example 1 test borings.	7
4.	Cross section of superstructure.	30
5.	Typical span resting on two bents.	31
6.	Typical Example 2 boring log.	33
7.	Corrected SPT results for Example 2 test borings.	34
8.	Pile cap configuration.	35
9.	Pile and idealized SPT profile.	38
10.	Mississippi embayment boundaries and cross section through embayment.	55
11.	Seismic source zones - south central United States (Johnston and Nava, 1994, reprinted by permission of ATC).	56
12.	Algermissen seismic hazard map.	58
13.	Seismic hazard curves for Shelby County (Allen and Hoshall, 1989, as quoted in Poe, 1992).	59
14.	Target spectrum and the spectra of three time histories.	62
15.	Earthquake acceleration time histories.	64
16.	Small-strain shear modulus profile.	65
17.	Corrected Example 3 SPT profile.	69
18.	Load diagram on retaining wall.	71

FIGURES (continued)

<u>Number</u>		<u>Page</u>
19.	Original topography and proposed grading.	84
20.	Example 4 boring log.	86
21.	Shear strength envelopes for site materials.	88
22.	Calculation of MCE peak ground acceleration.	89
23.	Critical failure mechanisms for Bench 1, static loading.	91
24.	Critical failure mechanisms for Bench 1, pseudo-static loading.	92
25.	Critical deep-seated failure mechanism static loading.	93
26.	Critical deep-seated failure mechanism, pseudo-static loading.	94
27.	Wedge analysis of anchor system.	96
28.	Example 5 site location and seismic source.	103
29.	Recurrence relationship for blind thrust and fold belt.	105
30.	Seismic hazard curves.	106
31.	Stratigraphic profile under embankment.	109
32.	Example 5 boring log.	110
33.	Field uncorrected SPT N value distribution.	111
34.	Shear wave velocity profile in channel.	112
35.	Critical failure surface for OLE.	114
36.	Critical failure surface for CLE.	115
37.	Distribution of factor of safety with depth in the free field.	116

FIGURES (continued)

Number

38.	Distribution of factor of safety with depth under the centerline of the embankment. . .	117
39.	Distribution of factor of safety with depth under the toe of the embankment.	118
40.	Post-liquefaction slope stability analysis.	121
41.	Post-liquefaction pseudo-static slope stability analysis (yield acceleration = 0.14 g). .	122
42.	Permanent seismic deformation chart (modified from Hynes and Franklin, 1984, reprinted by permission of U.S. Army Engineering Waterways Station)..	123
43.	Response spectra from SHAKE analysis for OLE events.	126
44.	Response spectra from SHAKE analysis for CLE events.	127
45.	Design response spectra.	128
46.	Stresses under an embankment (from Poulos and Davis, 1974, reprinted by permission of H.G. Poulos).	139

SYMBOLS

A	cross sectional area
A_t	pile tip area
a	distance
a_{max}	peak average acceleration, peak acceleration at the top of the embankment
B	foundation width (footing width) and/or width of the abutment wall and/or width of pile group
c	cohesion
C_{60}	product of correction factors for use in calculating N_{60}
C_d	pile perimeter at depth d
C_F	correction factor of K_δ when $\delta \neq \phi$
C_N	correction factor for use in calculating $(N_1)_{60}$
C_{HT}	SPT correction factor for nonstandard hammer type
C_{HW}	SPT correction factor for nonstandard hammer weight/height of fall
C_{SS}	SPT correction factor for nonstandard sample setup
C_{RL}	SPT correction factor for change in rod length
C_{BD}	SPT correction factor for nonsaturated borehole diameter
CLE	contingency level earthquake
CSR_{EQ}	critical stress ratio induced by earthquake
CSR_L	corrected critical stress ratio resisting liquefaction
d	displacement (equation 9-23 of volume I) and/or depth
d_i	distance from center of gravity of pile to pile i
D	pile diameter and/or embedded pile length
D_b	bracketed duration of strong ground motion
D_f	depth to the base of the footing from ground surface
D_r	relative density
D_s	significant duration of strong shaking
E	Young's modulus
E_s	Young's modulus of the soil
e_B	eccentricity along foundation width of footing
e_L	eccentricity along foundation length of footing
F	frictional capacity
FS	factor of safety
FS_L	factor of safety against liquefaction
g	acceleration of gravity
G	dynamic (secant) shear modulus
G_{max}	small strain (initial) shear modulus
H	height of the wall and/or resultant horizontal seismic load
H_x	horizontal load along x-axis
H_y	horizontal load along y-axis
I	moment of inertia of a pile

SYMBOLS (continued)

I_f	influence factor for group embedment
i_c, i_y, i_q	load inclination factors
K	stiffness matrix
K_{ECF}	stiffness matrix of equivalent circular footing
k_α	correction factor for the initial driving static shear stress
K_θ	rotational stiffness
K_δ	coefficient of lateral earth pressure at depth d
k_σ	correction factor for stress levels larger than 96 kPa
K_{11}, K_{22}	stiffness coefficient for horizontal rotation
K_2	factor for G_{max} calculation (equation 5-8 of volume I)
K_{33}	stiffness coefficient for vertical translation
K_{44}, K_{55}	stiffness coefficient for rocking rotation
K_{66}	stiffness coefficient for torsional rotation
k_a	active earth pressure coefficient
k_{ae}	seismic active earth pressure coefficient
k_{pe}	seismic passive earth pressure coefficient
k_h	horizontal seismic coefficient
$k_h g$	horizontal ground acceleration
K_{ij}	coefficient of stiffness matrix
k_M	correction factor for earthquake magnitudes other than $M_w 7.5$
k_{max}	peak horizontal average acceleration
K_o	coefficient of lateral earth pressure at rest
k_s	seismic coefficient
K_s	translational stiffness
k_v	vertical seismic coefficient
$k_v g$	vertical ground acceleration
k_y	yield acceleration
L	foundation length and/or length of pile
M	design moment
M_b	(short period) body wave magnitude
M_{JMS}	Japan Meteorological Agency Magnitude
M_L	Local (Richter) Magnitude
M_{max}	Maximum Magnitude
M_S	Surface Wave Magnitude
M_w	Moment Magnitude
M_x	moment in x direction
M_y	moment in y direction
n	number of piles in pile group and/or correction factor (equation 9.6 of volume I)
N	uncorrected Standard Penetration Test (SPT) blow count and/or yield acceleration (equation 9-23 of volume I)
N_{60}	standardized SPT blow count

SYMBOLS (continued)

$(N_1)_{60}$	N_{60} normalized to an effective overburden pressure of 96 kPa
$(N_1)_{60-CS}$	normalized standard "clean sand" blow count
N_c, N_γ, N_q	bearing capacity factors
P	vertical load on pile
P_a	static active earth force or thrust
P_{ac}	seismic active earth force or thrust
P_{pe}	seismic passive earth force or thrust
$(P_v)^{STAT}$	static vertical load
$(P_v)^{DYN}$	dynamic vertical load
$(P_H)^{DYN}$	dynamic horizontal load
P_d	effective overburden pressure at center of depth increment d
P_f	foundation pressure due to seismic load
PI	Plasticity Index
p_t	effective overburden pressure at the pile tip
q_a	allowable bearing capacity (allowable bearing pressure)
q_{max}	maximum applied vertical pressure
q_s	uniform surcharge load applied at ground surface
q_{ult}	ultimate bearing capacity (ultimate bearing pressure)
Q	static vertical load on pile cap
R	equivalent radius for circular footing
r	radius of pile and/or reduction factor for sliding resistance
r_d	stress reduction factor
R_E	epicentral distance
R_H	hypocentral distance
R_I	load inclination factor
R_J	Joyner and Boore distance
R_M	Richter magnitude
R_R	rupture distance
R_S	seismogenic distance or pile shaft resistance
R_T	pile tip resistance
s_c, s_γ, s_q	foundation shape factors
u_{max}	maximum permanent displacement
u_o	pore water pressure
V	resultant vertical seismic load and/or peak velocity of the earthquake record (equation 9-23 of volume I) and/or displaced soil volume (for driven piles)
V_{max}	maximum applied vertical load
V_s	shear wave velocity
α	inclination of resultant force and/or foundation shape correction factor

SYMBOLS (continued)

α_t	dimensionless factor (dependent on pile depth-width relationship)
β	slope of the back of the wall and/or foundation embedment factor
γ	unit weight
$\gamma_{\text{eff}} (G_{\text{eff}}/G_{\text{max}})$	hypothetical effective shear stress factor
γ_{eff}	effective shear strain
δ	angle of friction of the wall/backfill interface and/or pile/soil interface
δ_T	vertical deflection of foundation pile
Δd	length of pile segment
ν	Poisson's ratio
ρ	mass density
σ_m	mean normal total stress
σ'_m	mean normal effective stress
σ_v	vertical total stress
σ'_v	vertical effective stress
τ_{ho}	initial static shear strength on a horizontal plane
τ_{max}	maximum earthquake-induced shear stress at depth
ϕ	angle of internal friction
ω	angle of pile taper measured from vertical

ABBREVIATIONS AND ACRONYMS

AASHTO	American Association of State Highway and Transportation Officials
ASCE	American Society of Civil Engineers
ASTM	American Society for Testing and Materials
ATC	Applied Technology Council
BPT	Becker Penetration Test
CALTRANS	California Department of Transportation
CSSASW	Controlled Source Spectral Analysis of Surface Waves
CDMG	California Division of Mines and Geology
CLE	Contingency Level Event
CPT	Cone Penetration Test
CSR	Critical Stress Ratio
CyDSS	Cyclic Direct Simple Shear (Test)
EERC	Earthquake Engineering Research Center
EERI	Earthquake Engineering Research Institute
EPA	Effective Peak Acceleration
EPRI	Electric Power Research Institute
FEMA	Federal Emergency Management Agency
FHWA	Federal Highway Administration
FSAR	Final Safety Analysis Report
GEC	Geotechnical Engineering Circular
IDOT	Illinois Department of Transportation
JSSMFE	Japanese Society for Soil Mechanics and Foundation Engineering
MCE	Maximum Credible Earthquake
MFZ	Mendocino Fracture Zone
MHA	Maximum Horizontal Acceleration
MM	Modified Mercalli (Intensity Scale)
MCE	Maximum Credible Earthquake
MPE	Maximum Probable Earthquake
MSE	Mechanically Stabilized Earth
NAPP	National Aerial Photographic Program
NAVFAC	Naval Facilities Engineering Command
NCEER	National Center for Earthquake Engineering Research
NCHRP	National Cooperative Highway Research Program
NEHRP	National Earthquake Hazards Reduction Program
NGDC	National Geophysical Data Center
NHI	National Highway Institute
NISEE	National Information Service for Earthquake Engineering
NMSZ	New Madrid Seismic Zone
NRC	National Research Council
NTIS	National Technical Information Service

ABBREVIATIONS AND ACRONYMS (continued)

NYSDOT	New York State Department of Transportation
OLE	Operational Level Event
PGA	Peak Ground Acceleration
PGD	Peak Ground Displacement
PGV	Peak Ground Velocity
PHGA	Peak Horizontal Ground Acceleration
PHGD	Peak Horizontal Ground Displacement
PHGV	Peak Horizontal Ground Velocity
PSAR	Preliminary Safety Analysis Report
PVGA	Peak Vertical Ground Acceleration
RMS	Root Mean Square
RMSA	Root Mean Square of Acceleration Time History
SASW	Spectral Analysis of Surface Waves
SDOF	Single Degree of Freedom (System)
SPT	Standard Penetration Test
SSA	Seismological Society of America
UBC	Unified Building Code
USEPA	United States Environmental Protection Agency
USCS	Unified Soil Classification System
USGS	United States Geological Survey

ACKNOWLEDGEMENTS

The authors wish to express their appreciation to Dr. Rudolph Bonaparte of GeoSyntec Consultants for his contribution in the writing and review of this document. The authors also thank Mr. Richard S. Cheney, Mr. James C. Lyons, Mr. Chien-Tan Chang, and Mr. Barry D. Siel of Federal Highway Administration (FHWA), Dr. Abbas Abghari of the California Department of Transportation (CALTRANS), Mr. Victor Modeer of the Illinois Department of Transportation (IDOT), and Mr. Teh Sung of the New York State Department of Transportation (NYSDOT) who reviewed the manuscript and provided many valuable suggestions.

The authors also acknowledge the many individuals, too numerous to name here, who reviewed parts of this document and who, over the years, have shared their experiences and recommendations regarding seismic probability studies, liquefaction analysis, and dynamic stability evaluation.

INTRODUCTION

In the United States, design of constructed facilities to resist the effects of earthquakes is often considered a problem restricted to areas west of the Rocky Mountains. However, historical records show that damaging earthquakes can, and do, also occur over broad areas of the eastern and central United States. In fact, the areas over which damaging earthquakes may reasonably be expected to occur cover more than 40 percent of the continental United States. Until recently, highway facilities in many of these areas have not been designed for seismic loading. However, in response to a growing awareness of both the potential for strong motions due to earthquakes in the eastern and central United States and the impact of even modest levels of shaking on facilities not designed to resist earthquake effects, most states now require some consideration of seismic loading in design of new highway facilities.

To provide geotechnical engineers with general guidance on the seismic design of highway facilities, this two-volume guidance document has been prepared. The first volume presents narrative text on the principles of geotechnical earthquake engineering for highway projects. This second volume presents a series of five design examples illustrating the application of the design principles presented in the first volume.

The examples presented in this volume are based upon actual problems encountered in geotechnical earthquake engineering practice. Each example is self-supporting and contains all necessary information for the geotechnical engineer to conduct the required analyses. In example 1, the seismic bearing capacity and dynamic stiffness matrix of a shallow bridge foundation is evaluated. Example 2 is devoted to the seismic design of a deep foundation constructed with driven piles for a four-lane highway bridge. In example 3, a complete seismic hazard analysis is conducted to provide the seismic loading for design of a concrete gravity retaining wall. The seismic stability analysis of a cut slope in soft rock is presented in example 4. Example 5 illustrates the evaluation of liquefaction potential.

The objective of these examples is to illustrate application of the principles and methods described in volume I. In each example, reference is made to the appropriate chapters in volume I. Table 1 summarizes the topics covered in each of the five examples presented in this volume. For each example, a concise statement of the problem to be solved is presented along with the necessary information, detailed calculations, and the final recommendations for design. Equation numbers that appear in the right-hand margin of the calculation sheets refer back to volume I.

Table 1. Brief description of volume II examples.

Example	Title	Volume I Topics Covered
1	Seismic Analysis of a Shallow Bridge Foundation	<ul style="list-style-type: none"> • Correction of SPT N values • Static and dynamic bearing capacity • Dynamic stiffness matrix for shallow footings • Dynamic stiffness coefficient for shallow abutment wall • Seismic settlement evaluation
2	Seismic Design of a Deep Foundation System	<ul style="list-style-type: none"> • Deep foundation static and dynamic bearing capacity • Lateral deflection of a pile group • Vertical deflection of a pile
3	Seismic Design of a Retaining Wall	<ul style="list-style-type: none"> • Simplified seismic hazard analysis • Seismic response analysis • Pseudo-static analysis of a retaining wall • Evaluation of seismically-induced displacement
4	Slope Stability Analysis	<ul style="list-style-type: none"> • Deterministic seismic hazard analysis • Pseudo-static slope stability analysis
5	Liquefaction Potential Analysis	<ul style="list-style-type: none"> • Seed and Idriss simplified method for liquefaction potential evaluation • Probabilistic seismic hazard analysis • Seismic slope stability and deformation analysis • Post-liquefaction stability analysis • Liquefaction mitigation measures

EXAMPLE 1

SEISMIC ANALYSIS OF A SHALLOW BRIDGE FOUNDATION

1.1 INTRODUCTION

1.1.1 Description of the Project

This project involves a foundation performance evaluation for the construction of a new bridge in an alluvial valley. The geotechnical engineer has been asked to evaluate the allowable seismic bearing capacity of the proposed spread footing foundation and provide the structural engineer with the dynamic stiffness matrix for the footings and abutment walls. The bridge is 38 m long with a 5-m clearance. It is a composite structure with steel girders and precast concrete slabs forming the deck. The cross section of the bridge and soil profile are shown on figure 1. The bridge is 24 m wide, including sidewalks and barriers, as shown in figure 2. The seismic hazard and site response analyses were performed as part of earlier, preliminary, design work and are not part of this problem. The maximum credible earthquake design event is characterized by a moment magnitude equal to 7.5 and a peak horizontal ground acceleration equal to 0.55 g. Seismically-induced peak shear strains calculated in site response analyses were on the order of 0.02 percent.

1.1.2 Source Materials Required

The source materials necessary to solve this problem include:

- the configuration of the bridge;
- geotechnical subsurface information (e.g., boring logs with blow counts); and
- volume I of this document.

1.2 SITE GEOLOGY

Soil conditions in the valley are dominated by deep Holocene alluvium. Available information on regional geology indicates that the site is underlain by up to 450 m of this Holocene alluvium. Information obtained during initial site reconnaissance, from a review of surficial geology maps, and from a review of data from previous subsurface investigations in the vicinity of the site indicates that the soils at the site consist of sand, silty sands, sandy silts, and gravelly sands.

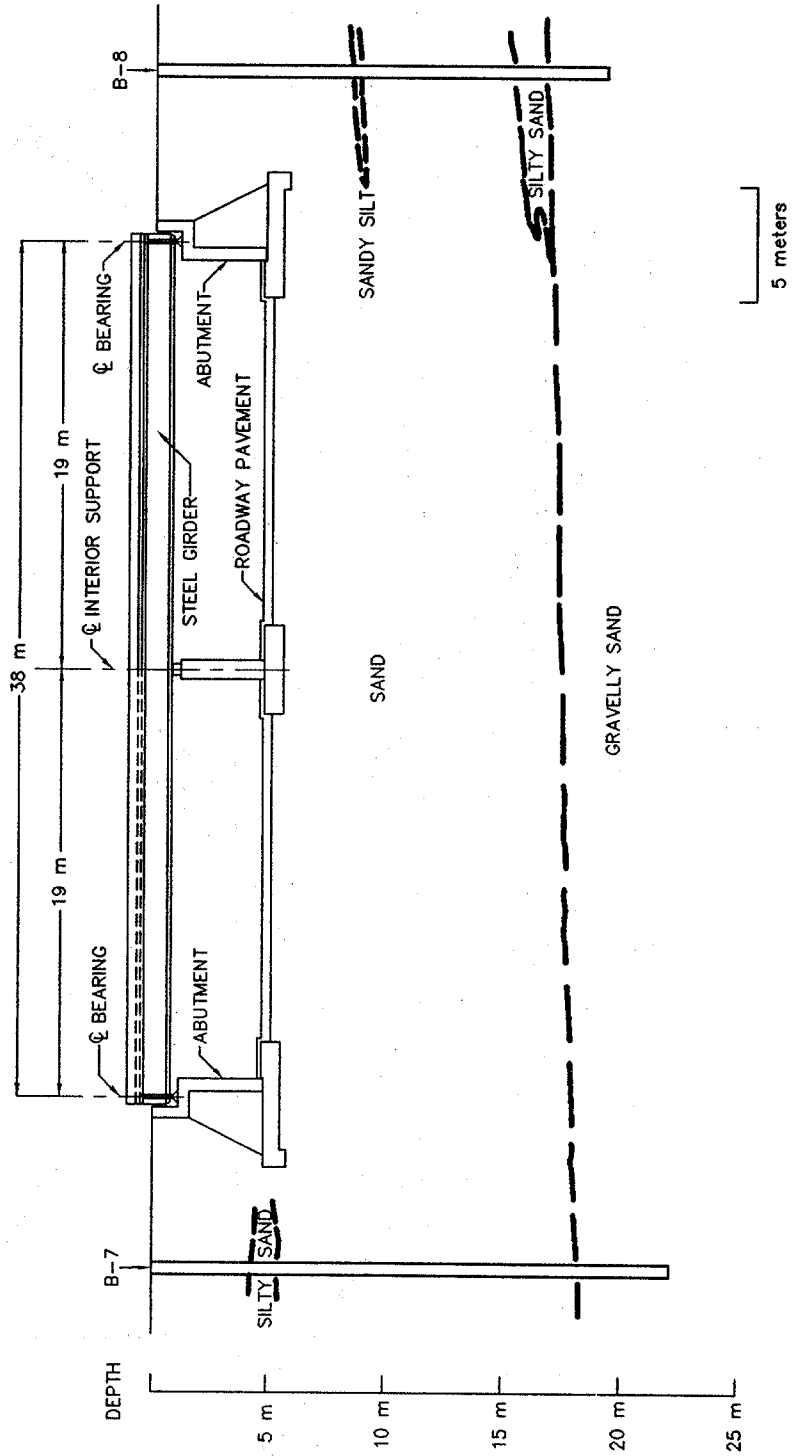
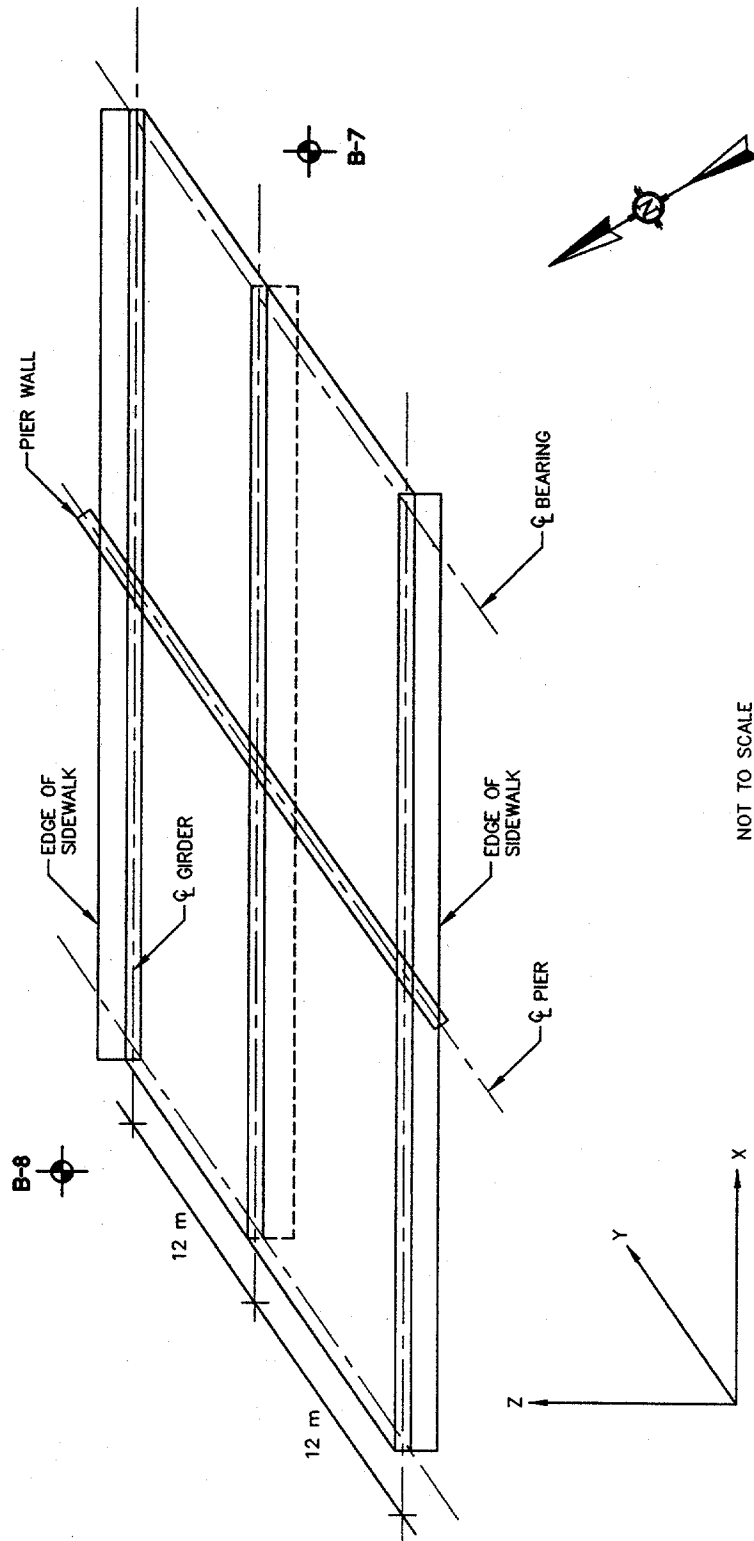


Figure 1. Cross section of proposed bridge and soil stratigraphy.



NOT TO SCALE

Figure 2. Location of the Example 1 test borings.

1.3 GEOTECHNICAL EXPLORATION

Soil conditions at the site were obtained from two soil borings (B-7 and B-8) located at either end of the proposed bridge, as shown on figure 1. Borings were advanced using a 0.2 m diameter hollow stem auger mounted on a CME-75 drill rig. The boring program included standard penetration tests (SPT) (ASTM D 1586) and California Drive Sampling (ASTM D 3550) in predominantly cohesionless soils. Standard penetration tests and drive sampling were performed alternately at 1.5-m intervals using a doughnut hammer with rope and pulley.

Borings B-7 and B-8 were drilled to refusal at depths of 24 m and 21 m, respectively, at the locations shown on figure 2. Groundwater was not encountered in either boring. The soil profile developed based on information from these borings is reported on figure 1.

Based upon the results of the laboratory and field tests, the site stratigraphy was idealized for engineering analysis. Table 2 presents this idealized soil profile and relevant soil parameters obtained from the laboratory test results and empirical correlations for use in the bearing capacity analysis.

Table 2. Summary of soil properties.

Depth (m)	Soil Type (USCS)	Dry Unit Weight (kN/m ³)	Total Unit Weight (kN/m ³)	Friction Angle (°)	Cohesion (kPa)
0-18	SP-SM	16.5	17.2	35	0
18-21	SP-GP	17.3	18.1	38	0

Note: Groundwater was not encountered in either boring.

The field blow counts and blow counts normalized to 96 kPa overburden pressure and standardized for 60 percent hammer efficiency are reported on figure 3. Details of the normalization and standardization procedures are provided in the attached calculation sheets. In general, the blow counts increase with depth. Average normalized and standardized values vary from approximately 25 blows per 300 mm at shallow depths (0 to 10 m) to approximately 30 blows per 300 mm at greater depths (11 to 20 m). Both borings were terminated due to refusal at the bottom of the hole (depths 21 m and 24 m). Refusal and the isolated high blow counts at shallower depths may be attributed to the presence of gravel, which is known to result in high blow counts.

SPT Blow Counts (Blows/300mm)

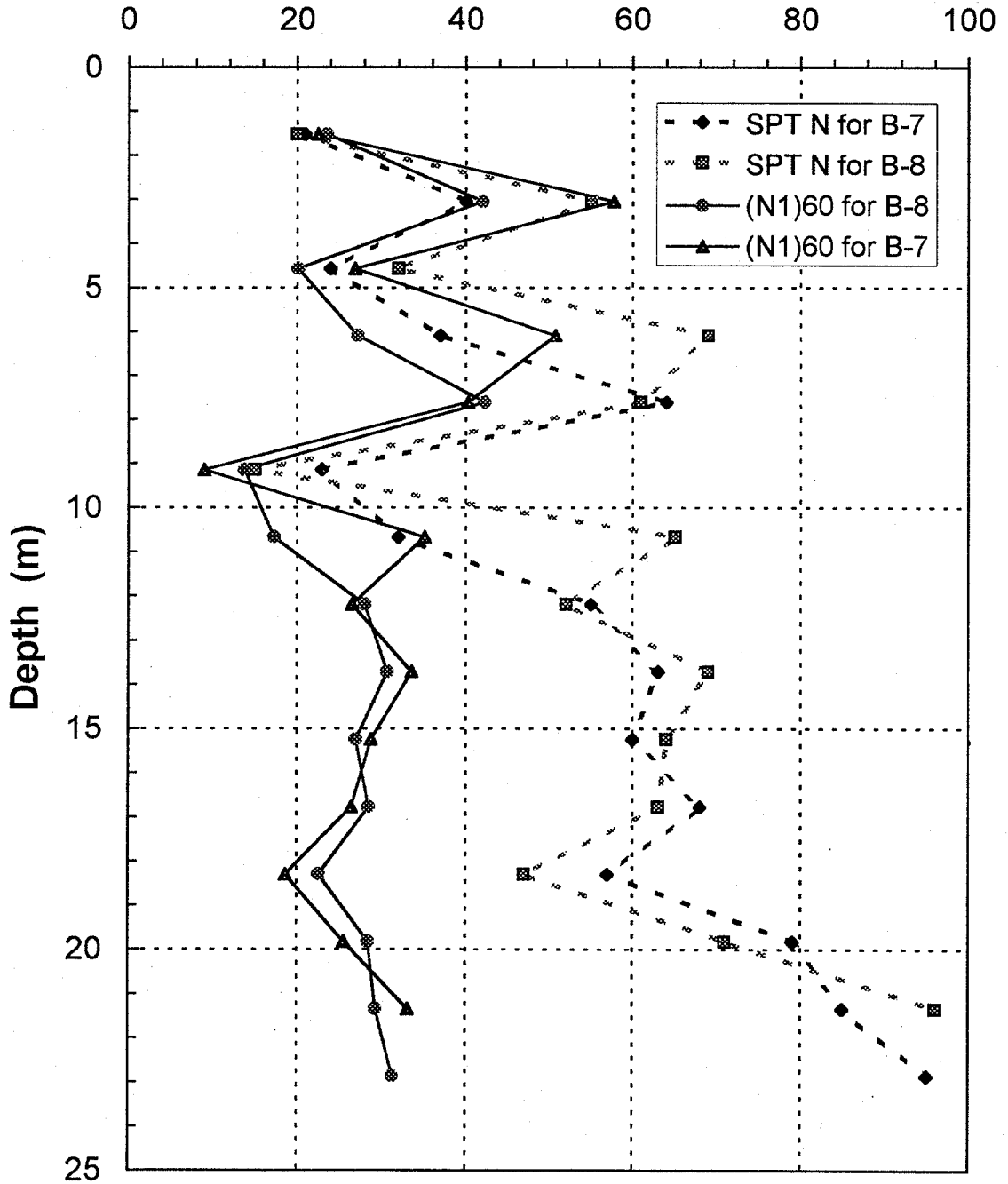


Figure 3. Corrected SPT results for Example 1 test borings.

1.4 DESIGN OF SHALLOW FOUNDATION

The proposed bridge will be supported by a central pier resting on a rectangular footing and two cast-in-place concrete abutment walls, as shown on figure 1. The bearing capacity and stiffness matrix of the central pier footing and the footings for the two abutment walls are needed by the structural engineer for the seismic analysis. The structural engineer also requires the rotational and translational stiffness of the abutment walls. The analysis was carried out in two phases. For the initial phase, an estimate of the static bearing capacity was made to enable the engineer to assess the adequacy of the dimensions of the footings. The footing dimensions were then used to evaluate the stiffness matrix. Using the stiffness matrix, the structural engineer performed the seismic response computations and provided the geotechnical engineer with estimates of the vertical and horizontal loads which may be imposed on the footings during the design earthquake. In the second phase, the bearing capacity of the footings under static and dynamic conditions was assessed for comparison to the loads from the dynamic analysis.

The geometry of the foundations shown on figure 1 is summarized in table 3.

Table 3. Geometry of bridge foundations.

Foundation	Length (m)	Width (m)	Depth Below Grade (m)
Central Pier Footing	25	4.25	5.5
Abutment Wall Footings	25	6.0	5.5

The allowable static bearing capacity was calculated using the method described in chapter 9.4.2.3 of volume I. The allowable static bearing capacity, including a factor of safety of 3, is approximately 420 kPa for the central pier footing and 580 kPa for the abutment wall footings. This static capacity is for vertical loads only and was used to size the foundations. The dynamic bearing capacity will be estimated once the magnitude of the seismic loads, and hence the magnitude and direction of the resultant force, are obtained from the structural engineer.

The stiffness matrix for the footings for soil-structure interaction computations was obtained using the procedure detailed in chapter 9.4.3 of volume I. The elements of the stiffness matrix for the footings are listed in table 4 below and the detailed calculations are provided in the calculation sheets at the end of this example.

The rotational and translational stiffness of the abutment walls were calculated using the procedure detailed in chapter 9.6.2.3 of volume I. The rotational stiffness was calculated as 4,294 MPa/m and the translational stiffness was calculated as 1,147 MPa/m². Detailed calculations are provided in the calculation sheets at the end of this example.

Table 4. Coefficients of stiffness matrix.

Motion	Central Pier Footing (MPa·m)	Abutment Wall Footings (MPa·m)
Vertical	$K_{33} = 4,015$	$K_{33} = 4,679$
Horizontal	$K_{11} = K_{22} = 3,430$	$K_{11} = K_{22} = 3,814$
X-Axis Rocking	$K_{44} = 2,992,156$	$K_{44} = 3,875,628$
Y-Axis Rocking	$K_{55} = 224,544$	$K_{55} = 486,130$
Z-Axis Rotation (Torsion)	$K_{66} = 2,800,657$	$K_{66} = 3,645,971$

Using the stiffness coefficients provided by the geotechnical engineer, estimates of the dynamic horizontal and vertical loads were provided by the structural engineer and are incorporated into the final check of the dynamic bearing capacity of the footing. For the central pier, the following dynamic loads were calculated:

$$\text{Peak Dynamic Vertical Load: } (P_V)^{\text{DYN}} = 7,000 \text{ kN}$$

$$\text{Peak Dynamic Horizontal Load: } (P_H)^{\text{DYN}} = 14,000 \text{ kN}$$

The calculations for the dynamic bearing capacity of the central pier are included in the attached calculation sheets.

1.5 SEISMIC SETTLEMENT AND LIQUEFACTION POTENTIAL

The seismic settlement of the foundation soil in the design earthquake was evaluated using the method described in chapter 8.5 of volume I. The calculated seismic settlement is 24 mm. The calculations are provided in the calculation sheets. The potential for earthquake-induced liquefaction is negligible because groundwater was not encountered in either of the borings, indicating that groundwater was at least 24 m below ground surface.

1.6 CALCULATIONS

The calculations sheets for example 1, "Seismic Analysis of a Shallow Bridge Foundation" follow. Equation numbers that appear in the right hand margin of the calculation sheets refer back to volume I.

Written by: T.H.H. Date: 96 / 03 / 19 Reviewed by: E.K. and N.M. Date: 96 / 03 / 20
YY MM DD YY MM DD

Client: FHWA Project: GEC-3 Project/Proposal No.: GE3686 Task No.: F

DETAILED CALCULATIONS
EXAMPLE 1 - SEISMIC ANALYSIS OF A SHALLOW BRIDGE FOUNDATION

Correlation of SPT N Values

1. Standardization

The standardized SPT blow count N_{60} is the standard penetration blow count for a hammer with an efficiency of 60 percent. If non-standard equipment is used, N_{60} is obtained from equation 8-4 of volume I.

$$N_{60} = N \cdot C_{60} \tag{8-4}$$

where N is the SPT blow count measured in the field.
 C_{60} is the product of various correlative factors.

$$C_{60} = C_{HT} \cdot C_{HW} \cdot C_{SS} \cdot C_{RL} \cdot C_{BD}$$

Values of the different factors are provided in table 9 of volume I.

The equipment used at the site included a donut hammer with rope and pulley. Other elements of the SPT equipment met the recommended standards listed in table 8 of volume I.

From table 9 of volume I:

$$\begin{aligned} C_{HT} &= 0.75 \\ C_{HW} &= 1.0 \\ C_{SS} &= 1.0 \\ C_{RL} &= 1.0 \\ C_{BD} &= 1.0 \\ \Rightarrow C_{60} &= (0.75)(1.0)(1.0)(1.0)(1.0) = 0.75 \end{aligned}$$



Written by: T.H.H. Date: 96 / 03 / 19 Reviewed by: E.K. and N.M. Date: 96 / 03 / 20
YY MM DD YY MM DD

Client: FHWA Project: GEC-3 Project/Proposal No.: GE3686 Task No.: F

2. Normalization

$(N_1)_{60}$ is the standardized blow count normalized to an effective stress of 96 kPa (1 ton per square foot) in order to eliminate the influence of confining pressure.

$$(N_1)_{60} = C_N \cdot N_{60} \tag{8-6}$$

where C_N is read from figure 57 of volume I (use table 4 or figure 37 from volume I for N-D_r correlation) or obtained using equation 8-5. A spreadsheet was developed to perform the calculation of the standardized normalized blow count at the site. The distributions with depth of both field measured and normalized and standardized blow count are shown in figure 3 of this example.

Normalization of SPT Blow Counts.

Depth	Vertical Effective Stress	C_N (Figure 57)	C_{60} (Table 9)	N		$(N_1)_{60} = N \cdot C_N \cdot C_{60}$	
				B-7	B-8	B-7	B-8
1.5 m	25.2 kPa	1.50	0.75	21	20	23.6	22.5
3.0 m	50.4 kPa	1.40	0.75	40	55	42.0	57.8
4.6 m	75.6 kPa	1.12	0.75	24	32	20.2	26.9
6.1 m	100.8 kPa	0.98	0.75	37	69	27.2	50.7
7.6 m	126.0 kPa	0.88	0.75	64	61	42.2	40.3
9.1 m	151.2 kPa	0.80	0.75	23	15	13.8	9.0
10.7 m	176.4 kPa	0.72	0.75	32	65	17.3	35.1
12.2 m	201.6 kPa	0.68	0.75	55	52	28.1	26.5
13.7 m	226.8 kPa	0.65	0.75	63	69	30.7	33.6
15.2 m	252.0 kPa	0.60	0.75	60	64	27.0	28.8
16.8 m	277.2 kPa	0.56	0.75	68	63	28.6	26.5
18.3 m	302.4 kPa	0.53	0.75	57	47	22.7	18.7
19.8 m	343.2 kPa	0.48	0.75	79	71	28.4	25.6
21.3 m	369.6 kPa	0.46	0.75	85	96	29.3	33.1
22.9 m	396.0 kPa	0.44	0.75	95	—	31.4	—



Written by: T.H.H. Date: 96 / 03 / 19 Reviewed by: E.K. and N.M. Date: 96 / 03 / 20
YY MM DD YY MM DD

Client: FHWA Project: GEC-3 Project/Proposal No.: GE3686 Task No.: F

Allowable Bearing Capacity

Allowable bearing capacity is evaluated using the procedure described in chapter 9.4.2.3 of volume I. The equation for ultimate bearing capacity can be written as:

$$q_{ult} = c N_c s_c i_c + 0.5 \gamma B N_\gamma s_\gamma i_\gamma + q_s N_q s_q i_q \tag{9-1}$$

Step 1: Evaluate the Coefficients and Soil Parameters (chapter 9.4.2.3 of volume I)

$$N_q = e^{\pi \tan \phi} \tan^2 (45 + \phi/2) \tag{9-2}$$

$$N_c = (N_q - 1) \cot \phi \tag{9-3}$$

$$N_\gamma = (N_q - 1) \tan (1.4\phi) \tag{9-4}$$

For preliminary calculations, it is assumed that the applied loads are vertical. This implies that, with respect to the load inclination factors in equation 9-1, $i_c = i_q = i_\gamma = 1$.

The foundation shape factors are given by (chapter 9.4.2.3 of volume I):

$$s_c = 1 + \frac{B}{L} (N_q/N_c) \tag{9-7a}$$

$$s_q = 1 + \frac{B}{L} \tan \phi \tag{9-7b}$$

$$s_\gamma = 1 - 0.4 \left(\frac{B}{L} \right) \tag{9-7c}$$

As the proposed foundations are shallow foundations, the soil parameters for the upper 18 m thick soil layer are used for this analysis. From table 2, these parameters are:

$$\phi = 35^\circ$$

$$\gamma = 17.2 \text{ kN/m}^3$$



Written by: T.H.H. Date: 96 / 03 / 19 Reviewed by: E.K. and N.M. Date: 96 / 03 / 20
YY MM DD YY MM DD

Client: FHWA Project: GEC-3 Project/Proposal No.: GE3686 Task No.: F

The footing length, L, was set at 25 m, the width of the bridge. After several trials, a footing width, B, of 4.25 m was established for the central pier, and a width of 6 m was established for the abutment wall.

Based upon these values, the following bearing capacity coefficients were calculated:

Summary of bearing capacity coefficients.

Factor	Central Pier; B = 4.25 m, L = 25 m	Abutment Wall; B = 6 m, L = 25 m
N_q	33.3	33.3
N_γ	37.2	37.2
N_c	46.1	46.1
s_q	1.12	1.17
s_γ	0.93	0.90
s_c	1.12	1.17

Step 2: Evaluate Bearing Capacity

For this computation, it is assumed that the footings are founded directly at the proposed grade elevation (no embedment). The effect of embedment on the bearing capacity of the abutment wall footings and the effect of the horizontal seismic loads on bearing capacity will be included in later analyses.

Therefore, the equation of bearing capacity (equation 9.1 in volume I), with $c = 0$ (cohesionless), $q_s = 0$ (no surcharge), and $i_\gamma = 1$ (no inclination), can be written as:

$$q_{ult} = 0.5 \gamma B N_\gamma s_\gamma$$

Assuming a factor of safety FS = 3 the allowable bearing capacities for static loading calculated using this equation are:

$$\text{Central Pier Footing: } q_a = \frac{1,265}{3} = 420 \text{ kPa}$$



Written by: T.H.H. Date: 96 / 03 / 19 Reviewed by: E.K. and N.M. Date: 96 / 03 / 20
YY MM DD YY MM DD

Client: FHWA Project: GEC-3 Project/Proposal No.: GE3686 Task No.: F

$$\text{Abutment Wall Footings: } q_a = \frac{1728}{3} = 580 \text{ kPa}$$

The estimated loads on each footing were:

Central Pier Footing: 44,625 kN
 Abutment Wall Footing: 87,000 kN

As the bridge is 25 m wide, and therefore the footings are 25 m long (L=25 m), the following footing widths were established for each footing.

$$\text{Central Pier Footing: } B_{\min} = \frac{44,625}{420 \cdot 25} = 4.25 \text{ m}$$

$$\text{Abutment Wall Footing: } B_{\min} = \frac{87,000}{25 \cdot 580} = 6.00 \text{ m}$$

These results indicated that 4.25 m was an acceptable width for the central pier and that 6 m was an acceptable width for the abutment wall.

Stiffness Matrix

The equation for the general footing stiffness matrix, K, is:

$$K = \alpha \beta K_{ECF} \tag{9-11}$$

where: α = foundation shape correction factor (chapter 9.4.3.4 of volume I)

β = foundation embedment factor (chapter 9.4.3.5 of volume I)

K_{ECF} = stiffness matrix of an equivalent circular surface footing, composed of coefficients K_{ij} , as described in chapter 9.4.3.2 of volume I.

The equations for the stiffness coefficients of a circular footing of radius R are: (chapter 9.4.3.2 of volume I)



Written by: T.H.H. Date: 96 / 03 / 19 Reviewed by: E.K. and N.M. Date: 96 / 03 / 20
YY MM DD YY MM DD

Client: FHWA Project: GEC-3 Project/Proposal No.: GE3686 Task No.: F

Vertical Translation $K_{33} = \frac{4GR}{1 - \nu}$ (9-12a)

Horizontal Translation $K_{11} = K_{22} = \frac{8GR}{2 - \nu}$ (9-12b)

X & Y-Axis Rocking $K_{44} = K_{55} = \frac{8GR^3}{3(1 - \nu)}$ (9-12d)

Z-Axis Rotation (Torsion) $K_{66} = \frac{16GR^3}{3}$ (9-12c)

where G is the shear modulus of soil and ν is Poisson's ratio.

Step 1: Evaluation of Equivalent Radius

Using the equations for evaluating the equivalent circular radius of a rectangular footing given in table 13 of volume I, the equivalent radius is calculated for each mode as follows:

Translational modes: $R_z = R_x = \sqrt{BL / \pi}$ (Vertical and Horizontal Translation)

Rotational modes: $R_{\psi_x} = \left[\frac{(16B)(L)^3}{3\pi} \right]^{1/4}$ X-Axis Rocking

$R_{\psi_y} = \left[\frac{(16B)^3(L)}{3\pi} \right]^{1/4}$ Y-Axis Rocking

$R_{\psi_z} = \left[\frac{16BL(B^2 + L^2)}{6\pi} \right]^{1/4}$ Z-Axis Rotation (Torsion)

where the x-axis is parallel to the B -dimension (width of the footing), the y-axis is parallel to the L -dimension (length of the footing) and Z is the vertical axis. Results of the calculations are presented in the following table:



Written by: T.H.H. Date: 96 / 03 / 19 Reviewed by: E.K. and N.M. Date: 96 / 03 / 20
YY MM DD YY MM DD

Client: FHWA Project: GEC-3 Project/Proposal No.: GE3686 Task No.: F

Results of equivalent radius calculation.

Motion	Equivalent Radius	
	Central Pier Footing (m)	Abutment Wall Footings (m)
Vertical and Horizontal Translation	$R_z = R_x = 5.82$	$R_z = R_x = 6.91$
X-Axis Rocking	$R_{\psi_x} = 18.32$	$R_{\psi_x} = 19.97$
Y-Axis Rocking	$R_{\psi_y} = 7.56$	$R_{\psi_y} = 9.78$
Z-Axis Rotation (Torsion)	$R_{\psi_z} = 15.52$	$R_{\psi_z} = 17.03$

Step 2: Evaluation of the Shear Modulus

As no direct measurements of the shear modulus or shear wave velocity are available, the small strain shear modulus of the upper layer of medium dense sand and silty sand at the site must be estimated for use in evaluating the stiffness coefficients. Available methods for estimating shear wave velocity or modulus include: (1) correlations using SPT blow count values; (2) typical values for dense sandy soils; or (3) empirical correlations such as those described in chapter 5.4.5.2 and table 6 of volume I.

Compute $G = G_{max}$ at a depth approximately equal to the equivalent radius for translation of the foundation. Use 6.5 meters as average value for both footings and use the properties reported in table 2 and figure 3 for the soils between 1 and 6.5 meters:

$$N_{60} = 28; \phi = 35^\circ; \gamma = 17.2 \text{ kN/m}^3$$

Two different methods are used herein to calculate G_{max} : (1) the Seed et al. (1984) empirical correlation based upon mean normal effective stress and blow count; and (2) the Imai and Tonouchi (1982) equation based solely on the SPT blow count values.

(1) Seed et al. (1984):

$$G_{max} = 220 (K_2)_{max} (\sigma'_m)^{1/2}$$



Written by: T.H.H. Date: 96 / 03 / 19 Reviewed by: E.K. and N.M. Date: 96 / 03 / 20
YY MM DD YY MM DD

Client: FHWA Project: GEC-3 Project/Proposal No.: GE3686 Task No.: F

$$\sigma'_m = \left(\frac{1+2K_o}{3} \right) \sigma'_v$$

$$\sigma'_v = (6.5)(17.2) = 112 \text{ kPa}$$

$$K_o = 1 - \sin\phi = 1 - \sin(35) = 0.43$$

$$\sigma'_m = \left(\frac{1+2(0.43)}{3} \right) (112) = 69 \text{ kPa}$$

$$(K_2)_{\max} = 20(N_{60})^{1/3} = (20)(28)^{1/3} = 60.73$$

$$G_{\max} = 220(60.73)(69)^{1/2} = 110,982 \text{ kPa}$$

$$G_{\max} = 110 \text{ MPa}$$

(2) Imai and Tonouchi (1982):

$$\begin{aligned} G_{\max} &= 15,560 (N_{60})^{0.68} \\ &= 15,560 (28)^{0.68} = 149,995 \text{ kPa} \end{aligned}$$

$$G_{\max} = 150 \text{ MPa}$$

Using average value from methods (1) and (2):

$$G_{\max} = 130 \text{ MPa}$$

Based on the results of a seismic site response analysis, it is assumed that the design earthquake will induce shear strains of about 0.02 percent. Therefore, following the recommendations from volume I, chapter 9.4.3.2, and using modulus reduction curve for sand shown on figure 41 of volume I ($\sigma'_m \approx 100 \text{ kPa}$), the small strain shear modulus will be reduced by 30 percent to 91 MPa for use in calculating the footing stiffness coefficients.

Step 3: Evaluation of the Stiffness Coefficient for Circular Footing

Using the G_{\max} value calculated above (including the 30 percent reduction), the equivalent radius values computed in step 1, and an assumed value of Poisson's ratio, $\nu = 0.35$ (see volume I,



Written by: T.H.H. Date: 96 / 03 / 19 Reviewed by: E.K. and N.M. Date: 96 / 03 / 20
YY MM DD YY MM DD

Client: FHWA Project: GEC-3 Project/Proposal No.: GE3686 Task No.: F

chapter 5.3.3), the stiffness coefficients for a circular footing are calculated using equations 9.12a through 9.12d. The results of this calculation are shown in the following table.

Results of stiffness coefficient calculation for equivalent circular footing.

Motion	Stiffness Coefficient for Circular Footing	
	Central Pier Footing MPa·m	Abutment Wall Footings MPa·m
Vertical Translation	$K_{33} = 3,260$	$K_{33} = 3,870$
Horizontal Translation	$K_{11} = K_{22} = 2,568$	$K_{11} = K_{22} = 3,049$
X-Axis Rocking	$K_{44} = 2,295,478$	$K_{44} = 2,973,247$
Y-Axis Rocking	$K_{55} = 161,310$	$K_{55} = 349,231$
Z-Axis Rotation (Torsion)	$K_{66} = 1,814,326$	$K_{66} = 2,397,088$

Step 4: Evaluation of Rectangular Footing Stiffness Coefficient

Once the stiffness coefficients for an “equivalent” circular footing are calculated, they can be multiplied by the shape and embedment factors α and β to get the stiffness coefficient for the embedded rectangular footing in accordance with equation 9-11. The shape and embedment factors, α and β , are functions of depth of embedment, dimensions of the footings, and type of motion. Values for these factors may be taken from figures 69 and 70 from volume I and combined with the stiffness values calculated in Step 3 to calculate the stiffness coefficients for the bridge foundations.

For both footings, use a footing thickness $D = 1$ m from the design drawings.

Since $L = 25$ m and $B = 4.25$ m, $L/B = 5.9$. To calculate the shape and embedment factors, use asymptotic values for $L/B = 4$ and D/R calculated with $D = 1$ and R from the table on page 7/18 of these calculation sheets. The resulting values of α and β (see figures 69 and 70 in volume I) and the calculated stiffness values for the central pier footing are given in the following table.



Written by: T.H.H. Date: 96 / 03 / 19 Reviewed by: E.K. and N.M. Date: 96 / 03 / 20
YY MM DD YY MM DD

Client: FHWA Project: GEC-3 Project/Proposal No.: GE3686 Task No.: F

Results of stiffness coefficient calculation for central pier footing.

Motion	D/R	β	α	K_{PIER} (MPa·m)
Vertical Translation	0.172	1.09	1.13	$K_{33} = 4,015$
Horizontal Translation	0.172	1.26	1.06	$K_{11} = K_{22} = 3,430$
X-Axis Rocking	0.055	1.1	1.185	$K_{44} = 2,992,156$
Y-Axis Rocking	0.13	1.2	1.16	$K_{55} = 224,544$
Z-Axis Rotation (Torsion)	0.06	1.3	1.17	$K_{66} = 2,800,657$

For the Abutment Wall Footings:

Since $L = 25$ m and $B = 6$ m, $L/B = 4.2$. Use asymptotic values for $L/B = 4$ and D/R calculated with $D = 1$ and R from the table on page 7/18 of these calculation sheets. The resulting values of α and β and the calculated stiffness values for the abutment footings are given in the following table:

Results of stiffness coefficient calculation for abutment wall footing.

Motion	D/R	β	α	$K_{ABUTMENT}$ (MPa·m)
Vertical Translation	0.145	1.07	1.13	$K_{33} = 4,679$
Horizontal Translation	0.145	1.18	1.06	$K_{11} = K_{22} = 3,814$
X-Axis Rocking	0.05	1.1	1.185	$K_{44} = 3,875,628$
Y-Axis Rocking	0.10	1.2	1.16	$K_{55} = 486,130$
Z-Axis Rotation (Torsion)	0.06	1.3	1.17	$K_{66} = 3,645,971$



Written by: T.H.H. Date: 96 / 03 / 19 Reviewed by: E.K. and N.M. Date: 96 / 03 / 20
YY MM DD YY MM DD

Client: FHWA Project: GEC-3 Project/Proposal No.: GE3686 Task No.: F

Stiffness Coefficient for Abutment Wall

The translational and rotational stiffness coefficients for the abutment walls are computed below using equations 9-26 and 9-27 from volume I.

$$K_S = 0.425 E_s B \tag{9-26}$$

$$K_\theta = 0.072 E_s B H^2 \tag{9-27}$$

where B and H are the width and height of the wall and E_s is the Young's modulus of the soil. Values for B and H were obtained from the design drawings and are equal to 25 m and 4.7 m, respectively.

The shear modulus of the backfill, G, is estimated from the values listed in table 5 of volume I.

Silty sand, medium compaction:

$$G = 80 \text{ MPa}$$

$$E_s = 2(1 + \nu) G = 2(1 + 0.35) 80 = 216 \text{ MPa}$$

As recommended in chapter 9.6.2.3, the value of Young's modulus is reduced to reflect a strain level of 0.02 percent. Following the logic used previously for the shear modulus and using modulus reduction curves for sand shown on figure 42 of volume I ($\sigma'_m \approx 25 \text{ kPa}$), E_s will be reduced by 50 percent.

$$E_s = (0.5)(216) = 108 \text{ MPa}$$

$$K_S = (0.425)(108)(25) = 1,147 \text{ MPa} \cdot \text{m}$$

$$K_\theta = (0.072)(108)(25)(4.7)^2 = 4,294 \text{ MPa} \cdot \text{m}^2$$



Written by: T.H.H. Date: 96 / 03 / 19 Reviewed by: E.K. and N.M. Date: 96 / 03 / 20
YY MM DD YY MM DD

Client: FHWA Project: GEC-3 Project/Proposal No.: GE3686 Task No.: F

Evaluate Dynamic Bearing Capacity of Central Pier Footing

Following performance of a seismic response analysis for the bridge, the structural engineer has provided the following estimates of the peak dynamic vertical and horizontal loads on top of the central pier footing:

$$(P_V)^{DYN} = 7,000 \text{ kN}$$

$$(P_H)^{DYN} = 14,000 \text{ kN}$$

These loads must be checked against the dynamic bearing capacity of the footing and the sliding resistance. Note that cited horizontal forces used in this example are transverse loads (perpendicular to the roadway). For actual design, the calculations also need to be performed for horizontal loads along the longitudinal direction of the bridge.

The footing is subjected to a combined vertical load and horizontal load. This combined system of loads is first replaced by a single inclined load. Then, the footing is analyzed for two load conditions, one in which the vertical load is assumed to act upwards (maximum dynamic load inclination) and another where the vertical load is assumed to act downwards (maximum vertical load).

- Maximum dynamic load inclination.

$$V = (P_V)^{STAT} - (P_V)^{DYN}$$

where $(P_V)^{STAT}$ is the static vertical load ($Q_a = 44,625 \text{ kN}$)

$$V = 44,625 - 7,000 = 37,625 \text{ kN}$$

This loading condition governs sliding, but it will also be used to evaluate bearing capacity.



Written by: T.H.H. Date: 96 / 03 / 19 Reviewed by: E.K. and N.M. Date: 96 / 03 / 20
YY MM DD YY MM DD

Client: FHWA Project: GEC-3 Project/Proposal No.: GE3686 Task No.: F

Since $H = (P_H)^{DYN} = 14,000$ kN, the load is inclined at an angle α from the horizontal evaluated as:

$$\alpha = \tan^{-1} \frac{37,625}{14,000} = 70^\circ$$

The magnitude of the load is evaluated as:

$$P = \sqrt{H^2 + V^2} = \sqrt{14,000^2 + 37,625^2} = 40,145 \text{ kN}$$

Since the central pier footing is founded directly at the proposed grade elevation on a cohesionless soil, the bearing capacity equation 9-1 reduces to:

$$q_{ult} = 0.5 \gamma B N_\gamma s_\gamma i_\gamma \tag{9-1}$$

For zero cohesion, i_γ is given by:

$$i_\gamma = \left[1 - \frac{H}{V} \right]^n \tag{9-5d}$$

and

$$n = \left[\left(2 + \frac{L}{B} \right) / \left(1 + \frac{L}{B} \right) \right] \cos^2 \theta + \left[\left(2 + \frac{B}{L} \right) / \left(1 + \frac{B}{L} \right) \right] \sin^2 \theta \tag{9-6a}$$

where: $\theta = \tan^{-1}(e_B/e_L)$

The parameters e_B and e_L are the load eccentricity factors (offset distances) in the transverse and longitudinal directions, respectively.

Since there is no eccentricity, $\theta = 0$ and:



Written by: T.H.H. Date: 96 / 03 / 19 Reviewed by: E.K. and N.M. Date: 96 / 03 / 20
YY MM DD YY MM DD

Client: FHWA Project: GEC-3 Project/Proposal No.: GE3686 Task No.: F

$$n = \left[\left(2 + \frac{L}{B} \right) / \left(1 + \frac{L}{B} \right) \right]$$

$$= \left[\left(2 + \frac{25}{4.25} \right) / \left(1 + \frac{25}{4.25} \right) \right] = 1.145$$

$$i_\gamma = \left(1 - \frac{14,000}{37,625} \right)^{1.145} = 0.59$$

$q_{ult} = (0.5)(17.2)(4.25)(37.2)(0.93)(0.59) = 746 \text{ kPa}$ (ultimate bearing capacity for the maximum dynamic load inclination).

$$q_{max} = \frac{P}{A} = \frac{40,145}{4.25(25)} = 378 \text{ kPa}$$

The factor of safety is then given by:

$$FS = \frac{746}{378} = 1.97$$

- Sliding Resistance

The frictional capacity is given by: $F = V(\tan \phi) r$, where r is a reduction factor varying from 0.67 to 0.8 (see chapter 9.4.2.5 of volume I for further discussion) that is applied to the friction coefficient of the soil to obtain the footing-soil interface friction coefficient. For concrete on sand, $r = 0.8$, so:

$$F = (37,625)(0.8) (\tan (35)) = 21,076 \text{ kN}$$

The factor of safety is then given by:

$$FS = \frac{20,006}{14,000} = 1.43$$



Written by: T.H.H. Date: 96 / 03 / 19 Reviewed by: E.K. and N.M. Date: 96 / 03 / 20
YY MM DD YY MM DD

Client: FHWA Project: GEC-3 Project/Proposal No.: GE3686 Task No.: F

- Maximum vertical load

This maximum load occurs when the dynamic vertical load acts down and is combined with the static load:

$$V_{\max} = (P_V)^{\text{STAT}} + (P_V)^{\text{DYN}}$$

$$= 44,625 + 7,000 = 51,625 \text{ kN}$$

Since $H = (P_H)^{\text{DYN}} = 14,000 \text{ kN}$, the load is inclined at an angle α from the horizontal evaluated as:

$$\alpha = \tan^{-1} \frac{51,625}{14,000} = 74.8^\circ$$

The magnitude of the load is evaluated as:

$$P = \sqrt{H^2 + V^2} = \sqrt{14,000^2 + 51,625^2} = 53,490 \text{ kN}$$

Since the central pier footing is founded directly at the proposed grade elevation on a cohesionless soil, the bearing capacity equation 9-1 reduces to:

$$q_{\text{ult}} = 0.5\gamma B N_\gamma s_\gamma i_\gamma \tag{9-1}$$

For zero cohesion, i_γ is given by:

$$i_\gamma = \left[1 - \frac{H}{V} \right]^n \tag{9-5d}$$

and

$$n = \left[\left(2 + \frac{L}{B} \right) / \left(1 + \frac{L}{B} \right) \right] \cos^2 \theta + \left[\left(2 + \frac{B}{L} \right) / \left(1 + \frac{B}{L} \right) \right] \sin^2 \theta \tag{9-6a}$$



Written by: T.H.H. Date: 96 / 03 / 19 Reviewed by: E.K. and N.M. Date: 96 / 03 / 20
YY MM DD YY MM DD

Client: FHWA Project: GEC-3 Project/Proposal No.: GE3686 Task No.: F

where: $\theta = \tan^{-1}(e_B/e_L)$

Since there is no eccentricity, $\theta = 0$ and:

$$n = \left[\left(2 + \frac{L}{B} \right) / \left(1 + \frac{L}{B} \right) \right]$$

$$= \left[\left(2 + \frac{25}{4.25} \right) / \left(1 + \frac{25}{4.25} \right) \right] = 1.145$$

$$i_\gamma = \left(1 - \frac{14,000}{51,625} \right)^{1.145} = 0.70$$

$q_{ult} = (0.5)(17.2)(4.25)(37.2)(0.93)(0.70) = 885 \text{ kPa}$ (ultimate bearing capacity for the maximum vertical load).

$$q_{max} = \frac{P}{A} = \frac{53,490}{4.25(25)} = 503 \text{ kPa}$$

The factor of safety is then given by:

$$FS = \frac{885}{503} = 1.76$$

Note that sliding need not be checked for this case, as the factor of safety against sliding will exceed that calculated for the upwards vertical load (since i_γ is greater for this case than when the load acts upwards). Also, the abutment footing must be checked for bearing capacity and sliding resistance. As these evaluations are similar to those for the central pier footing, they are not presented in this example.



Written by: T.H.H. Date: 96 / 03 / 19 Reviewed by: E.K. and N.M. Date: 96 / 03 / 20
YY MM DD YY MM DD

Client: FHWA Project: GEC-3 Project/Proposal No.: GE3686 Task No.: F

Evaluate Liquefaction Potential

As discussed in chapter 8.2 of volume I, the first step in assessing liquefaction potential is evaluating whether or not a potential for liquefaction exists. Five screening criteria are listed in chapter 8.2 of volume I. Of relevance to this problem are the depth to groundwater and soil penetration resistance. Groundwater was not encountered in either boring. Therefore, it can be assumed that the water table is at least 24 m below ground surface (the maximum boring depth). Furthermore, for depths deeper than 20 m, the normalized and standardized blowcounts are in excess of 60 blows per 300 mm. Given the depth of the groundwater table and the high blow counts, liquefaction is not expected at the site.

Estimate Seismic Settlement

The step by step method outlined in chapter 8.5 of volume I provides a means of evaluating the seismic settlement potential. The calculations are performed by subdividing the top 20 m into two 10-m-thick layers. These calculations are presented in the table below. Note that it was assumed that the seismic strains in the layers at depths greater than 20 m will be negligible due to the high blow counts (normalized and standardized blow counts greater than 60).



Written by: T.H.H. Date: 96 / 03 / 19 Reviewed by: E.K. and N.M. Date: 96 / 03 / 20
 YY MM DD YY MM DD

Client: FHWA Project: GEC-3 Project/Proposal No.: GE3686 Task No.: F

Evaluation of seismic settlement.

Equation Reference	0 to 10 m	10 to 20 m
σ_v at mid-depth	$(5 \cdot 17.2) = 86 \text{ kPa}$	$(15)(17.2) = 258 \text{ kPa}$
$\sigma_m = 0.65\sigma_v$	$(0.65)(86) = 55.9 \text{ kPa}$	$(0.65)(258) = 167.7 \text{ kPa}$
$r_d = 1-0.015z$	0.925	0.775
G_{max} (see calculation below) ^(*)	93,950 kPa	162,700 kPa
$\gamma_{eff} (G_{eff}/G_{max}) =$ $= (0.65a_{max} \sigma_v r_d)/g \cdot G_{max}$ where $a_{max} = 0.55 \text{ g}$ (given)	$3 \cdot 10^{-4}$	$4.4 \cdot 10^{-4}$
$\gamma_{eff} =$ (figure 63 of volume I)	$1.0 \cdot 10^{-3}$	$1.2 \cdot 10^{-3}$
$\Delta_h = \gamma_{eff} \cdot H$	$(1.0 \cdot 10^{-3})(10) = 1.0 \cdot 10^{-2} \text{ m}$	$(1.2 \cdot 10^{-3})(10) = 1.2 \cdot 10^{-2} \text{ m}$

$$\Delta H_{TOTAL} = 1.0 \cdot 10^{-2} + 1.2 \cdot 10^{-2} = 2.4 \cdot 10^{-2} = 0.024 \text{ m} = 24 \text{ mm}$$

* G_{max} was obtained for both depths using Seed et al. (1984) method used in the evaluation of the stiffness coefficients in this example.

$$G_{max} = 220 (K_2)_{max} \sigma'_m{}^{1/2}$$

$$\sigma'_m = \frac{1+2K_0}{3} \sigma'_v$$

$$(K_2)_{max} = 20 (N)_{60}{}^{1/2}$$

with $(N)_{60} = 25$ [average blow count (for both depths)]

Depth 5m: $\sigma_v = 86 \text{ kPa} = \sigma'_v$

$$\sigma'_m = \frac{1+2(0.43)}{3} 86 = 53 \text{ kPa}$$

$$(K_2)_{max} = (20)(25)^{1/2} = 58.48$$

$$\Rightarrow G_{max} = (220)(58.48)(53)^{1/2} = 93,950 \text{ kPa}$$

Depth 15 m: $\sigma_v = 258 \text{ kPa} = \sigma'_v$

$$\sigma'_m = \frac{1+2(0.43)}{3} 258 = 160 \text{ kPa}$$

$$(K_2)_{max} = (20)(25)^{1/2} = 58.48$$

$$\Rightarrow G_{max} = (220)(58.48)(160)^{1/2} = 162,700 \text{ kPa}$$



1.7 SUMMARY AND CONCLUSIONS

Preliminary dimensions for the shallow foundations for a highway bridge were estimated based upon the static loads. The stiffness matrix and dynamic bearing capacity for the proposed bridge foundations were evaluated based upon these dimensions. The structural engineer used the stiffness matrix provided by the geotechnical engineer to evaluate the seismic response of the bridge structure. Using the foundation loads calculated by the structural engineer in the seismic response analysis, the geotechnical engineer checked the dynamic bearing capacity and sliding resistance of the foundations and found them to be acceptable.

Liquefaction was not of concern due to the absence of groundwater within 24 m of the ground surface and the high blow count values encountered at depths greater than 20 m. Seismic-induced settlement was calculated to be 24 mm. This value was deemed to be acceptable by the structural engineer.

EXAMPLE 2

SEISMIC DESIGN OF A DEEP FOUNDATION SYSTEM

2.1 INTRODUCTION

2.1.1 Description of the Project

Portions of a new highway will be built on a viaduct over an existing roadway and railroad tracks. To minimize disruption to existing traffic and because of the low bearing capacity of the top few meters of soil, a driven pile foundation will be employed for the viaduct. The viaduct will be composed of simply supported sections resting on pile-supported bents. Each bent will consist of three columns, each 1 m in diameter, transferring the load to a cast-in-place pile cap on top of the foundation piles.

To accommodate four lanes of traffic, the central barrier, shoulders, and side barriers, the viaduct is about 25 m wide. Figure 4 shows a cross section of the superstructure. The superstructure is composed of nine AASHTO standard precast type VI I-beams. The typical span is 43 m long resting on two bents as shown in figure 5. The bottom of the bent is about 5 m above the top of the pile cap.

The structural engineer has made a preliminary estimate of the loads transferred to the bottom of the columns in the design earthquake. The geotechnical engineer must evaluate the lateral load-deformation behavior and the ultimate uplift and compressive capacities of the proposed pile foundation for use in final design.

2.1.2 Source Materials Required

The source materials necessary to solve this problem include:

- geotechnical information on subsurface conditions;
- the configuration of the bridge and anticipated foundation loads;
- volume I of this document;
- National Highway Institute manual for design and construction of driven pile foundations (NHI, 1996); and
- COM624 computer program for analysis of laterally loaded piles (Reese et al., 1984; or Wang and Reese, 1991).

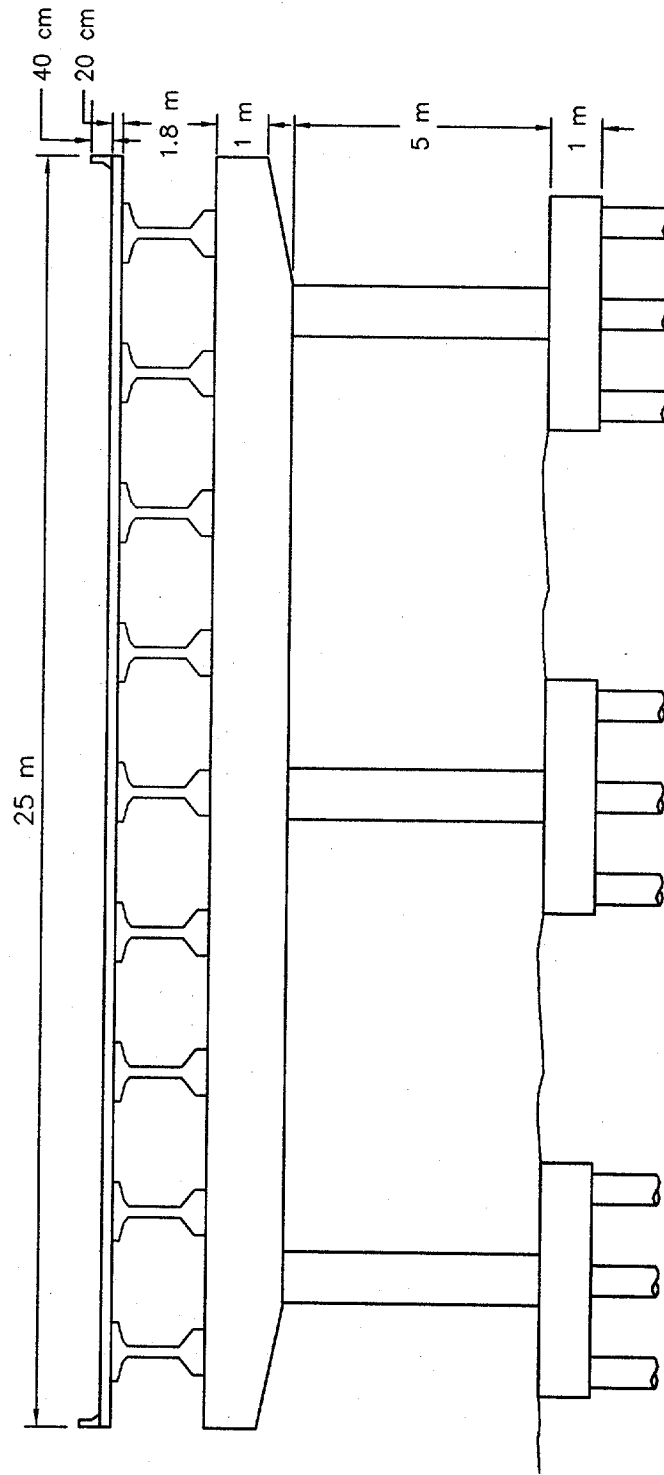


Figure 4. Cross section of superstructure.

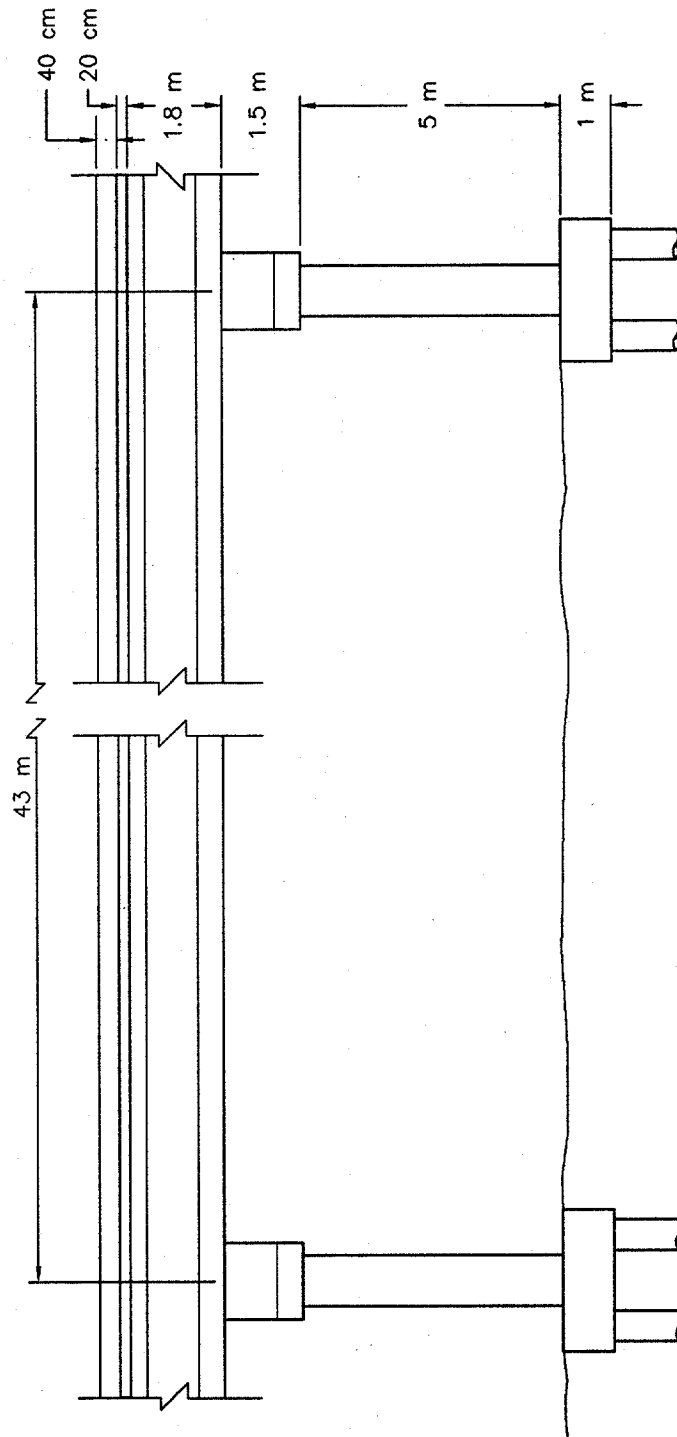


Figure 5. Typical span resting on two bents.

2.2 GEOTECHNICAL EXPLORATION

Three borings were drilled at the ends of the bridge. The borings were drilled to depths ranging from 23 to 25 m. Standard Penetration Tests (SPTs) were performed at 1.5-m intervals in the borings. The general stratigraphy at the site consists of sands and silty sands with a few lenses of low plasticity silts and clays. Figure 6 shows a typical boring log from the site. Groundwater was not encountered in any of the borings. Samples were recovered from the SPT split spoon for soil classification purposes. The distribution of normalized and standardized SPT blow count values with depth is shown on figure 7. The blow counts show that the material gets progressively denser with depth. The top 5 m are characterized by very variable normalized and standardized SPT values with an average value of about 10. From 5 to about 9 m below ground surface, the normalized and standardized SPT values are about 25 and then increase to about 50 from 9 to about 15 m below grade. At a depth of 16 m, the normalized and standardized SPT blow counts increase to about 70. The blow counts eventually reach refusal in a dense gravely sand layer 24 to 30 m below grade. The idealized normalized and standardized SPT profile used for design is shown on figure 7.

The isolated cohesive silt and clay seams and lenses encountered in the borings were of low plasticity and were not saturated. For the purposes of design analyses, the subsurface profile was simplified as a uniform layer of cohesionless soil that is progressively denser with depth. A total unit weight of 19 kN/m^3 was assigned to the soil and the friction angle was assumed to vary from 33 degrees at depths from 0 to 9 m to 38 degrees from 9 to 16 m. These friction angles were estimated using the normalized and standardized SPT blow counts and empirical correlations.

2.3 DESIGN OF PILE FOUNDATIONS

Preliminary values for the loads transferred from the superstructure to the top of the pile caps were provided by the structural engineer. The following preliminary loads were used for design analysis of the pile cap:

Static Load per Pile Cap

- Vertical Compressive Load (Q) = 3,110 kN

Dynamic Load per Pile Cap

- Horizontal Load Along Bridge, Longitudinal Axis (H_x) = 180 kN
- Horizontal Load Perpendicular to Bridge, Longitudinal Axis (H_y) = 602 kN
- Longitudinal Moment (M_x) = 903 kN·m
- Transverse Moment (M_y) = 3,010 kN·m

Based on the preliminary loads, octagonal 0.4-m-diameter driven concrete piles were selected for use in the foundation. Given the general stratigraphy of the site, it was decided to embed the pile in the denser sand layer that starts at 9 m depth. To provide sufficient end bearing capacity, the tip elevation was set at a depth of 12 m. Six 12-m-long piles, configured as shown in figure 8, were proposed for the cap under each column, resulting in a static vertical load of approximately 520

DEPTH BGS (m)	MATERIAL DESCRIPTION	SYMBOLIC LOG	EL. ABOVE MSL (m)	SAMPLES				
				NUMBER	SYMBOL	REC & RQD (%) OR REC (%)	SPT VALUES	
							BLOWS PER 150mm	N
5.0	Grey-brown, loose, fine to medium, sand		-30-	s-1			2-2-3	5
				s-2			3-5-4	9
				s-3			5-6-6	12
9.0	Dark brown, dense, silty sand with clay seams.		-20-	s-4			8-10-12	22
				s-5			12-14-12	26
				s-6			12-15-13	28
16.0	Dark brown, dense, sand.		-20-	s-7			8-22-23	45
				s-8			20-26-27	53
				s-9			26-26-29	55
17.0	Dark brown, silt		-20-	s-10			26-28-30	58
				s-11			32-35-35	70
				s-12			30-32-35	67
23.0	Very dense, silty sand.		-10-	s-13			30-34-36	70
				s-14			33-43-47	90
				s-15			42-46-55	101
	End of drilling at 23 m.			s-16			Refusal	

Figure 6. Typical Example 2 boring log.

Normalized and Standardized SPT N Values (Blows/300mm)

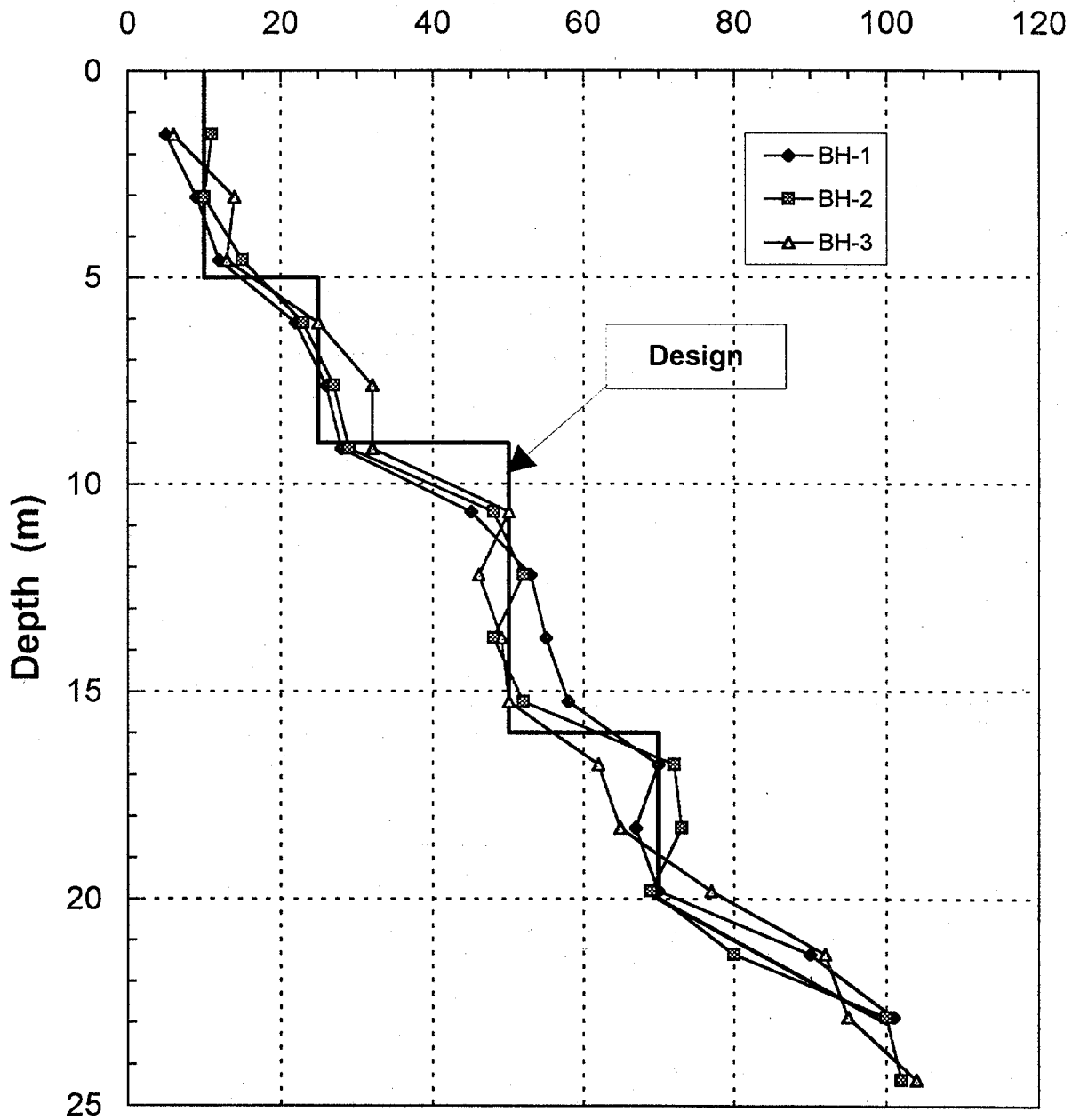
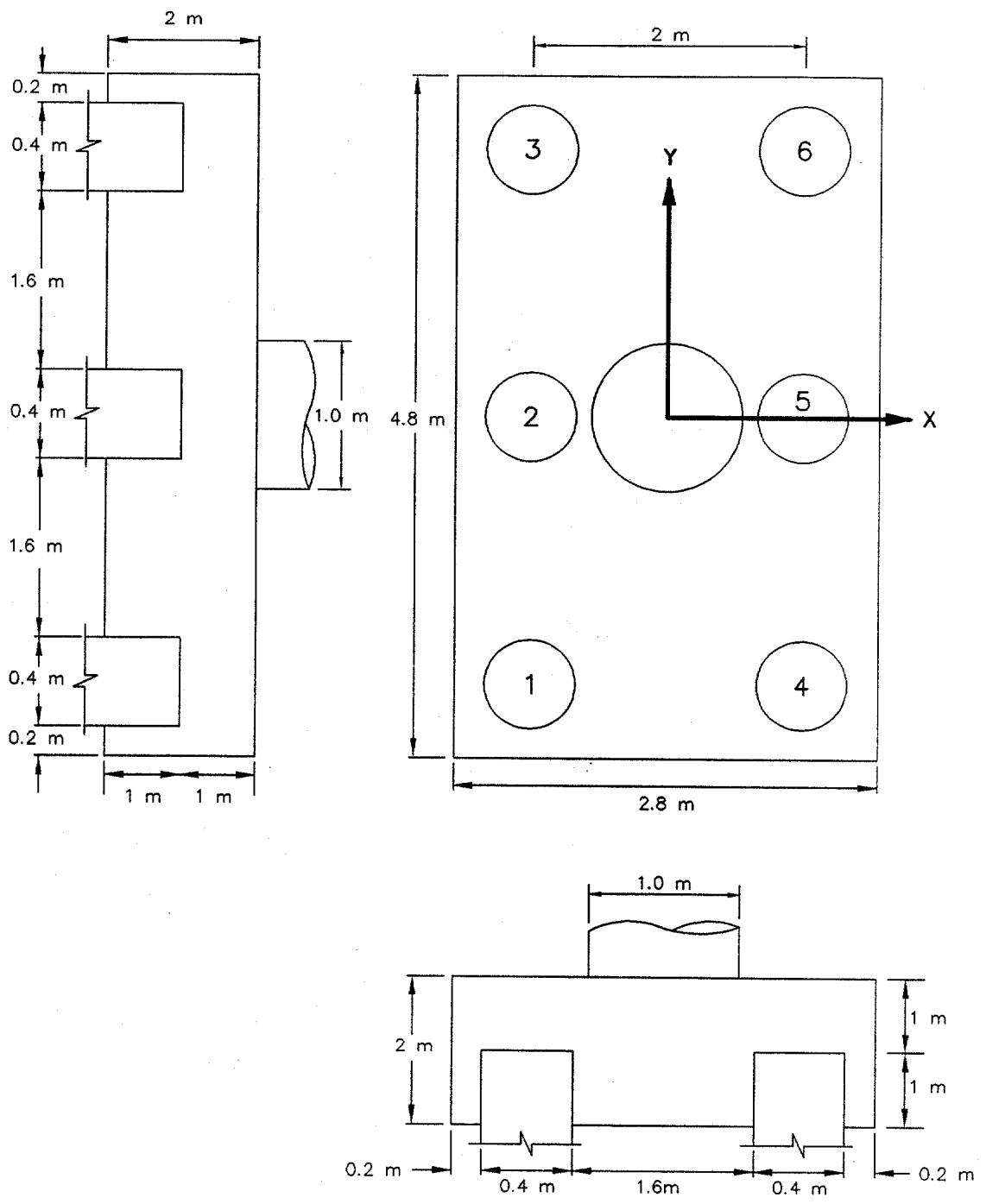


Figure 7. Corrected SPT results for Example 2 test borings.



NOT TO SCALE

Figure 8. Pile cap configuration.

kN/pile. To minimize group effects, the center-to-center spacing of piles in each cap was set at five pile diameters (i.e., 2.0 m). A pile cap embedment depth equal to 2.5 pile diameters (1 m) was used to fix the pile head with respect to the pile cap (no rotation of the pile head in the lateral load analysis). The ultimate static vertical compressive bearing capacity of a 12 m long, 0.4-m-diameter driven concrete pile at the site is on the order of 2,515 kN, resulting in a static factor of safety of almost 5. The calculations are provided in the attached calculation sheets.

In addition to the vertical compressive capacity of the piles, calculations were performed to evaluate vertical uplift capacity and lateral stiffness of the piles. The lateral capacity of the pile group was evaluated using the computer program COM624 (Reese et al., 1984). The p-y curves representing the lateral resistance of the soils were generated internally by the program based upon recommendations made by Reese et al. (1984) for cohesionless soils. Because the pile heads were fixed, the sand was medium dense to dense, and the piles were spaced at 5 pile diameters (center-to-center), group interaction behavior was ignored (the p-y curve for the trailing piles in the group was not modified). If the pile heads were free to rotate, "p-multipliers" of 0.85 and 0.75 would have been used to modify the p-y curves for the second and third row of piles, respectively, based upon the values presented in table 14 of volume I. The lateral load-deformation behavior of the cap would be calculated by assuming each pile deflected the same amount and summing up the lateral load carried by each pile to calculate the group load.

The loads provided by the structural engineer were resolved into individual pile loads, as shown in the attached calculations (see step 3) and summarized in table 5. Note that the vertical load on the pile analyzed for stiffness capacity was increased from the static load of 518 kN to 1,045 kN to account for the vertical load induced by moment loading (see calculations). Also listed in table 5 is the factor of safety against uplift or compression failure and the expected vertical and lateral deflection of the pile under the dynamic loads.

Table 5. Dynamic loading characteristics.

Type of Load	Maximum Load Per Pile (kN)	Factor of Safety (FS)	Deflection ⁽¹⁾ (mm)
Compression	1,045	FS = 2.4	6 ⁽²⁾
Uplift	9	FS > 1	N/A
Horizontal	100	N/A	5

- Notes: (1) Calculated deflections based on allowable capacities.
 (2) Reported value is incremental deflection under seismic load.

2.4 CALCULATIONS

The calculation sheets for example 2, "Seismic Design of a Deep Foundation System" follows.

Written by: T.A.W. Date: 96 / 08 / 01 Reviewed by: E.K. and N.M. Date: 96 / 08 / 02
YY MM DD YY MM DD

Client: FHWA Project: GEC-3 Project/Proposal No.: GE3686 Task No.: F

DETAILED CALCULATIONS
EXAMPLE 2 - SEISMIC DESIGN OF A DEEP FOUNDATION SYSTEM

Step 1: Design of Pile Group

- Piles are 12 m long
- Piles are octagonal 0.4 m diameter, driven concrete piles
- Piles are spaced 5 diameters apart (i.e., 2 m) center to center
- Piles are embedded 1 m (2.5 diameters) into the pile cap
- Each cap contains 6 piles
- Layout of piles is shown in figure 8

Step 2: Evaluate Static Bearing Capacity

Static bearing capacity is evaluated using the Nordlund Method as outlined in NHI (1996). The idealized normalized and standardized SPT profile and the pile profile are shown in figure 9. The ultimate bearing capacity, q_{ult} , is composed of a shaft resistance, R_S , tip resistance, R_T , such that $q_u = R_S + R_T$.

$$q_{ult} = \underbrace{\sum_{d=0}^{d=D} K_{\delta} C_F p_d \frac{\sin(\delta + \omega)}{\cos \omega} C_d \Delta d}_{R_S} + \underbrace{\alpha_t N'_q A_t p_t}_{R_T}$$

- where:
- d = depth;
 - D = embedded pile length;
 - K_{δ} = coefficient of lateral earth pressure at depth d;
 - C_F = correction factor of K_{δ} when $\delta \neq \phi$;
 - p_d = effective overburden pressure at the center of depth increment d;
 - δ = soil-pile friction angle;
 - ω = angle of pile taper;
 - C_d = pile perimeter at depth d;
 - Δd = length of pile segment;
 - α_t = dimensionless factor (dependent on pile depth-width relationship);



Written by: T.A.W. Date: 96 / 08 / 01 Reviewed by: E.K. and N.M. Date: 96 / 08 / 02
YY MM DD YY MM DD

Client: FHWA Project: GEC-3 Projct/Proposal No.: GE3686 Task No.: F

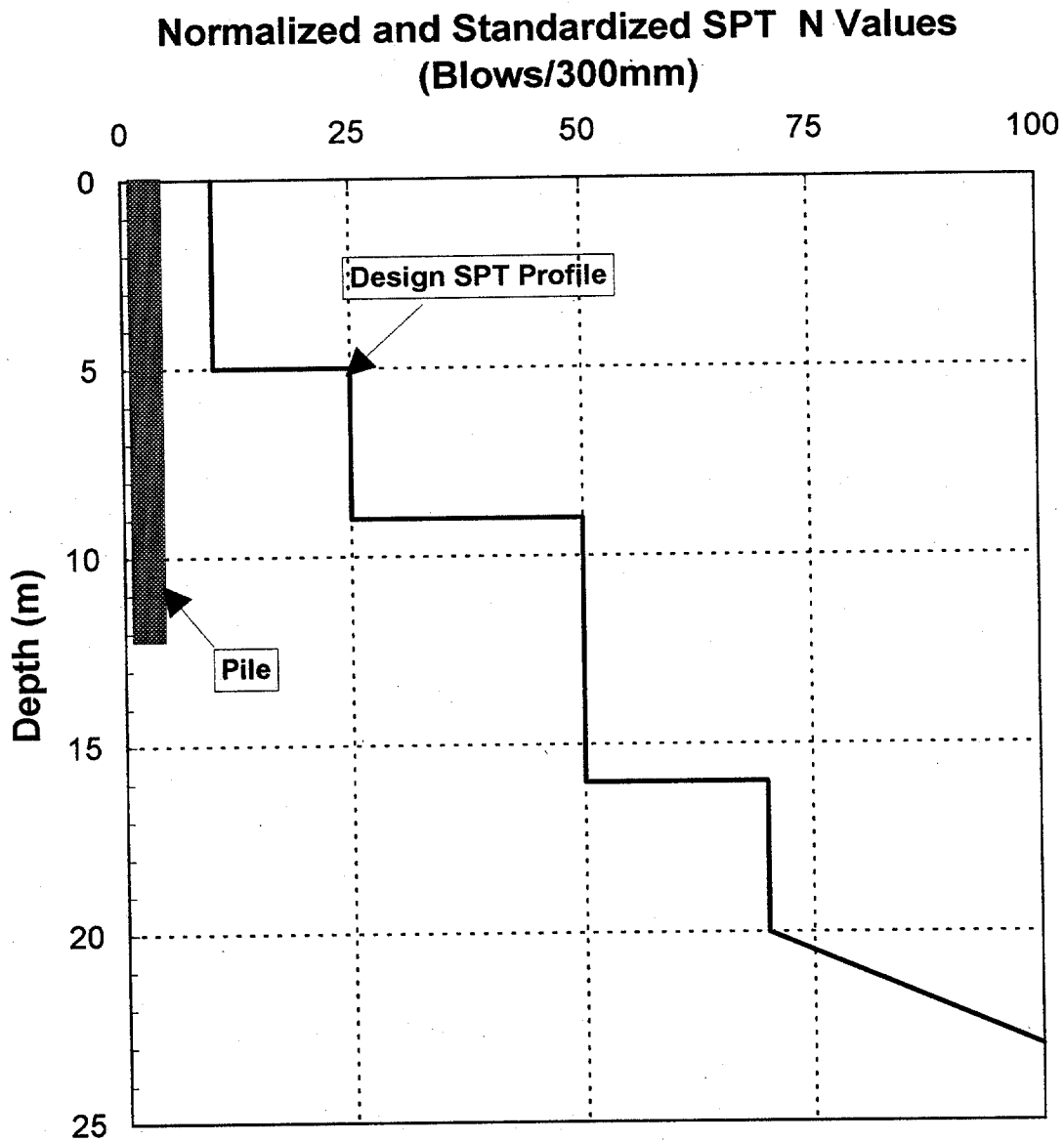


Figure 9. Pile and idealized SPT profile



Written by: T.A.W. Date: 96 / 08 / 01 Reviewed by: E.K. and N.M. Date: 96 / 08 / 02
YY MM DD YY MM DD

Client: FHWA Project: GEC-3 Project/Proposal No.: GE3686 Task No.: F

- N'_q = bearing capacity factor;
- A_t = pile tip area; and
- p_t = effective overburden pressure at the pile tip.

- Compute Tip Resistance, R_T

$$R_T = \alpha_T N'_q A_t p_t$$

$$\alpha_T = 0.7 \text{ for } \phi = 38^\circ \quad (\text{NHI, 1996})$$

$$N'_q = 100 \text{ for } \phi = 38^\circ \quad (\text{NHI, 1996})$$

$$A_t = \pi r^2 = \pi(0.4 \text{ m}/2)^2 = 0.126 \text{ m}^2$$

$$p_t = (12 \text{ m})(19 \text{ kN/m}^3) = 228 \text{ kPa}$$

The limiting value of p_t is 150 kPa (NHI, 1996), therefore, $p_t = 150 \text{ kPa}$ and $R_T = (0.7)(100)(0.126 \text{ m}^2)(150 \text{ kPa}) = 1,325 \text{ kN}$

However, R_T is limited to $R_T = q_L A_t$.
 $q_L = 12,000 \text{ kPa}$ for $\phi = 38^\circ$ (NHI, 1996)
 $R_T \text{ limiting} = (12,000 \text{ kPa})(0.126 \text{ m}^2) = 1,510 \text{ kN}$ (does not govern)

$\therefore R_T = 1,325 \text{ kN}$

- Compute Shaft Resistance, R_S

$$R_S = \sum_{d=1}^{d=D} K_\delta C_F P_d \frac{\sin(\delta + \omega)}{\cos \omega} C_d \Delta_d$$

For this calculation, the soil deposit has been divided into two layers as follows:

Stratigraphy and strength parameters for the two layers.

Layer	Depth Interval (m)	Friction Angle, ϕ (deg)
1	0-9	33
2	9-12	38

(see chapter 3.2 of this document for a discussion of the values of ϕ)



Written by: T.A.W. Date: 96 / 08 / 01 Reviewed by: E.K. and N.M. Date: 96 / 08 / 02
YY MM DD YY MM DD

Client: FHWA Project: GEC-3 Project/Proposal No.: GE3686 Task No.: F

Determine approximate circumference of pile, C_d .

$$C_d \approx 2\pi r = 2\pi(0.4\text{m}/2) = 1.26 \text{ m}$$

This is constant over the length of pile, i.e., the angle of the pile taper, ω , = 0.

Determine δ , the friction angle between pile and soil based on soil friction angle, ϕ . For a pre-cast concrete pile, $\delta/\phi = 0.72$ (NHI, 1996)

$$\delta_1 = (0.72)(33^\circ) = 24^\circ$$

$$\delta_2 = (0.72)(38^\circ) = 27^\circ$$

Determine K_δ for each material based upon displaced soil volume, V (NHI, 1996)

$$V_1 = V_2 = \frac{\pi r^2 \cdot 1 \text{ m}}{1 \text{ m}} = \frac{\pi \left(\frac{0.4}{2}\right)^2 \cdot 1 \text{ m}}{1 \text{ m}} = 0.126 \text{ m}^3 / \text{m}$$

for $\omega = 0$ (pile has no taper), using $V = 0.093 \text{ m}^3/\text{m}$ curve (approx.)

$$K_{\delta_1} = 1.15 + (0.6)(1.75-1.15) = 1.51$$

(interpolating between plots for $\phi = 30^\circ$ and $\phi = 35^\circ$)

$$K_{\delta_2} = 1.75 + (0.6)(3.00-1.75) = 2.5$$

(interpolating between plots for $\phi = 35^\circ$ and $\phi = 40^\circ$)

Determine correction factor, C_F , to be applied to K_δ if $\delta \neq \phi$ (NHI, 1996)

$$C_{F_1} = 0.85 \text{ for } \delta/\phi = 0.72 \text{ and } \phi = 33^\circ$$

$$C_{F_2} = 0.80 \text{ for } \delta/\phi = 0.72 \text{ and } \phi = 38^\circ$$

Determine effective overburden pressure at midpoint of each layer, P_d .

$$P_{d_1} = (19 \text{ kN/m}^3)(4.5 \text{ m}) = 85.5 \text{ kPa}$$

$$P_{d_2} = (19 \text{ kN/m}^3)(10.5 \text{ m}) = 199.5 \text{ kPa}$$



Written by: T.A.W. Date: 96 / 08 / 01 Reviewed by: E.K. and N.M. Date: 96 / 08 / 02
YY MM DD YY MM DD

Client: FHWA Project: GEC-3 Project/Proposal No.: GE3686 Task No.: F

Compute shaft resistance, R_s

$$R_s = R_{s_1} + R_{s_2}$$

$$R_s = (1.51)(0.85)(85.5 \text{ kPa})(\sin 24^\circ)(1.26 \text{ m})(9 \text{ m}) + (2.5)(0.80)(199.5 \text{ kPa})(\sin 27^\circ)(1.26 \text{ m})(3 \text{ m}) = 1,190 \text{ kN}$$

- Compute Static Bearing Capacity

$$q_{ult} = R_s + R_t$$

$$q_{ult} = 1,325 \text{ kN} + 1,190 \text{ kN} = 2,515 \text{ kN}$$

Step 3: Calculate Loads on Piles

- Compute vertical loads on piles from preliminary values provided by the structural engineer using the average vertical compressive load and the load induced by the moment distribution:

$$p = \frac{Q}{n} \pm \frac{M \cdot d_i}{\sum_{i=1}^n d_i^2}$$

where: p = vertical load on pile;
 Q = static vertical load on pile cap;
 n = number of piles in group (6 for this example);
 d_i = distance from center of gravity of pile group to pile i ; and
 M = design moment.

Transverse direction (y direction):

$$Q = 3,110 \text{ kN}$$

$$M_y = 3,010 \text{ kN} \cdot \text{m}$$

$$\sum_{i=1}^6 d_i^2 = 4 \cdot (2 \text{ m})^2 + 2 \cdot (0 \text{ m})^2 = 16 \text{ m}^2$$



Written by: T.A.W. Date: 96 / 08 / 01 Reviewed by: E.K. and N.M. Date: 96 / 08 / 02
YY MM DD YY MM DD

Client: FHWA Project: GEC-3 Project/Proposal No.: GE3686 Task No.: F

Piles on outer edge will experience the highest load. Calculated loads on each pile are listed on the following table:

Loads on individual piles (transverse direction).

Pile	Q/n (kN)	d (m)	$M_y d / \sum d^2$ (kN)
1	518	2	-376
2	518	0	0
3	518	2	376
4	518	2	-376
5	518	0	0
6	518	2	367

Note that the direction of action of M_y is arbitrary and piles 1 and 4 are symmetrical with respect to piles 3 and 6.

Longitudinal direction (x direction):

$$Q = 3,110 \text{ kN}$$

$$M_x = 903 \text{ kN} \cdot \text{m}$$

$$\sum_1^6 d_i^2 = 6 \cdot (1 \text{ m})^2 = 6 \text{ m}^2$$

Loads on individual piles (longitudinal direction).

Pile	Q/n (kN)	d (m)	$M_x d / \sum d^2$ (kN)
1	518	1	-151
2	518	1	-151
3	518	1	-151
4	518	1	151
5	518	1	151
6	518	1	151

Note that the direction of action of M_x is arbitrary and piles 1, 2, and 3 are symmetrical with respect to piles 4, 5, and 6.



Written by: T.A.W. Date: 96 / 08 / 01 Reviewed by: E.K. and N.M. Date: 96 / 08 / 02
YY MM DD YY MM DD

Client: FHWA Project: GEC-3 Project/Proposal No.: GE3686 Task No.: F

Calculate maximum and minimum pile loads by superimposing longitudinal and transverse moment loads.

Combined longitudinal and transverse moments on individual piles.

Pile	Q/n (kN)	$M_y/d/\Sigma d^2$ (Transverse Direction) (kN)	$M_x/d/\Sigma d^2$ (Longitudinal Direction) (kN)	P (kN)
1	518	-376	-151	-9
2	518	0	-151	367
3	518	376	-151	743
4	518	-376	151	293
5	518	0	151	669
6	518	376	151	1,045

Step 4: Verify Factors of Safety

- Compression Loads

Maximum static load on any pile = 518 kN
 Maximum vertical load on any pile = 1,045 kN
 Ultimate compression capacity of each pile = 2,515 kN

$$FS_{\text{STATIC}} = \frac{2,515 \text{ kN}}{518 \text{ kN}} = 4.9$$

$$FS_{\text{SEISMIC}} = \frac{2,515 \text{ kN}}{1,045 \text{ kN}} = 2.4$$

These factors of safety are considered acceptable.

- Uplift Forces

The maximum uplift force on any pile is 9 kN. This force is significantly less than the ultimate capacity of the pile, so uplift capacity is adequate.



Written by: T.A.W. Date: 96 / 08 / 01 Reviewed by: E.K. and N.M. Date: 96 / 08 / 02
YY MM DD YY MM DD

Client: FHWA Project: GEC-3 Project/Proposal No.: GE3686 Task No.: F

Step 5: Evaluate pile deflections

- Lateral deflection of the pile group

The effect of lateral forces on the piles was estimated using the program COM624 (Wang and Reese, 1991) in accordance with NHI, 1996 recommendations. Because pile spacing was 5D and the sand was dense, group interaction effects were ignored. Deformation of the pile is estimated to be 5 mm. COM624 input and output files are attached following these computation sheets.

Note: Maximum moment in pile from COM624 output (2.95 x 10⁶ in. · lbs (333 m · kN)) must be compared to pile capacity for structural adequacy.

- Vertical deflection of foundation pile.

Maximum vertical seismic deflection is calculated assuming that all load is carried at the pile tip. This is a conservative assumption. More detailed computations can be made using the t - z curve method (see chapter 9, volume I)

The vertical deflection of the foundation pile is calculated as the sum of the elastic deformation of the pile and the settlement of the soil at the pile tip. That is,
 $\delta_T = \delta_{PILE} + \delta_{SOIL AT TIP}$.

$$\delta_{PILE} = \frac{P_f \cdot L}{A \cdot E} = \frac{(527 \text{ kN})(12 \text{ m})}{(0.126 \text{ m}^2)(30,000,000 \text{ kPa})} \approx 2 \text{ mm} \approx 0.002 \text{ m}$$

- where:
- E = Young's modulus (30,000,000 kPa for concrete);
 - A = cross sectional area of pile;
 - P_f = the maximum vertical load imposed by the earthquake including the effect of the moments = 376 kN + 151 kN = 527 kN; and
 - L = Length of pile.



Written by: T.A.W. Date: 96 / 08 / 01 Reviewed by: E.K. and N.M. Date: 96 / 08 / 02
YY MM DD YY MM DD

Client: FHWA Project: GEC-3 Project/Proposal No.: GE3686 Task No.: F

$$\delta_{\text{SOIL AT TIP}} = \frac{0.96 P_f \sqrt{B} I_f}{(N_1)_{60}} \quad (\text{NHI, 1996})$$

$$\delta_{\text{SOIL AT TIP}} = \frac{0.96 \cdot 299 \cdot \sqrt{2.4} \cdot 0.5}{50} = 4.4 \text{ mm} = 0.004 \text{ m}$$

where: $\delta_{\text{SOIL AT TIP}}$ = estimated total settlement (mm) of soil;
 $N' \approx (N_1)_{60}$ = average normalized and standardized SPT N value
 within a depth B below pile tip level;
 P_f = foundation pressure due to seismic load (kPa);
 I_f = influence factor for group embedment = $1 - [D / 8B] \geq 0.5$;
 D = pile embedment depth (m);
 B = width of pile group (m);
 $P_f = \frac{(527 \text{ kN / pile})(6 \text{ piles})}{(4.4 \text{ m})(2.4 \text{ m})} = 299 \text{ kPa}$
 $I_f = 1 - [D / 8B] = 1 - [12 \text{ m} / 8 (2.4 \text{ m})] = 0.0375 \therefore I_f = 0.5$

The vertical deflection of the pile is:

$$\delta_T = \delta_{\text{PILE}} + \delta_{\text{SOIL AT TIP}} \approx 2 \text{ mm} + 4 \text{ mm} \approx 6 \text{ mm} \approx 0.006 \text{ m}$$



Written by: T.A.W. Date: 96 / 08 / 01 Reviewed by: E.K. and N.M. Date: 96 / 08 / 02
 YY MM DD YY MM DD

Client: FHWA Project: GEC-3 Project/Proposal No.: GE3686 Task No.: F

**Input Data
COM624 Sample Printout**

***** UNIT DATA. *****

SYSTEM OF UNITS
(UP TO 16 CHAR.)
ENGL

***** PILE DATA. *****

NO. INCREMENTS PILE IS DIVIDED	NO. SEGMENTS WITH DIFFERENT CHARACTERISTICS	LENGTH OF PILE	MODULUS OF ELASTICITY	DEPTH
48	1	.472E+03	.300E+08	.000E+00

TOP OF SEGMENT	DIAMETER OF PILE	MOMENT OF INERTIA	CROSS-SECT. AREA
.000E+00	.160E+02	.302E+04	.195E+03

***** SOIL DATA. *****

NUMBER OF LAYERS
2

LAYER NUMBER	P-Y CURVE CONTROL CODE	TOP OF LAYER	BOTTOM OF LAYER	INITIALSOIL MODULI CONST.	FACTOR 'A'	FACTOR 'F'
1	5	.000E+00	.354E+03	.225E+03	.000E+00	.000E+00
2	5	.354E+03	.472E+03	.225E+03	.000E+00	.000E+00

***** UNIT WEIGHT DATA. *****

NO. POINTS FOR PLOT
OF EFF. UNIT WEIGHT
VS. DEPTH
2

DEPTH BELOW TOP TO POINT	EFFECTIVE UNIT WEIGHT
.000E+00	.700E-01
.600E+03	.700E-01

***** PROFILE DATA. *****

NO. POINTS FOR
STRENGTH PARAMETERS
VS. DEPTH
3

DEPTH BELOW TOP OF PILE	UNDRAINED SHEAR STRENGTH OF SOIL	ANGEL OF INTERNAL FRICTION IN RADIANS	STRAIN AT 50% STRESS LEVEL
.000E+00	.000E+00	.576E+00	.200E-01
.354E+03	.000E+00	.663E+00	.200E-01
.500E+03	.000E+00	.663E+00	.200E-01

***** P-Y DATA. *****



Written by: T.A.W. Date: 96 / 08 / 01 Reviewed by: E.K. and N.M. Date: 96 / 08 / 02
YY MM DD YY MM DD

Client: FHWA Project: GEC-3 Projct/Proposal No.: GE3686 Task No.: F

NO. OF
P-Y CURVES
4

NO. POINTS ON
P-Y CURVES
9

X-COORD. TO
INPUT P-Y CURVE
.590E+02

DEFLECTION	SOIL RESISTANCE
.000E+00	.000E+00
.200E-01	.890E+02
.700E-01	.171E+03
.110E+00	.199E+03
.160E+00	.220E+03
.200E+00	.237E+03
.240E+00	.252E+03
.600E+00	.355E+03
.160E+02	.355E+03

X-COORD. TO
INPUT P-Y CURVE
.177E+03

DEFLECTION	SOIL RESISTANCE
.000E+00	.000E+00
.200E-01	.444E+03
.700E-01	.133E+04
.110E+00	.196E+04
.160E+00	.238E+04
.200E+00	.269E+04
.240E+00	.296E+04
.600E+00	.494E+04
.160E+02	.494E+04

X-COORD. TO
INPUT P-Y CURVE
.295E+03

DEFLECTION	SOIL RESISTANCE
.000E+00	.000E+00
.200E-01	.800E+03
.700E-01	.240E+04
.110E+00	.337E+04
.160E+00	.396E+04
.200E+00	.447E+04
.240E+00	.492E+04
.600E+00	.821E+04
.160E+02	.821E+04

X-COORD. TO
INPUT P-Y CURVE
.413E+03



Written by: T.A.W. Date: 96 / 08 / 01 Reviewed by: E.K. and N.M. Date: 96 / 08 / 02
YY MM DD YY MM DD

Client: FHWA Project: GEC-3 Projct/Proposal No.: GE3686 Task No.: F

DEFLECTION	SOIL RESISTANCE
.000E+00	.000E+00
.200E-01	.107E+04
.700E-01	.320E+04
.110E+00	.449E+04
.160E+00	.528E+04
.200E+00	.596E+04
.240E+00	.656E+04
.600E+00	.109E+05
.160E+02	.109E+05



Written by: T.A.W. Date: 96 / 08 / 01 Reviewed by: E.K. and N.M. Date: 96 / 08 / 02
YY MM DD YY MM DD

Client: FHWA Project: GEC-3 Project/Proposal No.: GE3686 Task No.: F

**Output Data
COM624 Sample Printout**

DATA	OUTPUT	P-Y	NO. DEPTHS TO
OUTPUT	INCREMENT	PRINTOUT	PRINT FOR
CODE	CODE	CODE	P-Y CURVES
1	2	1	7

DEPTH FOR
PRINTING
P-Y CURVES
.500E+02
.100E+03
.150E+03
.200E+03
.250E+03
.300E+03
.350E+03

***** PILE HEAD (BOUNDARY) DATA. *****

BOUNDARY	NO. OF SETS
CONDITION	OF BOUNDARY
CODE	CONDITIONS
2	2

PILE HEAD	LATERAL LOAD AT	VALUE OF SECOND	AXIAL LOAD
PRINTOUT CODE	TOP OF PILE	BOUNDARY CONDITION	ON PILE
0	.220E+05	.000E+00	.226E+05
1	.220E+05	.000E+00	.000E+00

***** CYCLIC DATA. *****

CYCLIC(0)	NO. CYCLES
OR STATIC(1)	OF LOADING
LOADING	
0	.000E+00

***** PROGRAM CONTROL DATA. *****

MAX. NO. OF	TOLERANCE ON	PILE HEAD DEFLECTION
ITERATIONS	SOLUTION	FLAG (STOPS RUN)
	CONVERGENCE	
200	.100E-02	.140E+02

COM624G INPUT DATA
OUTPUT DATA

GENERATED P-Y CURVES

THE NUMBER OF CURVES	= 7
THE NUMBER OF POINTS ON EACH CURVE	= 17

***** WARNING *****
P-Y CURVES CANNOT BE GENERATED IN LAYERS WHERE



Written by: T.A.W. Date: 96 / 08 / 01 Reviewed by: E.K. and N.M. Date: 96 / 08 / 02
 YY MM DD YY MM DD

Client: FHWA Project: GEC-3 Projct/Proposal No.: GE3686 Task No.: F

P-Y CURVES ARE INPUT
 1 1 CASE

UNITS--ENGL

OUTPUT INFORMATION

NO. OF ITERATIONS = 5
 MAXIMUM DEFLECTION ERROR = .991E-03 IN
 MAXIMUM MOMENT IMBALANCE FOR ANY ELEMENT = -.828E-01 IN-LBS
 MAX. LAT. FORCE IMBALANCE FOR ANY ELEMENT = .570E-02 LBS
 COMPUTED LATERAL FORCE AT PILE HEAD = .22000E+05 LBS
 COMPUTED SLOPE AT PILE HEAD = .14113E-17 IN/IN
 THE OVERALL MOMENT IMBALANCE = -.662E-01 IN-LBS
 THE OVERALL LATERAL FORCE IMBALANCE = -.578E-08 LBS
 PILE HEAD DEFLECTION = .171E+00 IN
 MAXIMUM BENDING MOMENT = -.295E+07 IN-LBS
 MAXIMUM TOTAL STRESS = .794E+04 LBS/IN**2
 MAXIMUM SHEAR FORCE = .426E+05 LBS

NO. OF ITERATIONS = 1
 MAXIMUM DEFLECTION ERROR = .181E-03 IN

PILE LOADING CONDITION

LATERAL LOAD AT PILE HEAD = .220E+05 LBS
 SLOPE AT PILE HEAD = .000E+00 IN/IN
 AXIAL LOAD AT PILE HEAD = .000E+00 LBS

X	DEFLEC	MOMENT	TOTAL STRESS	DISTR. LOAD	SOIL MODULUS	FLEXURAL RIGIDITY
IN	IN	LBS-IN	LBS/IN**2	LBS/IN	LBS/IN**2	LBS-IN**2
*****	*****	*****	*****	*****	*****	*****
.00	.171E+00	-.295E+07	.781E+04	.000E+00	-.526E+04	.906E+11
19.67	.165E+00	-.236E+07	.626E+04	.000E+00	-.311E+04	.906E+11
39.33	.149E+00	-.158E+07	.418E+04	.000E+00	-.875E+03	.906E+11
59.00	.126E+00	-.739E+06	.196E+04	.000E+00	.164E+04	.906E+11
78.67	.999E-01	.198E+05	.523E+02	.000E+00	.462E+04	.906E+11
98.33	.740E-01	.603E+06	.160E+04	.000E+00	.788E+04	.906E+11
118.00	.507E-01	.966E+06	.256E+04	.000E+00	.112E+05	.906E+11
137.67	.313E-01	.111E+07	.294E+04	.000E+00	.149E+05	.906E+11
157.33	.167E-01	.108E+07	.285E+04	.000E+00	.192E+05	.906E+11
177.00	.663E-02	.918E+06	.243E+04	.000E+00	.222E+05	.906E+11
196.67	.464E-03	.702E+06	.186E+04	.000E+00	.252E+05	.906E+11
216.33	-.271E-02	.480E+06	.127E+04	.000E+00	.281E+05	.906E+11
236.00	-.382E-02	.286E+06	.758E+03	.000E+00	.311E+05	.906E+11
255.67	-.371E-02	.138E+06	.365E+03	.000E+00	.341E+05	.906E+11
275.33	-.299E-02	.377E+05	.999E+02	.000E+00	.370E+05	.906E+11
295.00	-.210E-02	-.198E+05	.526E+02	.000E+00	.400E+05	.906E+11
314.67	-.128E-02	-.451E+05	.119E+03	.000E+00	.422E+05	.906E+11
334.33	-.653E-03	-.493E+05	.130E+03	.000E+00	.444E+05	.906E+11
354.00	-.231E-03	-.421E+05	.111E+03	.000E+00	.467E+05	.906E+11
373.67	.114E-04	-.305E+05	.809E+02	.000E+00	.489E+05	.906E+11
393.33	.124E-03	-.191E+05	.505E+02	.000E+00	.511E+05	.906E+11
413.00	.154E-03	-.998E+04	.264E+02	.000E+00	.533E+05	.906E+11
432.67	.141E-03	-.398E+04	.105E+02	.000E+00	.533E+05	.906E+11



Written by: T.A.W. Date: 96 / 08 / 01 Reviewed by: E.K. and N.M. Date: 96 / 08 / 02
YY MM DD YY MM DD

Client: FHWA Project: GEC-3 Project/Proposal No.: GE3686 Task No.: F

452.33 .110E-03 -.860E+03 .228E+01 .000E+00 .533E+05 .906E+11
 472.00 .746E-04 .000E+00 .000E+00 .000E+00 .533E+05 .906E+11

OUTPUT VERIFICATION

THE MAXIMUM MOMENT IMBALANCE FOR ANY ELEMENT = -.632E-01 IN-LBS
 THE MAX. LATERAL FORCE IMBALANCE FOR ANY ELEMENT = .485E-02 LBS
 COMPUTED LATERAL FORCE AT PILE HEAD = .22000E+05 LBS
 COMPUTED SLOPE AT PILE HEAD = .00000E+00 IN/IN
 THE OVERALL MOMENT IMBALANCE = .317E-01 IN-LBS
 THE OVERALL LATERAL FORCE IMBALANCE = -.560E-08 LBS

OUTPUT SUMMARY

PILE HEAD DEFLECTION = .171E+00 IN
 MAXIMUM BENDING MOMENT = -.295E+07 IN-LBS
 MAXIMUM TOTAL STRESS = .781E+04 LBS/IN**2
 MAXIMUM SHEAR FORCE = .426E+05 LBS

1 1 CASE

S U M M A R Y T A B L E

LATERAL LOAD (LBS)	BOUNDARY CONDITION BC2	AXIAL LOAD (LBS)	YT (IN)	ST (IN/IN)	MAX. MOMENT (IN-LBS)	MAX. STRESS (LBS/IN**2)
.220E+05	.000E+00	.226E+05	.171E+00	.141E-17	-.295E+07	.794E+04
.220E+05	.000E+00	.000E+00	.171E+00	.000E+00	-.295E+07	.781E+04

End COM624 Sample Output



2.5 SUMMARY AND CONCLUSIONS

A new highway will be built on a viaduct over an existing roadway and railroad tracks. Due to the relatively low bearing capacity of the near-surface soils and because it was necessary to minimize disruption to traffic, a pile foundation was selected. Precast concrete piles, 0.4 m in diameter driven in groups of six were used to support each column. The vertical and lateral static and pseudo-static loads were provided by the structural engineers.

The geotechnical investigation indicated that the top 5 m consisted of very loose fine sand underlain by about 4 m of silty sand with clay lenses. The bearing layer was identified to be a dense sand layer starting at depths of 10 m.

The static bearing capacity of each pile in the group was estimated based on methods presented in NHI (1996) to be 2,515 kN. The static factor of safety for the piles was 4.9.

The maximum pseudo-static load on any pile was calculated to be 1,045 kN, resulting in a seismic factor of safety of 2.4 for compressive loading. The maximum pseudo-static uplift force on any pile was estimated to be 9 kN, resulting in an adequate seismic factor of safety for uplift loading.

The lateral deflection due to seismic loading was estimated using the computer program COM624. The seismically-induced lateral deflection was estimated to be 5 mm. The upper bound vertical deformation was evaluated using NHI methods and assuming that all vertical loads were carried by the pile tip. The vertical incremental deflection due to seismic loading was estimated to be 6 mm.

EXAMPLE 3

SEISMIC DESIGN OF A RETAINING WALL

3.1 INTRODUCTION

3.1.1 Description of the Project

A retaining wall will be built as part of an underpass along the layout of a highway project in the south central United States. The wall will vary in height from 0.5 m to 6 m along the underpass alignment. To complete the seismic design of the wall, the following tasks need to be performed:

- evaluate seismicity information and select appropriate design earthquake events;
- perform a site specific seismic response analysis for the design earthquake; and
- perform pseudo-static stability analyses of the retaining wall.

The site is located in southwestern Shelby County, about 37 km south of Memphis, Tennessee.

3.1.2 Source Materials Required

The source materials required to solve this problem include:

- volume I of this document;
- subsurface profile information;
- Standard Specifications for Highway Bridges (AASHTO, 1992);
- Probabilistic Earthquake Acceleration and Velocity Maps for the United States and Puerto Rico (Algermissen et al., 1991);
- A Probabilistic Estimate of Maximum Acceleration in Rock in the Contiguous United States (Algermissen et al., 1976); and
- the computer program SHAKE for seismic site response analysis (Schnabel et al., 1972; and Idriss and Sun, 1992).

3.2 GEOLOGIC AND SEISMIC SETTING

The site is situated in the Gulf Coastal Plain section of the Coastal Plain Physiographic Province, as shown in figure 10. The region is referred to as the Mississippi Embayment. The topography of the area is characterized as gentle to steep, with occasional discontinuities created by the flat-lying alluvial plains of the streams in the area. These topographic features have formed as a result of the glacial erosion of the uppermost Tertiary and Quaternary formations and by subsequent deposition of a thick covering of loess deposits during late stages of the Pleistocene glaciation.

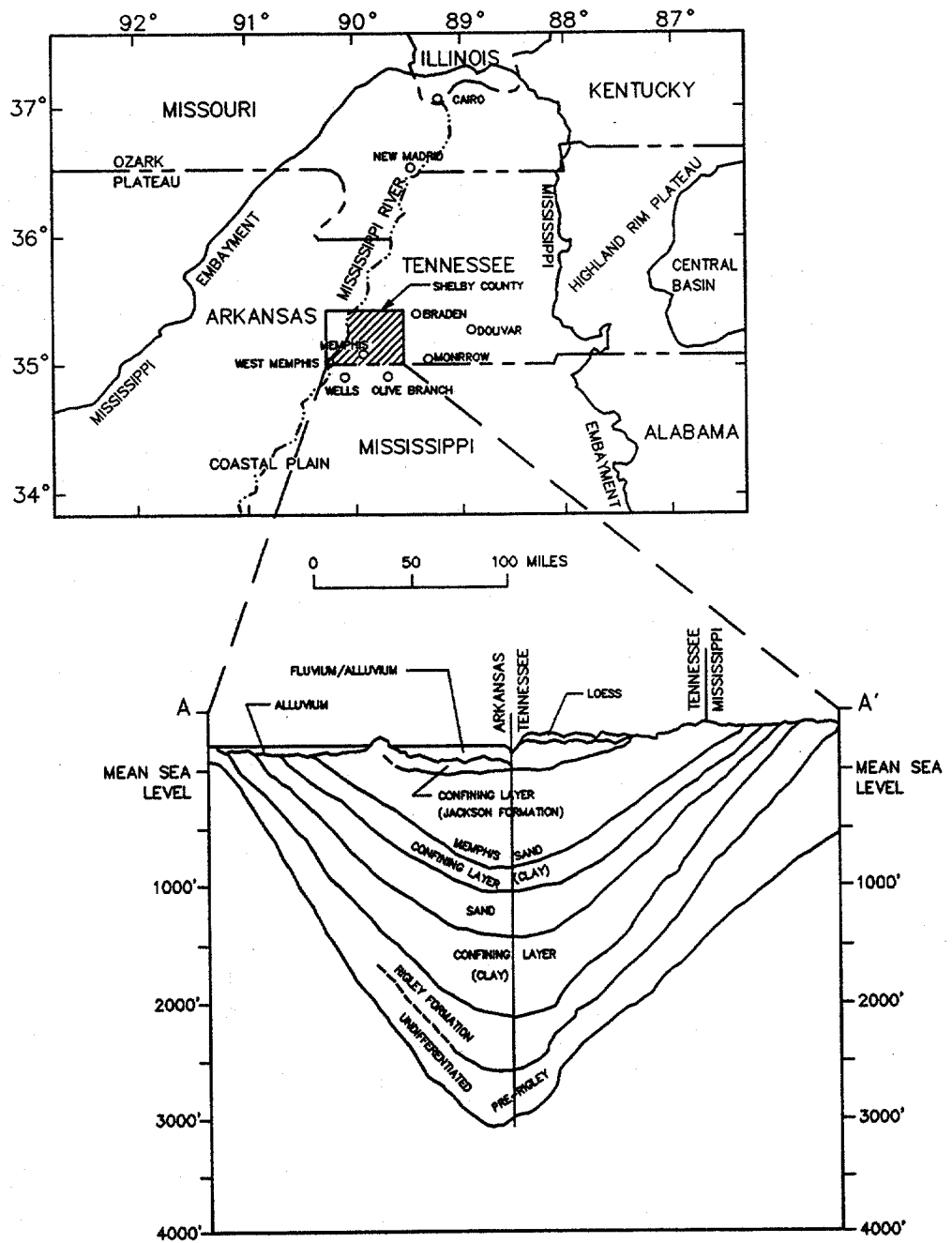
Approximately 915 to 1,200 m of Quaternary, Tertiary, and Cretaceous age sediments were deposited within the Mississippi embayment in the Memphis area. The surface and subsurface geologic units of this area consist predominantly of unconsolidated silt, sand, clay, gravel, and lignite deposits.

The project site is located within the New Madrid Seismic Zone (NMSZ), the source of three major earthquakes and several thousand aftershocks between 1811 and 1814. The NMSZ is defined primarily on the basis of micro-seismicity. It can be traced across the Mississippi river flood plain in the vicinity of New Madrid, Missouri. It strikes about 175 km in the northeasterly direction through the Mississippi embayment, from near Memphis, Tennessee in the south, to Cairo, Illinois in the north. The location of the site with respect to the NMSZ is shown in figure 11, the seismic source zonation map for the central United States from Johnston and Nava (1994) (figure 18 in volume I).

3.3 GEOTECHNICAL INVESTIGATION

The site is underlain by the Memphis sand formation, which consists mainly of coarse sand with lenses or beds of clay and silt at various horizons.

Subsurface information at the site was obtained through a series of cone penetration tests (CPTs) and borings drilled using rotary wash borings with drilling mud to depths of up to 60 m. Standard penetration tests (SPTs) were performed at intervals of 1.5 m in the borings. SPT split-spoon samples recovered from the borings were visually classified, and index property tests were performed on several samples. The normalized and standardized SPT N value (blow count) distribution with depth is provided in the attached calculation sheets.



MODIFIED AFTER BRAHANA, PARKS AND GAYDOS, (1987)

Figure 10. Mississippi Embayment boundaries and cross section through embayment.

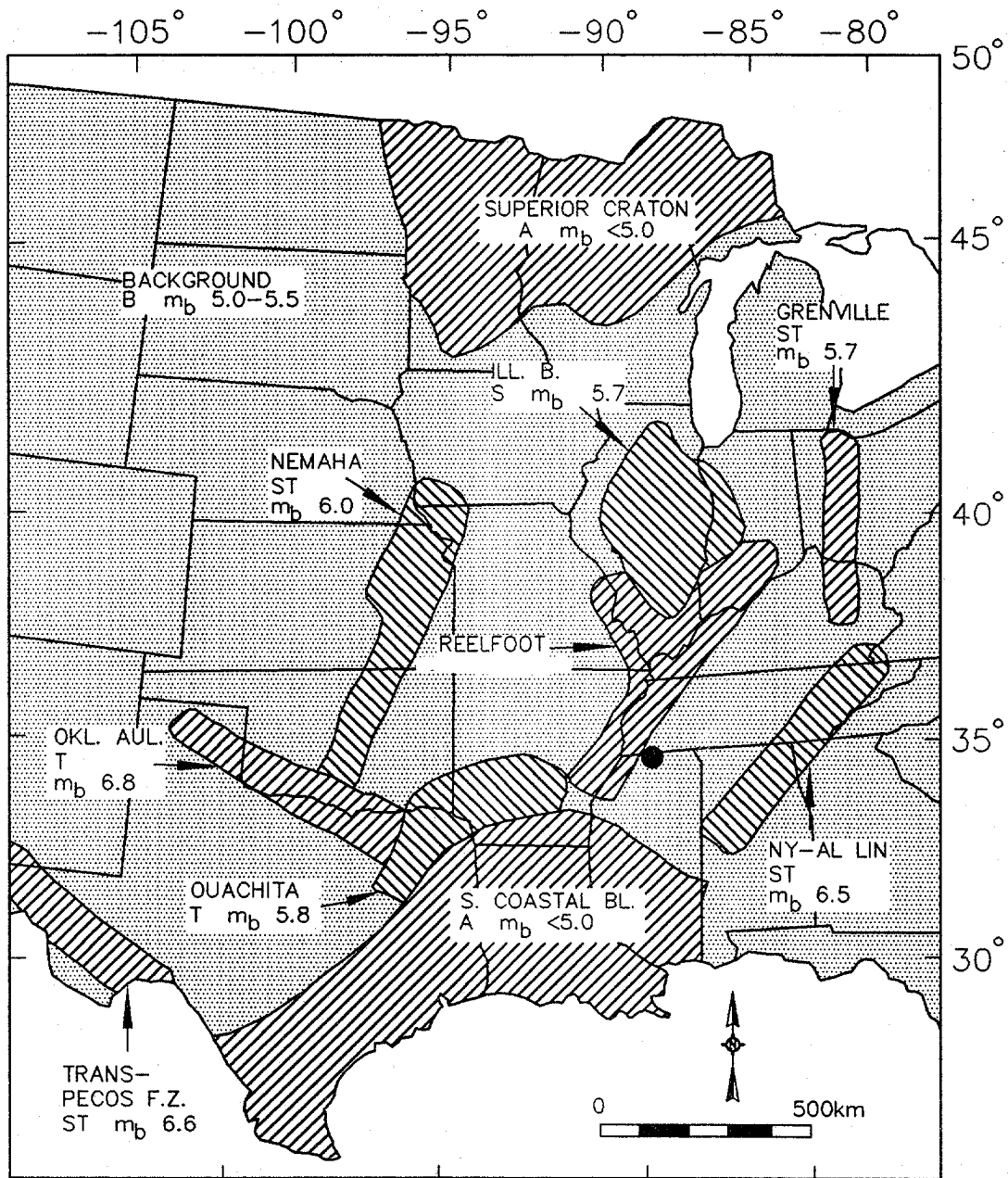


Figure 11. Seismic source zones - south central United States (Johnston and Nava, 1994, reprinted by permission of ATC).

3.4 SEISMIC HAZARD ANALYSIS

3.4.1 Introduction

A simplified probabilistic seismic hazard analysis based upon United States Geological Survey (USGS) maps, as described in chapter 3 of volume I of this document, was performed for the site, using the following three steps:

- interpolation from published maps of the peak ground acceleration in a hypothetical bedrock outcrop at the site for use in design;
- assessment of the magnitude associated with the design peak ground acceleration; and
- selection of representative time histories to model the design event.

3.4.2 Peak Horizontal Ground Acceleration

The peak horizontal ground acceleration for the site for use in design was selected from the latest USGS seismic hazard maps, USGS Map Sheet MF-2120 (Algermissen et al., 1991). These maps show the peak ground acceleration in rock in the contiguous United States, Alaska, Hawaii, and Puerto Rico with a 90 percent probability of not being exceeded in the time periods of 50 and 250 years (return periods of 474 and 2,372 years). In developing these maps, rock was defined as a material with a shear wave velocity (V_s) of between 750 and 900 m/s.

As recommended by AASHTO (1992), the peak ground acceleration was represented by a peak ground acceleration having a 10 percent probability of exceedance in 50 years. The portion of USGS Map Sheet MF-2120, presenting the peak ground acceleration with a 90 percent probability of not being exceeded in a 50-year exposure period, is reproduced in figure 12. By interpolation, the peak ground acceleration for the site was established from figure 12 as approximately 0.16 g.

To further substantiate the peak ground acceleration selected for design, other sources of information were examined. In a recent study by the Center for Earthquake Research and Information at Memphis State University reported in Poe (1992), the seismic hazard curves presented in figure 13 were developed for soil sites in three different parts of Shelby County, Tennessee. The curve for the south portion of the county yields a peak ground acceleration of 0.14 g for the same annual probability of exceedance (1/return period) as the above quoted Algermissen maps. This result is in agreement with the peak ground acceleration of 0.16 g estimated for the site based upon the Algermissen map. Therefore, it may be concluded that a peak ground acceleration of 0.16 g is a reasonable value to use for the design acceleration in a bedrock outcrop at the site.

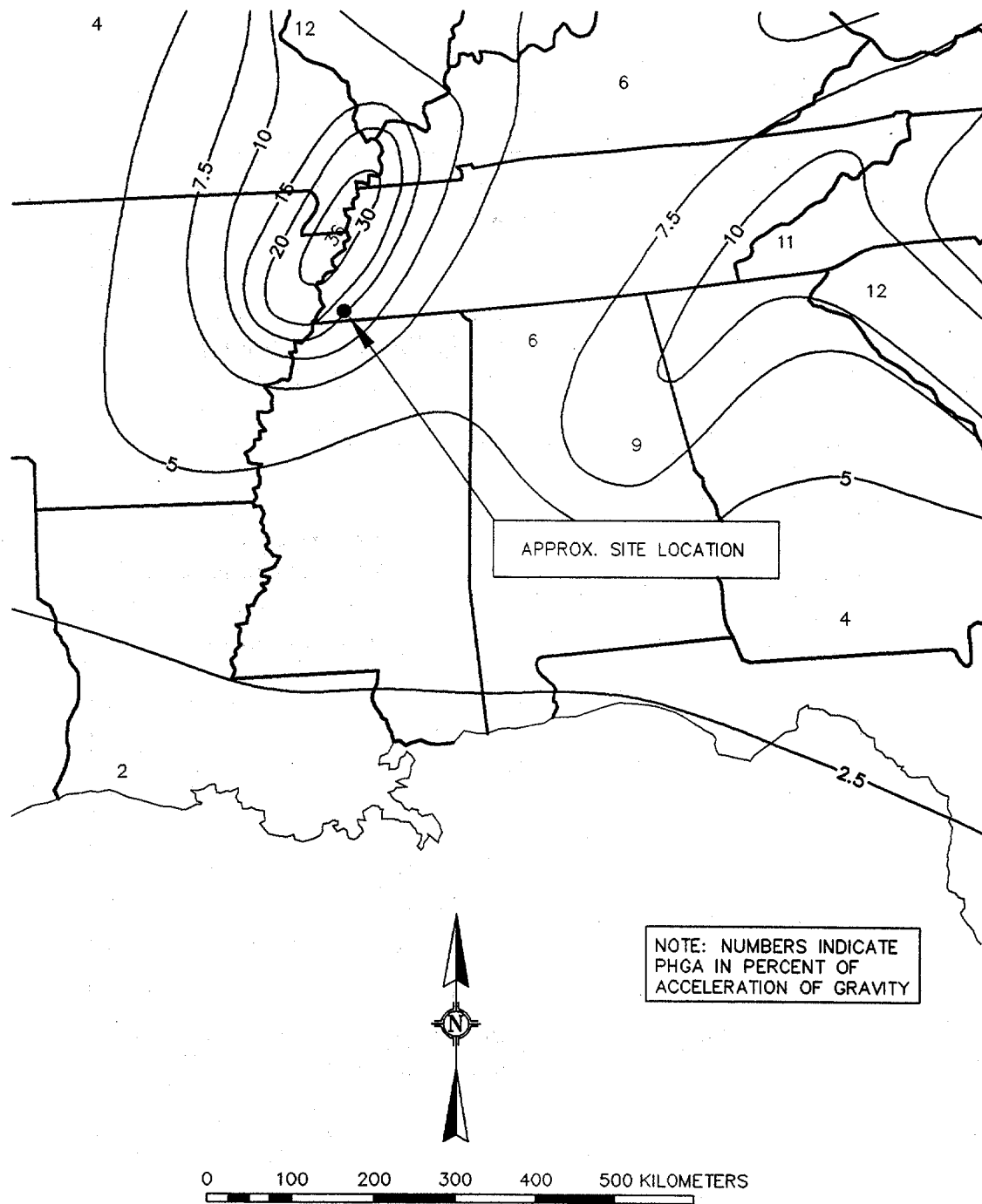


Figure 12. Algermissen seismic hazard map.

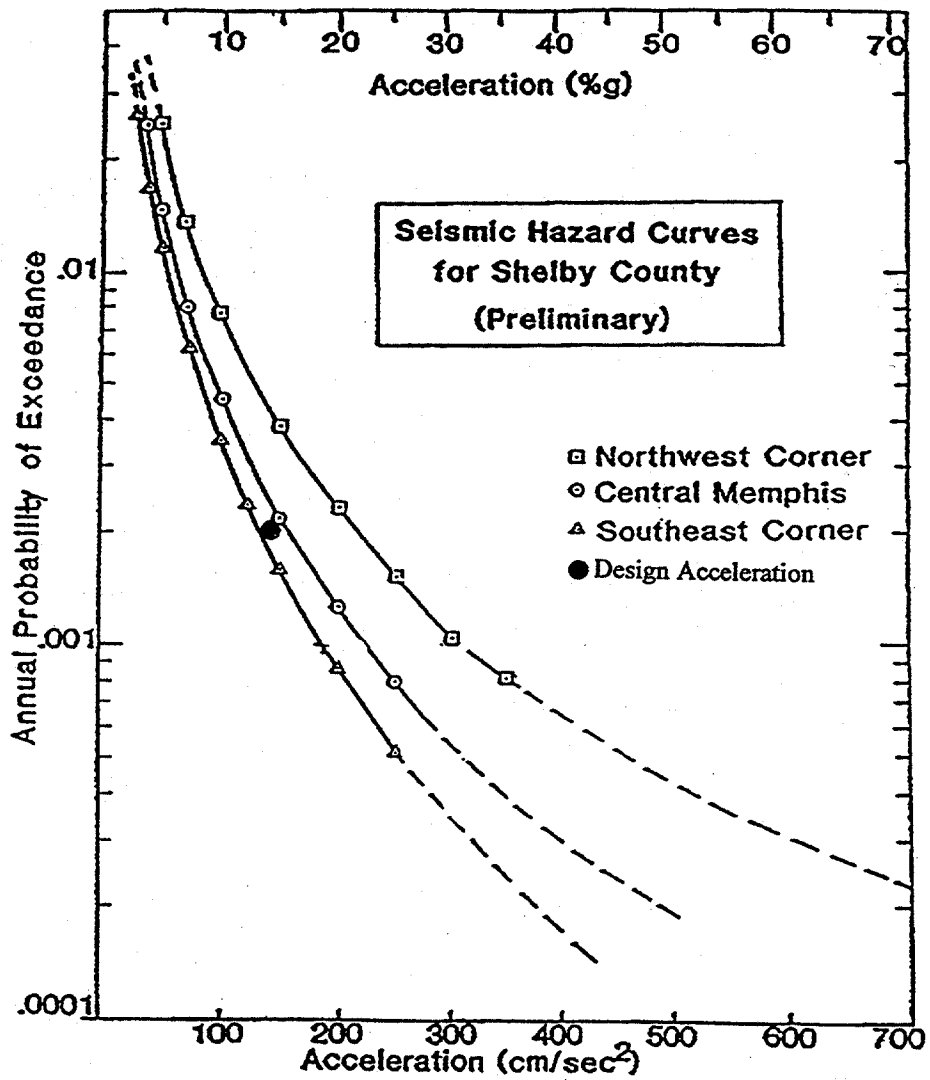


Figure 13. Seismic hazard curves for Shelby County (Allen and Hashall, 1989, as quoted in Poe, 1992).

3.4.3 Earthquake Magnitude

The project area is within the Reelfort rift area of the New Madrid Seismic Zone where some investigators believe that a great earthquake of $m_b \geq 7$, $M_s \geq 8.0$ can occur (Johnston and Nava, 1994). The peak ground acceleration for the site determined in the preceding section of this document was based upon USGS data. For the sake of consistency, the same source of information was employed to assess earthquake magnitude. USGS data for the NMSZ indicate a maximum earthquake magnitude, M_s , equal to 7.3 (Algermissen and Perkins, 1976).

Using the maximum magnitude to represent the design earthquake is a conservative assumption. The peak ground acceleration from the USGS map actually includes contributions from earthquakes smaller than the maximum magnitude but closer to the site than the distance at which the maximum magnitude event would induce the peak ground acceleration. For example, based upon mean attenuation relationships, the epicentral distance for the M_s 7.3 event is estimated to be larger than 50 km, while a magnitude 6.5 event within 5 km of the site would be expected to produce the same acceleration. The seismic hazard analysis used to generate the Algermissen map considers both the nearer, smaller magnitude events and the more distant, larger magnitude events. The resulting acceleration shown on the map is composed of contributions from both classes of events (near and far-field events). Use of the upper bound magnitude represents a conservative approach to the seismic analyses because the larger magnitude event is more likely to induce larger deformations.

3.4.4 Representative Acceleration Time Histories

The method outlined in chapter 4.7 of volume I is used herein to select a set of accelerograms to perform a seismic response analysis. This procedure involves the estimation of a target spectrum and then the selection of a recorded or synthetic time history whose spectral coordinates provide a reasonable envelope to those of the target spectrum. The target spectrum is estimated from available attenuation relationships. The lack of spectral attenuation relationships for the central United States makes it necessary to use a spectral attenuation relationship for the western United States. The attenuation relationship developed by Abrahamson and Silva was used herein (Abrahamson and Silva, 1996).

Unfortunately, the catalog of strong motion acceleration time histories for the central United States is very limited. The strongest earthquakes that have been recorded in the New Madrid Seismic Zone using strong motion instrumentation are the Risco ($M_w = 4.6$) and Cape Girardeau ($M_w = 4.8$), Missouri earthquakes. Acceleration time histories recorded during these NMSZ events cannot by themselves constitute a representative set of time histories for the site because of their relatively moderate magnitude. Time histories from a moderate magnitude NMSZ can, however, reasonably be used as a part of a suite of time histories selected for a liquefaction analysis. The function of a seismic response analysis in a liquefaction potential assessment is to evaluate the attenuation or amplification of seismic motions by the local soil profile. The magnitude of the time history used in the response analysis is of secondary importance in calculating these effects.

Acceleration time histories from western United States earthquakes (western earthquakes) are often used for seismic response analyses of large magnitude earthquakes in the central United States, mainly because of the lack of acceleration time histories from large central United States earthquakes. However, acceleration time histories from earthquakes in the western United States must be used with caution to model earthquakes in the central United States for the following reasons:

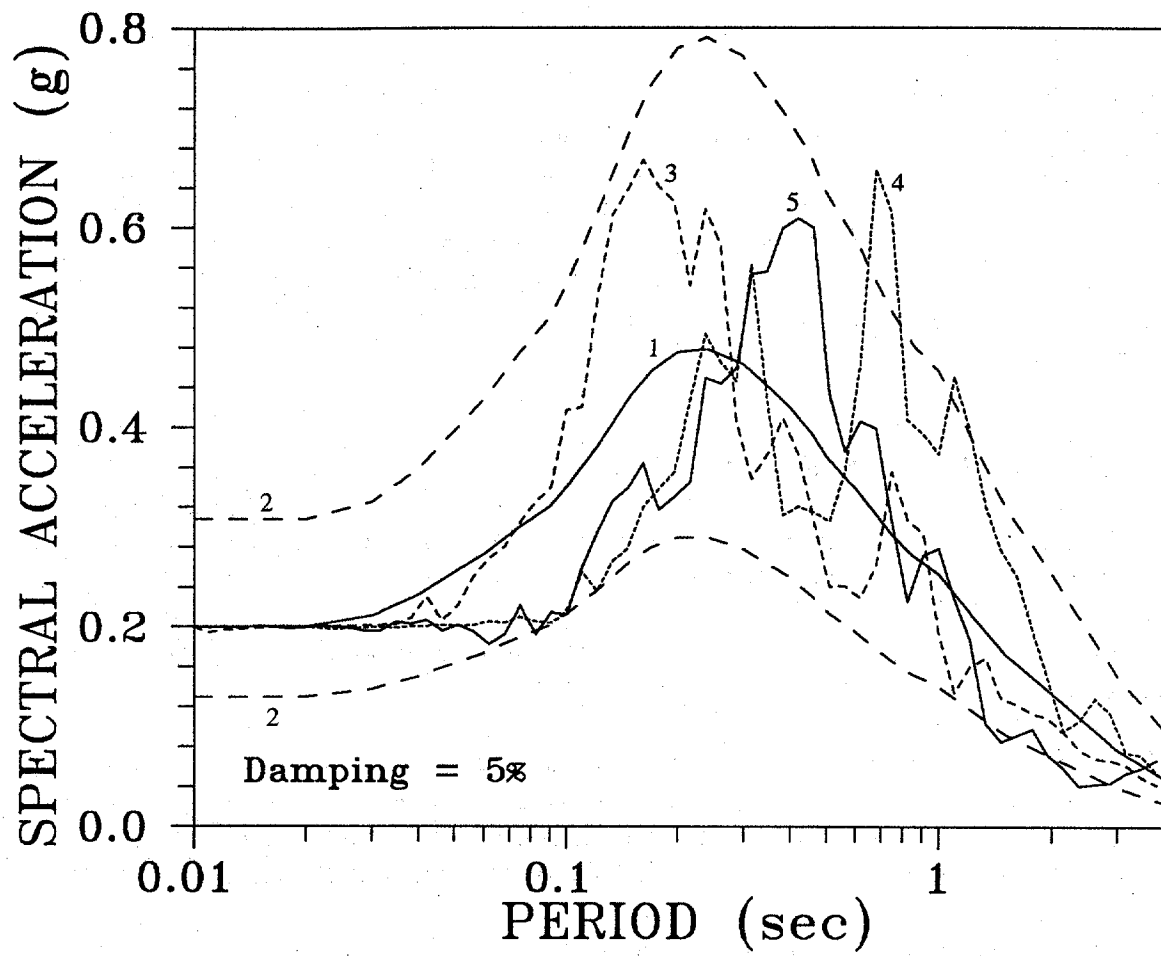
- Central United States earthquakes (central earthquakes) are believed to be enriched in high frequency energy compared to western earthquakes.
- A recorded acceleration time history from a western earthquake of a given magnitude is not likely to have a peak acceleration and duration that are consistent with a similar magnitude event at a central site. This lack of consistency is because the relationship between magnitude, peak acceleration, and duration depends largely on the attenuation of the motions between the source and the recording site. Available data indicate that attenuation in central geologic conditions is significantly less rapid than in western geologic conditions.
- Source mechanisms are believed to be different for central and western earthquakes. Typically, western earthquakes are associated with surface faulting, while central earthquakes are not.

Based upon the above logic, the suite of time histories selected for use in the seismic response analyses included one moderate magnitude NMSZ event, one large magnitude western United States event, and one large magnitude international event. The following set of accelerograms was selected:

- the N340 horizontal component of the Old Appleton accelerogram recorded during the Cape Girardeau ($M_w = 4.8$) earthquake of 26 September 1990;
- the 90 degree horizontal component of the Joshua Tree - Fire Station accelerogram recorded during the 28 June 1992 Landers, California earthquake ($M_w = 7.3$); and
- the transverse horizontal component of the Tabas-e-Golshan, Iran earthquake of 16 September 1968 ($M_w = 7.4$).

The Old Appleton time history was used primarily to represent the frequency content of a New Madrid event. As the primary function of the site response analysis was to evaluate the distribution of peak acceleration versus depth for pseudo-static analysis of a retaining wall, the $M_w = 4.8$ Old Appleton record was considered acceptable for this purpose. The Old Appleton record would not be acceptable for use in seismic deformation analyses due to the magnitude deficiency of the record.

Figure 14 shows the target spectrum and the spectra of the three time histories selected to represent the design event. Note that all three earthquake accelerograms were scaled to a peak ground



- 1 ——— Target Spectrum - median
- 2 - - - Target Spectrum - 16th and 84th percentiles
- 3 - - - Joshua Tree - Fire Station (90 deg) (M_w 7.3 Landers Eq.)
- 4 - - - Tabas (M_w 7.4 Tabas-e-Golshan Earthquake)
- 5 ——— Old Appleton (340 deg) (M_w 4.8 Cape Girardeau Earthquake)

Figure 14. Target spectrum and the spectra of three time histories.

acceleration of 0.16 g. The representative acceleration time histories selected for the site are shown in figure 15.

Information about the regional geology indicates that the bedrock underlying the site is approximately 1 km below ground. The 0.16 g peak ground acceleration value interpolated from the Algermissen Map which is partially reproduced in figure 12. It should be noted that this value describes the peak ground acceleration for a hypothetical bedrock outcrop at the site. The peak accelerations and seismically-induced shear stresses within the site soil profile in the design earthquake will, in general, differ from the hypothetical bedrock output motions due to the influence of the soil profile on the earthquake ground motions. Therefore, a site specific seismic response analysis was conducted.

3.5 SEISMIC RESPONSE ANALYSIS

The site specific seismic response analysis was performed to evaluate the peak average acceleration and, if necessary, the time history of the average acceleration within the retaining wall backfill. The peak average acceleration of the wall backfill is required for the pseudo-static stability analysis of the wall, while the time history of the average acceleration of the wall backfill would be required if a seismic deformation analysis was to be performed.

To model the influence of local soil conditions on site response, the computer program SHAKE (Schnabel et al., 1972; Idriss and Sun, 1992) was used to perform the one-dimensional frequency domain site response analysis with an equivalent linear soil model. Chapter 6.4 of volume I discusses the required input parameters and the advantages and limitations of SHAKE.

The subsurface profile was established through review of existing information and from the geotechnical investigation carried out at the site. The top 90 m of the soil profile were modeled in the response analyses. While the soil profile at the site is considerably deeper than 90 m, experience has shown that modeling soil profiles greater than 90 m in thickness can lead to erroneous results. Values of G_{max} for each layer were obtained using the methods developed in chapter 5 of volume I. Calculation of the low strain modulus G_{max} at depths of 10 m and 90 m are detailed on the calculation sheets attached to this example. A distribution of G_{max} with depth is reported on figure 16.

Site response analyses were performed using the three representative acceleration time histories identified in chapter 3.4.4 of this volume. The liquefaction and pseudo-static retaining wall analysis were based upon the "critical" case from the analyses (i.e., the case with the highest average acceleration).

The selected acceleration time histories described in chapter 3.4.4 of this volume were input to the SHAKE program as bedrock outcrop motions. The design peak horizontal acceleration was 0.16 g. The input and output files for the SHAKE analysis with the Joshua Tree accelerogram are provided in the attached calculation sheets.

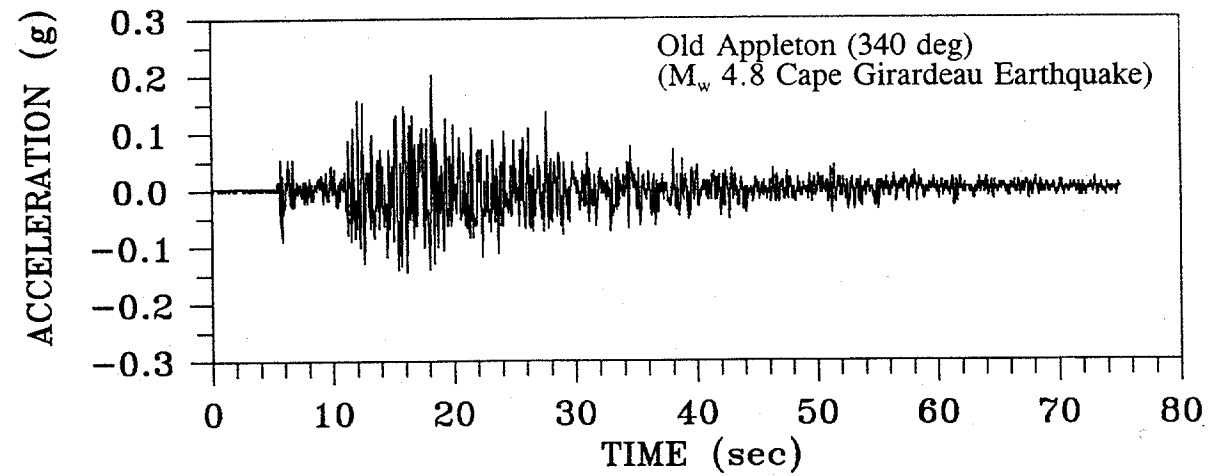
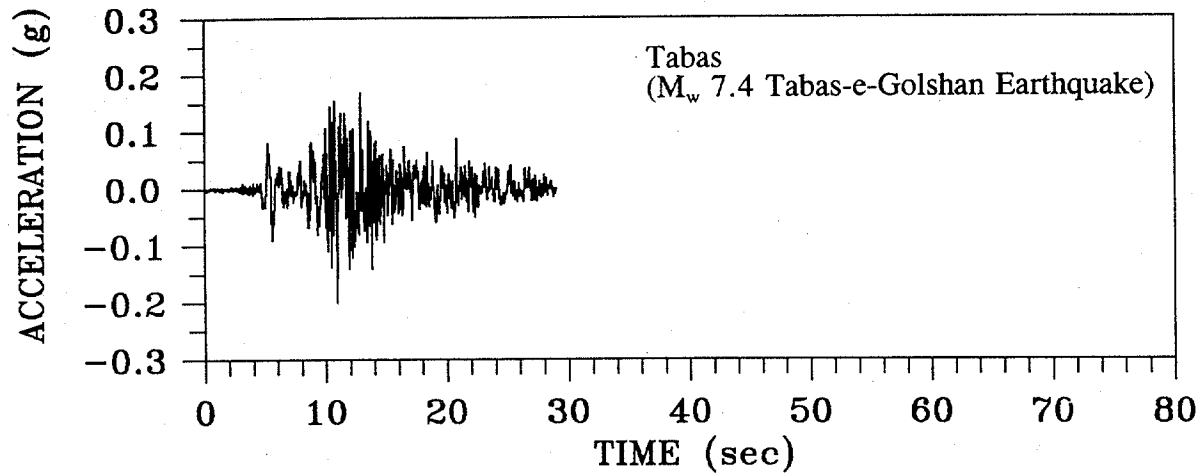
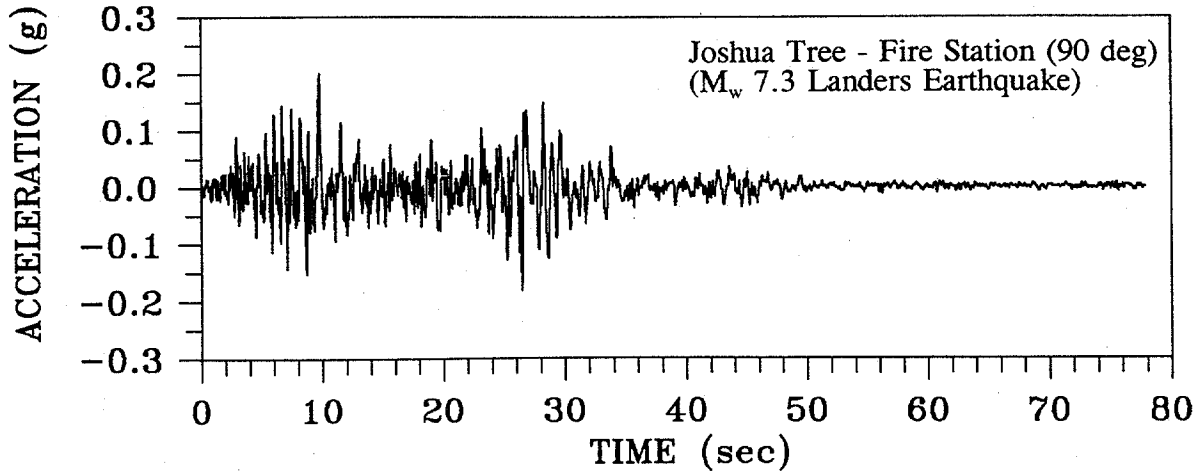


Figure 15. Earthquake acceleration time histories.

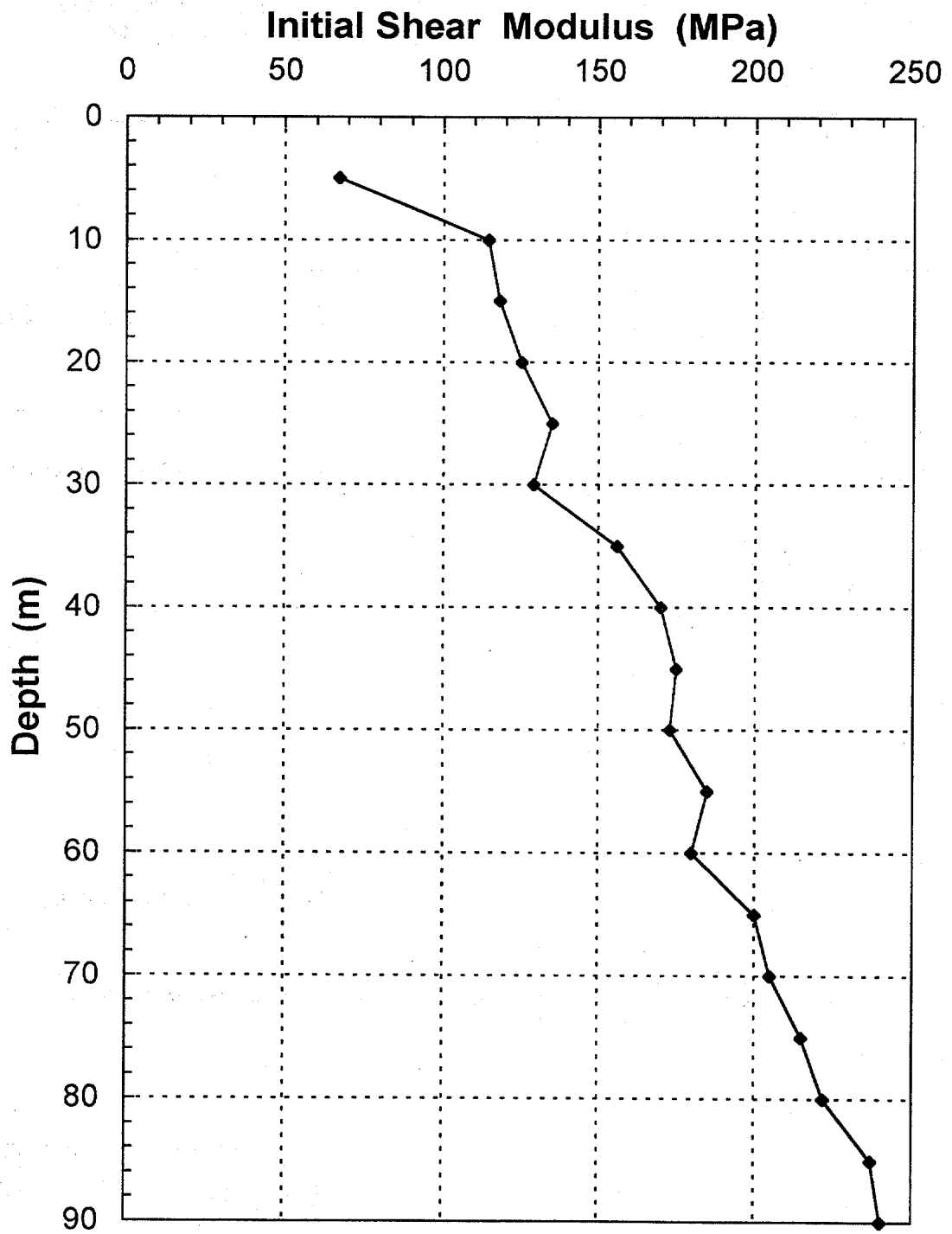


Figure 16. Small-strain shear modulus profile.

3.6 DESIGN OF THE WALL

The height of the wall in the cut section varies as the roadway descends and passes under the proposed highway. The wall will be a maximum of 6 m high. The backfill will be well-compacted silty sand with a unit weight of 19 kN/m³ and a drained friction angle of 35 degrees. The dynamic behavior of the fill is deemed comparable to that of the soil in place prior to the excavation of the underpass.

Recognizing that the peak ground acceleration at the top of the wall is a conservative value for use in design, the acceleration selected for the pseudo-static design of the retaining wall was the peak acceleration at mid-height of the wall. The acceleration calculated by SHAKE at a depth 3 m (mid-height) for each accelerogram is listed in table 6 along with the peak ground acceleration. The peak horizontal ground velocity at depth 3 m was evaluated by integrating the acceleration time histories provided by the SHAKE analysis. Table 6 lists the peak velocity computed at 3 m depth for all three accelerograms.

The peak horizontal ground acceleration at mid-height of the wall is from the Joshua Tree accelerogram and equals 0.15 g. The pseudo-static approach described in chapter 9.6.2.1 of volume I is followed in the calculation sheets to evaluate the static and seismic active earth force against the wall.

Results indicate that the magnitude of the seismic active earth force against the wall, given in kN per meter (kN/m) of wall as a function of the height of the wall is 3.23 times the square of the wall height (see attached calculation sheets). The total earth pressure is uniformly distributed over the height of the wall as discussed in chapter 9.6.2.1 of volume I.

Table 6. Peak horizontal acceleration and velocity values.

Accelerogram	Peak Acceleration at 3 m	Peak Velocity at 3 m	Peak Ground Acceleration
Tabas	0.12 g	0.18 m/s	0.14 g
Joshua Tree	0.15 g	0.22 m/s	0.16 g
Old Appleton	0.10 g	0.38 m/s	0.11 g

The simplified formulation developed by Richards and Elms (1979) presented in chapter 9.6.2.2 of volume I was used to evaluate the displacement of the wall. The formula involves the yield acceleration, the peak acceleration, and the peak velocity imposed on the wall by the earthquake. Following the recommendation of Lam and Martin (1986), the yield acceleration can be taken as half the peak acceleration. The calculated displacement was 5.2 mm.

3.7 CALCULATIONS

The calculation sheets for example 3, "Seismic Design of a Retaining Wall" follow. Equation numbers that appear in the right hand margin of the calculation sheets refer back to volume I.

Written by: T.H.H. Date: 96 / 03 / 19 Reviewed by: E.K. and N.M. Date: 96 / 03 / 20
YY MM DD YY MM DD

Client: FHWA Project: GEC-3 Project/Proposal No.: GE3686 Task No.: F

DETAILED CALCULATIONS
EXAMPLE 3 - DESIGN OF A RETAINING WALL

Calculation of Shear Modulus G_{max}

Values of G_{max} were evaluated with depth for input in the SHAKE program. The SPT values were used for depths of up to 25 m to evaluate G_{max} . For depths greater than 25 m, empirical correlations such as those presented in chapter 5.4.5.2 of volume I were used.

It is assumed in evaluating G_{max} over the top 25 m of the deposit that the material behaves as a sand.

Distribution of the normalized and standardized SPT values are reported on figure 17. The design profile was used to evaluate G_{max} .

- Depth 10 m in sand layer
 $\gamma = 18 \text{ kN/m}^3$; no water
 $\phi = 32^\circ$; $(N_1)_{60} = 14$ (figure 17)

Using the Seed et al. (1984) correlation (table 6 of volume I)

$$\sigma'_v = 10 \text{ m} \cdot 18 \text{ kN/m}^3 = 180 \text{ kPa}$$

$$K_o = 1 - \sin \phi' = 1 - \sin (32) = 0.47$$

$$\sigma'_m = (1+2K_o) \sigma'_v / 3 = (1+2 \cdot 0.47) 180 / 3 = 116.4 \text{ kPa}$$

$$G_{max} = 220 (K_2)_{max} (\sigma'_m)^{1/2}$$

$$(K_2)_{max} \approx 20 \{(N_1)_{60}\}^{1/3} = (20)(14)^{1/3} = 48$$

$$G_{max} = (220)(48)(116.4)^{1/2} = 113,930 \text{ kPa}$$

$$\Rightarrow G_{max} = 114 \text{ MPa at 10 m}$$



Written by: T.H.H. Date: 96 / 03 / 19 Reviewed by: E.K. and N.M. Date: 96 / 03 / 20
YY MM DD YY MM DD

Client: FHWA Project: GEC-3 Project/Proposal No.: GE3686 Task No.: F

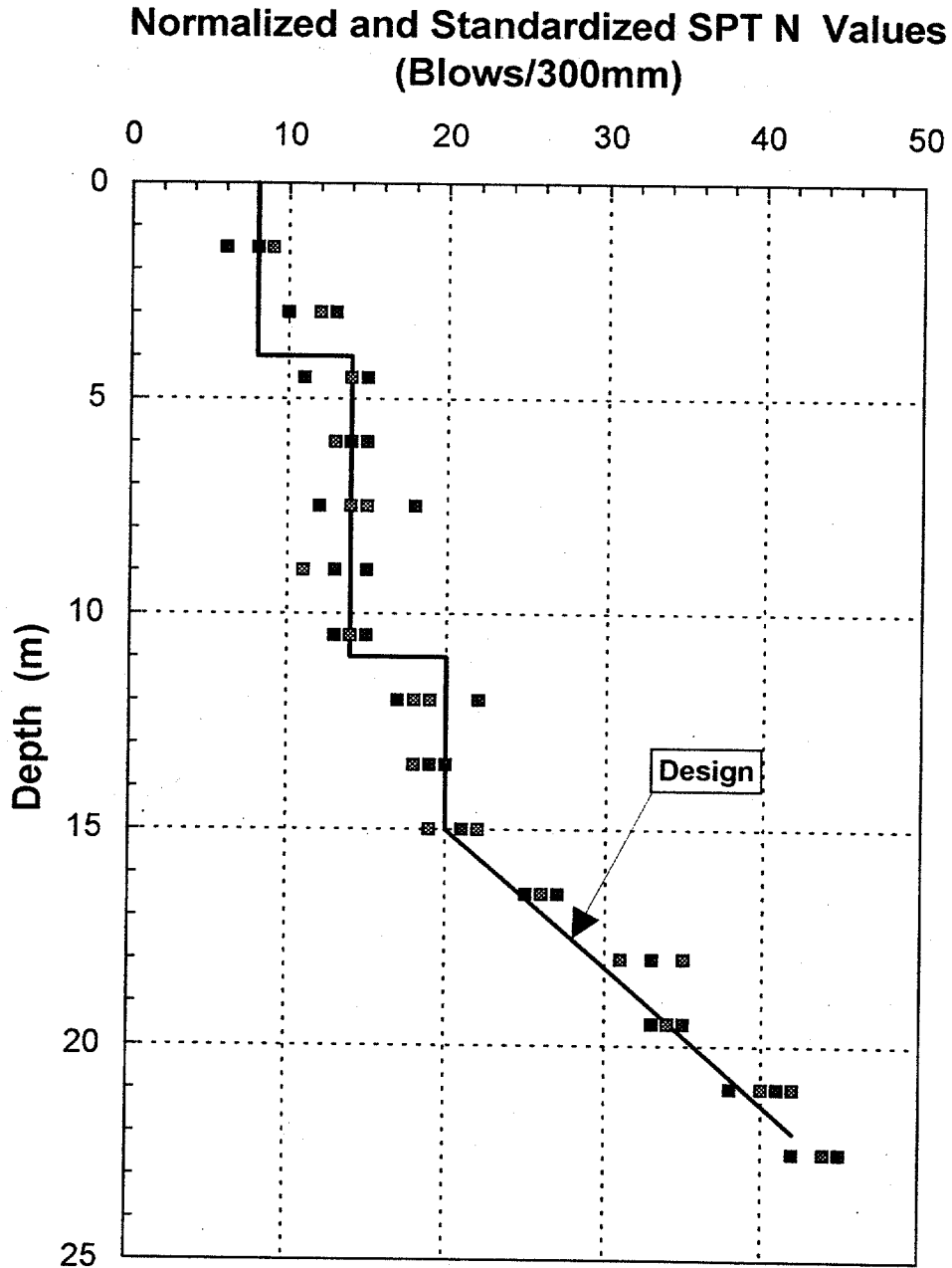


Figure 17. Corrected Example 3 SPT Profile



Written by: T.H.H. Date: 96 / 03 / 19 Reviewed by: E.K. and N.M. Date: 96 / 03 / 20
YY MM DD YY MM DD

Client: FHWA Project: GEC-3 Project/Proposal No.: GE3686 Task No.: F

From table 5 of volume I, the shear modulus for the dense sand at a depth of 90 m was assumed to be 240 mPa.

$$\Rightarrow G_{\max} = 240 \text{ MPa at } 90 \text{ m}$$

Figure 16 shows the distribution of G_{\max} with depth that was used to calculate seismic site response.

Design of Retaining Wall

Evaluation of Earth Pressure

The wall is a cast-in-place reinforced concrete cantilever wall of variable height (figure 18). Based on the results of the site response analysis, $k_h = 0.16$.

Backfill will be composed of well compacted sand, i.e.,

$$\gamma = 19 \text{ kN/m}^3 \text{ and } \phi = 35^\circ$$

From figure 74 of volume I, the seismic coefficients are

$$k_{AE} = 0.34 \text{ and } k_v = 0$$

The dynamic earth force or thrust against the wall is

$$P_{AE} = 1/2 k_{AE} \gamma H^2 (1 - k_v) \\ = 1/2 (0.34)(19) H^2 (1 - 0.0) = 3.23 H^2$$

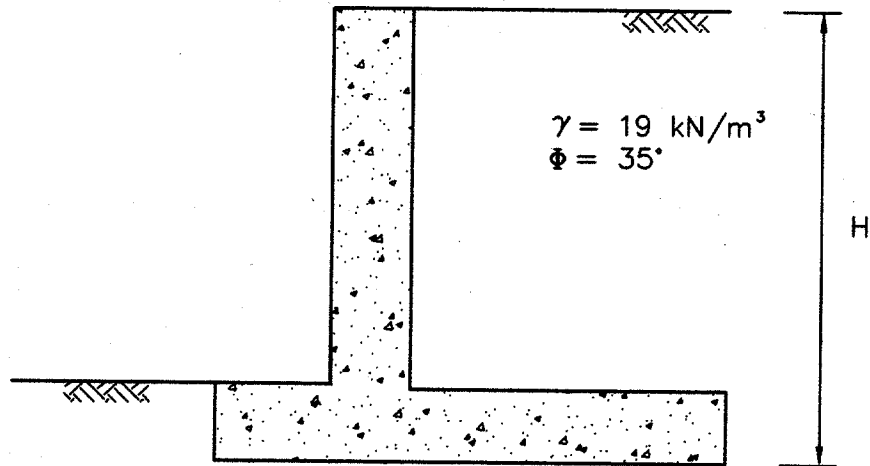
The static earth force or thrust is given by

$$P_a = 1/2 k_a \gamma H^2 = 1/2 (0.27)(19)(H^2) = 2.57 H^2 \\ \text{with } k_a = (1 - \sin \phi) / (1 + \sin \phi) = 0.27$$

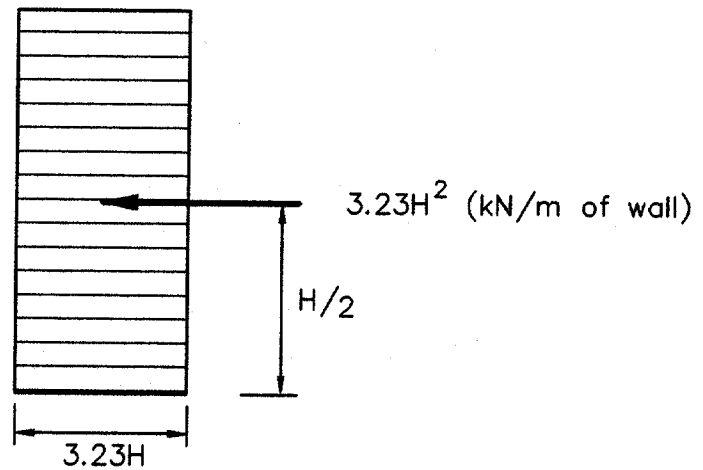


Written by: T.H.H. Date: 96 / 03 / 19 Reviewed by: E.K. and N.M. Date: 96 / 03 / 20
YY MM DD YY MM DD

Client: FHWA Project: GEC-3 Project/Proposal No.: GE3686 Task No.: F



TOTAL EARTH PRESSURE



(NOTE: H in meters, stress in kPa)

Figure 18. Load diagram on retaining wall.



Written by: T.H.H. Date: 96 / 03 / 19 Reviewed by: E.K. and N.M. Date: 96 / 03 / 20
YY MM DD YY MM DD

Client: FHWA Project: GEC-3 Project/Proposal No.: GE3686 Task No.: F

Following the recommendation of FHWA (1986) reported in chapter 9.6.2.1 of volume I, the total earth pressure is uniformly distributed over the height of the wall, i.e., the earth pressure resultant acts at midheight of the wall.

Evaluation of Displacement

The simplified formulation proposed by Richards and Elms (1979) is used to estimate the displacement of this cantilever wall. Richards and Elms proposed the following equation to evaluate the displacement of the wall:

$$d = 0.087 (V^2/A \cdot g) (N/A)^{-4} \cdot 25.4 \tag{9-23}$$

where d is the displacement of the wall in mm, V is the peak ground velocity, N is the yield acceleration for the wall-backfill system, A is the peak horizontal acceleration in the earthquake record, and g is acceleration of gravity.

$$V = 0.38 \text{ m/s (from the SHAKE analysis, Old Appleton accelerogram)}$$

$$A = 0.10 \text{ g (from the SHAKE analysis, Old Appleton accelerogram)}$$

$$N = (1/2 A) = 0.05 \text{ g (based on Lam and Martin (1986) recommendations)}$$

$$d = 0.087 (0.38^2/0.10 \cdot 9.81) \left(\frac{0.10 / 2}{0.10} \right)^{-4} 25.4 = 5.2 \text{ mm}$$

The analysis should be repeated for the other two accelerograms. Calculated displacements of up to 100 mm are deemed acceptable (Richards and Elms, 1979).



Written by: T.H.H. Date: 96/03/19 Reviewed by: E.K. and N.M. Date: 96/03/20
YY MM DD YY MM DD

Client: FHWA Project: GEC-3 Project/Proposal No.: GE3686 Task No.: F

Output File for SHAKE Analysis

```

*****
* SHAKE -- A COMPUTER PROGRAM FOR EARTHQUAKE RESPONSE *
* ANALYSIS OF HORIZONTALLY LAYERED SITES *
* by: Per B. Schnabel & John Lysmer -- 1970 *
* ----- *
* Shake85 : IBM-PC version of SHAKE *
* by: S.S. (Willie) Lai, January 1985 *
* ----- *
* Shake88 : New modulus reduction curves for clays *
* added using results from Sun et al. (1988) *
* by: J. I. Sun & Ramin Golesorkhi *
* February 26, 1988 *
* ----- *
* Shake90/91: Adjust last iteration; Input now is either *
* Gmax or max Vs; up to 13 material types can *
* be specified by user; up to 50 Layers can *
* be specified; object motion can be read in *
* from a separate file and can have user *
* specified format; Different periods for *
* response spectral calculations; options *
* are renumbered; and general cleanup *
* by: J. I. Sun, I. M. Idriss & P. Dirrim *
* June 1990 - February 1991 *
* ----- *
* Shake91 : General cleanup and finalization of input / *
* output format ... etc *
* by: I. M. Idriss *
* December 1991 *
* ----- *
* Shake94 : Routine for direct calculation of average *
* (ál) acceleration is added to the program. Out- *
* put format is modified to enable the two - *
* - page landscape printing. The following *
* modulus reduction and damping curves are *
* added: Kavazanjian & Matasovic (1995) for *
* municipal solid waste; Matasovic & Vucetic *
* (1993) for SMB sand; and Vucetic and Dobry *
* (1991) for clays of various plasticities. *
* by: Neven Matasovic *
* August 1993 - May 1994 *
*****

```

MAX. NUMBER OF TERMS IN FOURIER TRANSFORM = 4096
 NECESSARY LENGTH OF BLANK COMMON X = 25619

***** OPTION 1 *** READ RELATION BETWEEN SOIL PROPERTIES AND STRAIN

 MATERIAL TYPE NO. 4

CURVE NO. 7: #4 Modulus for Clay (PI=15) (Vucetic and Dobry, 1991)



Written by: T.H.H. Date: 96 / 03 / 19 Reviewed by: E.K. and N.M. Date: 96 / 03 / 20
YY MM DD YY MM DD

Client: FHWA Project: GEC-3 Project/Proposal No.: GE3686 Task No.: F

CURVE NO. 8: Damping for Clay (PI=15) (Vucetic and Dobry, 1991)

CURVE NO. 7		CURVE NO. 8	
STRAIN	G/Gmax	STRAIN	DAMPING
.0001	1.000	.0001	.85
.0003	1.000	.0003	1.04
.0010	.995	.0010	1.55
.0032	.936	.0032	2.58
.0100	.818	.0100	4.64
.0316	.640	.0316	7.77
.1000	.405	.1000	11.67
.3160	.210	.3160	16.08
1.0000	.095	1.0000	20.12
3.1600	.034	3.1600	23.17

 MATERIAL TYPE NO. 8

CURVE NO. 15:
 CURVE NO. 16:

CURVE NO.15		CURVE NO.16	
STRAIN	G/Gmax	STRAIN	DAMPING

 MATERIAL TYPE NO. 5

CURVE NO. 9: #5 Modulus for Clay (PI=30) (Vucetic and Dobry, 1991)
 CURVE NO. 10: Damping for Clay (PI=30) (Vucetic and Dobry, 1991)

CURVE NO. 9		CURVE NO.10	
STRAIN	G/Gmax	STRAIN	DAMPING
.0001	1.000	.0001	.85
.0003	1.000	.0003	.85
.0010	1.000	.0010	1.36
.0032	.976	.0032	2.18
.0100	.901	.0100	3.82
.0316	.743	.0316	6.00
.1000	.538	.1000	8.72
.3160	.332	.3160	12.41
1.0000	.158	1.0000	16.90
3.1600	.048	3.1600	21.26



GEOSYNTEC CONSULTANTS

Written by: T.H.H. Date: 96 / 03 / 19 Reviewed by: E.K. and N.M. Date: 96 / 03 / 20
YY MM DD YY MM DD

Client: FHWA Project: GEC-3 Project/Proposal No.: GE3686 Task No.: F

MATERIAL TYPE NO. 7

CURVE NO. 13:
CURVE NO. 14:

CURVE NO.13		CURVE NO.14	
STRAIN	G/Gmax	STRAIN	DAMPING

MATERIAL TYPE NO. 2

CURVE NO. 3: #2 ATTENUATION OF ROCK AVERAGE
CURVE NO. 4: DAMPING IN ROCK

CURVE NO. 3		CURVE NO. 4	
STRAIN	G/Gmax	STRAIN	DAMPING
.0001	1.000	.0001	.40
.0003	1.000	.0010	.80
.0010	.988	.0100	1.50
.0030	.952	.1000	3.00
.0100	.900	1.0000	4.60
.0300	.810	.0000	.00
.1000	.725	.0000	.00
1.0000	.550	.0000	.00

MATERIAL TYPE NO. 6

CURVE NO. 11:
CURVE NO. 12:

CURVE NO.11		CURVE NO.12	
STRAIN	G/Gmax	STRAIN	DAMPING

MATERIAL TYPE NO. 3

CURVE NO. 5: #3 Modulus for sand (PI=0) (Vucetic and Dobry, 1991)
CURVE NO. 6: Damping for Sand (PI=0) (Vucetic and Dobry, 1991)



Written by: T.H.H. Date: 96 / 03 / 19 Reviewed by: E.K. and N.M. Date: 96 / 03 / 20
 YY MM DD YY MM DD

Client: FHWA Project: GEC-3 Project/Proposal No.: GE3686 Task No.: F

CURVE NO. 5		CURVE NO. 6	
STRAIN	G/Gmax	STRAIN	DAMPING
.0001	1.000	.0001	.85
.0003	1.000	.0003	1.04
.0010	.964	.0010	1.66
.0032	.870	.0032	3.00
.0100	.712	.0100	5.48
.0316	.474	.0316	10.01
.1000	.253	.1000	15.40
.3160	.103	.3160	20.23
1.0000	.028	1.0000	23.94
3.1600	.004	.0000	.00

***** OPTION 2 *** READ SOIL / WASTE PROFILE

SOIL PROFILE NO. 1 Wall example deposit
 NUMBER OF LAYERS 9
 DEPTH TO BEDROCK 270.0

NO.	TYPE	THICKNESS (ft)	DEPTH (ft)	TOT. PRESS. (psf)	MODULUS (ksf)	DAMPING (%)	UNIT WT. (pcf)	SH. VEL. (fps)
1	3	10.00	5.00	550.00	950.	5.00	110.00	527.3
2	4	10.00	15.00	1650.00	1500.	5.00	110.00	662.6
3	5	30.00	35.00	3925.00	2378.	5.00	115.00	816.0
4	3	50.00	75.00	8650.00	3000.	5.00	120.00	897.2
5	1	50.00	125.00	14775.00	3505.	5.00	125.00	950.2
6	1	40.00	170.00	20460.00	3725.	5.00	128.00	968.0
7	3	40.00	210.00	25620.00	4100.	5.00	130.00	1007.7
8	1	40.00	250.00	30620.00	4525.	5.00	120.00	1101.9
9	BASE				5000.	1.00	140.00	1072.4

PERIOD = 1.158 sec FROM AVERAGE SHEAR WAVE VELOCITY OF 932.8 ft/sec

FREQUENCY AMPLITUDE:
 MAXIMUM AMPLIFICATION = 13.35
 FOR FREQUENCY (f) = .95 c/sec
 FOR PERIOD (1 / f) = 1.05 sec

***** OPTION 3 *** READ INPUT MOTION

FILE NAME FOR INPUT MOTION = JOSHUA90.SAR
 NO. OF INPUT ACCEL. POINTS = 4000
 NO. OF POINTS USED IN FFT = 4096
 NO. OF HEADING LINES = 7
 NO. OF POINTS PER LINE = 8
 TIME STEP FOR INPUT MOTION = .0200
 FORMAT FOR OF TIME HISTORY = (8F9.6)



Written by: T.H.H. Date: 96 / 03 / 19 Reviewed by: E.K. and N.M. Date: 96 / 03 / 20
 YY MM DD YY MM DD

Client: FHWA Project: GEC-3 Project/Proposal No.: GE3686 Task No.: F

***** ACCELEROGRAM HEADER *****

LANDERS EQ.; JOSHUA TREE - FIRE STATION (90 Deg); 4000 points @ 0.02 sec
 1-story building on shallow alluvium which is overlying granite bedrock
 UNCorr.Max. = 0.287g @ 9.778 sec; Max. in file = +0.283866g @ 9.780 sec
 RMS acc. (uncorr.) = 0.44g; Predom. freq.= 1.47Hz; Mn. Sq. freq.= 2.07Hz
 Epicent. dist.= 14 km; Focal depth= 9.0 km; Bracketed duration: 41.1 sec
 LANDERS EQ. 28 JUNE 1992 4:58 PDT; Right-Lateral Slip on Camp Rock fault
 HYPOCENTER (USGS): 34.217N,116.433W, H=9 km. Ms=7.5 (NEIC), Mw=7.4 (CIT)

** FIRST & LAST 5 LINES OF INPUT MOTION *****

```

1 .004793 -.008643 -.013358 -.004243 .004904 .004550 -.015163 -.022346
2 -.010351 -.000739 -.007081 -.018615 -.021747 -.017897 -.012727 -.005326
3 .001259 .004162 .011625 .011065 .006764 .004994 .012114 .020316
4 .018054 .018607 .018994 .016094 .006357 -.002759 -.007146 -.008494
5 -.007122 -.001046 .002054 .001218 .001994 .004918 -.000156 -.018718
..... INPUT MOTION READ NOT ECHOED.....
496 -.001827 -.000118 .001032 .003296 .004509 .004355 .003855 .002413
497 .001412 -.000005 .000240 .000915 .001288 .001901 .001506 .003389
498 .003879 .002985 .002056 .001758 .002524 .002618 .000791 .000514
499 -.000946 -.002436 -.004001 -.004878 -.004714 -.004489 -.002658 .000588
500 .003148 .004309 .005547 .005048 .003879 .003333 .001518 .000976
    
```

MAXIMUM ACCELERATION = .283866
 AT TIME = 9.78 sec

THE VALUES WILL BE MULTIPLIED BY A FACTOR = .56364630
 TO GIVE NEW MAXIMUM ACCELERATION = .16000000

MEAN SQUARE FREQUENCY = 2.07 c/sec

***** OPTION 4 *** READ WHERE OBJECT MOTION IS GIVEN

OBJECT MOTION IN LAYER NUMBER 9 OUTCROPPING

***** OPTION 5 *** OBTAIN STRAIN COMPATIBLE SOIL PROPERTIES

MAXIMUM NUMBER OF ITERATIONS = 8
 FACTOR FOR UNIFORM STRAIN IN TIME DOMAIN = .60

ACCELEROGRAM - JOSHUA90.SAR
 P R O F I L E - Wall example deposit

ITERATION NUMBER 1

VALUES IN TIME DOMAIN

NO	TYPE	DEPTH (ft)	UNIFRM. STRAIN	<---- NEW	DAMPING USED	----> ERROR	<---- NEW	SHEAR MODULUS USED	----> ERROR	G/Go RATIO
1	3	5.0	.00604	.044	.050	-14.1	742.1	950.0	-28.0	1.000
2	4	15.0	.01121	.049	.050	-1.1	1200.5	1500.0	-25.0	1.000
3	5	35.0	.01581	.047	.050	-6.7	1992.9	2378.0	-19.3	1.000
4	3	75.0	.02412	.089	.050	44.1	1589.6	3000.0	-88.7	1.000
5	1	125.0	.02891	.050	.050	.4	2268.0	3505.0	-54.5	1.000
6	1	170.0	.03134	.053	.050	5.1	2347.6	3725.0	-58.7	1.000



Written by: T.H.H. Date: 96 / 03 / 19 Reviewed by: E.K. and N.M. Date: 96 / 03 / 20
 YY MM DD YY MM DD

Client: FHWA Project: GEC-3 Project/Proposal No.: GE3686 Task No.: F

7	3	210.0	.03112	.099	.050	49.7	1956.5	4100.0	-109.6	1.000
8	1	250.0	.02976	.051	.050	1.6	2902.9	4525.0	-55.9	1.000

ACCELEROGRAM - JOSHUA90.SAR
 P R O F I L E - Wall example deposit

ITERATION NUMBER 2

VALUES IN TIME DOMAIN

NO	TYPE	DEPTH (ft)	UNIFRM. STRAIN	<---- DAMPING ---->			<---- SHEAR MODULUS ---->			G/Go RATIO
				NEW	USED	ERROR	NEW	USED	ERROR	
1	3	5.0	.00775	.049	.044	11.0	709.7	742.1	-4.6	.781
2	4	15.0	.01402	.056	.049	11.0	1148.6	1200.5	-4.5	.800
3	5	35.0	.01906	.050	.047	7.0	1932.0	1992.9	-3.2	.838
4	3	75.0	.04490	.117	.089	23.2	1219.9	1589.6	-30.3	.530
5	1	125.0	.04150	.064	.050	21.1	1988.2	2268.0	-14.1	.647
6	1	170.0	.04405	.066	.053	20.1	2063.0	2347.6	-13.8	.630
7	3	210.0	.05391	.125	.099	20.5	1523.2	1956.5	-28.4	.477
8	1	250.0	.03520	.057	.051	11.2	2733.8	2902.9	-6.2	.642

ACCELEROGRAM - JOSHUA90.SAR
 P R O F I L E - Wall example deposit

ITERATION NUMBER 3

VALUES IN TIME DOMAIN

NO	TYPE	DEPTH (ft)	UNIFRM. STRAIN	<---- DAMPING ---->			<---- SHEAR MODULUS ---->			G/Go RATIO
				NEW	USED	ERROR	NEW	USED	ERROR	
1	3	5.0	.00772	.049	.049	-.1	710.1	709.7	.1	.747
2	4	15.0	.01404	.056	.056	.1	1148.3	1148.6	.0	.766
3	5	35.0	.01868	.050	.050	-.8	1938.5	1932.0	.3	.812
4	3	75.0	.05580	.127	.117	8.0	1094.8	1219.9	-11.4	.407
5	1	125.0	.04406	.066	.064	3.5	1941.1	1988.2	-2.4	.567
6	1	170.0	.04665	.068	.066	3.3	2015.1	2063.0	-2.4	.554
7	3	210.0	.06320	.133	.125	5.6	1398.2	1523.2	-8.9	.372
8	1	250.0	.03348	.055	.057	-3.5	2784.7	2733.8	1.8	.604

ACCELEROGRAM - JOSHUA90.SAR
 P R O F I L E - Wall example deposit

ITERATION NUMBER 4

VALUES IN TIME DOMAIN

NO	TYPE	DEPTH (ft)	UNIFRM. STRAIN	<---- DAMPING ---->			<---- SHEAR MODULUS ---->			G/Go RATIO
				NEW	USED	ERROR	NEW	USED	ERROR	
1	3	5.0	.00753	.049	.049	-1.1	713.4	710.1	.5	.747
2	4	15.0	.01374	.055	.056	-1.1	1153.2	1148.3	.4	.766
3	5	35.0	.01842	.050	.050	-.5	1943.1	1938.5	.2	.815



GEOSYNTEC CONSULTANTS

Written by: T.H.H. Date: 96 / 03 / 19 Reviewed by: E.K. and N.M. Date: 96 / 03 / 20
YY MM DD YY MM DD

Client: FHWA Project: GEC-3 Project/Proposal No.: GE3686 Task No.: F

4	3	75.0	.06134	.131	.127	3.4	1040.2	1094.8	-5.2	.365
5	1	125.0	.04400	.066	.066	-.1	1942.2	1941.1	.1	.554
6	1	170.0	.04652	.068	.068	-.2	2017.5	2015.1	.1	.541
7	3	210.0	.06646	.135	.133	1.7	1358.6	1398.2	-2.9	.341
8	1	250.0	.03171	.053	.055	-4.0	2839.8	2784.7	1.9	.615

ACCELEROGRAM - JOSHUA90.SAR
 PROFILE - Wall example deposit

ITERATION NUMBER 5

VALUES IN TIME DOMAIN

NO	TYPE	DEPTH (ft)	UNIFRM. STRAIN		DAMPING			SHEAR MODULUS			G/Go RATIO
			NEW	USED	NEW	USED	ERROR	NEW	USED	ERROR	
1	3	5.0	.00747	.048	.049	-.3	714.3	713.4	.1	.751	
2	4	15.0	.01360	.055	.055	-.5	1155.6	1153.2	.2	.769	
3	5	35.0	.01830	.050	.050	-.3	1945.3	1943.1	.1	.817	
4	3	75.0	.06451	.133	.131	1.8	1011.3	1040.2	-2.9	.347	
5	1	125.0	.04353	.066	.066	-.6	1950.5	1942.2	.4	.554	
6	1	170.0	.04600	.068	.068	-.6	2026.9	2017.5	.5	.542	
7	3	210.0	.06756	.136	.135	.6	1345.8	1358.6	-1.0	.331	
8	1	250.0	.03080	.052	.053	-2.2	2869.1	2839.8	1.0	.628	

ACCELEROGRAM - JOSHUA90.SAR
 PROFILE - Wall example deposit

ITERATION NUMBER 6

VALUES IN TIME DOMAIN

NO	TYPE	DEPTH (ft)	UNIFRM. STRAIN		DAMPING			SHEAR MODULUS			G/Go RATIO
			NEW	USED	NEW	USED	ERROR	NEW	USED	ERROR	
1	3	5.0	.00746	.048	.048	-.1	714.5	714.3	.0	.752	
2	4	15.0	.01357	.055	.055	-.1	1156.1	1155.6	.0	.770	
3	5	35.0	.01825	.050	.050	-.1	1946.1	1945.3	.0	.818	
4	3	75.0	.06636	.135	.133	1.0	995.0	1011.3	-1.6	.337	
5	1	125.0	.04314	.065	.066	-.5	1957.6	1950.5	.4	.556	
6	1	170.0	.04559	.067	.068	-.5	2034.5	2026.9	.4	.544	
7	3	210.0	.06788	.136	.136	.2	1342.0	1345.8	-.3	.328	
8	1	250.0	.03042	.052	.052	-1.0	2882.0	2869.1	.4	.634	

ACCELEROGRAM - JOSHUA90.SAR
 PROFILE - Wall example deposit

ITERATION NUMBER 7

VALUES IN TIME DOMAIN



Written by: T.H.H. Date: 96 / 03 / 19 Reviewed by: E.K. and N.M. Date: 96 / 03 / 20
 YY MM DD YY MM DD

Client: FHWA Project: GEC-3 Project/Proposal No.: GE3686 Task No.: F

NO	TYPE	DEPTH (ft)	UNIFRM. STRAIN	<---- DAMPING ---->			<---- SHEAR MODULUS ---->			G/Go RATIO
				NEW	USED	ERROR	NEW	USED	ERROR	
1	3	5.0	.00746	.048	.048	.0	714.5	714.5	.0	.752
2	4	15.0	.01357	.055	.055	.0	1156.1	1156.1	.0	.771
3	5	35.0	.01824	.050	.050	.0	1946.4	1946.1	.0	.818
4	3	75.0	.06746	.136	.135	.6	985.5	995.0	-1.0	.332
5	1	125.0	.04288	.065	.065	-.4	1962.4	1957.6	.2	.559
6	1	170.0	.04532	.067	.067	-.3	2039.4	2034.5	.2	.546
7	3	210.0	.06795	.136	.136	.0	1341.2	1342.0	-.1	.327
8	1	250.0	.03026	.051	.052	-.4	2887.1	2882.0	.2	.637

ACCELEROGRAM - JOSHUA90.SAR
 P R O F I L E - Wall example deposit

ITERATION NUMBER 8

VALUES IN TIME DOMAIN

NO	TYPE	DEPTH (ft)	UNIFRM. STRAIN	<---- DAMPING ---->			<---- SHEAR MODULUS ---->			G/Go RATIO
				NEW	USED	ERROR	NEW	USED	ERROR	
1	3	5.0	.00746	.048	.048	.0	714.5	714.5	.0	.752
2	4	15.0	.01358	.055	.055	.0	1156.0	1156.1	.0	.771
3	5	35.0	.01823	.050	.050	.0	1946.4	1946.4	.0	.818
4	3	75.0	.06813	.136	.136	.3	979.9	985.5	-.6	.329
5	1	125.0	.04272	.065	.065	-.2	1965.3	1962.4	.2	.560
6	1	170.0	.04516	.067	.067	-.2	2042.3	2039.4	.1	.547
7	3	210.0	.06793	.136	.136	.0	1341.5	1341.2	.0	.327
8	1	250.0	.03021	.051	.051	-.1	2888.9	2887.1	.1	.638

VALUES IN TIME DOMAIN

LAYER	MAT. TYPE	THICKNESS (ft)	DEPTH (ft)	MAX. STRAIN (%)	MAX. STRESS (psf)	AVG. ACC. (g)	TIME (sec)
1	3	10.0	5.0	.01244	88.88	.16161	10.18
2	4	10.0	15.0	.02263	261.60	.15854	10.18
3	5	30.0	35.0	.03039	591.49	.15070	10.16
4	3	50.0	75.0	.11354	1119.00	.12936	10.18
5	1	50.0	125.0	.07120	1397.29	.09457	10.14
6	1	40.0	170.0	.07527	1534.94	.07502	10.10
7	3	40.0	210.0	.11321	1518.40	.05927	10.12
8	1	40.0	250.0	.05035	1453.63	.04747	10.06

PERIOD = 1.614 sec FROM AVERAGE SHEAR WAVE VELOCITY OF 669.3 ft/sec

FREQUENCY AMPLITUDE:
 MAXIMUM AMPLIFICATION = 6.82
 FOR FREQUENCY (f) = .64 c/sec
 FOR PERIOD (1 / f) = 1.55 sec



Written by: T.H.H. Date: 96 / 03 / 19 Reviewed by: E.K. and N.M. Date: 96 / 03 / 20
 YY MM DD YY MM DD

Client: FHWA Project: GEC-3 Project/Proposal No.: GE3686 Task No.: F

***** OPTION 6 *** COMPUTE MOTION IN NEW SUBLAYERS

ACCELEROGRAM - JOSHUA90.SAR
 D E P O S I T - Wall example deposit

LAYER	DEPTH (ft)	MAX. ACC. (g)	TIME (sec)	MN.SQ.FR. (c/sec)	ACC. RATIO QUIET ZONE	TH SAVED ACC.REC.
OUTCR.	.0	.16010	10.16	1.31	.040	512
WITHIN	10.0	.15627	10.16	1.23	.040	0
WITHIN	20.0	.14892	10.16	1.14	.039	0
WITHIN	50.0	.12763	10.12	1.02	.039	0
WITHIN	100.0	.09521	10.00	1.49	.040	0
WITHIN	150.0	.07691	9.94	1.47	.058	0
WITHIN	190.0	.08485	9.88	1.78	.056	0
WITHIN	230.0	.09707	9.82	2.11	.048	512



3.8 SUMMARY AND CONCLUSIONS

A retaining wall is to be built as part of a highway project in the south central United States. The wall is a cast-in-place concrete gravity wall up to 6 m in height. The general geology at the site is characteristic of the Mississippi Embayment and consists of deep deposits of Quaternary, Tertiary, and Cretaceous sediments.

A subsurface investigation was carried out using rotary wash drilling up to depths of 60 m. In addition, in-situ testing using the SPT and CPT was performed to derive representative soil properties for use in design.

To estimate the design acceleration for pseudo-static analysis of the retaining wall, a seismic response analysis was performed using the computer program SHAKE. Three acceleration time histories were selected based on a target spectrum. The calculated peak horizontal ground acceleration at the site was on the order of 0.16 g. The peak average acceleration for use in retaining wall design was on the order of 0.15 g.

The pseudo-static analysis provided the structural engineer with both static earth pressure and pseudo-static earth pressure as a function of wall height. The computed permanent seismic deformation of the gravity wall was on the order of 5 mm. This deformation was considered acceptable.

EXAMPLE 4

SLOPE STABILITY ANALYSIS

4.1 INTRODUCTION

4.1.1 Description of the Project

Construction of a new highway will require extensive excavation and regrading of a hillside. Figure 19 shows the original topography and the proposed final grading. The highest cut slope rises approximately 44 m above grade. The existing topography is at an average inclination of 2.9H:1V (Horizontal:Vertical) and the proposed final grading calls for 1.5H:1V slopes. In general, the hillside is composed of interbedded weak sedimentary rock that, in some cases, dips out of slope. To complete the seismic design of the slope, the following tasks need to be performed:

- develop a representative geological and geotechnical profile;
- perform a pseudo-static stability of the cut slope; and
- design slope stabilization measures, if needed.

The local highway department required minimum factors of safety of 1.5 for static conditions and 1.1 for pseudo-static conditions with a seismic coefficient equal to one-half the peak ground acceleration.

4.1.2 Source Materials Required

The source materials necessary to solve this problem includes:

- topography of the proposed cut;
- geologic and geotechnical information;
- seismological data;
- slope stability computer program such as STABL4; and
- volume I of this document.

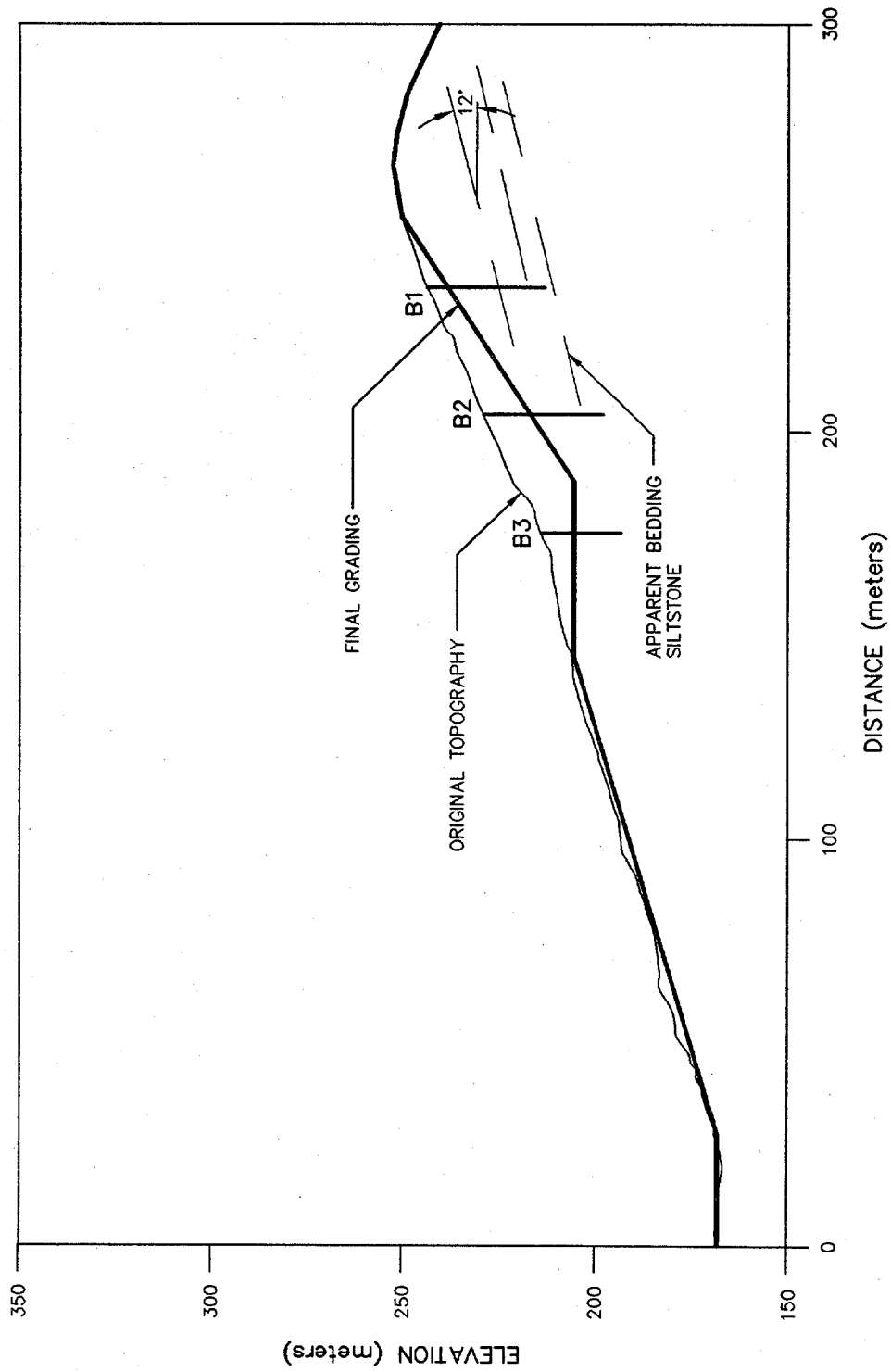


Figure 19. Original topography and proposed grading.

4.2 SITE GEOLOGY

Previous investigations identified two bedrock formations and five classes of surficial deposits within the area. The surficial deposits include terrace deposits, landslide debris, colluvium, alluvium, and artificial fill. The bedrock formations consist of marine sediments. The bedrock formations are divided into an upper group of Miocene formations and an underlying group of Pliocene age formations.

The Pliocene formation group is a siltstone unit, exposed over much of the area. It is described in boring logs as a light tan sandy siltstone, clayey siltstone, and silty sandstone with local silty claystone interbed seams. It was reported that the siltstone bedrock materials are massive with thin interbedded sandstone layers and abundant gypsum- and clay-lined joints. Weak seams are typically parallel to bedding and, by definition, have lower shear strengths than the predominant bedrock. In slope areas where adverse (i.e., out-of-slope) bedding is present, these weak seams may provide a mechanism for slope instability.

Regionally, bedding planes generally dip toward the north except where there has been local deformation due to faulting and folding. This regional trend is inferred to exist at the site based upon previous mapping.

4.3 GEOTECHNICAL EXPLORATION

4.3.1 General

Data from previous exploration programs and knowledge of the local geology indicate that the geomorphology will have a great influence on the stability of the cut slopes. Consequently, the geotechnical exploration program was designed to provide information on the orientation of the beds and on the shear strength of both the rock mass of the bedrock and on the bedding plane interfaces and weak seam material. To that effect, and to complement traditional borings and sampling procedures, a series of three 0.6-m-diameter test borings were excavated with a bucket auger. Downhole logging was performed in these borings to note bedding attitudes and to collect block samples for direct shear testing along bedding planes. The log of Boring B-1 is reported on figure 20. The geologic lithology of the section analyzed in this example is predominantly siltstone. The bedding dips out of the proposed cut slope at an apparent angle of approximately 12 degrees.

4.3.2 Geotechnical Properties

4.3.2.1 Intact Rock

The claystone and siltstone materials within the different bedrock formations exhibit similar shear strength parameters. Based upon laboratory test results, a cohesion of 50 kPa, a friction angle of 35 degrees, and a unit weight of 18.8 kN/m³ were assigned to intact claystone and siltstone bedrock.

LAYER DEPTH (M)	MATERIAL DESCRIPTION	ATTITUDE	SYMBOLIC LOG	EL. (M)	SAMPLES		COMMENTS
					NUMBER	REC (%) REC & RQD (%)	
4.0	Bedrock on surface, very dry Buff colors some gravel, siltstone some sand.			805			Monitor with PID: Oppm O2 = 16.3 at bottom exp = 0% Will pump O2 downhole during logging
6.0	Light to medium grey, clayey diatomaceous siltstone	N85W 19S					
	3 cm. Sandstone, grey, ironstained Back to dense grey siltstone as above						
9.0	Slickenside surface in clayey siltstone 2 cm. thick very clayey, medium to dark grey silty claystone with slickensides. Orange stained sand 1/4 to 1/2" thick Dense, medium grey siltstone again	N88E 21S		800	S1		
		N45W 45NE					
15.0	Dense siltstone as above	N80E 20S		795	S2	90	
		N10E 25SE					
21.0	21-22.5 m. Hard brittle zone (hard and chipped) breaks irregular - a bit cemented in siltstone still.	N85W 24S		790	S2		
22.5	Siltstone as above						
26.5	Hard zone same as 21-22.5 m. above						
27.0	27-28 m. Hard cemented siltstone tan to medium grey Back to medium grey siltstone, more cemented than as above - shaley siltstone, hard to chip out.	N56W 22SW		785	S3		
31.0	15 cm. very well cemented siltstone, light tan as zone 27-28 m. Grey siltstone, cemented	N35E 8SE		780	S4		
34.0	large gravel/cobbles cemented siltstone						
35.0	4" thick light tan/orange tan highly cemented siltstone. Back to grey siltstone, firm and hard thin bedded	N75W 22SW N8E 6SE		775	S4	95	
40.0	Due to unstable rock, downhole logging completed at Total depth 40 m	N55W 13SW		770			

CONTRACTOR
EQUIPMENT CME 75
DRILL MTHD BUCKET AUGER
DIAMETER 24 cm
LOGGER TW/EH **REVIEWER** THH
NORTHING 776.7
EASTING 2816.6
ANGLE Vertical
BEARING —
PRINTED 18 MAR 96

REMARKS:

 SEE KEY SHEET FOR SYMBOLS AND ABBREVIATIONS

Figure 20. Example 4 boring log.

4.3.2.2 Bedding Plane/Claystone and Siltstone Seam Material

A limited number of laboratory direct shear and triaxial shear test results were performed on intact and remolded samples of claystone and siltstone material. Data on other claystone and siltstone strata of similar origins but different locations were also available. Due to the similarity in the index properties reported for these strata and those reported for material from the project site, and considering that these bedrock formations are marine deposits that are typically relatively uniform over large areas, the data from the other claystone and siltstone strata in the area were used in developing shear strength parameters for the stability analyses. In addition to this laboratory data, there were a number of landslides in the area from which shear strengths could be back calculated.

Analysis of this data indicated that the peak shear strength of the claystone and siltstone materials could be conservatively characterized by a lower bound strength envelope with a friction angle of 19 degrees and cohesion of 50 kPa. Based largely on strength parameters back-analyzed from landslides in the same formations, a friction angle of 12 degrees and a cohesion value of 10 kPa were assigned to the residual shear strength parameters for the claystone and siltstone seam material. A unit weight of 18.8 kN/m³ was assigned to the claystone and siltstone seam material. The shear strength envelopes for the different materials are reported on figure 21.

4.4 DETERMINISTIC SEISMIC HAZARD ANALYSIS

The project site is located about 7.5 km from a strike-slip fault capable of generating a maximum credible earthquake (MCE) with a moment magnitude, M_w , of 7. In order to evaluate the value of maximum horizontal acceleration at the site from the MCE, five different attenuation relationships for rock sites were considered.

Figure 22 illustrates the calculation of the MCE peak ground acceleration. This figure provides the reference for each attenuation relationships and the mean and mean plus one standard deviation peak ground acceleration at the site for each attenuation relationship.

The average of the mean values of peak ground acceleration, 0.4 g, will be used in the design.

4.5 SLOPE STABILITY ANALYSIS

4.5.1 Design Criteria

The slope stability criteria imposed by local regulators required a minimum static factor of safety of 1.5. For seismic conditions, a factor of safety of 1.0 when using a seismic coefficient equal to $0.5 a_{max}/g$ in a pseudo-static limit equilibrium analysis was considered acceptable. The rationale for this seismic design criterion is discussed in chapter 7.2.2 of volume I. The seismic coefficient established using this criteria was $(0.5)(0.4g)/g = 0.20$.

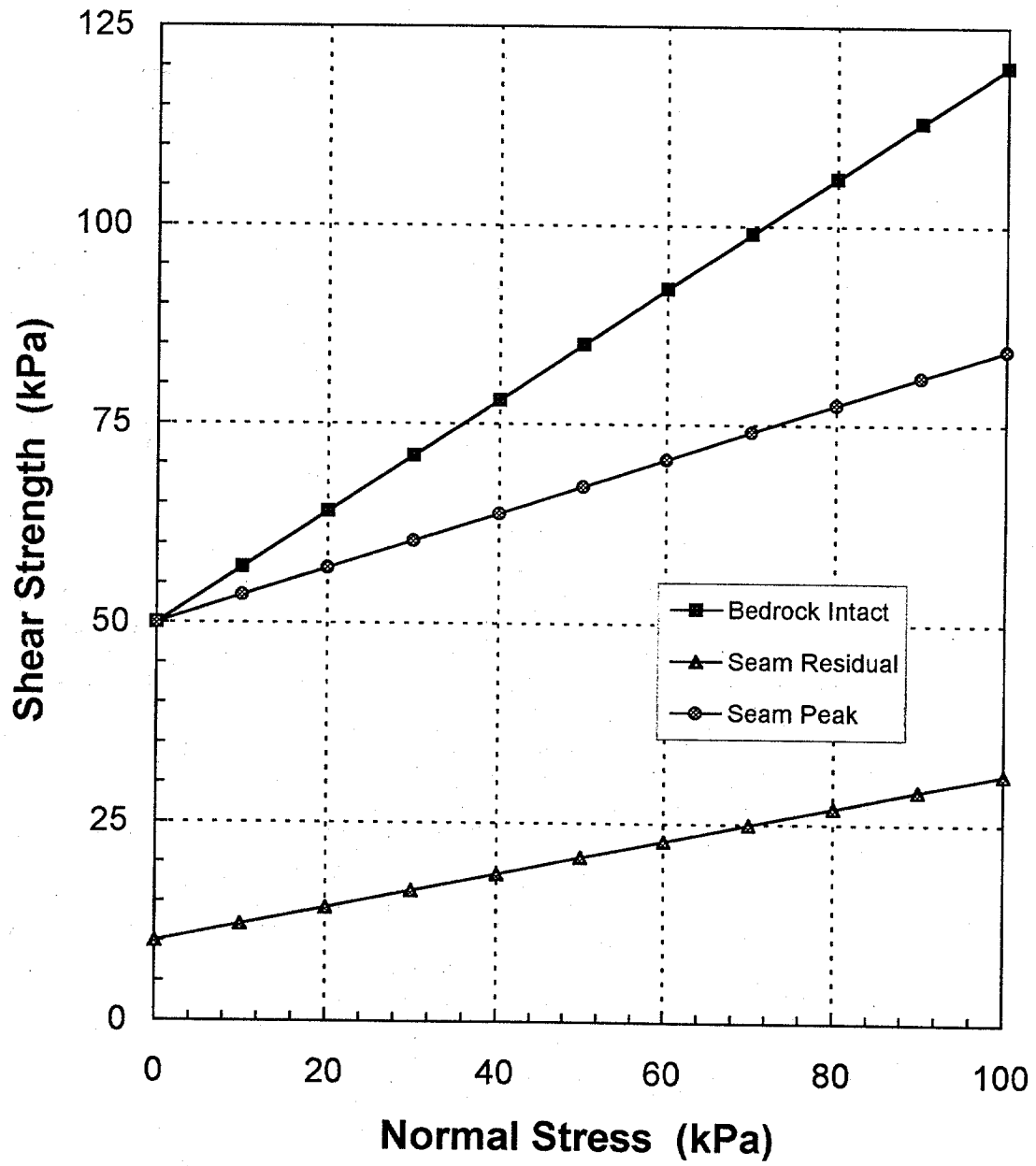
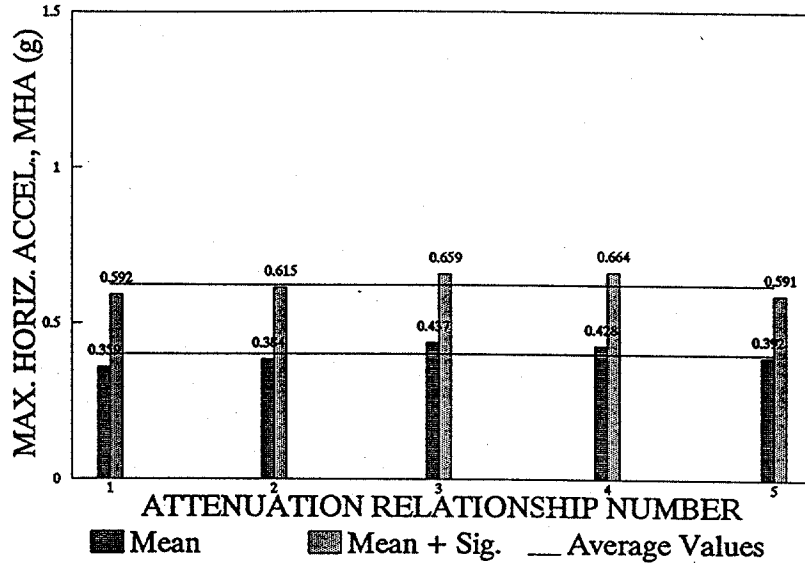


Figure 21. Shear strength envelopes for site materials.

MHA VALUES BY SELECTED ATTENUATION RELATIONSHIPS

$M_w = 7.0$

SITE TO SOURCE DISTANCE = 7.5 km



Attenuat. Relat. Number	SELECTED ATTENUATION RELATIONSHIPS ROCK SITES/STRIKE-SLIP FAULTS		MAX. HORIZONTAL ACCELERATION	
	Reference	Summary	Mean	Mean + Sig.
1	Campbell, K.W. (1993) "Empirical Prediction of Near-Source Ground Motion From Large Earthquakes," Proc. Internat. Workshop on Earthquake Hazard and Large Dams in the Himalaya, Sponsored by the Indian National Trust for Art and Cultural Heritage (INTACH), New Delhi, India, 7 p. (plus Appendices).	Hard Rock (< 10 m of Sediments) Updated by W.W. Near Source Events Strong Earthquakes ($M_w = 8$) World-Wide (W.W.) Data Set Focal Depth < 25 km	0.359	0.592
2	Boore, D.M., Joyner, W.B. and Fumal, T.E. (1993) "Estimation of Response Spectra and Peak Accelerations From Western North America Earthquakes: An Interim Report," U.S. Geological Survey Open File Report 93-509, 15 p.	Rock Site B ($360 < V_s < 750$ m/s) Western U.S. Data Set $M_w < 7.5$; $R < 80$ km Shallow Earthquakes (< 20 km) Prediction of Larger Horizontal Comp.	0.384	0.615
3	Sadigh, K., Chang, C.-Y., Abrahamson, N.A., Chiou, S.J., and Power, M.S. (1993) "Specification of Long-Period Ground Motions: Updated Attenuation Relationships for Rock Site Conditions and Adjustment Factors for Near-Fault Effects," Proc. ATC-17 Seminar on Seismic Isolation, Passive Energy Dissipation, and Active Control, Applied Technology Council, Vol. 1, 59-70.	Rock Sites West. U.S. + World-Wide Data Set Shallow Earthquakes (< 20 km) $M_w = < 8$; Near Fault Option Both Horiz. Components Considered	0.437	0.659
4	Silva, W.J. and Abrahamson, N.A. (1993) "Attenuation of Long Period Strong Ground Motions," Proc. American Society of Military Engineers PVP Conference, Denver, Colorado, 5 p.	Rock Sites World-Wide $M_w 6^+$ Data Set Average of Horiz. Components Used	0.428	0.664
5	Idris, I.M. (1993) "Procedures for Selecting Earthquake Ground Motions at Rock Sites," Report NIST GCR 93-625, U.S. Department of Commerce, National Institute of Standards and Technology, Gaithersburg, Maryland, 7 p.	Rock Sites $4.6 < M_w < 7.4$; $1 < R < 60$ km Randomly Oriented Horizontal Comp.	0.392	0.591

6 AVERAGE OF THE FIVE PGA VALUES LISTED ABOVE:

0.400 0.624

Figure 22. Calculation of MCE peak ground acceleration.

The shear strength parameters used in the long term static stability were the peak values for the intact rock and the residual values for the claystone and siltstone seams. The shear strength parameters used in the pseudo-static seismic (short term) analysis were the peak values for both the intact rock and the claystone and siltstone seams.

4.5.2 Stability Analyses

The computer program STABL4 (Lovell et al., 1984) was used to assess the stability of the slope. STABL4 employs limit equilibrium principles to provide general solutions to slope stability problems using the Modified Bishop or Modified Janbu methods to calculate factors of safety. Potential sliding surfaces can be pre-specified or randomly generated. The Modified Janbu method was used for the slope stability analyses performed herein.

Both circular and planar failure surfaces were evaluated. Planar failure surfaces generated for analysis considered the presence of weak zones such as the claystone and siltstone seams. The locations of the potential failure surfaces were varied in the slope stability analyses to evaluate the depth to the potential failure surface (the seam of weak material along the bedding).

The STABL4 input and output for the critical surface (the surface with the lowest pseudo-static factor of safety) are provided following this design example.

4.6 RESULTS

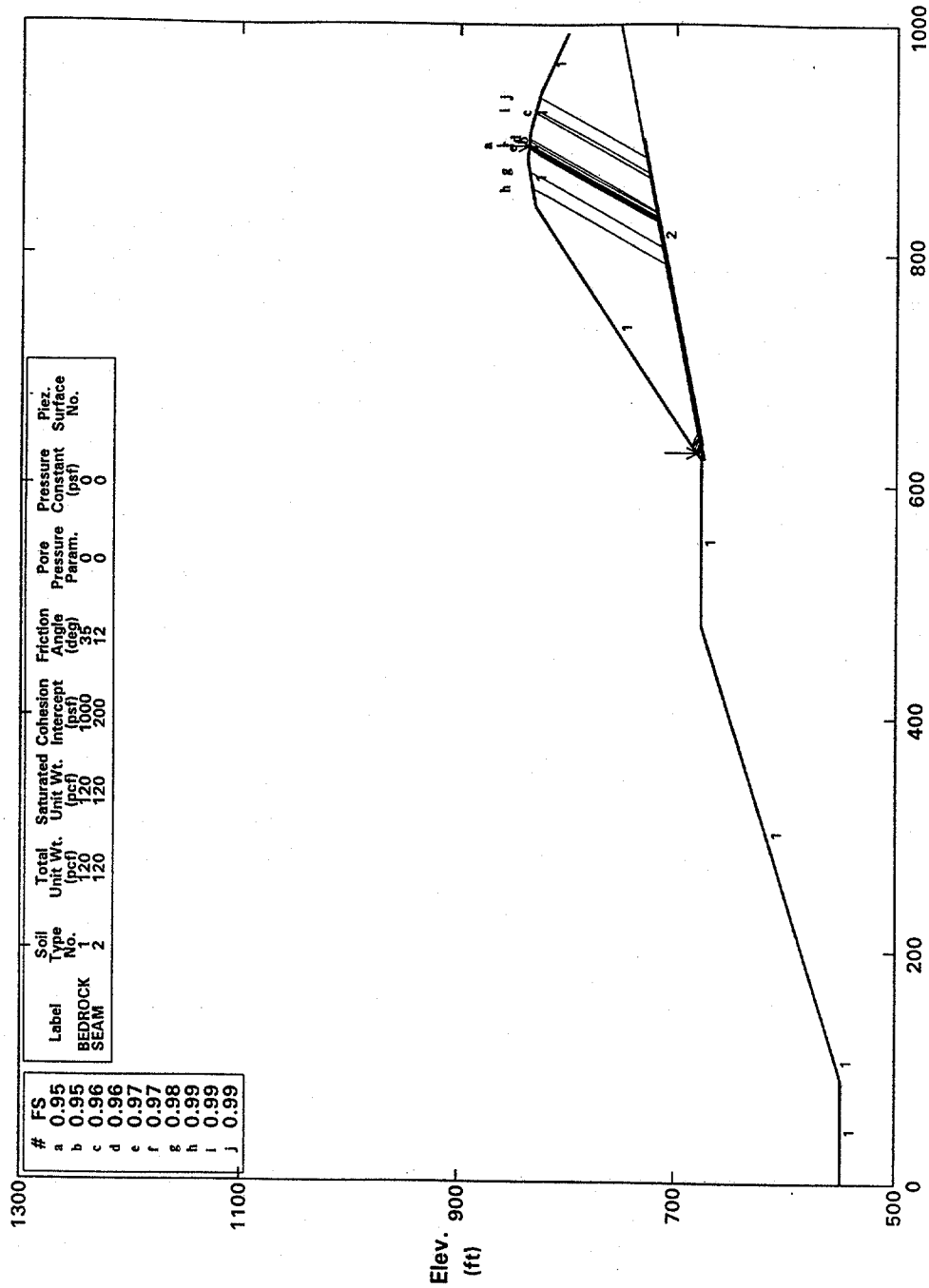
Figure 23 shows the most critical failure mechanisms for the slope. A wedge analysis was performed assuming sliding along the weak seam dipping at a 12-degree angle out of slope. The minimum calculated factor of safety under static loading conditions is 0.95. Under a seismic coefficient of 0.2, the pseudo-static factor of safety of the slope is 0.93, which is also not sufficient, as shown on figure 24.

Figures 25 and 26 show the stability analysis for circular deep seated failures under static and pseudo-static conditions. The analyses using circular surfaces give higher factors of safety than the wedge analyses, indicating that stability is controlled by the strength of the weak seams in the rock mass.

The results indicate that the proposed grading plan for the highway cut does not meet the requirements for either static or seismic conditions. Geometric constraints did not allow the engineers to flatten the slopes to increase stability. Therefore, structural stabilization solutions were investigated.

Highway Cut - GEC#2 - Static Analysis Seam daylight at road level

Ten Most Critical. R:GEC-F23.PLT By: THH 09-03-96 11:56am



PCSTABLE FSmin = 0.95 X-Axis (ft)
 Factors Of Safety Calculated By The Modified Janbu Method
 Note: 1 ft=0.3048 m, 1 psf=47.9 N/m², 1 pcf = 0.157 kN/m³

Figure 23. Critical failure mechanisms for Bench 1, static loading.

Highway Cut - GEC#2 - Seismic Analysis Seam daylight at first bench
 Ten Most Critical. R:GEC-F24.PLT By: THH 09-03-96 11:58am

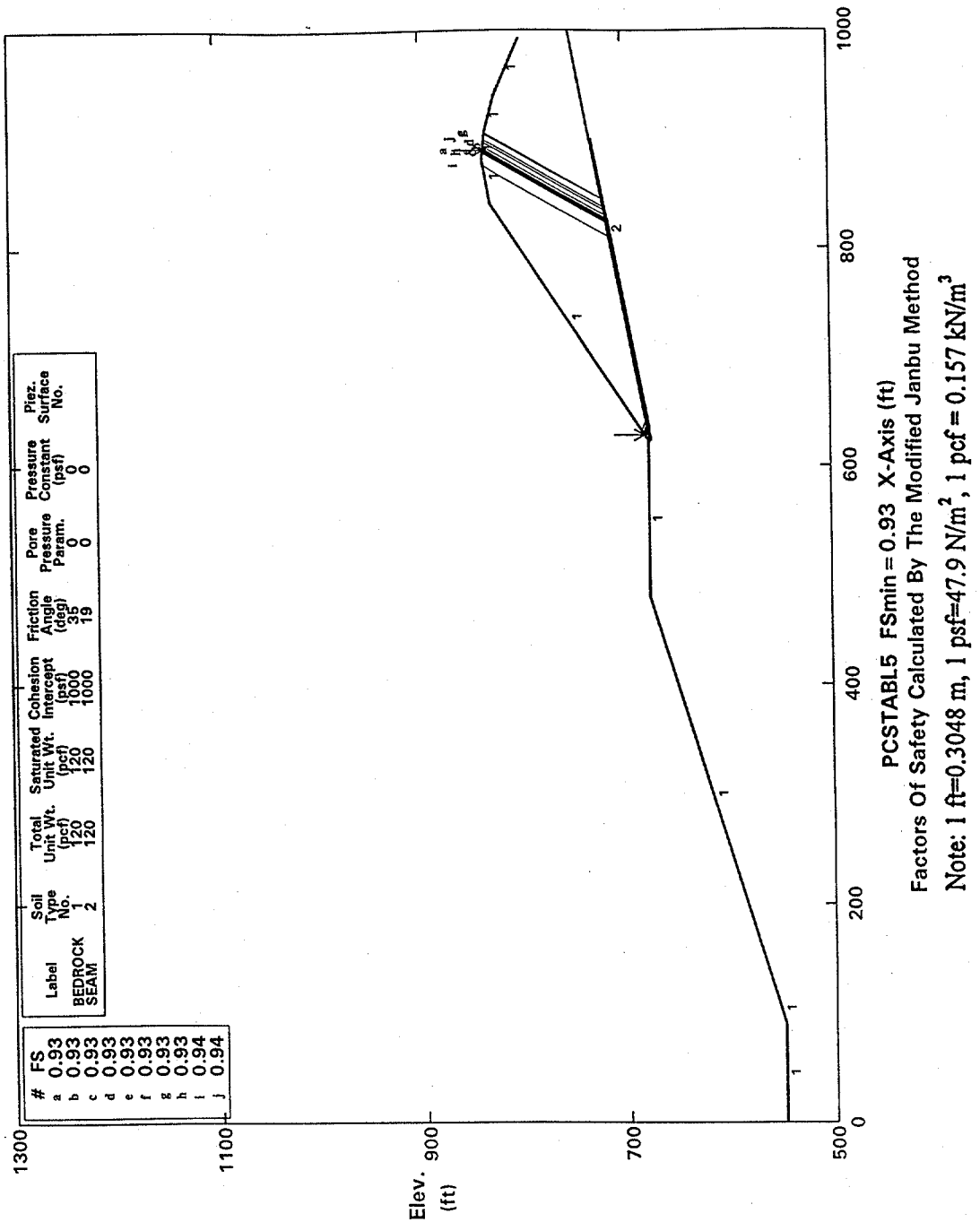
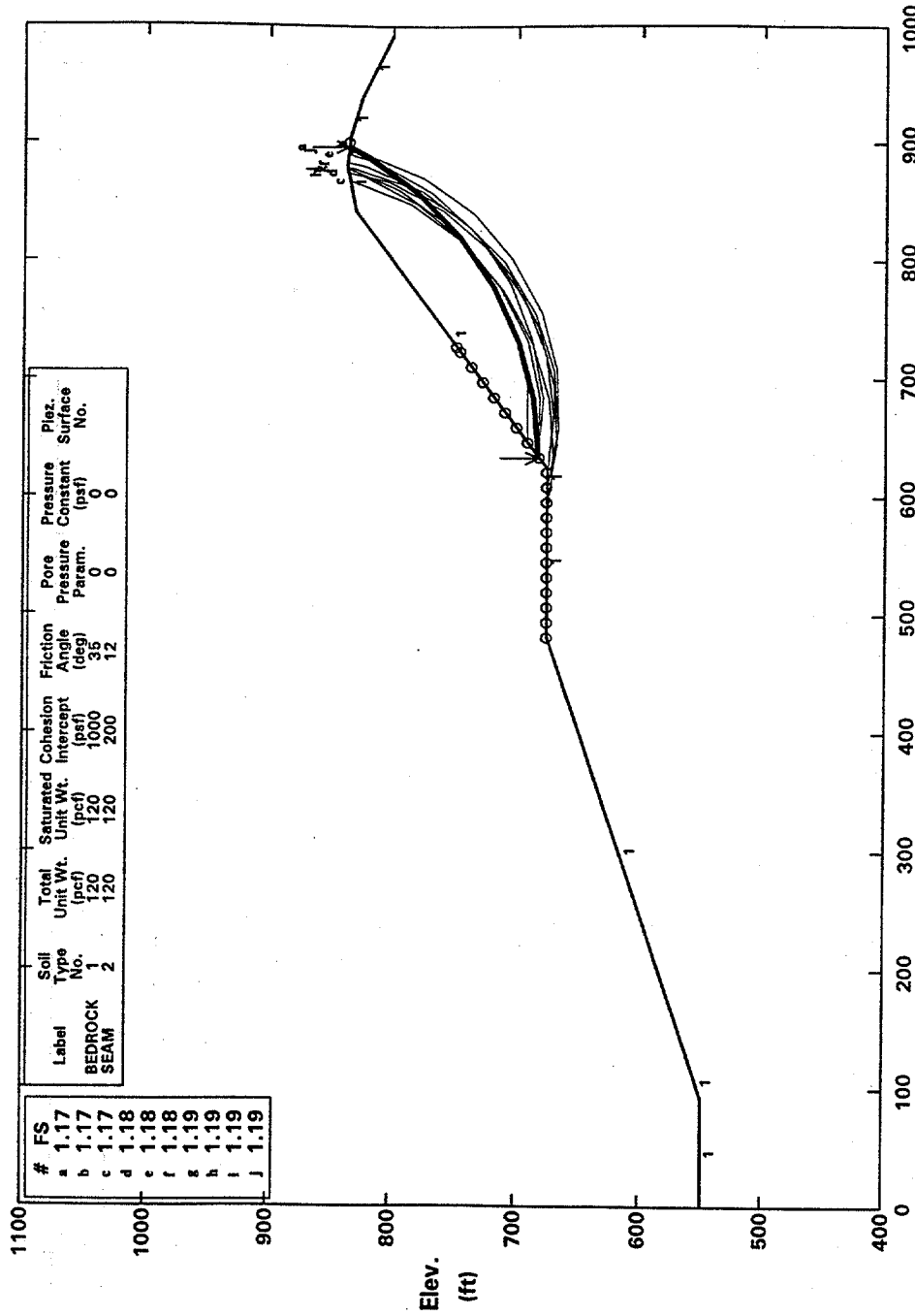


Figure 24. Critical failure mechanisms for Bench 1, pseudo-static loading.

Highway Cut - GEC#2 - Static analysis - Deep seated circular mechanism
 Ten Most Critical. R:GEC-F25N.PLT By: THH 09-03-96 10:10am



PCSTABL FSmin = 1.17 X-Axis (ft)
 Factors Of Safety Calculated By The Modified Janbu Method
 Note: 1 ft=0.3048 m, 1 psf=47.9 N/m², 1 pcf = 0.157 kN/m³

Figure 25. Critical deep-seated failure mechanism, static loading.

Highway Cut - GEC#2 - Seismic analysis - Deep seated circular mechanism

Ten Most Critical. R:GEC-F26N.PLT By: THH 09-03-96 10:12am

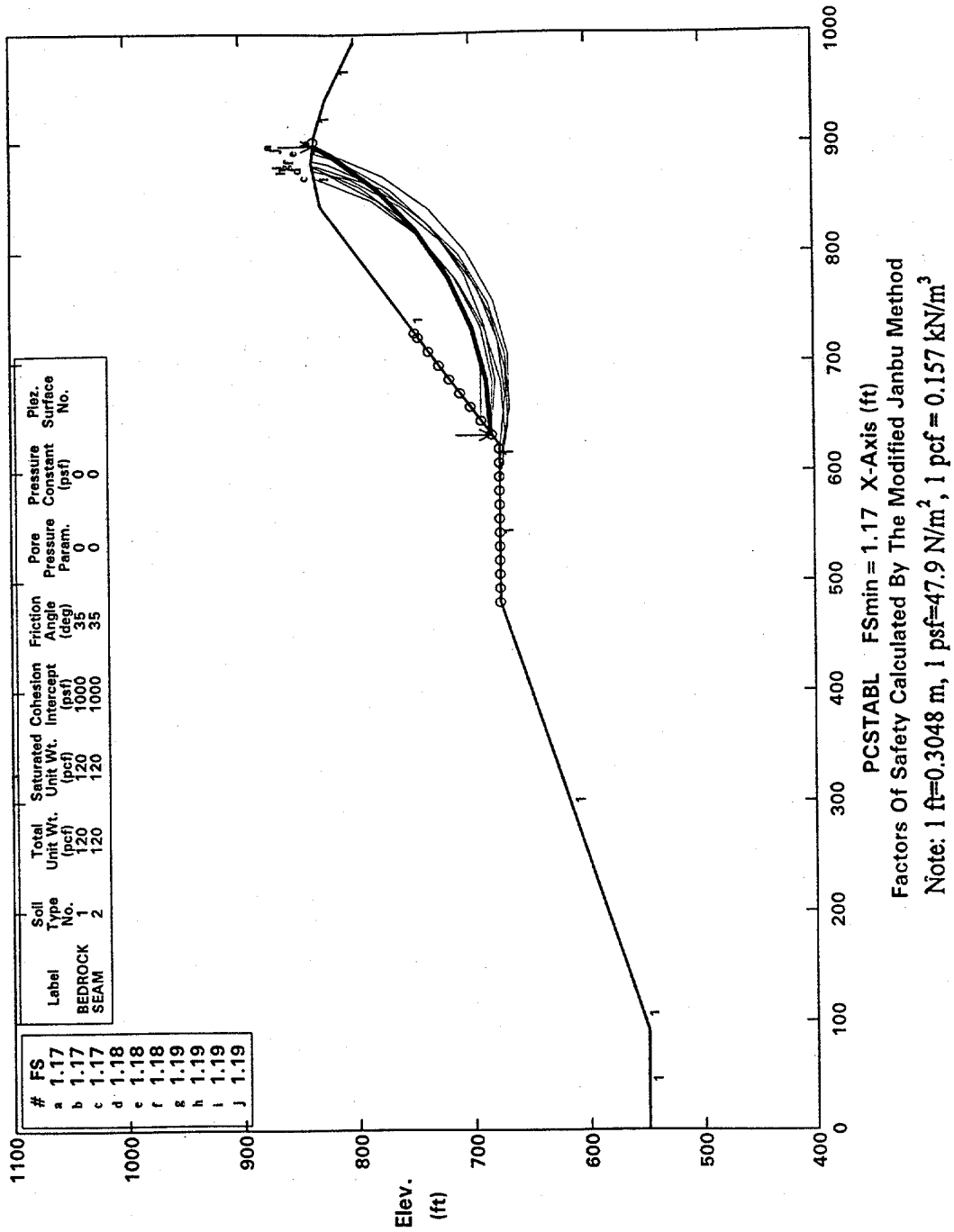


Figure 26. Critical deep-seated failure mechanism, pseudo-static loading.

4.7 REMEDIAL SOLUTION

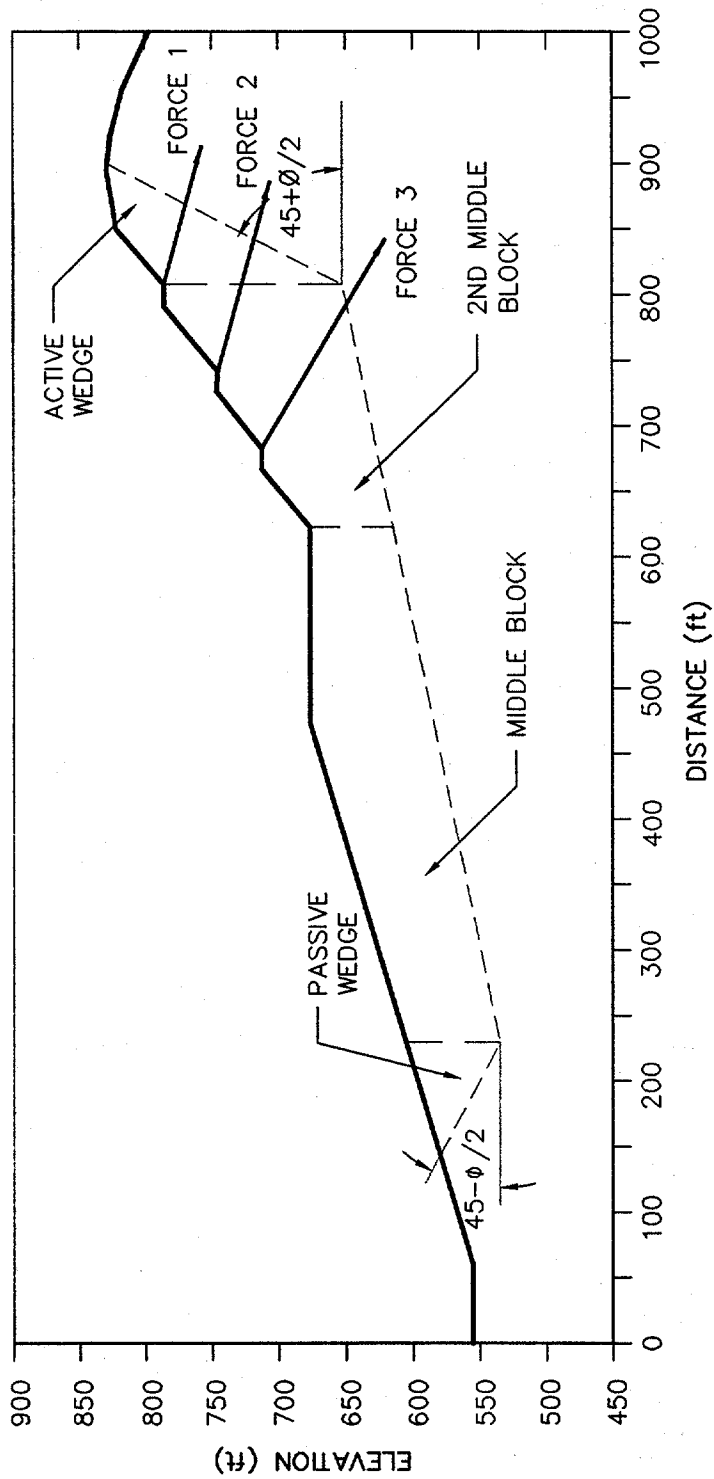
To increase the factors of safety to the required level, structural stabilization of the slope was required. The proposed stabilization system consisted of three rows of soil anchors located on benches. In general, the lowest row of anchors was designed to stabilize a global potential failure surface that extends parallel to the apparent dip and would daylight at road level or pass under the proposed roadway. The upper two rows of anchors were designed to stabilize the potential failure mass contained within the 1.5H:1V slopes. While many engineers prefer not to use benches on slopes above highways due to the potential for rockfalls, that potential was considered relatively low for this slope and the benches facilitate both access to the anchors for maintenance and monitoring and surface water drainage control.

The required anchor capacities were computed using hand calculations. Anchor loads were evaluated for all surfaces with a factor of safety below the desired value to find the required anchor capacity. The pseudo-static load due to a seismic coefficient of 0.20 was included in these calculations. The critical failure mechanisms were modeled as 4-block wedge mechanisms consisting of an upper (active) wedge, two middle sliding blocks, and a lower (passive) wedge, as shown on figure 27. The 4-block wedge slope stability hand calculations were performed using force equilibrium. In these inclinations, the interslice forces were assumed to be inclined at 12 degrees to the horizontal (i.e., parallel to the weak bedding plane). The calculation used an iterative approach to find a set of four normal forces, three interslice forces, and an anchor force that produced the required factor of safety against instability. The set of simultaneous equations were programmed into commercially available spreadsheet software.

The purpose of this chapter is not to show the detailed design of anchors; however, it is important to note that there are several potential failure mechanisms that need to be considered in anchor design:

- failure of the grout-reinforcement interface in shear;
- failure of the anchor reinforcement in tension (i.e., breakage of the anchor);
- failure of the soil-grout interface in shear (i.e., pullout of the anchor); and
- pull out of the anchor from the moving soil mass.

The anchors were installed on the benches from the top row down as the cut progressed. Each anchor was designed to resist the calculated anchor force and to develop this resistance below the potential failure surfaces (i.e., below the weak bedding plane). Information on the analysis and design of permanent ground anchors can be found in Cheney (1988).



NOTE: 1ft=0.3048 m 1psf=47.9 N/m² 1pcf=0.157kN/m³

Figure 27. Wedge analysis of anchor system.

Written by: T.A.W. Date: 96 / 08 / 01 Reviewed by: E.K. and N.M. Date: 96 / 08 / 02
 YY MM DD YY MM DD

Client: FHWA Project: GEC-3 Project/Proposal No.: GE3686 Task No.: F

EXAMPLE 4 - SLOPE STABILITY ANALYSIS
PCSTABL Output File

** pcSTABL4 **
 by
 Purdue University

--Slope Stability Analysis--
 Simplified Janbu Method of Slices
 or Simplified Bishop Method

Run Date:
 Time of Run:
 Run By:
 Input Data Filename: gec-f23.inp
 Output Filename: gec-f23.ouu

PROBLEM DESCRIPTION Highway Cut - GEC#2 - Static Analysis
 Seam daylight at first bench

BOUNDARY COORDINATES

9 Top Boundaries
 10 Total Boundaries

Boundary No.	X-Left (ft)	Y-Left (ft)	X-Right (ft)	Y-Right (ft)	Soil Type Below Bnd
1	.00	49.00	90.00	49.00	1
2	90.00	49.00	110.00	55.00	1
3	110.00	55.00	480.00	176.00	1
4	480.00	176.00	623.00	176.00	1
5	623.00	176.00	840.00	330.00	1
6	840.00	330.00	880.00	337.50	1
7	880.00	337.50	905.00	335.00	1
8	905.00	335.00	940.00	325.00	1
9	940.00	325.00	993.00	300.00	1
10	623.00	175.00	1000.00	251.70	2

ISOTROPIC SOIL PARAMETERS

2 Type(s) of Soil

Soil Type No.	Total Unit Wt. (pcf)	Saturated Unit Wt. (pcf)	Cohesion Intercept (psf)	Friction Angle (deg)	Pore Pressure Param. (psf)	Pressure Constant (psf)	Piez. Surface No.
1	120.0	120.0	1000.0	35.0	.00	.0	0
2	120.0	120.0	200.0	12.0	.00	.0	0

A Critical Failure Surface Searching Method, Using A Random Technique For Generating Sliding Block Surfaces, Has Been Specified.

The Active And Passive Portions Of The Sliding Surfaces Are Generated According To The Rankine Theory.

50 Trial Surfaces Have Been Generated.



Written by: T.A.W. Date: 96 / 08 / 01 Reviewed by: E.K. and N.M. Date: 96 / 08 / 02
 YY MM DD YY MM DD

Client: FHWA Project: GEC-3 Project/Proposal No.: GE3686 Task No.: F

2 Boxes Specified For Generation Of Central Block Base

Length Of Line Segments For Active And Passive Portions Of Sliding Block Is 62.0

Box No.	X-Left (ft)	Y-Left (ft)	X-Right (ft)	Y-Right (ft)	Width (ft)
1	623.00	174.00	723.00	194.30	.10
2	723.10	194.30	900.00	230.30	.10

Following Are Displayed The Ten Most Critical Of The Trial Failure Surfaces Examined. They Are Ordered - Most Critical First.

* * Safety Factors Are Calculated By The Modified Janbu Method * *

Failure Surface Specified By 8 Coordinate Points

*** .947 ***

Failure Surface Specified By 8 Coordinate Points

*** .952 ***

Failure Surface Specified By 7 Coordinate Points

*** .960 ***

Failure Surface Specified By 8 Coordinate Points

*** .963 ***

Failure Surface Specified By 8 Coordinate Points

*** .968 ***

Failure Surface Specified By 8 Coordinate Points

*** .972 ***

Failure Surface Specified By 8 Coordinate Points

*** .979 ***

Failure Surface Specified By 8 Coordinate Points

*** .989 ***

Failure Surface Specified By 7 Coordinate Points

*** .990 ***



Written by: T.A.W. Date: 96 / 08 / 01 Reviewed by: E.K. and N.M. Date: 96 / 08 / 02
YY MM DD YY MM DD

Client: FHWA Project: GEC-3 Project/Proposal No.: GE3686 Task No.: F

Failure Surface Specified By 7 Coordinate Points

*** .991 ***

Note: Failure surface coordinates omitted from the original PCSTABL output.



4.8 SUMMARY AND CONCLUSIONS

Construction of a new highway required regrading of a hillside. The highest cut slope rose about 44 m above grade at an inclination of 1.5H:1V. The site geology is characterized as sedimentary bedrock of marine origin. It is described as a light tan sandy siltstone with local interbedded clay seams. The bedding dips out at the proposed cut slope at an apparent angle of 12 degrees. The site is located about 7.5 km from a strike-slip fault capable of generating earthquakes of moment magnitude (M_w) of 7.0. A seismic hazard analysis was conducted using five attenuation relationships, resulting in a maximum horizontal ground acceleration of 0.4 g for use in design at the site.

Slope stability criteria called for a static factor of safety of 1.5 and a pseudo-static factor of safety of 1.1 for a seismic coefficient of 0.2 (one-half the peak ground acceleration). Initial slope stability analyses indicated that the proposed grading design would not meet the static and pseudo-static criteria.

A remedial solution was developed to stabilize the slope. The solution was based on using permanent ground anchors located on benches. The ground anchors were also designed for a seismic coefficient of 0.2 g.

EXAMPLE 5

LIQUEFACTION POTENTIAL ANALYSIS

5.1 INTRODUCTION

5.1.1 Description of the Project

A highway project includes a channel crossing with an approach embankment and a major cable-stayed bridge structure. The embankment, which will reach a maximum height of 3.5 m near the abutment wall, is founded upon potentially liquefiable soil. The bridge will be supported on a large diameter concrete pier founded upon steel H-piles in the center of the channel. The tasks of the geotechnical engineer are to:

- evaluate the stability of the approach embankment, including the effects of seismic loading; and
- provide the structural engineer with response spectra for design of the bridge structure.

Of primary concern in this case is the evaluation of the liquefaction potential of the foundation soil for the approach embankment and the effect of local soil conditions upon the response spectra.

5.1.2 Source Materials Required

The source materials required to solve this problem include:

- volume I of this document;
- geotechnical subsurface information;
- computer program SHAKE91 for seismic site response analysis (Schnabel et al., 1972, and Idriss and Sun, 1992); and
- computer program STABL4 for slope stability analyses (Lovell et al., 1984).

5.2 GEOLOGICAL SETTING

5.2.1 Regional Setting

The site is located along a broad coastal plain of limited relief surrounded by mountains to the north and east, and water to the south and west. The site lies in an area of high seismic exposure due to its proximity to three major fault zones. Figure 28 shows the site location relative to these known faults (Faults A, B, and C). Evaluation of the historical seismicity indicated that not all of the major earthquakes (magnitude > 5.0) in the region can be attributed to the three major faults. Recent studies indicated that the seismicity not attributable to these identified faults may be attributable to an unmapped buried thrust and fold belt that is capable of producing earthquakes up to magnitude 6.5 to 7.0. Therefore, in addition to the three recognized faults, the blind thrust and fold belt has been identified as a seismic source zone impacting the site. Figure 28 shows the location of the fold and thrust zone established on the basis of micro-seismicity studies and seismic reflection profiling.

5.2.2 Local Geology

Available data from previous subsurface investigations indicated that schist and basalt basement rocks can be found at a depth of approximately 40 to 60 m in the vicinity of the site. These basement rocks are overlain by approximately 20 m of Miocene marine shale and sandstone deposits which are, in turn, overlain by Pleistocene and Holocene sediments. Borings indicate that, on shore, the top 30 m at the site consists of Pleistocene marine terrace deposits covered by 3 to 5 m of alluvium. The channel is filled with recent sediments, having been incised into the Pleistocene marine terrace and Miocene shale and sandstone deposits when sea level fell below its present elevation during the Late Pleistocene period and being subject to periodic dredging. At the project site, the channel is filled with approximately 30 m of recent deposits of silts, clays, and sand.

5.3 SEISMIC DESIGN CRITERIA

Two levels of ground motions were established by the owner in developing the seismic design criteria for the project: an "operational" level at which the structure is assumed to respond elastically with little to no damage and a "contingency" level at which some "acceptable" level of damage is expected. The amount of damage considered to be acceptable at the contingency level depends on the function of the facility, the ease of repair, and the availability of alternative transportation routes. For critical facilities defined as lifelines, the criteria for acceptable damage requires the structure to remain serviceable. For important facilities where loss of service for limited periods of time can be accommodated, the criteria is that the damage be easily repairable. For ordinary facilities, where alternative transportation routes are available, it is simply necessary to prevent collapse of the structure and loss of life. For this project, the approach embankment and bridge crossing were judged to be important, but not critical facilities, as they were important for moving freight but there were alternative routes that could accommodate emergency services. Due to the importance of the route as a freight corridor, acceptable "downtime" following a major

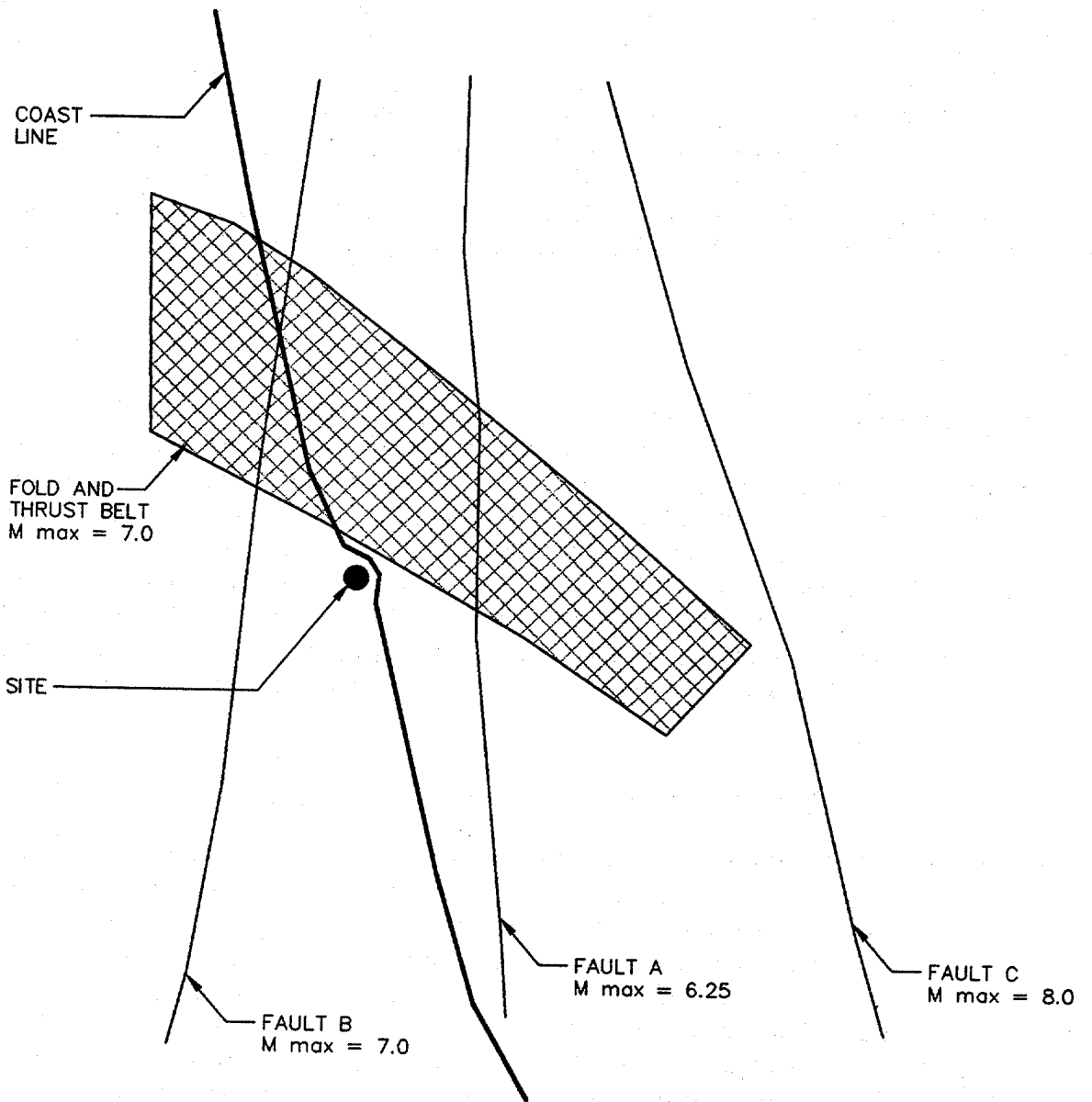


Figure 28. Example 5 site location and seismic source.

earthquake was limited to 2 to 4 weeks.

The Operational Level Event (OLE) and Contingency Level Event (CLE) were defined by the owner on a probabilistic basis. The OLE is defined as the most damaging event with a peak horizontal ground acceleration (PHGA) that has 50 percent probability of not being exceeded in a 50 year period. The CLE is defined as the most damaging event with a PHGA that has 10 percent probability of not being exceeded in a 50 year period.

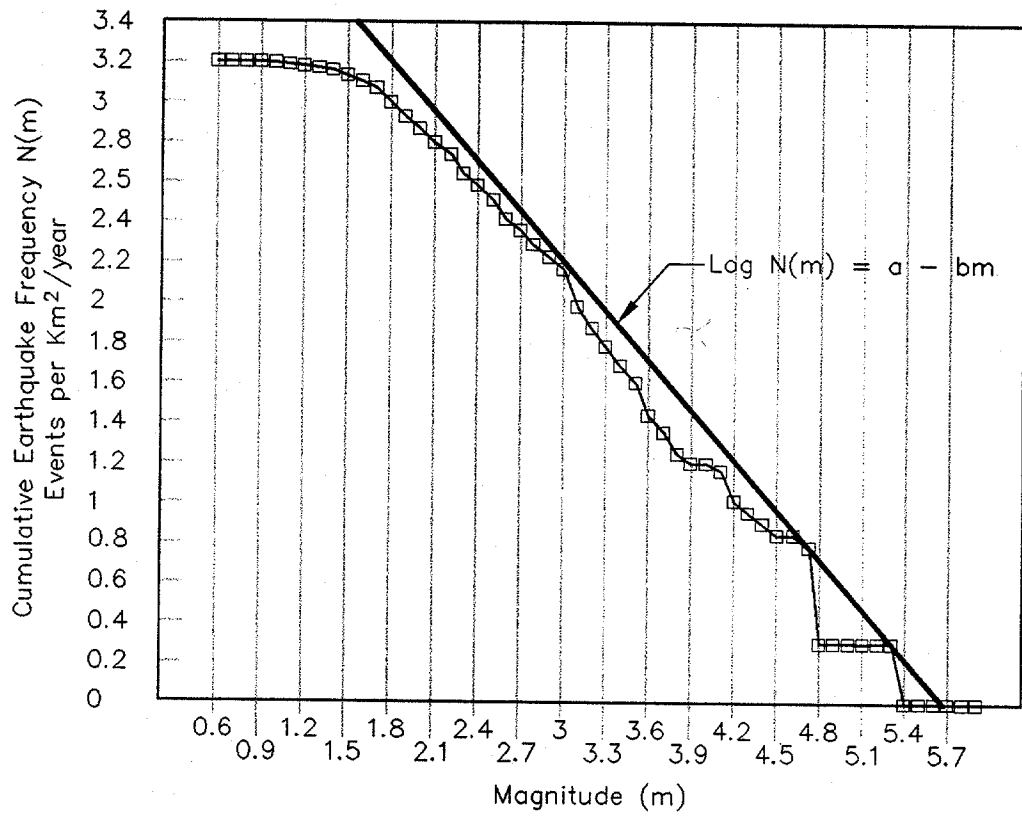
5.4 PROBABILISTIC SEISMIC HAZARD ANALYSIS

The firm ground intensity levels for the OLE and CLE design motions were evaluated on the basis of a conventional probabilistic strong shaking seismic hazard evaluation. The analyses followed the procedure originally suggested by Cornell (1968), as embodied in the computer program EQRISK (McGuire, 1976). Active faults within 100 km of the project site were identified, assigned earthquake magnitude recurrence rates on the basis of observed slip rates and historic seismicity, and assigned maximum magnitudes on the basis of the length of the fault segments. Historical seismicity and regional deformation not assigned to active faults were then assigned to either "random" seismicity or to buried blind fold and thrust belts. The three major known active faults were treated as line seismic sources while the blind thrust and fold belts and the sources of the "random" seismicity were treated as area sources. Figure 29 presents the Gutenberg-Richter recurrence plot developed for the blind thrust and fold belt on the basis of the historical seismicity. Once the magnitude-recurrence relationships were established for each source, the contribution of each source to the PHGA hazard at the site was calculated using the EQRISK computer program on the basis of the attenuation relationships developed by Campbell (1993). The sensitivity of the results to the choice of attenuation relationship and to assumptions regarding the "random" seismicity and the blind thrust and fold belt events was then investigated in subsequent analyses. The resulting seismic hazard curve adopted for the project is shown in figure 30. On the basis of this curve, the PHGA on firm soil in the OLE was established as 0.2 g. The PHGA on firm soil in the CLE was established as 0.4 g. Analysis of the results indicated that the most damaging source of the 0.2 g PHGA for the OLE would be a magnitude 8.0 event on Fault C (see figure 28) at a distance of 52 km. The most damaging event associated with the 0.4 g PHGA for the CLE was determined to be a magnitude 7.0 event within the blind thrust and fold belt at a distance of 11.3 km from the site. Table 7 summarizes the parameters of the design earthquakes.

5.5 GEOTECHNICAL INFORMATION

A subsurface exploration program which consisted of 12 geotechnical borings, 6 cone penetrometer tests (CPT), and laboratory testing on samples recovered from the borings was conducted at the site. Four of the soil borings were drilled from a barge in the channel. Cross hole seismic profiling was conducted within three of these channel borings to develop a shear wave velocity profile for seismic response analyses. The soil borings were drilled using rotary wash drilling equipment. Relatively undisturbed samples of the silts and clays in the channel were obtained for laboratory testing using

FOLD AND THRUST ZONE



$$a = 4.50$$

$$b = 0.80$$

Data covers a 34 year period

Figure 29. Recurrence relationship for blind thrust and fold belt.

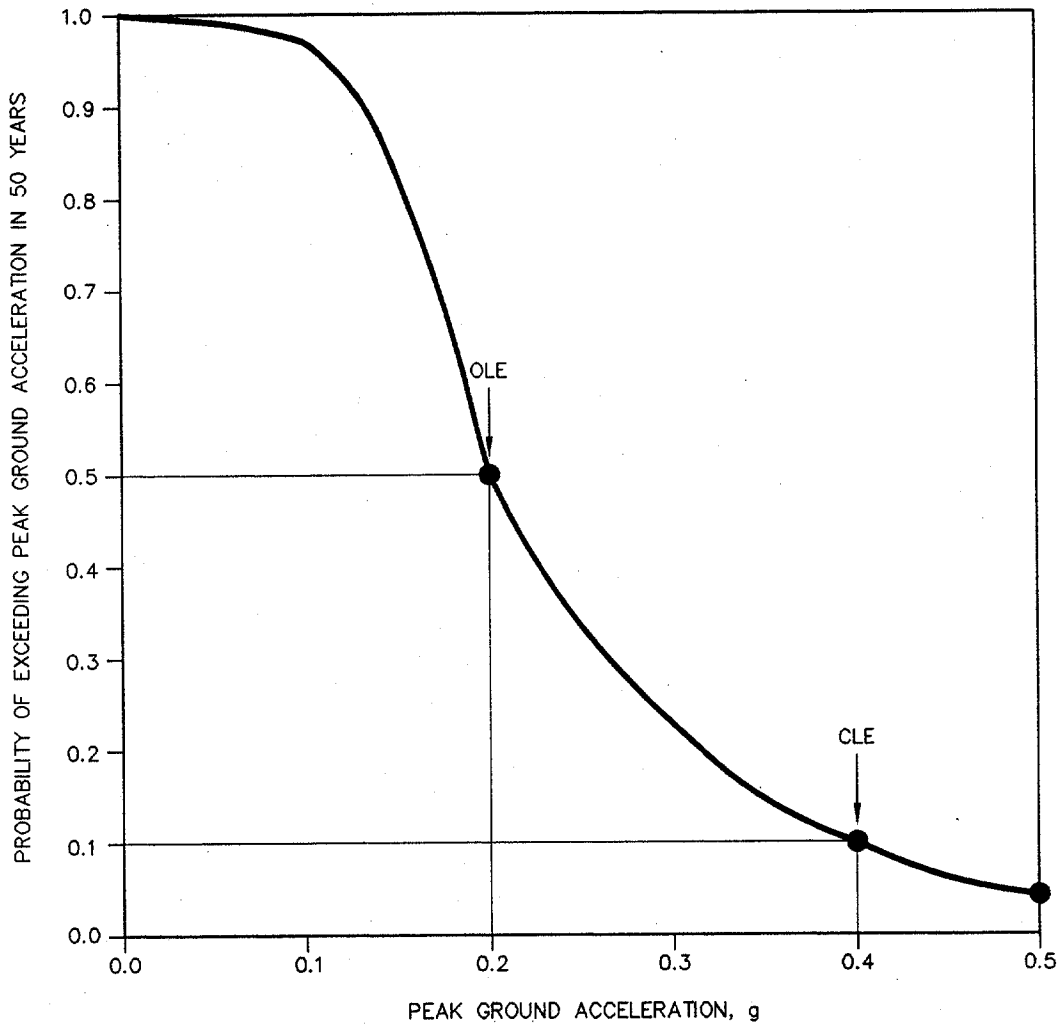


Figure 30. Seismic hazard curves.

Table 7. Summary of design earthquake parameters.

Design Event		Estimated Site-To-Source Distance	Assumed Local Site Conditions	Design Strong Motion Parameters		
Earthquake	Style of Faulting			MCE Magnitude ⁽¹⁾	Peak Ground Acceleration ⁽³⁾	Significant Duration ⁽⁴⁾
CLE (Faults A and B and the Blind Thrust)	Reverse (Blind-Thrust)	$M_w = 7$	Weak Rock (Joyner and Boore Site Class B) ⁽²⁾	PGA = 0.4 g	$D_s \approx 14.2$ sec	0.09 g
OLE (Fault C)	Strike-Slip (Right Lateral)	$M_w = 8$	Weak Rock (Joyner and Boore Site Class B) ⁽²⁾	PGA = 0.2 g	$D_s \approx 38.3$ sec	0.03 g

- Notes:
- (1) Moment Magnitude (M_w) corresponding to the Maximum Credible Earthquake (MCE).
 - (2) Joyner and Boore Site Class B assumes that shear wave velocity (V_s) in the upper 30 m of profile is between 360 and 750 m/s.
 - (3) Estimated median Peak Horizontal Ground Acceleration (PHGA) in hypothetical bedrock outcrop at geometric center of the site.
 - (4) Significant duration of strong shaking (D_s) defined by Trifunac and Brady (1975) as the time needed for the Husid plot to build from 5 to 95 percent of its final value. In this study, D_s was estimated, according to Dobry et al. (1978), as: $\log D_s = 0.432 M_w - 1.83$.
 - (5) Root Mean Square Acceleration (RMSA) over the significant duration of the record. In this study, RMSA was estimated using the Kavazanjian et al. (1985) attenuation equation for RMSA [Model I (TB)].

75-mm-diameter Shelby tubes. In the land-side borings, Standard Penetration Tests were conducted in accordance with ASTM Standard D 1586-84 at 1.5 m intervals. The six CPT soundings were advanced on land to continuously log the resistance of soil strata at the site to identify weak layers that may go unnoticed in traditional borings. The SPT blow counts and equivalent blow counts from the CPT soundings were used in the liquefaction potential analysis.

Based on the results of the subsurface exploration program, characteristic stratigraphic profiles were developed for the site. For the purpose of geotechnical analyses, typical properties were assigned to each of the characteristic stratigraphic units. The stratigraphic profile beneath the approach embankment is shown in figure 31. The log for Boring B-2 is shown in figure 32. The idealized stratigraphic profile of sediments found beneath the embankment near the bridge abutment consists of 1.5 m of soft organic silt underlain by 7 m of medium-dense sand underlain by 5 m of medium dense to dense silty sands underlain by dense to very dense sand and gravel. The representative profile of uncorrected SPT blow counts beneath the approach embankment, developed from both the borings and the CPT soundings, is shown in figure 33. The stratigraphic profile at the center of the channel consists of 18 m of silt, sand, and clay layers underlain by dense sand and gravel. Figure 34 shows the shear wave velocity profile within the channel developed from the cross hole soundings. Figure 34 also shows the shear wave design profile used in the SHAKE analyses.

5.6 DESIGN OF THE EMBANKMENT

5.6.1 Design Considerations

Preliminary design called for an approach embankment with an 18-m-wide crest and side slopes at an inclination of 1.5H:1V. The design called for excavation of the 1.5-m layer of organic silt, placement of a geotextile separation layer, and construction of the embankment. The embankment was compacted to 95 percent of the maximum dry density determined using ASTM D-1557, the Modified Proctor Compaction Test. The embankment is about 150 m long and varies in height to reach a maximum of 3.5 m over the last 100 m near the abutment wall of the bridge. Conventional geotechnical analyses performed for design of the embankment, including static slope stability and settlement analyses, were performed but are not described herein. Seismic performance analyses for the embankment that are described herein include:

- dynamic slope stability;
- liquefaction potential of the underlying soil; and
- the consequence of liquefaction.

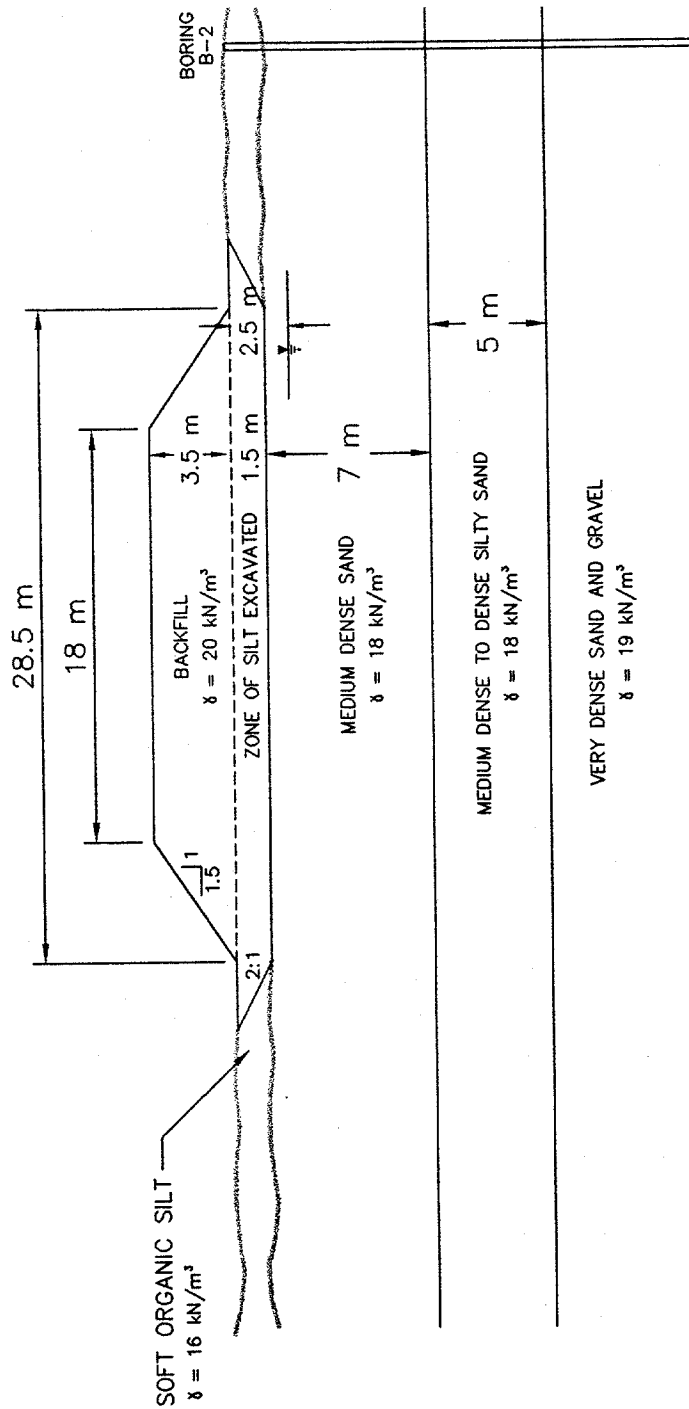


Figure 31. Stratigraphic profile under embankment.

GEOSYNTEC CONSULTANTS		BORING B-2		SHEET 1 OF 1							
2100 Main Street, Suite 150 Huntington Beach, California 92648 Tel: (714) 969-0800 Fax: (714) 969-0820		START DATE 12 JAN 96		FINISH DATE 12 JAN 96							
GS FORM: SOIL2 3 March 96		PROJECT GEC#2		LOCATION ANYWHERE, U.S.A.							
BORING RECORD			NUMBER CE 5200								
DEPTH BGS (m)	MATERIAL DESCRIPTION	SYMBOLIC LOG	EL. ABOVE MSL (m)	SAMPLES		COMMENTS	TEST RESULTS				
				REC & ROD (%) OR REC (%)	SPT VALUES BLOWS PER 150mm N		MOISTURE CONTENT (%)	LIQUID LIMIT (%)	PLASTIC LIMIT (%)	X FINES < #200 SIEVE	
	Yellow, loose silty sand with some shell fragments.		-30			Max. water table					
				r-1	5-4-5	9					6
				r-2	5-5-7	12					5
				r-3	6-7-7	14					4
7.8				r-4	7-8-7	15					7
	Sand, yellow-brown, medium dense to dense with some silt and clay lenses.		-20	r-5	9-8-9	17					8
				r-6	9-8-11	19					6
13.0				r-7	11-14-12	26					8
	Dense sand and gravel			r-8	15-16-16	32					10
				r-9	16-19-21	40					6
				r-10	24-23-25	48					7
				r-11	28-32-30	62					8
20.0	End of drilling at 20 m.		-10								

CONTRACTOR	NORTHING 31786.4	REMARKS:
LICENSE	EASTING 30363.5	
DRILL MTHD CME 75	ANGLE Vertical	
DIAMETER 8.25 HSA	BEARING	
LOGGER BH	REVIEWER TH	
	PRINTED 28 MAR 96	SEE KEY SHEET FOR SYMBOLS AND ABBREVIATIONS

Figure 32. Example 5 boring log.

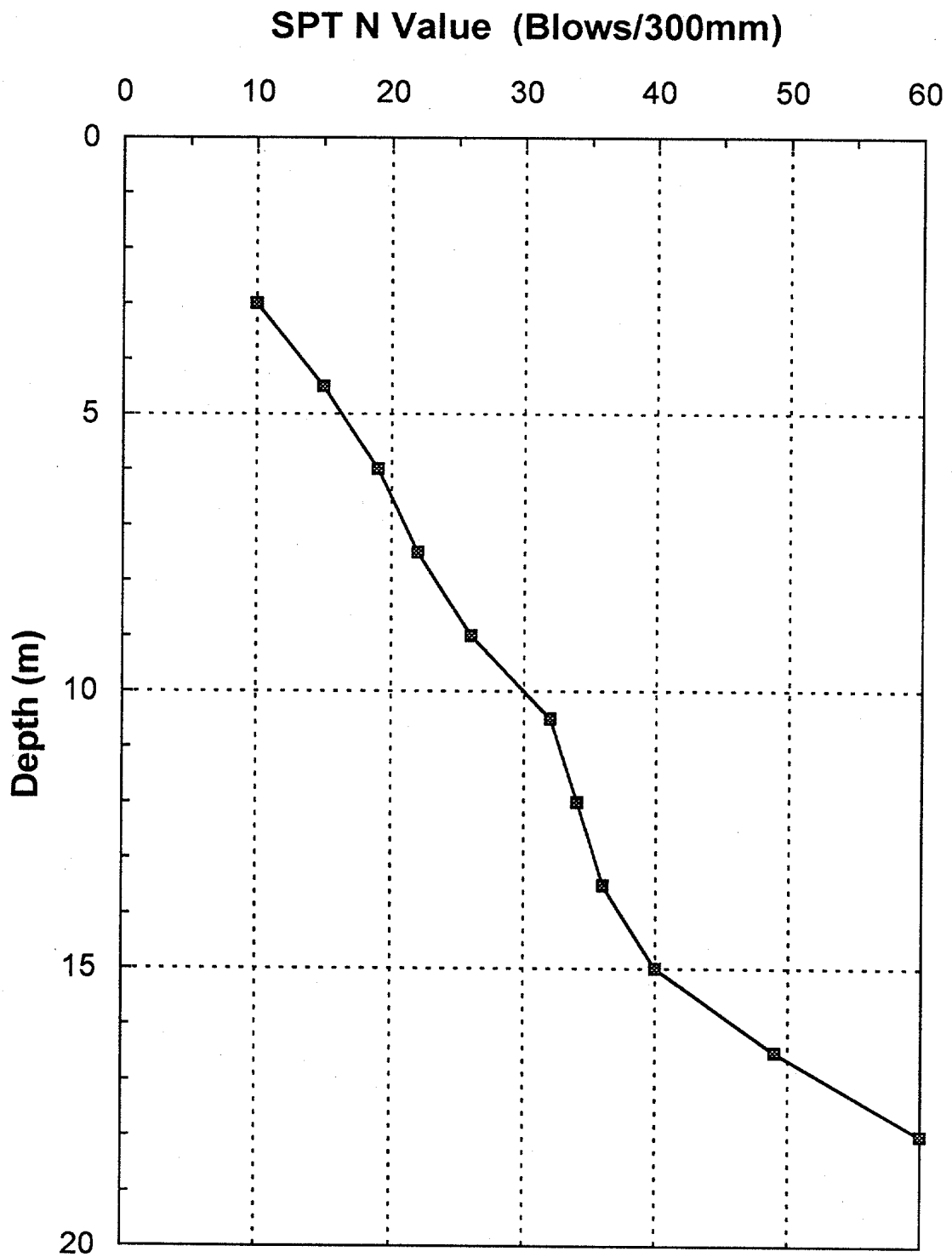


Figure 33. Field uncorrected SPT N value distribution.

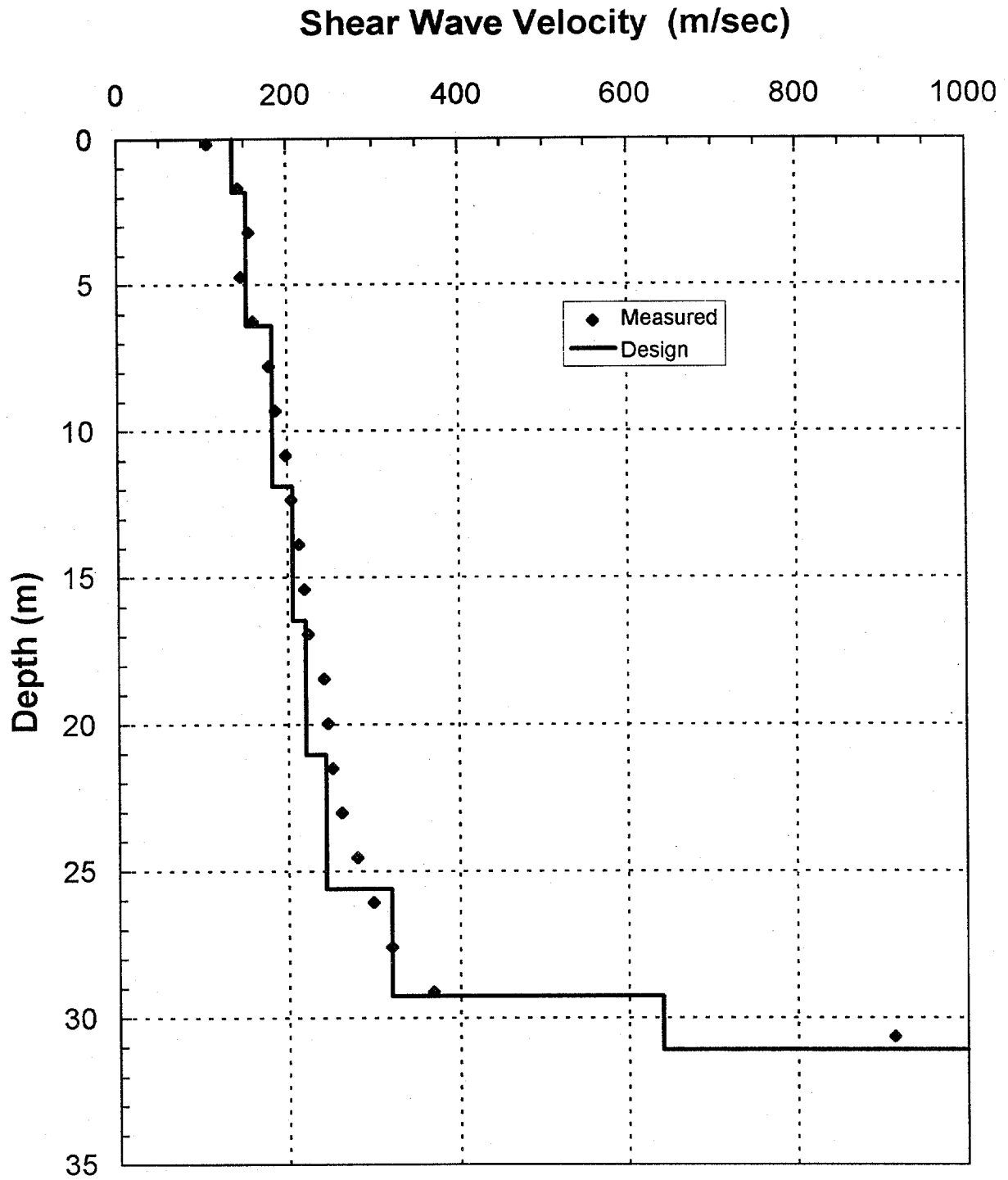


Figure 34. Shear wave velocity profile in channel.

5.6.2 Seismic Slope Stability

Pseudo-static slope stability analyses of the embankment were performed using the computer program STABL4 assuming that liquefaction would not occur. In the dynamic stability analyses, the seismic coefficient was set equal to one-half the PHGA divided by the acceleration of gravity, or 0.1 for the OLE and 0.2 for the CLE. Results of the analyses yielded a factor safety greater than 1.5 for both cases, indicating acceptable seismic performance in the absence of liquefaction. The critical failure surfaces are shown in figure 35 for the OLE and figure 36 for the CLE. Post-liquefaction stability analyses are described subsequently.

The input and output files for the STABL4 analyses using the OLE are provided in the attached calculation sheets.

5.6.3 Liquefaction Potential

Evaluation of liquefaction and seismic settlement potential is described in detail in volume I. The step-by-step methodology developed in chapter 8.3 of volume I will be followed in this example.

First, the uncorrected blow counts were normalized to a confining pressure of 96 kPa and standardized for a hammer efficiency of 60 percent. As a safety hammer was used in the rotary wash borings, the standardization factor for hammer efficiency was 1.0 (see chapter 8.3 of volume I). The normalization procedure is illustrated in the calculations and summarized in tables 10 through 12. Next, the factor of safety against liquefaction was calculated at each 1.5 m interval within the potentially liquefiable strata for both design earthquake loadings (the OLE and the CLE). Liquefaction potential was evaluated under the centerline of the embankment, beneath the toe of the embankment, and in the free-field beyond the embankment toe. Detailed calculations for liquefaction potential are provided in the attached calculation sheets.

Figure 37 shows the distribution of the factor of safety against liquefaction with depth for the free-field conditions. Under both the OLE and CLE conditions, liquefaction is expected to occur within approximately the top 10 m of the sand layer.

Figure 38 shows the distribution of the factor of safety against liquefaction with depth under the center of the embankment. Figure 38 shows that, due to the increase in confining stress imposed by the embankment, liquefaction is not anticipated under the embankment centerline in the OLE event but is expected to occur in the CLE event.

Figure 39 shows the distribution of the factor of safety under the toe of the embankment. At this location, liquefaction is also anticipated in the CLE but not in the OLE due to the beneficial influence of the initial static shear stress from the embankment on liquefaction potential. Note, however, that if the initial relative density of the surficial sand layer was less than 40 percent, the initial static shear stress from the embankment would increase the liquefaction potential. As indicated in figure 61 of volume I, the initial static shear stress correction factor k_α is larger than

Ten Most Critical. R:\LIQ3OLE.PLT 03-21-96 4:48pm

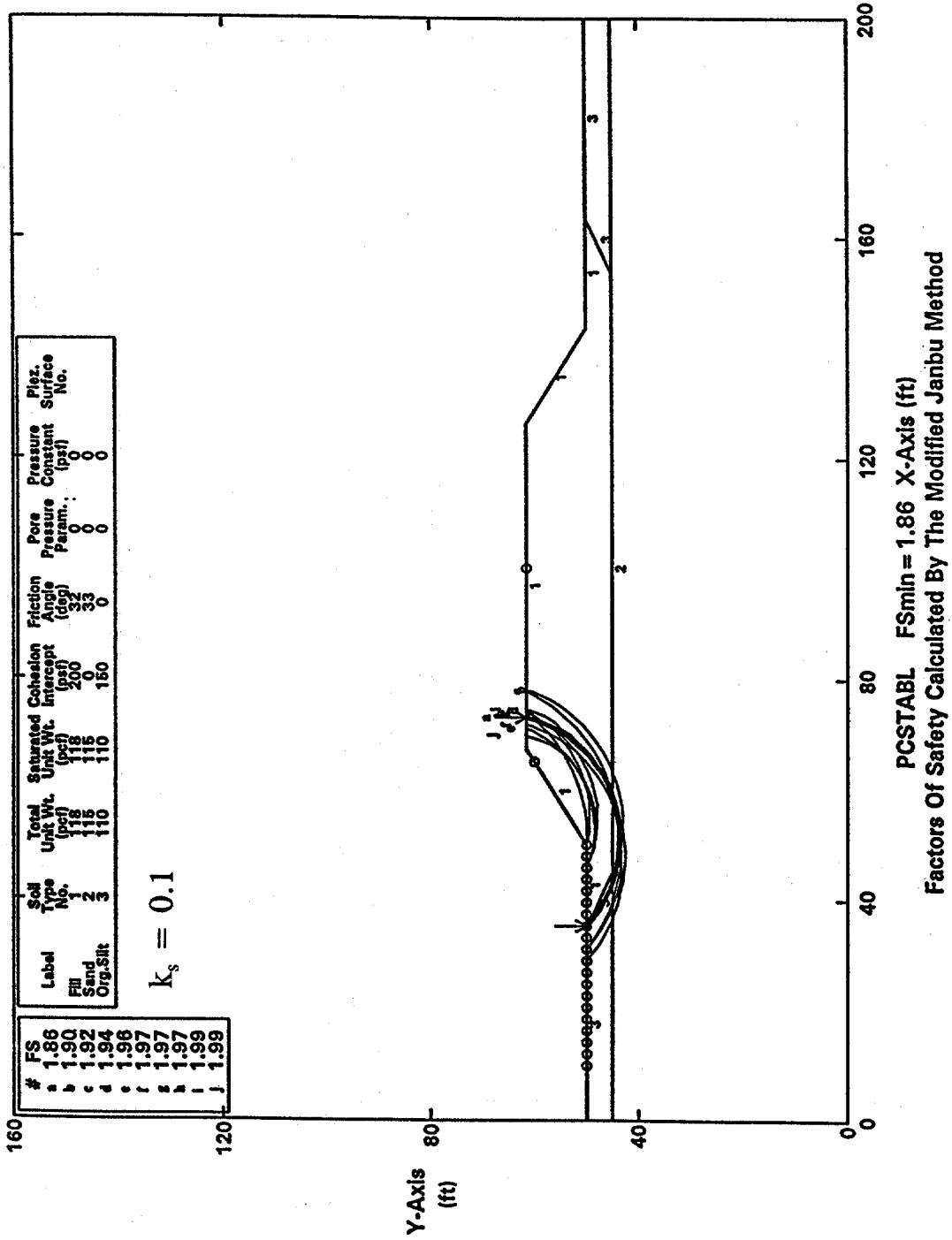
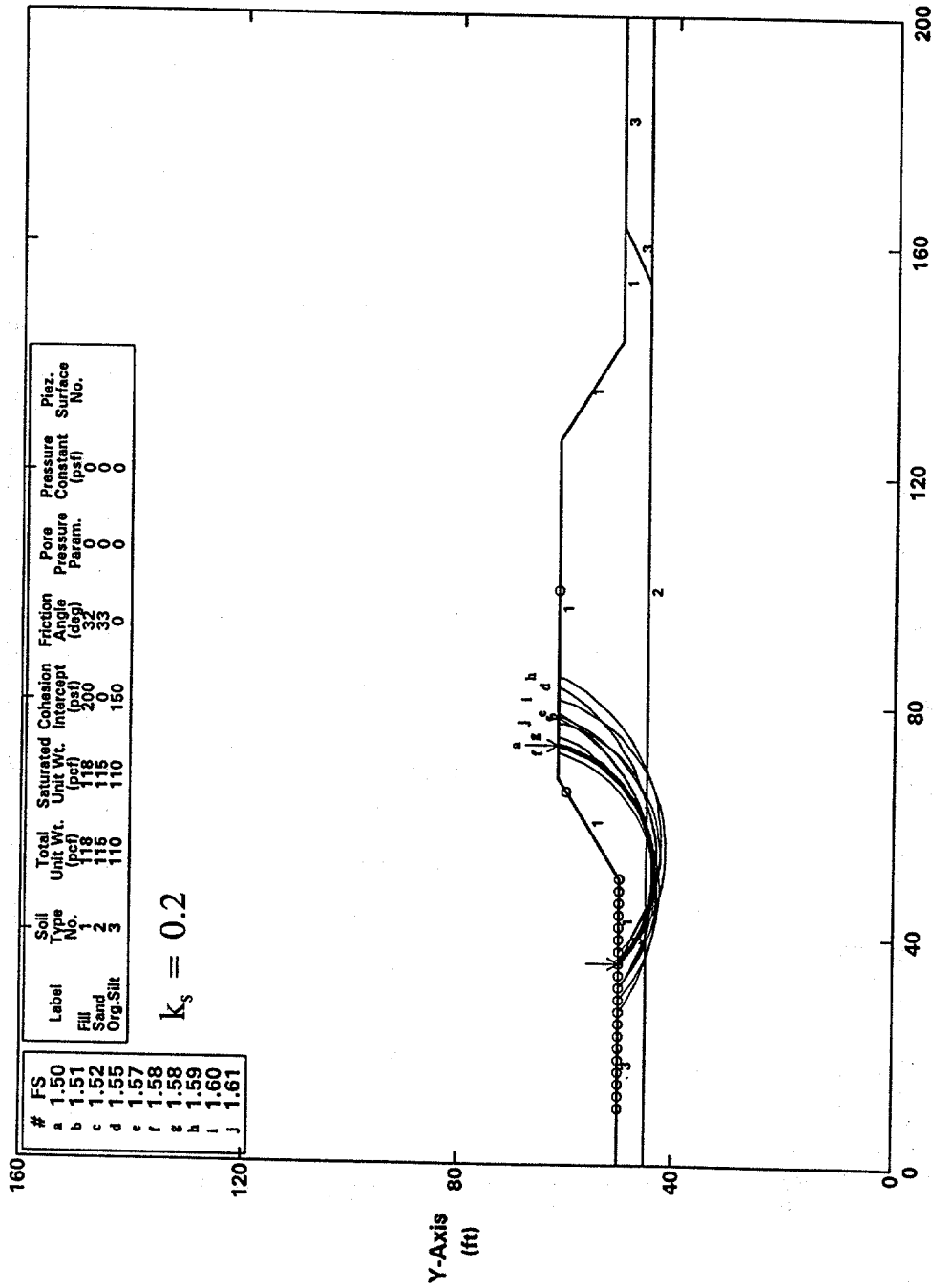


Figure 35. Critical failure surface for OLE.

Ten Most Critical. R:LIQ3CLE.PLT 03-21-96 4:47pm



#	FS	Soil Type No.	Total Unit Wt. (pcf)	Saturated Unit Wt. (pcf)	Cohesion Intercept (psf)	Friction Angle (deg)	Pore Pressure Param.	Pressure Constant (psf)	Piez. Surface No.
a	1.50	1	118	118	200	32	0	0	0
b	1.51	2	116	116	0	33	0	0	0
c	1.52	3	110	110	150	0	0	0	0
d	1.55								
e	1.57								
f	1.58								
g	1.58								
h	1.59								
i	1.60								
j	1.61								

$K_s = 0.2$

PCSTABL FSmin = 1.50 X-Axis (ft)
Factors Of Safety Calculated By The Modified Janbu Method

Note: 1 ft = 0.3048 m, 1 psf = 47.9 N/m², 1 pcf = 0.157 kN/m³

Figure 36. Critical failure surface for CLE.

Factor of Safety Against Liquefaction in the Free-Field

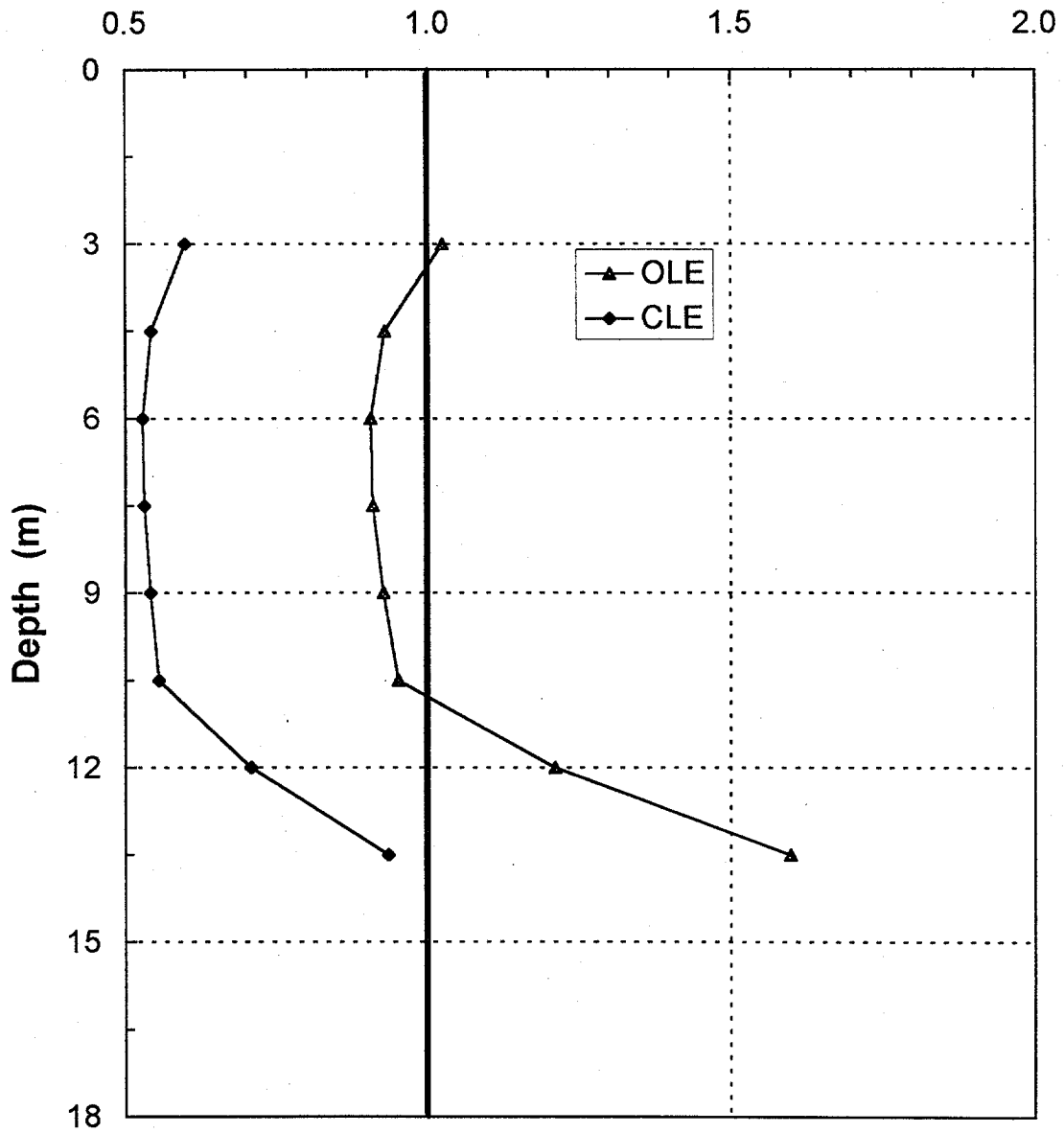


Figure 37. Distribution of factor of safety with depth in the free field.

Factor of Safety Against Liquefaction Under the Centerline of the Embankment

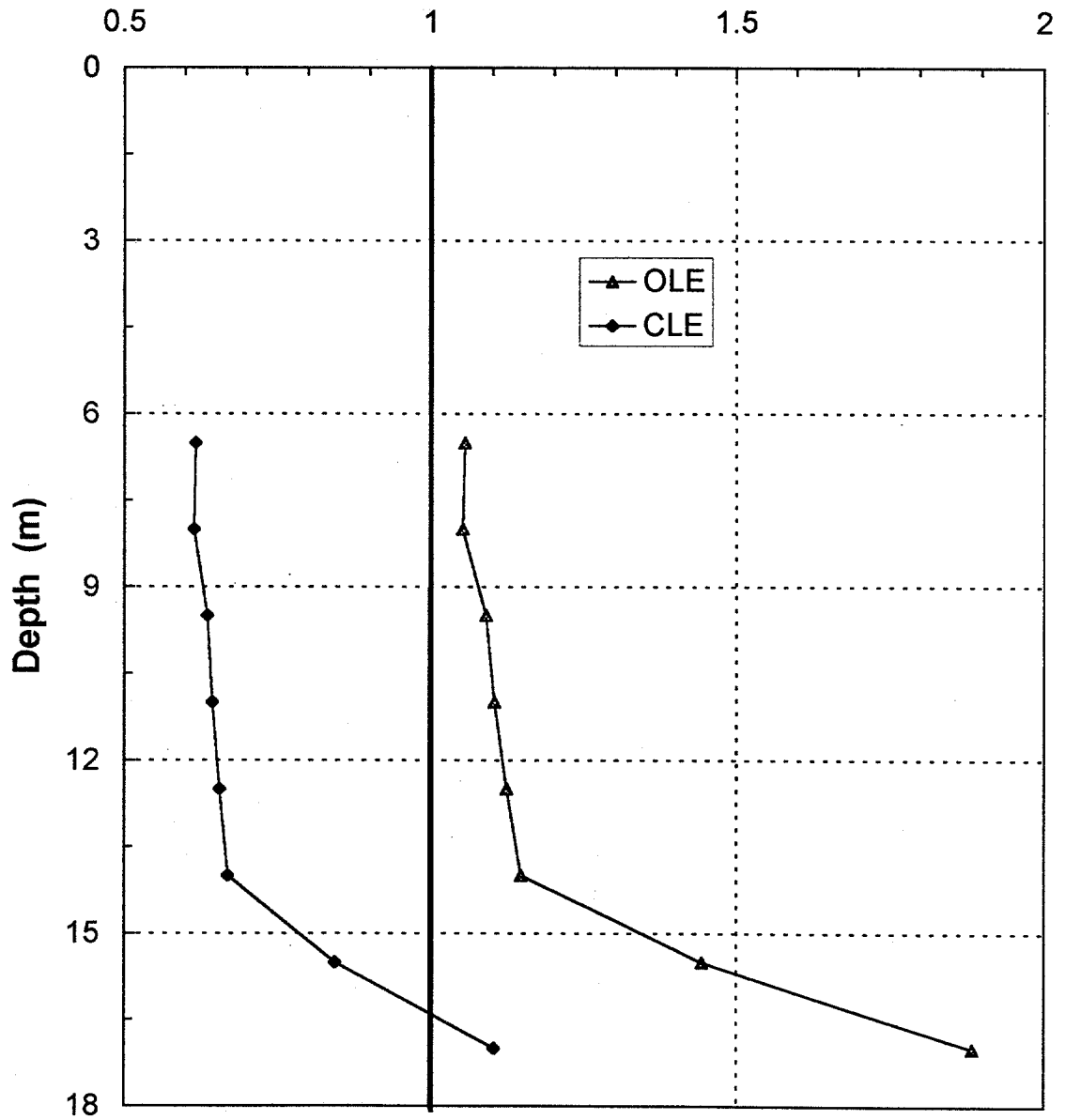


Figure 38. Distribution of factor of safety with depth under the centerline of the embankment.

Factor of Safety Against Liquefaction Under the Toe of the Embankment

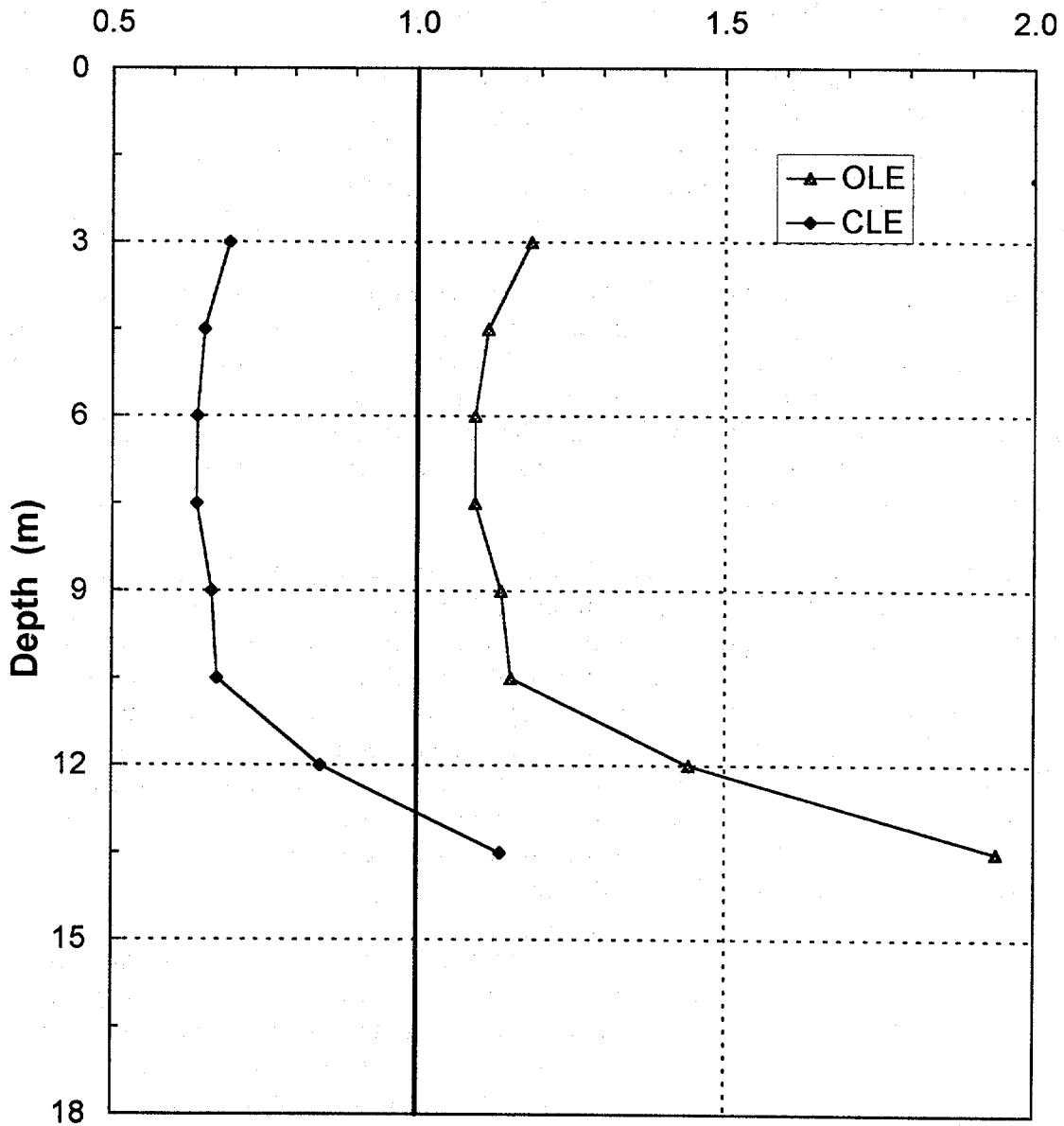


Figure 39. Distribution of factor of safety with depth under the toe of the embankment.

one for relative densities greater than 40 percent and less than one for relative densities less than 40 percent. The coefficient k_α appears in tables 10 through 12 in the attached computations and, for this example, is always larger than one since the sand found at the site has estimated relative densities varying from 40 to 55 percent.

5.6.4 Evaluation of the Consequences of Liquefaction

Since the analyses indicate that there is a potential for liquefaction in the free-field and under the embankment in both the OLE and CLE, the engineer must evaluate the consequences of liquefaction in these events. As discussed in chapter 5.3 of this volume, the design criteria are that in the OLE the embankment should remain usable and that in the CLE the damage will be repairable in 2 to 4 weeks.

The liquefaction analyses indicate that in the OLE liquefaction will occur in the free-field, as the factor of safety is on the order of 0.9. Furthermore, the factor of safety against liquefaction in the OLE under the centerline and toe of the embankment is very near one, indicating that some permanent seismic deformation is likely in the OLE. In the CLE, the factor of safety varies from about 0.5 in the free-field to about 0.7 under the embankment. Such low values indicate that extensive liquefaction may occur, resulting in large displacements (lateral spreading) and potential slope failure along the embankment.

To lower the risk of liquefaction, it was decided to densify the top 10 m of the sand layer. Target factors of safety of 1.1 under the embankment and 1.0 in the free-field during the CLE event were established. To achieve these factors of safety, it was determined that the cyclic shear ratio at which liquefaction will occur (the liquefaction resistance of the soil) must be greater than or equal to 0.3 over the top 10 m of sand layer. Based on figure 58 of volume I, to achieve a liquefaction resistance of 0.3 for a soil with a fines content of 5 percent requires a value of $(N_1)_{60}$ of about 25. The remedial ground improvement program was designed on this basis to provide an $(N_1)_{60}$ of 25 or greater at the site. As the site was an open, undeveloped area with no structures or utilities nearby, dynamic compaction was selected as the most economical ground improvement method with which to achieve the required liquefaction resistance.

Even with a standardized and normalized blow count of 25, there is still a risk of liquefaction in the free-field in the OLE and CLE, as only the soil under the embankment footprint was designated for densification. The potential consequence of liquefaction in the free-field adjacent to the toe of the embankment is lateral spreading of the embankment. Lateral spreading can occur subsequent to liquefaction both during the earthquake (assuming liquefaction occurs prior to the cessation of strong shaking) and after the event. To evaluate the potential for lateral spreading in the CLE, a limit equilibrium analysis was performed using the residual shear strength for the potentially liquefiable soil beyond the toe of the embankment. The rationale for the use of residual shear strength in this analysis is discussed in chapter 8.4 of volume I. The residual shear strength of the liquefied soil was evaluated using the correlation with SPT $(N_1)_{60-cs}$ values shown in figure 44 of volume I.

Because the area outside the footprint of the embankment was not treated with dynamic compaction, the value of residual shear strength was obtained using the average initial SPT values over the top 10 m of the sand layer and the lower-bound curve on figure 44 of volume I. On this basis, a value of 15 kPa was selected to characterize the residual shear strength of the sand.

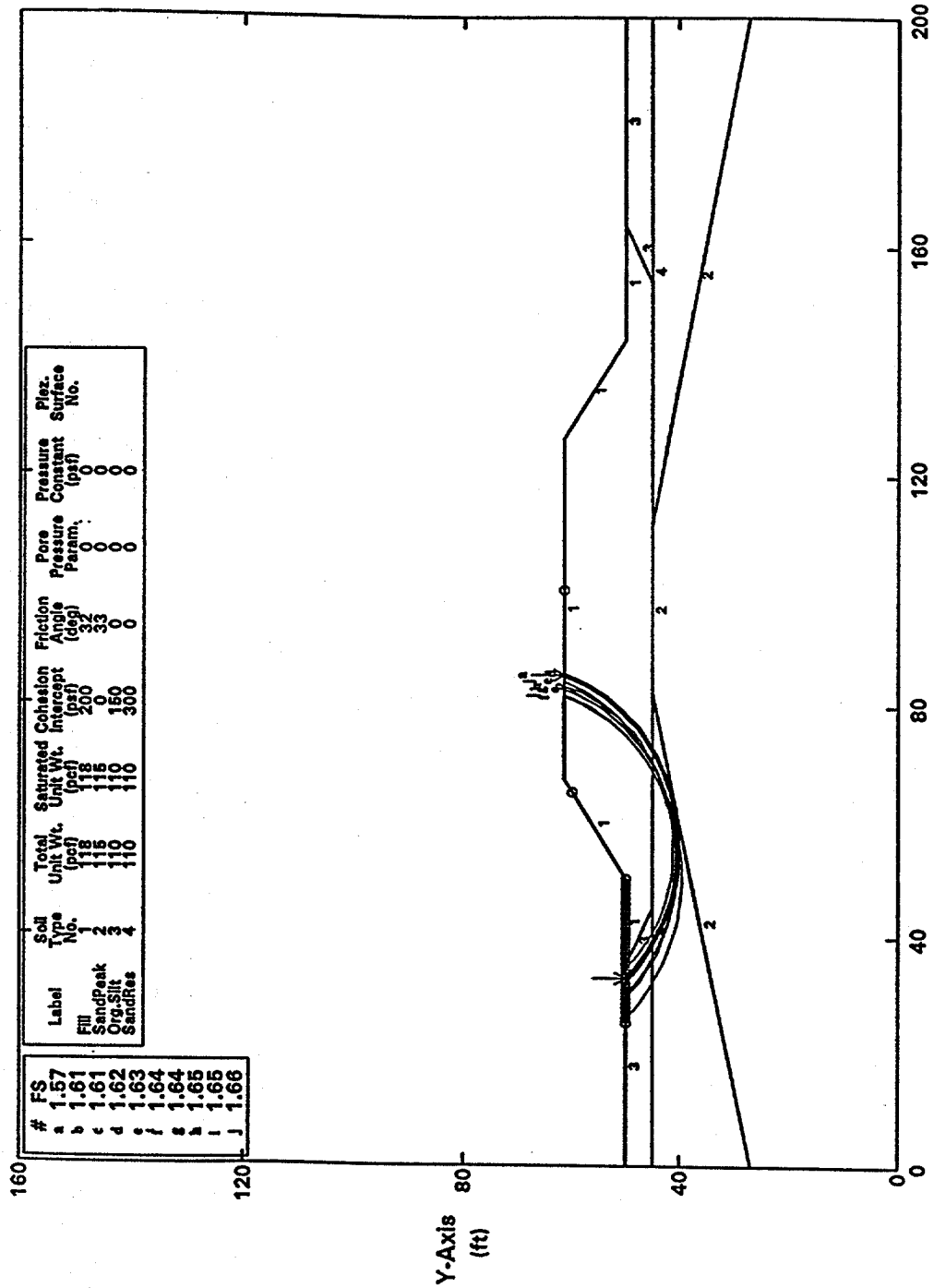
Results of the residual strength stability analysis presented in figure 40 of this volume, indicate a static factor of safety of 1.57 for the embankment using residual shear strength parameters. This analysis indicates that, once the strong shaking stops, the embankment will be stable and lateral spreading will cease. The yield acceleration calculated using residual shear strength beyond the toe of the embankment is 0.14 g (figure 41). Using this value in conjunction with the CLE PHGA of 0.4 g results in a value of 0.35 for the ratio of yield to peak acceleration. From the Hynes and Franklin (1984) chart presented in figure 51 of volume I, this results in an upper bound permanent seismic deformation of 0.36 m, as shown in figure 42. This is assumed to be the upper bound value for the lateral spreading anticipated during the CLE, calculated assuming that the soil liquefies immediately following the start of strong ground motion. As this potential amount of lateral spreading at the toe of the embankment was considered to be repairable in the designated time period by the design engineers, no additional remedial action was considered necessary. Note that for the OLE, the ratio of yield to peak acceleration is 0.7 and the upper bound on the anticipated amount of lateral spreading is less than 0.15 m. This magnitude of lateral spreading is considered negligible.

5.7 SITE RESPONSE ANALYSES

A site specific response analysis was conducted to develop response spectra for the OLE and CLE for use in design of the bridge structure. The response analysis was conducted using the in-house modified computer program SHAKE91 (Schnabel et al., 1972; Idriss and Sun, 1992). Input time histories were selected using the methods described in chapter 4 of volume I. Table 7 presents the target values for acceleration intensity, duration, and energy content for the two design events. Tables 8 and 9 show the time histories that were screened for use in the analyses and identify the selected time histories for the CLE and OLE, respectively.

The input time histories, scaled to the appropriate peak acceleration, were specified as outcrop motions in the SHAKE analyses. The soil profile for the SHAKE analyses were based upon the cross hole velocity profile shown in figure 34, laboratory density and shear strength values for the silt and clay strata, and modulus reduction and damping curves from Vucetic and Dobry (1991). Results of the SHAKE analyses are presented in figures 43 and 44. In figure 43, response spectra at the top of the silty clay stratum in the channel are plotted for the three input OLE time histories. Also shown in this figure is the smoothed response spectra recommended for use in design. Figure 44 presents the same information for the CLE. In figure 45, the smoothed response spectra for the OLE and CLE are plotted together for comparison. These results clearly demonstrate the focusing of seismic energy around the predominant period of the site, estimated to be approximately 0.3 seconds, and the influence of the long period motions of the CLE design event on site response.

Ten Most Critical. R:LI03PL.PLT 03-21-96 4:45pm



PCSTABL FSmin = 1.57 X-Axis (ft)
 Factors Of Safety Calculated By The Modified Janbu Method

Note: 1 ft = 0.3048 m, 1 psf = 47.9 N/m², 1 pcf = 0.157 kN/m³

Figure 40. Post-liquefaction slope stability analysis.

Ten Most Critical. R:LIQ3CLE.PLT 03-21-96 4:47pm

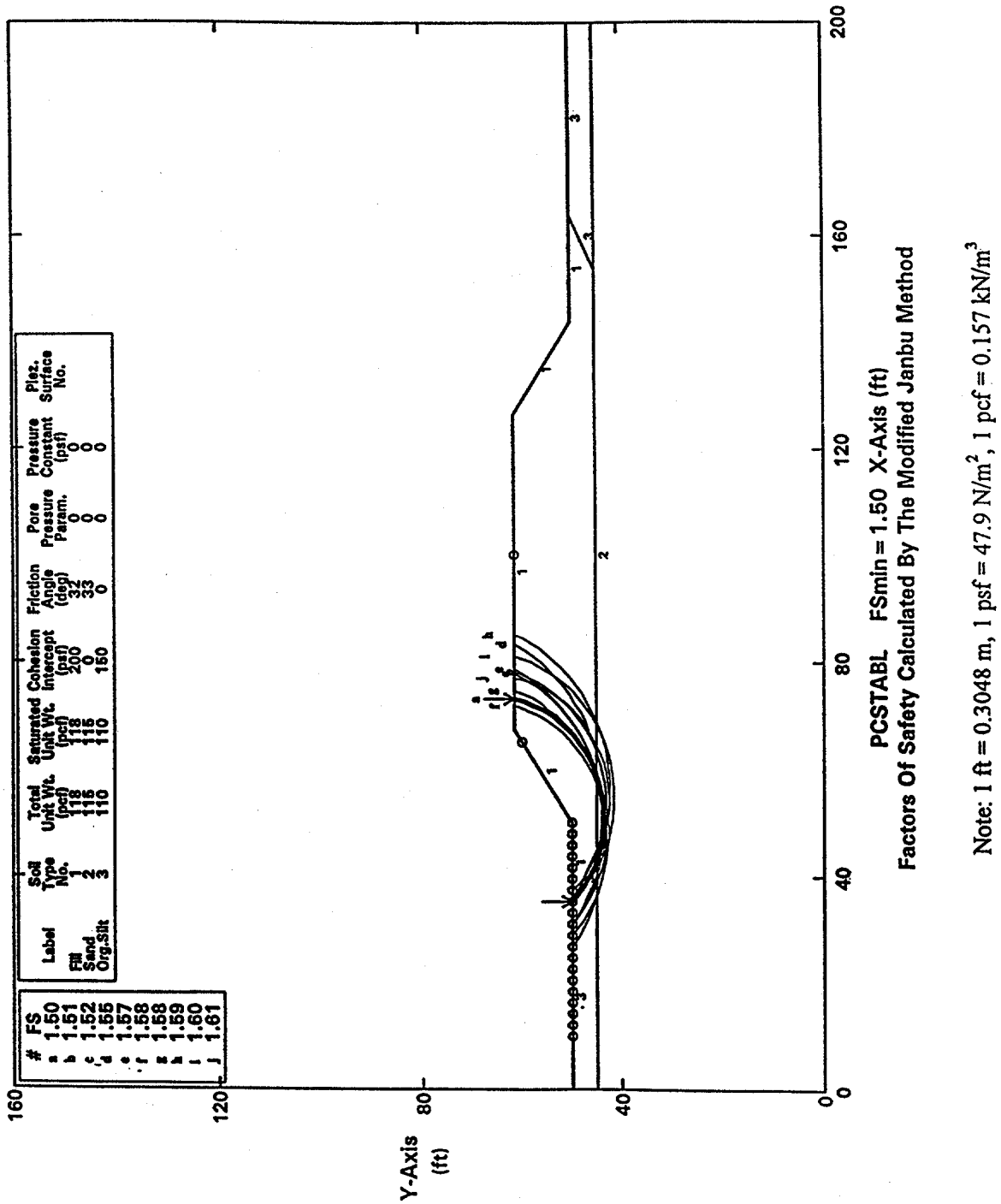


Figure 41. Post-liquefaction pseudo-static slope stability analysis (yield acceleration = 0.14 g).

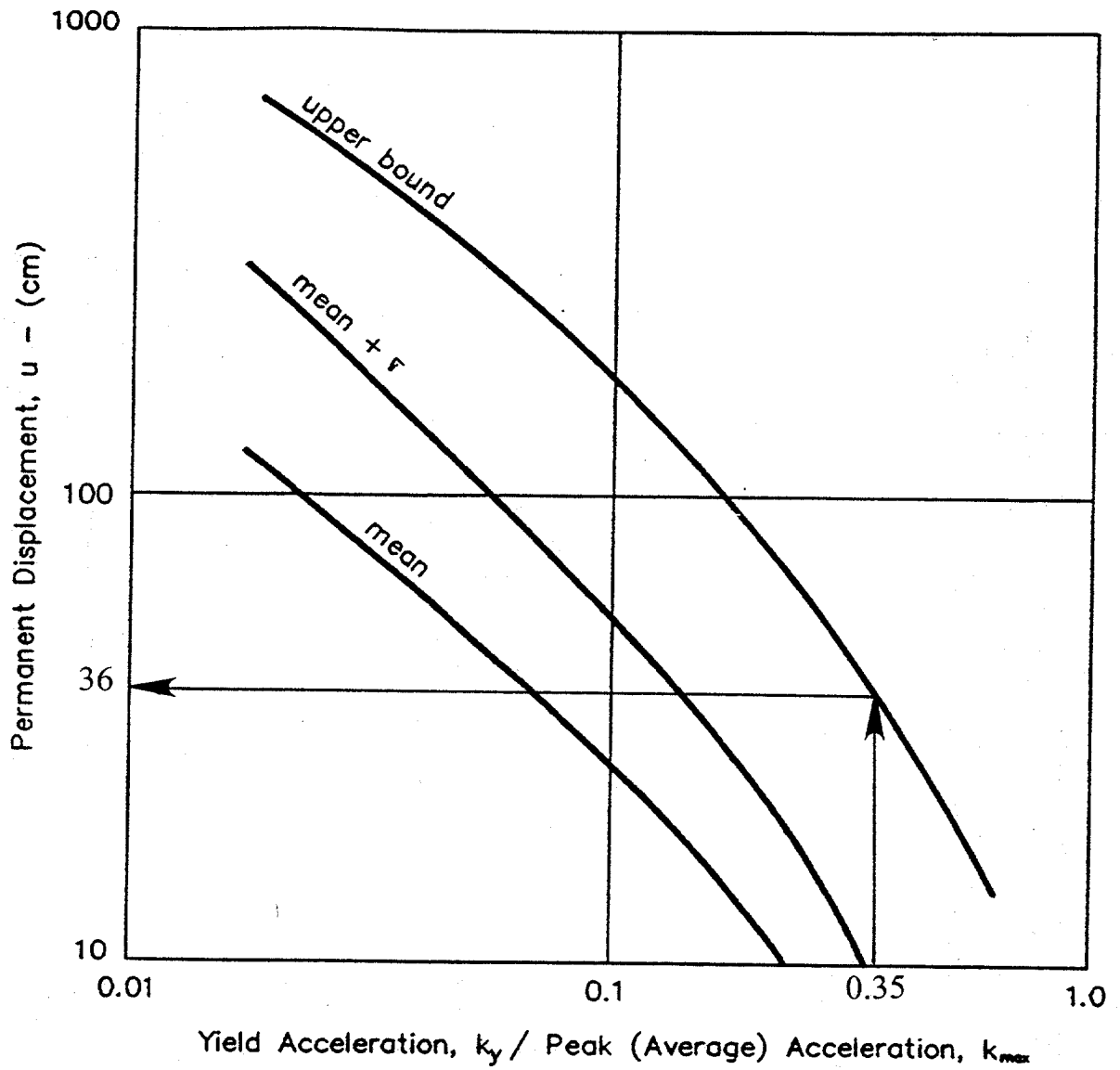


Figure 42. Permanent seismic deformation chart (modified from Hynes and Franklin, 1984, reprinted by permission of U.S. Army Engineer Waterways Experiment Station).

Table 8. Main characteristics of candidate CLE accelerograms.

Accelerogram	Earthquake	Recording Station		Strong Motion Characteristics		
		Epicentral Distance	Local Site Conditions	Uncorr. PHGA ⁽¹⁾	Significant Duration ⁽²⁾	RMSA ⁽³⁾
Los Angeles Dam-Right Abutment (S20W)	Northridge ($M_w = 6.7$)	11 km	Weak Rock (Non-marine deposit)	0.32 g	6.51 sec	0.113 g
Los Angeles Dam-Downhole (116 deg)	Northridge ($M_w = 6.7$)	11 km	Weak Rock (Non-marine deposit)	0.35 g	3.01 sec	0.088 g
Pacoma Dam-Downstream (265 deg)	Northridge ($M_w = 6.7$)	17.7 km	Hard Rock (Highly jointed Diorite gneiss)	0.446 g	4.11 sec	0.105 g
Pacoma-Kugel Canyon Fire Station (360 deg)	Northridge ($M_w = 6.7$)	17.7 km	Hard Rock (Sedimentary)	0.434 g	9.82 sec	0.104 g
Griffith Park (260 deg)	Northridge ($M_w = 6.7$)	24 km	Rock	0.166 g	11.4 sec	0.047 g
Castaic - Old Ridge Route (90 deg)	Northridge ($M_w = 6.7$)	41 km	Rock (Sedimentary)	0.58 g	9.06 g	0.14 g
Corralitos-Eureka Canyon Road (0 deg)	Santa Cruz Mountains ($M_w = 6.9$)	14 km	Weak Rock (Pliocene Sediments)	0.643 g	6.86 sec	0.170 g
Saratoga-Alhambra Avenue (0 deg)	Santa Cruz Mountains ($M_w = 6.9$)	11.7 km	Soft Rock (Plio-Pleistocene Sediment)	0.52 g	9.40 sec	0.099 g
Petrolia (90 deg)	Cape Mendocino/Petrolia ($M_w = 7.0$)	5 km	Weak Rock (Joyner & Boore Class B)	0.685 g	16.95 sec	0.122 g
Rio Dell (270 deg)	Cape Mendocino/Petrolia ($M_w = 7.0$)	15 km	Alluvium (50 ft or 15 m)	0.385 g	15.36 sec	0.076 g
C4 - Synthetic (Silva, 1995)	Synthesized for Northridge Earthquake ($M_w = 6.7$)	8.4 km	Weak Rock	0.417 g	6.70 sec	0.154 g
PEAEP2TA - Synthetic (Chin, 1996)	Synthesized for Elysian Park Thrust ($M_w = 7.25$)	10-16 km	Weak Rock	0.85 g	8.33 sec	0.30 g

- Notes:
- (1) Uncorrected peak horizontal acceleration (PHGA) value of strong motion record before digital processing.
 - (2) Significant duration of strong shaking, D_s , as defined by Trifunac and Brady (1975).
 - (3) Root Mean Square Acceleration (RMSA) over the significant duration of the record scaled to PHGA. Redlined Accelerograms eliminated from further consideration.

Table 9. Main characteristics of candidate OLE accelerograms.

Accelerogram	Earthquake	Recording Station		Strong Motion Characteristics		
		Epicentral Distance	Local Site Conditions	Uncorr. PHGA ⁽¹⁾	Significant Duration ⁽²⁾	RMSA ⁽³⁾
Indro-Cosechella Canal (90 deg)	Landers ($M_w = 7.3$)	61 km	Deep alluvium	0.111 g	39.66 sec	0.023 g
Joshua Tree-Fire Station (90 deg)	Landers ($M_w = 7.3$)	14 km	Shallow alluvium over granite bedrock	0.287 g	28.22 sec	0.071 g
Taft-Lincoln School Tunnel (S69E)	Kern County ($M_w = 7.4$)	42 km	Weak Rock	0.187 g	28.87 sec	0.036 g
Olympia-Washington Highway Test Lab (N86E)	Western Washington ($M_w = 7.1$)	39 km	Deep Cohesionless Soil	0.275 g	18.08 sec	0.059 g
Tabas	Tabas-e-Golshan	3 km	Sedimentary and Conglomerated Rock	0.785 g	16.28 sec	0.176 g
Managua	Managua, Nicaragua ($M_w = 6.3$)	5 km	Soil (1-S)	0.382 g	6.50 sec	0.066 g
Lima	Lima, Peru ($M_w = 7.6$)	38 km	Soil	0.255 g	47.81 sec	0.041 g
Old Appleton (N340)	Cape Girardeau ($M_w = 4.8$)	46 km		0.175 g	34.90 sec	0.040 g
Sitka Observatory	Alaska ($M_w = 7.7$)	45 km	Soil	0.108 g	28.86 sec	0.016 g
University of Hawaii (344 deg)	Island of Hawaii ($M_w = 7.2$)	43 km		0.197 g	0.027 sec	0.027 g
A1 (Jennings et al., 1968)	Synthetic earthquake on San Andreas fault ($M_w = 8^+$)	General near-field	General stiff soil site	0.390 g	41.51 sec	0.120 g
MAG-8 (Seed and Idriss, 1969)	Synthetic earthquake on San Andreas fault ($M_w = 8.25$)	General near-field	General rock site	0.420 g	38.60 sec	0.102 g

- Notes:
- (1) Uncorrected peak horizontal acceleration (PHGA) value of strong motion record before digital processing.
 - (2) Significant duration of strong shaking, D_s , as defined by Trifunac and Brady (1975).
 - (3) Root Mean Square Acceleration (RMSA) over the significant duration of the record scaled to PHGA. Redlined Accelerograms eliminated from further consideration.

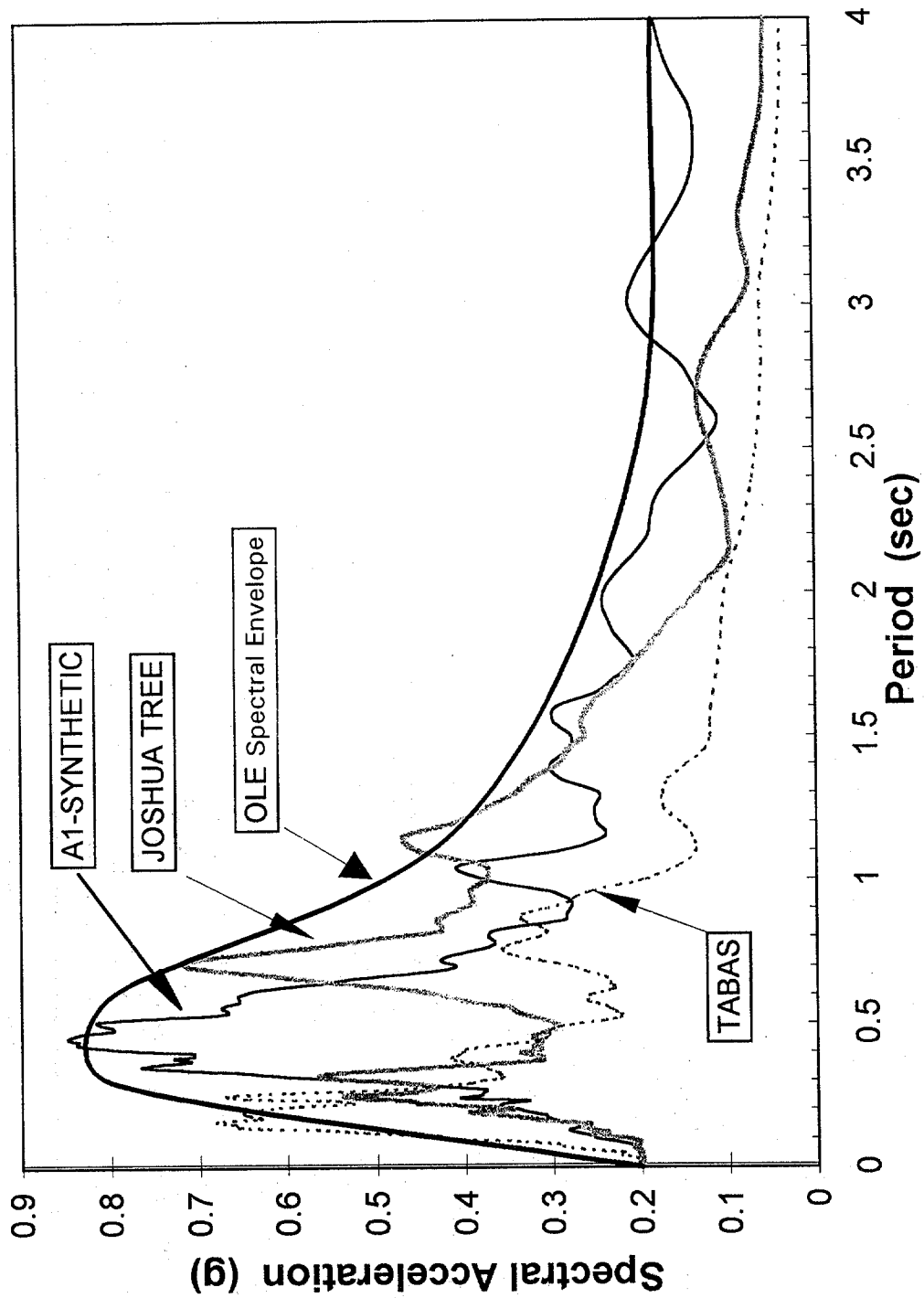


Figure 43. Response spectra from SHAKE analysis for OLE events.

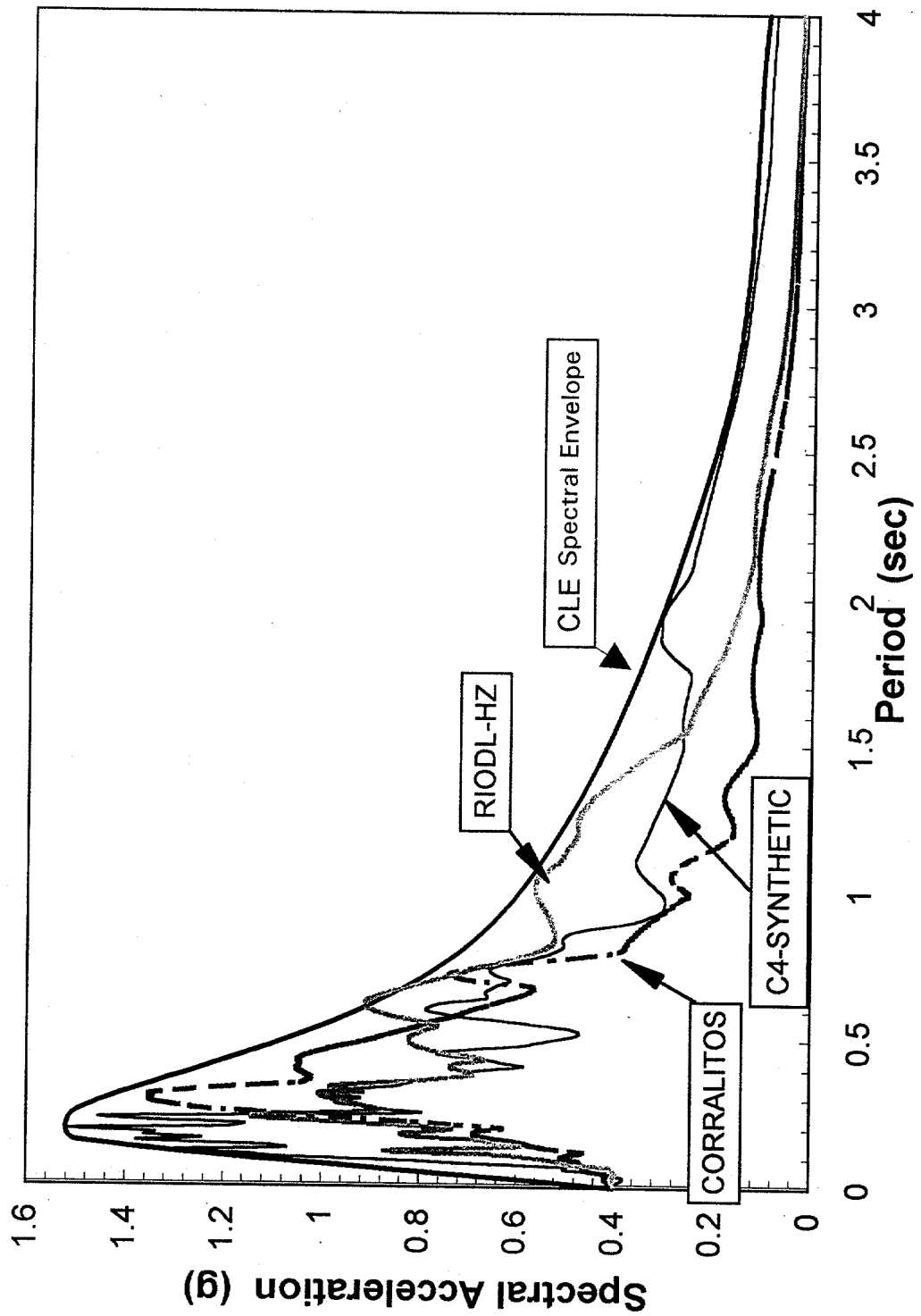


Figure 44. Response spectra from SHAKE analysis for CLE events.

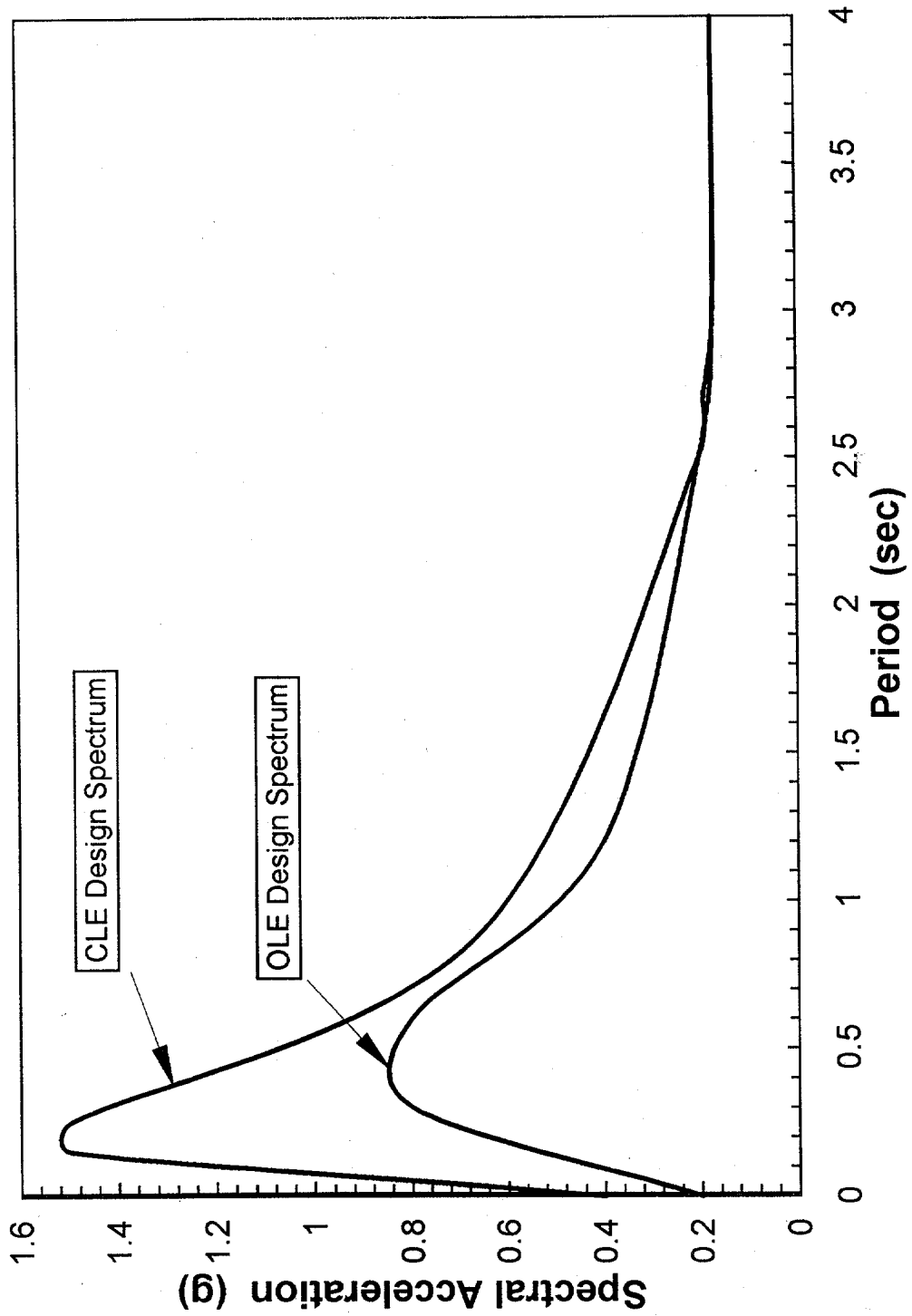


Figure 45. Design response spectra.

5.8 CALCULATIONS

The calculation sheets for example 5, "Liquefaction Potential Analysis" follow. Equation numbers that appear in the right margin of the calculation sheets refer back to volume I. Included are input and output files for a sample PCSTABL4 and SHAKE analysis.

Written by: T.H.H. Date: 96 / 03 / 19 Reviewed by: E.K. and N.M. Date: 96 / 03 / 21
YY MM DD YY MM DD

Client: FHWA Project: GEC-3 Project/Proposal No.: GE3686 Task No.: F

DETAILED CALCULATIONS
EXAMPLE 5 - LIQUEFACTION POTENTIAL ANALYSIS
(DEPTH = 4.5 m)

The liquefaction potential at depth 4.5 m below the original ground surface is evaluated in this example. For other depths, a spreadsheet was developed and the calculations are shown in tables 10, 11, and 12. The liquefaction potential analysis described in this example is found in chapter 8 of volume I.

Free-Field

Step 1: Develop Subsurface Profile (see figures 31 and 32)

Step 2: Evaluate Initial Stresses

$$\sigma_o = (1.5 \text{ m})(16 \text{ kN/m}^3) + (3 \text{ m})(18 \text{ kN/m}^3) = 78 \text{ kPa}$$

$$u_o = (2 \text{ m})(9.8 \text{ kN/m}^3) = 20 \text{ kPa}$$

$$\sigma'_o = \sigma_o - u_o = 78 - 20 = 58 \text{ kPa}$$

Step 3: Evaluate Stress Reduction Factor

$$r_d = 1 - 0.015z = 1 - 0.015(4.5) = 0.9325 \tag{8-1}$$

Step 4: Evaluate the Critical Stress Ratio Induced by the Earthquake

$$CSR_{eq} = 0.65 (a_{max}/g) r_d \sigma_v/\sigma'_v \tag{8-3}$$

Evaluate CSR_{eq} for two design events:

(1) OLE ($a_{max} = 0.2 \text{ g}$; $M_w = 8.0$)

$$CSR_{eq} = (0.65)(0.2)(0.9325) 78/58 = 0.16$$

(2) CLE ($a_{max} = 0.4 \text{ g}$; $M_w = 7.0$)

$$CSR_{eq} = (0.65)(0.4)(0.9325) 78/58 = 0.33$$



Written by: T.H.H. Date: 96 / 03 / 19 Reviewed by: E.K. and N.M. Date: 96 / 03 / 21
YY MM DD YY MM DD

Client: FHWA Project: GEC-3 Project/Proposal No.: GE3686 Task No.: F

Step 5: Standardized Blow Count Value

Tables 8 and 9 in volume I are used to evaluate the standardized blow count. For this example, no corrections are necessary to apply since standard equipment was used for the SPT tests.

Step 6: Correction for SPT N value for Overburden Pressure

$$C_N = 9.79 (1/\sigma'_o)^{1/2} = 9.79(1/58)^{1/2} \approx 1.29 \tag{8-5}$$

$$(N_1)_{60} = C_N N_{60} = (1.29)(11) = 14 \tag{8-6}$$

Step 7: Evaluate Critical Stress Ratio Resisting Liquefaction (figure 58 in volume I)

For $(N_1)_{60} = 14$ and a fines content of 5%, $CSR_{7.5} = 0.16$

Step 8: Correct Critical Stress Ratio Resisting Liquefaction

$$CSR_L = CSR_{7.5} k_M k_\alpha k_\sigma$$

- k_M is read from figure 59 in volume I

$$M_w = 8.0 \quad k_M = 0.93$$

$$M_w = 7.0 \quad k_M = 1.08$$

- k_σ is read from figure 60 in volume I

$$\sigma'_v = 58 \text{ kPa} \quad k_\sigma = 1.05$$

- $k_\alpha = 1.0$, no initial static shear

(1) OLE ($a_{max} = 0.2 \text{ g}$; $M_w = 8.0$)

$$CSR_L = (0.16)(1)(1.05)(0.93) \approx 0.156$$

(2) CLE ($a_{max} = 0.4 \text{ g}$; $M_w = 7.0$)

$$CSR_L = (0.16)(1)(1.05)(1.08) \approx 0.181$$



Written by: T.H.H. Date: 96 / 03 / 19 Reviewed by: E.K. and N.M. Date: 96 / 03 / 21
YY MM DD YY MM DD

Client: FHWA Project: GEC-3 Project/Proposal No.: GE3686 Task No.: F

Step 9: Calculate Factor of Safety

- (1) OLE ($a_{max} = 0.2 \text{ g}; M_w = 8.0$)
 $FS_L = CSR_L / CSR_{eq} = 0.156 / 0.16 = 0.975$
- (2) CLE ($a_{max} = 0.4 \text{ g}; M_w = 7.0$)
 $FS_L = CSR_L / CSR_{eq} = 0.181 / 0.33 = 0.548$

A spreadsheet was developed to perform the calculation for the other depths. The results are presented in table 10.



Written by: T.H.H. Date: 96 / 03 / 19 Reviewed by: E.K. and N.M. Date: 96 / 03 / 21
 YY MM DD YY MM DD

Client: FHWA Project: GEC-3 Project/Proposal No.: GE3686 Task No.: F

Table 10. Liquefaction potential in the free-field.

Depth (m)	Fines Content	N _{field}	σ _v	σ _v '	C _N	C ₆₀	(N ₁) ₆₀	r _d	CLE event: a _{max} = 0.4 g; M _w = 7						
									k _M	k _s	k _σ	CSR _{eq}	CSR _{7.5}	CSR _L	FS
3	6	9	51.0	46	1.44	1	13	0.955	1.08	1.000	1.065	0.275	0.143	0.165	0.598
4.5	5	11	78.0	58	1.28	1	14	0.933	1.08	1.000	1.050	0.326	0.155	0.177	0.543
6	6	13	105.0	70	1.17	1	15	0.910	1.08	1.000	1.036	0.355	0.167	0.188	0.529
7.5	7	15	132.0	82	1.08	1	16	0.888	1.08	1.000	1.022	0.371	0.178	0.197	0.531
9	4	17	159.0	94	1.01	1	17	0.865	1.08	1.000	1.007	0.380	0.189	0.206	0.541
10.5	5	19	186.0	106	0.95	1	18	0.843	1.08	1.000	0.993	0.384	0.199	0.214	0.556
12	8	26	214.5	120	0.89	1	23	0.820	1.08	1.000	0.977	0.383	0.256	0.271	0.708
13.5	6	32	243.0	133	0.85	1	27	0.798	1.08	1.000	0.960	0.379	0.340	0.354	0.934
15	11	40	271.5	147	0.81	1	32	0.775	1.08	1.000	0.944	0.373	N/A	N/A	N/A
16.5	12	49	300.0	160	0.77	1	38	0.753	1.08	1.000	0.928	0.367	N/A	N/A	N/A
18	13	60	328.5	174	0.74	1	45	0.730	1.08	1.000	0.912	0.359	N/A	N/A	N/A
									OLE event: a _{max} = 0.2 g; M _w = 8						
3	6	9	51.0	46	1.44	1	13	0.955	0.93	1.000	1.065	0.138	0.143	0.141	1.024
4.5	5	11	78.0	58	1.28	1	14	0.933	0.93	1.000	1.050	0.163	0.155	0.151	0.928
6	6	13	105.0	70	1.17	1	15	0.910	0.93	1.000	1.036	0.177	0.167	0.161	0.905
7.5	7	15	132.0	82	1.08	1	16	0.888	0.93	1.000	1.022	0.186	0.178	0.169	0.909
9	4	17	159.0	94	1.01	1	17	0.865	0.93	1.000	1.007	0.190	0.189	0.176	0.926
10.5	5	19	186.0	106	0.95	1	18	0.843	0.93	1.000	0.993	0.192	0.199	0.183	0.951
12	8	26	214.5	120	0.89	1	23	0.820	0.93	1.000	0.977	0.191	0.256	0.232	1.211
13.5	6	32	243.0	133	0.85	1	27	0.798	0.93	1.000	0.960	0.189	0.340	0.303	1.598
15	11	40	271.5	147	0.81	1	32	0.775	0.93	1.000	0.944	0.187	N/A	N/A	N/A
16.5	12	49	300.0	160	0.77	1	38	0.753	0.93	1.000	0.928	0.183	N/A	N/A	N/A
18	13	60	328.5	174	0.74	1	45	0.730	0.93	1.000	0.912	0.180	N/A	N/A	N/A

- | | | | |
|---------------------------------|---|------------------|--|
| N _{field} | SPT blow-count from field investigations | σ _v | Total normal stress |
| C _N | Correction factor for overburden pressure (equation 8-5 or figure 57 of volume I) | σ _v ' | Effective normal stress |
| C ₆₀ | Correction factor for equipment (tables 8 and 9 of volume I) | FS _L | Factor of Safety against liquefaction |
| (N ₁) ₆₀ | SPT blow count corrected as per equation 8-6 | a _{max} | Peak ground acceleration |
| r _d | Stress reduction factor (equation 8-1 or figure 56 of volume I) | M _w | Moment magnitude |
| k _M | Magnitude correction factor (figure 59 of volume I) | CLE | Contingency Level Event |
| k _s | Initial static shear stress correction factor (figure 61 of volume I) | OLE | Operational Level Event |
| k _σ | Stress level correction factor (figure 60 of volume I) | N/A | Not Applicable (for (N ₁) ₆₀ > 30, CSR _{7.5} becomes very large as shown on figure 58 of volume I) |
| CSR _{eq} | Critical stress ratio imposed by the earthquake (equation 8-3 of volume I) | | |
| CSR _{7.5} | Critical stress ratio read from figure 58 of volume I | | |
| CSR _L | Critical stress ratio from figure 58 corrected as per equation 8-7 of volume I | | |



Written by: T.H.H. Date: 96 / 03 / 19 Reviewed by: E.K. and N.M. Date: 96 / 03 / 21
YY MM DD YY MM DD

Client: FHWA Project: GEC-3 Project/Proposal No.: GE3686 Task No.: F

Under Centerline of Embankment (Depth = 8 m below top of embankment)

Step 1: Develop Subsurface Profile (see figures 31 and 32)

Step 2: Evaluate Initial Stresses

$$\sigma_v = (5 \text{ m})(20 \text{ kN/m}^3) + (3 \text{ m})(18 \text{ kN/m}^3) = 154 \text{ kPa}$$

$$u_o = (2 \text{ m})(9.8 \text{ kN/m}^3) = 20 \text{ kPa}$$

$$\sigma'_v = \sigma_v - u_o = 154 - 20 = 134 \text{ kPa}$$

Step 3: Evaluate Stress Reduction Factor

$$r_d = 1 - 0.015z = 1 - 0.015(4.5) = 0.9325 \tag{8-1}$$

Step 4: Evaluate the Critical Stress Ratio Induced by the Earthquake

$$CSR_{eq} = 0.65 (a_{max}/g) r_d \sigma_o/\sigma'_o \tag{8-3}$$

Evaluate CSR_{eq} for two design events:

(1) OLE ($a_{max} = 0.2 \text{ g}$; $M_w = 8.0$)

$$CSR_{eq} = (0.65)(0.2)(0.88)154/134 = 0.131$$

(2) CLE ($a_{max} = 0.4 \text{ g}$; $M_w = 7.0$)

$$CSR_{eq} = (0.65)(0.4)(0.88)154/134 = 0.263$$

Step 5: Standardized Blow Count Value

Tables 8 and 9 in volume I are used to evaluate the standardized blow count. For this example, no corrections are necessary to apply since standard equipment was used for the SPT tests.



Written by: T.H.H. Date: 96 / 03 / 19 Reviewed by: E.K. and N.M. Date: 96 / 03 / 21
YY MM DD YY MM DD

Client: FHWA Project: GEC-3 Project/Proposal No.: GE3686 Task No.: F

Step 6: Correction for SPT N value for Overburden Pressure

The construction of the embankment has an effect on the overburden pressure but it is assumed that it will not affect the SPT values. Under the 3.5 meters of fill, the settlement of the sand layer will be negligible; consequently, the liquefaction resistance of the sand as measured by the SPT value is not affected by the increase in overburden pressure. Therefore the corrected SPT values to use in the analysis are the same as for the free-field analysis.

$$(N_1)_{60} = (N_1)_{60 \text{ free-field}} = 14$$

Step 7: Evaluate Critical Stress Ratio Resisting Liquefaction (figure 58 in volume I)

For N = 14 and a fines content of 5% $CSR_{7.5} = 0.16$

Step 8: Correct Critical Stress Ratio Resisting Liquefaction

$$CSR_L = CSR_{7.5} k_M k_\alpha k_\sigma$$

- k_M is read from figure 59 in volume I

$$M_w = 8.0 \quad k_M = 0.93$$

$$M_w = 7.0 \quad k_M = 1.08$$

- k_α read from figure 60 of volume I

$$\sigma'_v = 134 \text{ kPa} \quad k_\alpha = 0.96$$

- $k_\sigma = 1.0$, no initial static shear

(1) $OLE (a_{max} = 0.2 \text{ g}; M_w = 8.0)$

$$CSR_L = (0.16)(1)(0.96)(0.93) \approx 0.138$$

(2) $CLE (a_{max} = 0.4 \text{ g}; M_w = 7.0)$

$$CSR_L = (0.16)(1)(0.96)(1.08) \approx 0.162$$



Written by: T.H.H. Date: 96 / 03 / 19 Reviewed by: E.K. and N.M. Date: 96 / 03 / 21
YY MM DD YY MM DD

Client: FHWA Project: GEC-3 Project/Proposal No.: GE3686 Task No.: F

Step 9: Calculate Factor of Safety Against Liquefaction

(1) OLE ($a_{max} = 0.2 \text{ g}$; $M_w = 8.0$)

$$FS_L = CSR_L / CSR_{eq} = 0.138 / 0.131 = 1.05$$

(2) CLE ($a_{max} = 0.4 \text{ g}$; $M_w = 7.0$)

$$FS_L = CSR_L / CSR_{eq} = 0.162 / 0.262 = 0.614$$

A spreadsheet was developed to perform the calculation for the other depths. The results are presented in table 11.



Written by: T.H.H. Date: 96 / 03 / 19 Reviewed by: E.K. and N.M. Date: 96 / 03 / 21
 YY MM DD YY MM DD

Client: FHWA Project: GEC-3 Project/Proposal No.: GE3686 Task No.: F

Table 11. Liquefaction potential under the centerline of the embankment.

Depth (m)	Fines Content	N _{field}	σ _v	σ _v '	C _N	C ₆₀	(N ₁) ₆₀	r _d	OLE event: a _{max} = 0.2 g; M _w = 8						
									k _M	k _σ	k _σ	CSR _{eq}	CSR _{7.5}	CSR _L	FS _L
3	6	9	127	122	1.44	1	13	0.903	1.08	1.000	0.794	0.244	0.143	0.151	0.617
4.5	5	11	154	134	1.28	1	14	0.880	1.08	1.000	0.959	0.263	0.155	0.162	0.614
6	6	13	181	151	1.17	1	15	0.858	1.08	1.000	0.939	0.267	0.167	0.170	0.636
7.5	7	15	208	163	1.08	1	16	0.835	1.08	1.000	0.924	0.277	0.178	0.179	0.644
9	4	17	235	175	1.01	1	17	0.813	1.08	1.000	0.910	0.284	0.189	0.186	0.656
10.5	5	19	262	187	0.95	1	18	0.790	1.08	1.000	0.896	0.288	0.199	0.193	0.670
12	8	26	290.5	200.5	0.89	1	23	0.768	1.08	1.000	0.879	0.289	0.256	0.244	0.843
13.5	6	32	319	214	0.85	1	27	0.745	1.08	1.000	0.863	0.289	0.340	0.318	1.102
15	11	40	347.5	227.5	0.81	1	32	0.723	1.08	1.000	0.847	0.287	N/A	N/A	N/A
16.5	12	49	376	241	0.77	1	38	0.700	1.08	1.000	0.831	0.284	N/A	N/A	N/A
18	13	60	404.5	254.5	0.74	1	45	0.678	1.08	1.000	0.815	0.280	N/A	N/A	N/A

									OLE event: a _{max} = 0.2 g; M _w = 8						
3	6	9	127	122	1.44	1	13	0.903	0.93	1.000	0.794	0.122	0.143	0.129	1.055
4.5	5	11	154	134	1.28	1	14	0.880	0.93	1.000	0.959	0.131	0.155	0.138	1.051
6	6	13	181	151	1.17	1	15	0.858	0.93	1.000	0.939	0.134	0.167	0.145	1.089
7.5	7	15	208	163	1.08	1	16	0.835	0.93	1.000	0.924	0.139	0.178	0.153	1.102
9	4	17	235	175	1.01	1	17	0.813	0.93	1.000	0.910	0.142	0.189	0.159	1.122
10.5	5	19	262	187	0.95	1	18	0.790	0.93	1.000	0.896	0.144	0.199	0.165	1.145
12	8	26	290.5	200.5	0.89	1	23	0.768	0.93	1.000	0.879	0.145	0.256	0.209	1.443
13.5	6	32	319	214	0.85	1	27	0.745	0.93	1.000	0.863	0.144	0.340	0.272	1.884
15	11	40	347.5	227.5	0.81	1	32	0.723	0.93	1.000	0.847	0.143	N/A	N/A	N/A
16.5	12	49	376	241	0.77	1	38	0.700	0.93	1.000	0.831	0.142	N/A	N/A	N/A
18	13	60	404.5	254.5	0.74	1	45	0.678	0.93	1.000	0.815	0.140	N/A	N/A	N/A

- N_{field} SPT blow-count from field investigation
- C_N Correction factor for overburden pressure (equation 8-5 or figure 57 of volume I)
- C₆₀ Correction factor for equipment (tables 8 and 9 of volume I)
- (N₁)₆₀ SPT blow count corrected as per equation 8-6
- r_d Stress reduction factor (equation 8-1 or figure 56 of volume I)
- k_M Magnitude correction factor (figure 59 of volume I)
- k_σ Initial static shear stress correction factor (figure 61 of volume I)
- k_σ Stress level correction factor (figure 60 of volume I)
- CSR_{eq} Critical stress ratio imposed by the earthquake (equation 8-3 of volume I)
- CSR_{7.5} Critical stress ratio read from figure 58 of volume I
- CSR_L Critical stress ratio from figure 58 corrected as per equation 8-7 of volume I
- σ_v Total normal stress
- σ_v' Effective normal stress
- FS_L Factor of Safety
- a_{max} Peak ground acceleration
- M_w Moment magnitude
- CLE Contingency Level Event
- OLE Operational Level Event
- N/A Not Applicable (for (N₁)₆₀>30, CSR_{7.5} becomes very large as shown on figure 58 of volume I)



Written by: T.H.H. Date: 96 / 03 / 19 Reviewed by: E.K. and N.M. Date: 96 / 03 / 21
YY MM DD YY MM DD

Client: FHWA Project: GEC-3 Project/Proposal No.: GE3686 Task No.: F

Under Toe of Embankment

Step 1: Develop Subsurface Profile (see figures 31 and 32)

Step 2: Evaluate Initial Stresses

The sloping embankment will affect both vertical and horizontal stresses in the ground. The additional stress applied at depth by the embankment is evaluated using the elastic solutions collected by Poulos and Davis (1974).

Use figure 46 (solution by Gray, 1936; replotted in Poulos and Davis, 1974 as figure 3.12) to compute the stresses at depth of 4.5 m under the toe of the embankment.

$$\sigma_v = \sigma_v \text{ free-field} + \Delta\sigma_{\text{embankment}}$$

$$\Delta\sigma_{\text{embankment}} = [P/(\pi a)] \cdot (a\beta + \alpha x) \text{ (equation 13-2a in Poulos and Davis)}$$

$$a = 5.25\text{m}; x=0; \alpha \approx 0.862 \text{ rad}; \beta \approx 0.709 \text{ rad}; p = (3.5 \text{ m})(20 \text{ kN/m}^3) = 70 \text{ kPa}$$

$$\Delta\sigma_{\text{embankment}} = (70)/[(\pi)(5.25)] [(5.25)(0.709)+0] = 15.8 \text{ kPa}$$

$$\sigma_v = \sigma_v \text{ free-field} + \Delta\sigma_{\text{embankment}}$$

$$= (1.5 \text{ m})(20 \text{ kN/m}^3) + (3 \text{ m})(18 \text{ kN/m}^3) + (15.8 \text{ kPa}) = 99.8 \text{ kPa}$$

$$u_o = (2 \text{ m})(9.8 \text{ kN/m}^3) = 20 \text{ kPa}$$

$$\sigma'_v = \sigma_v - u_o = 99.8 - 20 = 79.8 \text{ kPa}$$

Calculate the initial static shear stress.

$$\tau = \rho \alpha z / \pi a \text{ (equation 3-21c in Poulos and Davis)}$$

$$a_{\text{max}} = 5.25 \text{ m}, \alpha \approx 0.862 \text{ radians}; p = 70 \text{ kPa}$$

$$\tau = (70)(0.862)(4.5)/(\pi)(5.25) = 16.5 \text{ kPa}$$



Written by: T.H.H. Date: 96 / 03 / 19 Reviewed by: E.K. and N.M. Date: 96 / 03 / 21
YY MM DD YY MM DD

Client: FHWA Project: GEC-3 Project/Proposal No.: GE3686 Task No.: F

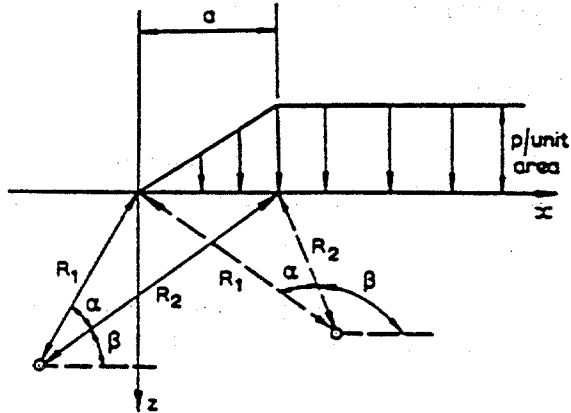


FIG. 3.12

$$\sigma_z = \frac{p}{\pi a} [a\beta + \alpha] \quad \dots (3.12a)$$

$$\sigma_x = \frac{p}{\pi a} [a\beta + \alpha + 2z \log_e \frac{R_2}{R_1}] \quad \dots (3.12b)$$

$$\tau_{xz} = -\frac{p}{\pi a} z \alpha \quad \dots (3.12c)$$

$$\left. \begin{matrix} \sigma_1 \\ \sigma_3 \end{matrix} \right\} = \frac{p}{\pi a} [(a\beta + \alpha + z \log_e \frac{R_2}{R_1}) \pm z (\log_e^2 \frac{R_2}{R_1} + \alpha^2)^{\frac{1}{2}}] \quad \dots (3.12d)$$

$$\tau_{max} = \frac{pz}{\pi a} (\log_e^2 \frac{R_2}{R_1} + \alpha^2)^{\frac{1}{2}} \quad \dots (3.12e)$$

Figure 46. Stresses under an embankment (Poulos and Davis, 1974, reprinted by permission of H.G. Poulos).



Written by: T.H.H. Date: 96 / 03 / 19 Reviewed by: E.K. and N.M. Date: 96 / 03 / 21
YY MM DD YY MM DD

Client: FHWA Project: GEC-3 Project/Proposal No.: GE3686 Task No.: F

Step 3: Evaluate Stress Reduction Factor

$$r_d = 1 - 0.015z = 1 - 0.015(4.5) = 0.9325 \tag{8-1}$$

Step 4: Evaluate the Critical Stress Ratio Induced by the Earthquake

$$CSR_{eq} = 0.65 (a_{max}/g) r_d \sigma_v/\sigma'_v \tag{8-3}$$

Evaluate CSR_{eq} for two design events:

- (1) OLE ($a_{max} = 0.2 \text{ g}$; $M_w = 8.0$)
 $CSR_{eq} = (0.65)(0.2)(0.9325)99.8/79.8 = 0.152$
- (2) CLE ($a_{max} = 0.4 \text{ g}$; $M_w = 7.0$)
 $CSR_{eq} = (0.65)(0.4)(0.9325)99.8/79.8 = 0.303$

Step 5: Standardized Blow Count Value

Tables 8 and 9 in volume I are used to evaluate the standardized blow count. For this example, no corrections are necessary to apply since standard equipment was used for the SPT tests.

Step 6: Correction for SPT N value for Overburden Pressure

The construction of the embankment has an effect on the overburden pressure but it assumed that it will not affect the SPT values. Under the 3.5 meters of fill, the settlement of the sand layer will be negligible; consequently, the liquefaction resistance of the sand as measured by the SPT value is not affected by the increase in overburden pressure. Therefore the corrected SPT values to use in the analysis are the same as for the free-field analysis.

$$(N_1)_{60} = (N_1)_{60 \text{ free-field}} = 14$$

Step 7: Evaluate Critical Stress Ratio Resisting Liquefaction (figure 58 in volume I)

For $N = 14$ and a fines content of 5% $CSR_{7.5} = 0.16$



Written by: T.H.H. Date: 96 / 03 / 19 Reviewed by: E.K. and N.M. Date: 96 / 03 / 21
YY MM DD YY MM DD

Client: FHWA Project: GEC-3 Project/Proposal No.: GE3686 Task No.: F

Step 8: Correct Critical Stress Ratio Resisting Liquefaction

$$CSR_L = CSR_{7.5} k_M k_\alpha k_\sigma$$

- k_M is read from figure 59 in volume I

$$M_w = 8.0 \quad k_M = 0.93$$

$$M_w = 7.0 \quad k_M = 1.08$$

- k_σ is read from figure 60 in volume I

$$\sigma'_v = 79.8 \text{ kPa} \quad k_\sigma = 1.025$$

- k_α = read from figure 61 in volume I

$$\alpha = \tau_{ho} / \sigma'_v = 16.5 / 79.8 = 0.21$$

$$k_\alpha \approx 1.15 \text{ for } \alpha = 0.21$$

(value obtained using lower bound curve for medium-dense soils, i.e., relative density = 45-50%)

(1) OLE ($a_{max} = 0.2 \text{ g}$; $M_w = 8.0$)

$$CSR_L = (0.16)(1.15)(1.025)(0.93) \approx 0.169$$

(2) CLE ($a_{max} = 0.4 \text{ g}$; $M_w = 7.0$)

$$CSR_L = (0.16)(1.15)(1.025)(1.08) \approx 0.197$$

Step 9: Calculate Factor of Safety

(1) OLE ($a_{max} = 0.2 \text{ g}$; $M_w = 8.0$)

$$FS_L = CSR_L / CSR_{eq} = 0.169 / 0.151 = 1.11$$



Written by: T.H.H. Date: 96 / 03 / 19 Reviewed by: E.K. and N.M. Date: 96 / 03 / 21
 YY MM DD YY MM DD

Client: FHWA Project: GEC-3 Project/Proposal No.: GE3686 Task No.: F

(2) CLE ($a_{max} = 0.4 \text{ g}$; $M_w = 7.0$)

$$FS_L = CSR_L / CSR_{eq} = 0.197 / 0.302 = 0.651$$

A spreadsheet was developed to perform the calculation for the other depths. The results are presented in table 12.

Table 12. Liquefaction potential under the toe of the embankment.

									CLE event: $a_{max} = 0.4 \text{ g}$; $M_w = 7$						
Depth (m)	Fines Content	N_{field}	σ_v	σ_v'	C_N	C_{60}	$(N_1)_{60}$	r_d	k_M	k_s	k_n	CSR_{eq}	$CSR_{7.5}$	CSR_L	FS_L
3	6	9	68.6	64	1.44	1	13	0.955	1.08	1.147	1.044	0.268	0.143	0.185	0.692
4.5	5	11	99.8	80	1.28	1	14	0.933	1.08	1.144	1.024	0.303	0.155	0.197	0.651
6	6	13	130.0	95	1.17	1	15	0.910	1.08	1.135	1.006	0.324	0.167	0.207	0.639
7.5	7	15	159.4	109	1.08	1	16	0.888	1.08	1.124	0.989	0.336	0.178	0.215	0.639
9	4	17	188.2	123	1.01	1	17	0.865	1.08	1.147	0.972	0.344	0.189	0.228	0.664
10.5	5	19	216.7	137	0.95	1	18	0.843	1.08	1.136	0.956	0.347	0.199	0.234	0.673
12	8	26	244.8	150	0.89	1	23	0.820	1.08	1.126	0.940	0.348	0.256	0.294	0.843
13.5	6	32	272.7	163	0.85	1	27	0.798	1.08	1.157	0.925	0.348	0.340	0.394	1.134
15	11	40	300.5	175	0.81	1	32	0.775	1.08	1.147	0.909	0.345	N/A	N/A	N/A
16.5	12	49	328.1	188	0.77	1	38	0.753	1.08	1.138	0.894	0.341	N/A	N/A	N/A
18	13	60	355.7	201	0.74	1	45	0.730	1.08	1.130	0.879	0.336	N/A	N/A	N/A
									OLE event: $a_{max} = 0.2 \text{ g}$; $M_w = 8$						
3	6	9	68.6	63.6	1.44	1	13	0.955	0.93	1.147	1.044	0.134	0.143	0.158	1.183
4.5	5	11	99.8	79.8	1.28	1	14	0.933	0.93	1.144	1.024	0.152	0.155	0.169	1.114
6	6	13	130.0	95.0	1.17	1	15	0.910	0.93	1.135	1.006	0.162	0.167	0.177	1.093
7.5	7	15	159.4	109.4	1.08	1	16	0.888	0.93	1.124	0.989	0.168	0.178	0.184	1.092
9	4	17	188.2	123.2	1.01	1	17	0.865	0.93	1.147	0.972	0.172	0.189	0.195	1.135
10.5	5	19	216.7	136.7	0.95	1	18	0.843	0.93	1.136	0.956	0.174	0.199	0.200	1.151
12	8	26	244.8	149.8	0.89	1	23	0.820	0.93	1.126	0.940	0.174	0.256	0.251	1.442
13.5	6	32	272.7	162.7	0.85	1	27	0.798	0.93	1.157	0.925	0.174	0.340	0.337	1.940
15	11	40	300.5	175.5	0.81	1	32	0.775	0.93	1.147	0.909	0.173	N/A	N/A	N/A
16.5	12	49	328.1	188.1	0.77	1	38	0.753	0.93	1.138	0.894	0.141	N/A	N/A	N/A
18	13	60	355.7	200.7	0.74	1	45	0.730	0.93	1.130	0.879	0.168	N/A	N/A	N/A

N_{field} SPT blow-count from field investigation
 C_N Correction factor for overburden pressure (equation 8-5 or figure 57 of volume I)
 C_{60} Correction factor for equipment (tables 8 and 9 of volume I)
 $(N_1)_{60}$ SPT blow count corrected as per equation 8-6
 r_d Stress reduction factor (equation 8-1 or figure 56 of volume I)
 k_M Magnitude correction factor (figure 59 of volume I)
 k_s Initial static shear stress correction factor (figure 61 of volume I)
 k_n Stress level correction factor (figure 60 of volume I)
 CSR_{eq} Critical stress ratio imposed by the earthquake (equation 8-3 of volume I)
 $CSR_{7.5}$ Critical stress ratio read from figure 58 of volume I
 CSR_L Critical stress ratio from figure 58 corrected as per equation 8-7 of volume I

σ_v Total normal stress
 σ_v' Effective normal stress
 FS Factor of Safety
 a_{max} Peak ground acceleration
 M_w Moment magnitude
 CLE Contingency Level Event
 OLE Operational Level Event
 N/A Not Applicable (for $(N_1)_{60} > 30$, $CSR_{7.5}$ becomes very large as shown on figure 58 of Volume I)



Written by: T.H.H. Date: 96 / 03 / 19 Reviewed by: E.K. and N.M. Date: 96 / 03 / 21
 YY MM DD YY MM DD

Client: FHWA Project: GEC-3 Project/Proposal No.: GE3686 Task No.: F

EXAMPLE 5

PCSTABL Output File

** pcSTABL4 **

by
 Purdue University

--Slope Stability Analysis--
 Simplified Janbu Method of Slices
 or Simplified Bishop Method

Run Date: 7-23-96
 Time of Run: 10:33
 Run By: THH
 Input Data Filename: liq3ole
 Output Filename: liq3ole.out

PROBLEM DESCRIPTION Liquefaction example
 Dynamic analysis

BOUNDARY COORDINATES

7 Top Boundaries
 10 Total Boundaries

Boundary No.	X-Left (ft)	Y-Left (ft)	X-Right (ft)	Y-Right (ft)	Soil Type Below Bnd
1	.00	50.00	35.00	50.00	3
2	35.00	50.00	50.00	50.00	1
3	50.00	50.00	67.22	61.48	1
4	67.22	61.48	126.26	61.48	1
5	126.26	61.48	143.48	50.00	1
6	143.48	50.00	163.60	50.00	1
7	163.60	50.00	200.00	50.00	3
8	35.00	50.00	45.00	45.00	3
9	153.60	45.00	163.60	50.00	3
10	.00	45.00	200.00	45.00	2

ISOTROPIC SOIL PARAMETERS

3 Type(s) of Soil

Soil Type No.	Total Unit Wt. (pcf)	Saturated Unit Wt. (pcf)	Cohesion Intercept (psf)	Friction Angle (deg)	Pore Pressure Param.	Pressure Constant (psf)	Piez. Surface No.
1	118.0	118.0	200.0	32.0	.00	.0	0
2	115.0	115.0	.0	33.0	.00	.0	0
3	110.0	110.0	150.0	.0	.00	.0	0



Written by: T.H.H. Date: 96 / 03 / 19 Reviewed by: E.K. and N.M. Date: 96 / 03 / 21
YY MM DD YY MM DD

Client: FHWA Project: GEC-3 Project/Proposal No.: GE3686 Task No.: F

A Horizontal Earthquake Loading Coefficient
Of .100 Has Been Assigned

A Vertical Earthquake Loading Coefficient
Of .000 Has Been Assigned

Cavitation Pressure = .0 psf
A Critical Failure Surface Searching Method, Using A Random
Technique For Generating Circular Surfaces, Has Been Specified.

400 Trial Surfaces Have Been Generated.

20 Surfaces Initiate From Each Of 20 Points Equally Spaced
Along The Ground Surface Between X = 10.00 ft.
and X = 50.00 ft.

Each Surface Terminates Between X = 65.00 ft.
and X = 100.00 ft.

Unless Further Limitations Were Imposed, The Minimum Elevation
At Which A Surface Extends Is Y = .00 ft.

2.00 ft. Line Segments Define Each Trial Failure Surface.

Following Are Displayed The Ten Most Critical Of The Trial
Failure Surfaces Examined. They Are Ordered - Most Critical
First.

* * Safety Factors Are Calculated By The Modified Janbu Method * *

Failure Surface Specified By 26 Coordinate Points

*** 1.856 ***

Failure Surface Specified By 28 Coordinate Points

*** 1.901 ***

Failure Surface Specified By 29 Coordinate Points

*** 1.919 ***

Failure Surface Specified By 16 Coordinate Points

*** 1.935 ***

Failure Surface Specified By 17 Coordinate Points

*** 1.962 ***



Written by: T.H.H. Date: 96 / 03 / 19 Reviewed by: E.K. and N.M. Date: 96 / 03 / 21
YY MM DD YY MM DD

Client: FHWA Project: GEC-3 Project/Proposal No.: GE3686 Task No.: F

Failure Surface Specified By 27 Coordinate Points

*** 1.968 ***

Failure Surface Specified By 19 Coordinate Points

*** 1.968 ***

Failure Surface Specified By 15 Coordinate Points

*** 1.971 ***

Failure Surface Specified By 29 Coordinate Points

*** 1.986 ***

Failure Surface Specified By 17 Coordinate Points

*** 1.987 ***

Note: Failure surface coordinates omitted from the original PCSTABL output.



Written by: T.H.H. Date: 96 / 03 / 19 Reviewed by: E.K. and N.M. Date: 96 / 03 / 21
 YY MM DD YY MM DD

Client: FHWA Project: GEC-3 Project/Proposal No.: GE3686 Task No.: F

SHAKE Output File

```
*****
* SHAKE -- A COMPUTER PROGRAM FOR EARTHQUAKE RESPONSE *
* ANALYSIS OF HORIZONTALLY LAYERED SITES *
* by: Per B. Schnabel & John Lysmer -- 1970 *
* ----- *
* Shake85 : IBM-PC version of SHAKE *
* by: S.S. (Willie) Lai, January 1985 *
* ----- *
* Shake88 : New modulus reduction curves for clays *
* added using results from Sun et al. (1988) *
* by: J. I. Sun & Ramin Golesorkhi *
* February 26, 1988 *
* ----- *
* Shake90/91: Adjust last iteration; Input now is either *
* Gmax or max Vs; up to 13 material types can *
* be specified by user; up to 50 Layers can *
* be specified; object motion can be read in *
* from a separate file and can have user *
* specified format; Different periods for *
* response spectral calculations; options *
* are renumbered; and general cleanup *
* by: J. I. Sun, I. M. Idriss & P. Dirrim *
* June 1990 - February 1991 *
* ----- *
* Shake91 : General cleanup and finalization of input / *
* output format ... etc *
* by: I. M. Idriss *
* December 1991 *
* ----- *
* Shake94 : Routine for direct calculation of average *
* (á1) acceleration is added to the program. Out- *
* put format is modified to enable the two - *
* - page landscape printing. The following *
* modulus reduction and damping curves are *
* added: Kavazanjian & Matasovic (1995) for *
* municipal solid waste; Matasovic & Vucetic *
* (1993) for SMB sand; and Vucetic and Dobry *
* (1991) for clays of various plasticities. *
* by: Neven Matasovic *
* August 1993 - May 1994 *
*****
```

MAX. NUMBER OF TERMS IN FOURIER TRANSFORM = 4096
 NECESSARY LENGTH OF BLANK COMMON X = 25619

***** OPTION 1 *** READ RELATION BETWEEN SOIL PROPERTIES AND STRAIN

 MATERIAL TYPE NO. 4

CURVE NO. 7: #4 Modulus for Clay (PI=15) (Vucetic and Dobry, 1991)
 CURVE NO. 8: Damping for Clay (PI=15) (Vucetic and Dobry, 1991)

CURVE NO. 7		CURVE NO. 8	
STRAIN	G/Gmax	STRAIN	DAMPING
.0001	1.000	.0001	.85
.0003	1.000	.0003	1.04



GEOSYNTEC CONSULTANTS

Written by: T.H.H. Date: 96 / 03 / 19 Reviewed by: E.K. and N.M. Date: 96 / 03 / 21
 YY MM DD YY MM DD

Client: FHWA Project: GEC-3 Project/Proposal No.: GE3686 Task No.: F

.0010	.995	.0010	1.55
.0032	.936	.0032	2.58
.0100	.818	.0100	4.64
.0316	.640	.0316	7.77
.1000	.405	.1000	11.67
.3160	.210	.3160	16.08
1.0000	.095	1.0000	20.12
3.1600	.034	3.1600	23.17

 MATERIAL TYPE NO. 8

CURVE NO. 15:
 CURVE NO. 16:

CURVE NO.15		CURVE NO.16	
=====		=====	
STRAIN	G/Gmax	STRAIN	DAMPING
-----	-----	-----	-----

 MATERIAL TYPE NO. 5

CURVE NO. 9: #5 Modulus for Clay (PI=50) (Vucetic and Dobry 1991)
 CURVE NO. 10: Damping for Clay (PI=50) (Vucetic and Dobry, 1991)

CURVE NO. 9		CURVE NO.10	
=====		=====	
STRAIN	G/Gmax	STRAIN	DAMPING
-----	-----	-----	-----
.0001	1.000	.0001	.85
.0003	1.000	.0003	1.04
.0010	1.000	.0010	1.09
.0032	.996	.0032	1.91
.0100	.957	.0100	3.00
.0316	.846	.0316	4.36
.1000	.672	.1000	6.27
.3160	.461	.3160	9.41
1.0000	.245	1.0000	13.57
3.1600	.064	3.1600	18.21

 MATERIAL TYPE NO. 7

CURVE NO. 13:
 CURVE NO. 14:

CURVE NO.13		CURVE NO.14	
=====		=====	
STRAIN	G/Gmax	STRAIN	DAMPING
-----	-----	-----	-----

 MATERIAL TYPE NO. 2



Written by: T.H.H. Date: 96 / 03 / 19 Reviewed by: E.K. and N.M. Date: 96 / 03 / 21
 YY MM DD YY MM DD

Client: FHWA Project: GEC-3 Project/Proposal No.: GE3686 Task No.: F

CURVE NO. 3: #2 ATTENUATION OF ROCK AVERAGE
 CURVE NO. 4: DAMPING IN ROCK

CURVE NO. 3		CURVE NO. 4	
STRAIN	G/Gmax	STRAIN	DAMPING
.0001	1.000	.0001	.40
.0003	1.000	.0010	.80
.0010	.988	.0100	1.50
.0030	.952	.1000	3.00
.0100	.900	1.0000	4.60
.0300	.810	.0000	.00
.1000	.725	.0000	.00
1.0000	.550	.0000	.00

 MATERIAL TYPE NO. 6

CURVE NO. 11:
 CURVE NO. 12:

CURVE NO.11		CURVE NO.12	
STRAIN	G/Gmax	STRAIN	DAMPING

 MATERIAL TYPE NO. 3

CURVE NO. 5: #3 Modulus for Peat (TETC modification of Seed & Idriss
 CURVE NO. 6: Damping for Clay used for Peat (Seed & Idriss, 1990)

CURVE NO. 5		CURVE NO. 6	
STRAIN	G/Gmax	STRAIN	DAMPING
.0001	1.000	.0001	1.98
.0003	.830	.0003	2.03
.0010	.680	.0010	2.69
.0030	.550	.0030	3.54
.0100	.450	.0100	4.59
.0300	.366	.0300	6.56
.1000	.293	.1000	9.18
.3000	.225	.3000	3.77
1.0000	.160	1.0000	19.48
3.0000	.099	3.1600	25.38
10.0000	.020	10.0000	28.00

***** OPTION 2 *** READ SOIL / WASTE PROFILE

SOIL PROFILE NO. 1 Channel deposit

NUMBER OF LAYERS 9
 DEPTH TO BEDROCK 112.0

NO.	TYPE	THICKNESS (ft)	DEPTH (ft)	TOT. PRESS. (psf)	MODULUS (ksf)	DAMPING (%)	UNIT WT. (pcf)	SH. VEL. (fps)
-----	------	-------------------	---------------	----------------------	------------------	----------------	-------------------	-------------------



Written by: T.H.H. Date: 96 / 03 / 19 Reviewed by: E.K. and N.M. Date: 96 / 03 / 21
 YY MM DD YY MM DD

Client: FHWA Project: GEC-3 Project/Proposal No.: GE3686 Task No.: F

1	3	6.00	3.00	300.00	629.	5.00	100.00	450.0
2	5	15.00	13.50	1425.00	854.	5.00	110.00	500.0
3	1	18.00	30.00	3285.00	1286.	5.00	115.00	600.0
4	4	15.00	46.50	5220.00	1698.	5.00	120.00	675.0
5	1	15.00	61.50	7057.50	2040.	5.00	125.00	725.0
6	1	15.00	76.50	8955.00	2544.	5.00	128.00	800.0
7	1	12.00	90.00	10695.00	4502.	5.00	130.00	1056.0
8	4	16.00	104.00	12435.00	16435.	5.00	120.00	2100.0
9	BASE				39130.	1.00	140.00	3000.0

PERIOD = .500 sec FROM AVERAGE SHEAR WAVE VELOCITY OF 895.3 ft/sec

FREQUENCY AMPLITUDE:
 MAXIMUM AMPLIFICATION = 14.13
 FOR FREQUENCY (f) = 2.02 c/sec
 FOR PERIOD (1 / f) = .50 sec

***** OPTION 3 *** READ INPUT MOTION

FILE NAME FOR INPUT MOTION = riodl-hz.sar
 NO. OF INPUT ACCEL. POINTS = 1800
 NO. OF POINTS USED IN FFT = 4096
 NO. OF HEADING LINES = 5
 NO. OF POINTS PER LINE = 8
 TIME STEP FOR INPUT MOTION = .0200
 FORMAT FOR OF TIME HISTORY = (8F9.6)

***** ACCELEROGRAM HEADER *****

CAPE MENDOCINO, CA EQ.; Mw = 7.0; Ms = 7.1; H = 15 km; Thrust
 RIO DELL - 101/PAINTER ST. OVERPASS; CHAN 4: 270 Deg. (free-field)
 UNCOR MAX = -0.385 g @ 5.575 sec; MAX IN FILE = .385732 @ 5.58 sec
 RMS ACCEL OF (UNCOR) RECORD = .041 g; Mean sq. freq. = 3.01 Hz
 8*225 = 1800 POINTS OF ACCEL DATA EQUALLY SPACED AT .020 SEC. (UNITS: g)

** FIRST & LAST 5 LINES OF INPUT MOTION *****

1	-.002296	-.001777	.000569	.000731	-.003688	-.000583	.004051	.002788
2	.000964	-.002422	-.004550	-.004451	-.005423	-.008852	-.014746	-.015439
3	-.011380	-.006311	-.005492	-.008705	-.008035	-.006091	-.004255	-.001129
4	.002864	.006916	.010118	.005313	-.004705	-.003748	.003541	.005366
5	.000370	-.000956	.004816	.007193	.010419	.013203	.011285	.008016
..... INPUT MOTION READ NOT ECHOED.....								
221	-.005527	-.003620	-.002145	-.002337	-.002461	-.004595	-.007641	-.008303
222	-.007946	-.006056	-.005096	-.005324	-.005166	-.005233	-.004698	-.004398
223	-.002852	-.002130	-.002072	-.002438	-.002967	-.001687	.001139	.004567
224	.006282	.006832	.006628	.008013	.009033	.007818	.006191	.003176
225	.000796	-.001591	-.001767	.000490	.000460	-.001572	.000280	.001179

MAXIMUM ACCELERATION = .385732
 AT TIME = 5.58 sec

THE VALUES WILL BE MULTIPLIED BY A FACTOR = 1.03698900
 TO GIVE NEW MAXIMUM ACCELERATION = .40000000

MEAN SQUARE FREQUENCY = 3.02 c/sec

***** OPTION 4 *** READ WHERE OBJECT MOTION IS GIVEN

OBJECT MOTION IN LAYER NUMBER 9 OUTCROPPING

***** OPTION 5 *** OBTAIN STRAIN COMPATIBLE SOIL PROPERTIES



Written by: T.H.H. Date: 96 / 03 / 19 Reviewed by: E.K. and N.M. Date: 96 / 03 / 21
 YY MM DD YY MM DD

Client: FHWA Project: GEC-3 Project/Proposal No.: GE3686 Task No.: F

MAXIMUM NUMBER OF ITERATIONS = 8
 FACTOR FOR UNIFORM STRAIN IN TIME DOMAIN = .80

ACCELEROGRAM - ri odl-hz.sar
 P R O F I L E - Channel deposit

ITERATION NUMBER 1

VALUES IN TIME DOMAIN

NO	TYPE	DEPTH (ft)	UNIFRM. STRAIN	<---- DAMPING ---->			<---- SHEAR MODULUS ---->			G/Go RATIO
				NEW	USED	ERROR	NEW	USED	ERROR	
1	3	3.0	.02549	.063	.050	20.2	238.0	628.9	-164.2	1.000
2	5	13.5	.08523	.060	.050	16.7	594.5	854.0	-43.6	1.000
3	1	30.0	.11440	.105	.050	52.4	445.8	1285.7	-188.4	1.000
4	4	46.5	.12843	.126	.050	60.4	615.7	1698.0	-175.8	1.000
5	1	61.5	.13289	.113	.050	55.7	654.6	2040.5	-211.7	1.000
6	1	76.5	.12099	.108	.050	53.7	857.5	2544.1	-196.7	1.000
7	1	90.0	.07291	.086	.050	41.6	1984.8	4502.1	-126.8	1.000
8	4	104.0	.02222	.068	.050	26.6	11413.7	16434.8	-44.0	1.000

ACCELEROGRAM - ri odl-hz.sar
 P R O F I L E - Channel deposit

ITERATION NUMBER 2

VALUES IN TIME DOMAIN

NO	TYPE	DEPTH (ft)	UNIFRM. STRAIN	<---- DAMPING ---->			<---- SHEAR MODULUS ---->			G/Go RATIO
				NEW	USED	ERROR	NEW	USED	ERROR	
1	3	3.0	.07669	.086	.063	27.1	194.4	238.0	-22.4	.378
2	5	13.5	.14287	.072	.060	17.1	518.0	594.5	-14.8	.696
3	1	30.0	.39431	.167	.105	37.3	202.2	445.8	-120.4	.347
4	4	46.5	.36728	.166	.126	24.0	331.1	615.7	-86.0	.363
5	1	61.5	.38060	.166	.113	32.0	327.0	654.6	-100.2	.321
6	1	76.5	.29116	.153	.108	29.7	471.1	857.5	-82.0	.337
7	1	90.0	.13044	.112	.086	23.4	1458.8	1984.8	-36.1	.441
8	4	104.0	.02521	.072	.068	4.8	11092.5	11413.7	-2.9	.694

ACCELEROGRAM - ri odl-hz.sar
 P R O F I L E - Channel deposit

ITERATION NUMBER 3

VALUES IN TIME DOMAIN

NO	TYPE	DEPTH (ft)	UNIFRM. STRAIN	<---- DAMPING ---->			<---- SHEAR MODULUS ---->			G/Go RATIO
				NEW	USED	ERROR	NEW	USED	ERROR	
1	3	3.0	.06958	.084	.086	-2.5	198.1	194.4	1.9	.309
2	5	13.5	.12044	.068	.072	-6.9	544.8	518.0	4.9	.607
3	1	30.0	.60652	.187	.167	10.5	156.3	202.2	-29.4	.157
4	4	46.5	.43734	.172	.166	3.6	301.5	331.1	-9.8	.195
5	1	61.5	.48310	.177	.166	6.2	286.5	327.0	-14.1	.160
6	1	76.5	.38556	.166	.153	7.8	404.9	471.1	-16.3	.185
7	1	90.0	.12972	.112	.112	-.3	1463.2	1458.8	.3	.324
8	4	104.0	.01833	.063	.072	-13.8	11902.5	11092.5	6.8	.675



Written by: T.H.H. Date: 96 / 03 / 19 Reviewed by: E.K. and N.M. Date: 96 / 03 / 21
 YY MM DD YY MM DD

Client: FHWA Project: GEC-3 Project/Proposal No.: GE3686 Task No.: F

ACCELEROGRAM - riodl-hz.sar
 P R O F I L E - Channel deposit

ITERATION NUMBER 4

VALUES IN TIME DOMAIN

NO	TYPE	DEPTH (ft)	UNIFRM. <---- DAMPING ---->			<---- SHEAR MODULUS ---->			G/Go RATIO	
			STRAIN	NEW	USED	ERROR	NEW	USED		ERROR
1	3	3.0	.05954	.081	.084	-4.2	204.0	198.1	2.9	.315
2	5	13.5	.10029	.063	.068	-8.0	573.5	544.8	5.0	.638
3	1	30.0	.69363	.193	.187	3.2	141.9	156.3	-10.1	.122
4	4	46.5	.41420	.170	.172	-1.1	310.7	301.5	3.0	.178
5	1	61.5	.50639	.179	.177	1.2	278.6	286.5	-2.9	.140
6	1	76.5	.40123	.168	.166	1.1	396.5	404.9	-2.1	.159
7	1	90.0	.11523	.105	.112	-5.8	1555.4	1463.2	5.9	.325
8	4	104.0	.01550	.058	.063	-7.8	12328.8	11902.5	3.5	.724

ACCELEROGRAM - riodl-hz.sar
 P R O F I L E - Channel deposit

ITERATION NUMBER 5

VALUES IN TIME DOMAIN

NO	TYPE	DEPTH (ft)	UNIFRM. <---- DAMPING ---->			<---- SHEAR MODULUS ---->			G/Go RATIO	
			STRAIN	NEW	USED	ERROR	NEW	USED		ERROR
1	3	3.0	.05622	.079	.081	-1.6	206.2	204.0	1.1	.324
2	5	13.5	.09239	.061	.063	-2.3	584.1	573.5	1.8	.671
3	1	30.0	.74033	.196	.193	1.5	135.0	141.9	-5.2	.110
4	4	46.5	.38865	.168	.170	-1.3	321.5	310.7	3.4	.183
5	1	61.5	.50932	.179	.179	.1	277.6	278.6	-.4	.137
6	1	76.5	.39803	.168	.168	-.2	398.2	396.5	.4	.156
7	1	90.0	.10570	.101	.105	-4.4	1622.6	1555.4	4.1	.345
8	4	104.0	.01470	.057	.058	-2.6	12464.9	12328.8	1.1	.750

ACCELEROGRAM - riodl-hz.sar
 P R O F I L E - Channel deposit

ITERATION NUMBER 6

VALUES IN TIME DOMAIN

NO	TYPE	DEPTH (ft)	UNIFRM. <---- DAMPING ---->			<---- SHEAR MODULUS ---->			G/Go RATIO	
			STRAIN	NEW	USED	ERROR	NEW	USED		ERROR
1	3	3.0	.05531	.079	.079	-.5	206.8	206.2	.3	.328
2	5	13.5	.09023	.061	.061	-.6	587.2	584.1	.5	.684
3	1	30.0	.76916	.198	.196	.9	130.9	135.0	-3.1	.105
4	4	46.5	.37179	.167	.168	-.9	329.0	321.5	2.3	.189
5	1	61.5	.50659	.179	.179	-.1	278.5	277.6	.3	.136
6	1	76.5	.39215	.167	.168	-.4	401.3	398.2	.8	.157
7	1	90.0	.10045	.098	.101	-2.7	1662.3	1622.6	2.4	.360
8	4	104.0	.01446	.056	.057	-.8	12506.2	12464.9	.3	.758

ACCELEROGRAM - riodl-hz.sar
 P R O F I L E - Channel deposit

ITERATION NUMBER 7



Written by: T.H.H. Date: 96 / 03 / 19 Reviewed by: E.K. and N.M. Date: 96 / 03 / 21
 YY MM DD YY MM DD

Client: FHWA Project: GEC-3 Project/Proposal No.: GE3686 Task No.: F

VALUES IN TIME DOMAIN

NO	TYPE	DEPTH (ft)	UNIFRM. STRAIN	DAMPING			SHEAR MODULUS			G/Go RATIO
				NEW	USED	ERROR	NEW	USED	ERROR	
1	3	3.0	.05511	.079	.079	-.1	207.0	206.8	.1	.329
2	5	13.5	.08976	.061	.061	-.1	587.8	587.2	.1	.688
3	1	30.0	.78798	.199	.198	.6	128.3	130.9	-2.0	.102
4	4	46.5	.36169	.166	.167	-.6	333.7	329.0	1.4	.194
5	1	61.5	.50253	.179	.179	-.2	279.9	278.5	.5	.136
6	1	76.5	.38679	.167	.167	-.4	404.2	401.3	.7	.158
7	1	90.0	.09757	.097	.098	-1.2	1690.6	1662.3	1.7	.369
8	4	104.0	.01437	.056	.056	-.3	12522.0	12506.2	.1	.761

ACCELEROGRAM - ri odl-hz.sar
 P R O F I L E - Channel deposit

ITERATION NUMBER 8

VALUES IN TIME DOMAIN

NO	TYPE	DEPTH (ft)	UNIFRM. STRAIN	DAMPING			SHEAR MODULUS			G/Go RATIO
				NEW	USED	ERROR	NEW	USED	ERROR	
1	3	3.0	.05511	.079	.079	.0	207.0	207.0	.0	.329
2	5	13.5	.08973	.061	.061	.0	587.9	587.8	.0	.688
3	1	30.0	.80060	.200	.199	.4	126.6	128.3	-1.3	.100
4	4	46.5	.35575	.165	.166	-.4	336.5	333.7	.8	.197
5	1	61.5	.49852	.178	.179	-.2	281.2	279.9	.5	.137
6	1	76.5	.38247	.166	.167	-.3	406.6	404.2	.6	.159
7	1	90.0	.09561	.096	.097	-.8	1711.1	1690.6	1.2	.376
8	4	104.0	.01432	.056	.056	-.2	12530.8	12522.0	.1	.762

VALUES IN TIME DOMAIN

LAYER	MAT. TYPE	THICKNESS (ft)	DEPTH (ft)	MAX. STRAIN (%)	MAX. STRESS (psf)	AVG. ACC. (g)	TIME (sec)
1	3	6.0	3.0	.06888	142.57	.47524	5.90
2	5	15.0	13.5	.11217	659.38	.46272	5.90
3	1	18.0	30.0	1.00075	1284.00	.39087	5.92
4	4	15.0	46.5	.44469	1483.86	.28427	5.90
5	1	15.0	61.5	.62315	1743.93	.24710	6.00
6	1	15.0	76.5	.47809	1932.67	.21582	5.94
7	1	12.0	90.0	.11951	2020.45	.18892	5.90
8	4	16.0	104.0	.01790	2241.34	.18024	5.88

PERIOD = .815 sec FROM AVERAGE SHEAR WAVE VELOCITY OF 549.8 ft/sec

FREQUENCY AMPLITUDE:
 MAXIMUM AMPLIFICATION = 3.79
 FOR FREQUENCY (f) = .81 c/sec
 FOR PERIOD (1 / f) = 1.23 sec

***** OPTION 6 *** COMPUTE MOTION IN NEW SUBLAYERS

ACCELEROGRAM - ri odl-hz.sar
 D E P O S I T - Channel deposit

LAYER	DEPTH (ft)	MAX. ACC. (g)	TIME (sec)	MN.SQ.FR. (c/sec)	ACC. RATIO QUIET ZONE	TH SAVED ACC.REC.
-------	---------------	------------------	---------------	----------------------	--------------------------	----------------------



Written by: T.H.H. Date: 96 / 03 / 19 Reviewed by: E.K. and N.M. Date: 96 / 03 / 21
YY MM DD YY MM DD

Client: FHWA Project: GEC-3 Project/Proposal No.: GE3686 Task No.: F

OUTCR.	.0	.47618	5.88	1.16	.001	512
WITHIN	6.0	.46614	5.88	1.09	.001	512

***** OPTION 9 *** COMPUTE RESPONSE SPECTRUM

RESPONSE SPECTRUM ANALYSIS FOR LAYER NUMBER 9
 CALCULATED FOR DAMPING .050

TIMES AT WHICH MAX. SPECTRAL VALUES OCCUR
 TD = TIME FOR MAX. RELATIVE DISP.
 TV = TIME FOR MAX. RELATIVE VEL.
 TA = TIME FOR MAX. ABSOLUTE ACC.
 DAMPING RATIO = .05

PER = .01	TIMES FOR MAX.	- TD = 5.5600	TV = 5.6400	TA = 5.5600
PER = .03	TIMES FOR MAX.	- TD = 5.5600	TV = 6.1200	TA = 5.5600
PER = .04	TIMES FOR MAX.	- TD = 5.5600	TV = 4.3600	TA = 5.5600
PER = .05	TIMES FOR MAX.	- TD = 5.5600	TV = 6.1200	TA = 5.5600
PER = .06	TIMES FOR MAX.	- TD = 5.5800	TV = 6.1200	TA = 5.5800
PER = .07	TIMES FOR MAX.	- TD = 5.5400	TV = 4.4400	TA = 5.5400
PER = .08	TIMES FOR MAX.	- TD = 5.5600	TV = 5.4600	TA = 5.5600
PER = .09	TIMES FOR MAX.	- TD = 5.5800	TV = 4.8000	TA = 5.5800
PER = .10	TIMES FOR MAX.	- TD = 5.5000	TV = 5.6200	TA = 5.5000
PER = .11	TIMES FOR MAX.	- TD = 5.5200	TV = 5.8800	TA = 6.1400
PER = .12	TIMES FOR MAX.	- TD = 6.1600	TV = 6.1400	TA = 6.1600
PER = .13	TIMES FOR MAX.	- TD = 6.1800	TV = 6.1400	TA = 6.1800
PER = .14	TIMES FOR MAX.	- TD = 6.8200	TV = 5.9000	TA = 6.8200
PER = .15	TIMES FOR MAX.	- TD = 5.5400	TV = 5.9200	TA = 5.5400
PER = .16	TIMES FOR MAX.	- TD = 5.5600	TV = 5.9200	TA = 5.5400
PER = .17	TIMES FOR MAX.	- TD = 5.5600	TV = 6.2200	TA = 5.5600
PER = .18	TIMES FOR MAX.	- TD = 6.2000	TV = 6.2400	TA = 6.2000
PER = .19	TIMES FOR MAX.	- TD = 5.6000	TV = 5.6600	TA = 5.6000
PER = .20	TIMES FOR MAX.	- TD = 7.6400	TV = 6.5800	TA = 7.6400
PER = .21	TIMES FOR MAX.	- TD = 6.4400	TV = 6.6000	TA = 6.5400
PER = .22	TIMES FOR MAX.	- TD = 6.5600	TV = 6.6200	TA = 6.5600
PER = .23	TIMES FOR MAX.	- TD = 6.4600	TV = 6.5200	TA = 6.4600
PER = .24	TIMES FOR MAX.	- TD = 6.4800	TV = 6.5400	TA = 6.4800
PER = .25	TIMES FOR MAX.	- TD = 6.8800	TV = 6.4400	TA = 6.8600
PER = .26	TIMES FOR MAX.	- TD = 5.4800	TV = 5.4000	TA = 5.0600
PER = .27	TIMES FOR MAX.	- TD = 5.5000	TV = 5.4200	TA = 5.5000
PER = .28	TIMES FOR MAX.	- TD = 5.5200	TV = 5.4400	TA = 5.5200
PER = .29	TIMES FOR MAX.	- TD = 5.5400	TV = 6.1000	TA = 5.5400
PER = .30	TIMES FOR MAX.	- TD = 5.5600	TV = 6.1000	TA = 5.5600
PER = .31	TIMES FOR MAX.	- TD = 6.0600	TV = 5.9800	TA = 6.0600
PER = .32	TIMES FOR MAX.	- TD = 5.6000	TV = 6.0000	TA = 5.6000
PER = .33	TIMES FOR MAX.	- TD = 8.7800	TV = 8.8600	TA = 8.7800
PER = .34	TIMES FOR MAX.	- TD = 8.8000	TV = 8.7200	TA = 8.8000
PER = .35	TIMES FOR MAX.	- TD = 8.8200	TV = 8.7400	TA = 8.8000
PER = .36	TIMES FOR MAX.	- TD = 8.8200	TV = 8.7400	TA = 8.8200
PER = .37	TIMES FOR MAX.	- TD = 8.8400	TV = 8.7400	TA = 8.8200
PER = .38	TIMES FOR MAX.	- TD = 8.8400	TV = 4.6600	TA = 8.8400
PER = .39	TIMES FOR MAX.	- TD = 4.5800	TV = 4.6600	TA = 4.5800
PER = .40	TIMES FOR MAX.	- TD = 5.6200	TV = 4.6800	TA = 5.6200
PER = .41	TIMES FOR MAX.	- TD = 5.6400	TV = 5.7400	TA = 5.6200
PER = .42	TIMES FOR MAX.	- TD = 5.6400	TV = 5.7600	TA = 5.6400
PER = .43	TIMES FOR MAX.	- TD = 4.6000	TV = 4.7000	TA = 4.6000
PER = .44	TIMES FOR MAX.	- TD = 5.1000	TV = 4.7000	TA = 5.1000
PER = .45	TIMES FOR MAX.	- TD = 5.1200	TV = 5.2200	TA = 5.1000
PER = .46	TIMES FOR MAX.	- TD = 5.1200	TV = 5.2200	TA = 5.1200
PER = .47	TIMES FOR MAX.	- TD = 5.1400	TV = 5.2400	TA = 5.1200
PER = .48	TIMES FOR MAX.	- TD = 5.1400	TV = 5.2400	TA = 5.1400
PER = .49	TIMES FOR MAX.	- TD = 5.1600	TV = 5.2600	TA = 5.1400
PER = .50	TIMES FOR MAX.	- TD = 5.1600	TV = 5.2800	TA = 5.1600
PER = .51	TIMES FOR MAX.	- TD = 5.1800	TV = 5.0600	TA = 5.1600



Written by: T.H.H. Date: 96 / 03 / 19 Reviewed by: E.K. and N.M. Date: 96 / 03 / 21
YY MM DD YY MM DD

Client: FHWA Project: GEC-3 Project/Proposal No.: GE3686 Task No.: F

PER = .52	TIMES FOR MAX.	- TD = 5.1800	TV = 5.0600	TA = 5.1800
PER = .53	TIMES FOR MAX.	- TD = 5.1800	TV = 5.0800	TA = 5.1800
PER = .54	TIMES FOR MAX.	- TD = 5.2000	TV = 5.0800	TA = 5.1800
PER = .55	TIMES FOR MAX.	- TD = 5.5400	TV = 5.0800	TA = 5.5200
PER = .56	TIMES FOR MAX.	- TD = 5.5600	TV = 5.7200	TA = 5.5400
PER = .57	TIMES FOR MAX.	- TD = 5.5800	TV = 5.7400	TA = 5.5600
PER = .58	TIMES FOR MAX.	- TD = 5.6000	TV = 5.7600	TA = 5.5800
PER = .60	TIMES FOR MAX.	- TD = 5.6200	TV = 5.7800	TA = 5.6000
PER = .62	TIMES FOR MAX.	- TD = 5.6400	TV = 5.7800	TA = 5.6200
PER = .64	TIMES FOR MAX.	- TD = 5.6600	TV = 5.8000	TA = 5.6400
PER = .66	TIMES FOR MAX.	- TD = 5.6600	TV = 5.8000	TA = 5.6600
PER = .68	TIMES FOR MAX.	- TD = 5.6800	TV = 5.8200	TA = 5.6600
PER = .70	TIMES FOR MAX.	- TD = 5.6800	TV = 5.8200	TA = 5.6800
PER = .72	TIMES FOR MAX.	- TD = 5.7000	TV = 5.8400	TA = 5.6800
PER = .74	TIMES FOR MAX.	- TD = 5.7200	TV = 6.3200	TA = 5.7000
PER = .76	TIMES FOR MAX.	- TD = 5.7200	TV = 6.3400	TA = 5.7000
PER = .78	TIMES FOR MAX.	- TD = 5.7200	TV = 6.3400	TA = 5.7200
PER = .80	TIMES FOR MAX.	- TD = 5.7400	TV = 6.3400	TA = 5.7200
PER = .82	TIMES FOR MAX.	- TD = 6.1600	TV = 6.3600	TA = 6.1600
PER = .84	TIMES FOR MAX.	- TD = 6.1800	TV = 6.3600	TA = 6.1800
PER = .86	TIMES FOR MAX.	- TD = 6.2000	TV = 6.3800	TA = 6.1800
PER = .88	TIMES FOR MAX.	- TD = 6.2200	TV = 6.0000	TA = 6.2000
PER = .90	TIMES FOR MAX.	- TD = 6.2200	TV = 6.0200	TA = 6.2200
PER = .92	TIMES FOR MAX.	- TD = 6.2400	TV = 6.0200	TA = 6.2200
PER = .94	TIMES FOR MAX.	- TD = 6.2600	TV = 6.0200	TA = 6.2400
PER = .96	TIMES FOR MAX.	- TD = 6.2600	TV = 6.0200	TA = 6.2400
PER = .98	TIMES FOR MAX.	- TD = 6.2800	TV = 6.0200	TA = 6.2600
PER = 1.00	TIMES FOR MAX.	- TD = 6.2800	TV = 6.0200	TA = 6.2800
PER = 1.05	TIMES FOR MAX.	- TD = 6.3200	TV = 6.0400	TA = 6.3000
PER = 1.10	TIMES FOR MAX.	- TD = 6.3600	TV = 6.0600	TA = 6.3400
PER = 1.15	TIMES FOR MAX.	- TD = 7.0400	TV = 6.1800	TA = 7.0200
PER = 1.20	TIMES FOR MAX.	- TD = 8.3400	TV = 7.4000	TA = 8.3200
PER = 1.25	TIMES FOR MAX.	- TD = 9.0400	TV = 8.7600	TA = 9.0200
PER = 1.30	TIMES FOR MAX.	- TD = 9.1400	TV = 8.8200	TA = 9.1200
PER = 1.35	TIMES FOR MAX.	- TD = 9.2200	TV = 8.9000	TA = 9.2000
PER = 1.40	TIMES FOR MAX.	- TD = 8.6600	TV = 8.9600	TA = 8.6400
PER = 1.45	TIMES FOR MAX.	- TD = 8.7000	TV = 6.9600	TA = 8.6800
PER = 1.50	TIMES FOR MAX.	- TD = 9.5000	TV = 6.9800	TA = 9.4800
PER = 1.55	TIMES FOR MAX.	- TD = 9.5800	TV = 7.0600	TA = 9.5600
PER = 1.60	TIMES FOR MAX.	- TD = 6.7600	TV = 7.0800	TA = 6.7400
PER = 1.65	TIMES FOR MAX.	- TD = 6.8000	TV = 7.1000	TA = 6.7600
PER = 1.70	TIMES FOR MAX.	- TD = 6.8200	TV = 5.6400	TA = 6.7800
PER = 1.75	TIMES FOR MAX.	- TD = 6.8400	TV = 5.6400	TA = 6.8000
PER = 1.80	TIMES FOR MAX.	- TD = 6.0400	TV = 5.6400	TA = 6.0000
PER = 1.85	TIMES FOR MAX.	- TD = 6.1000	TV = 5.6400	TA = 6.0800
PER = 1.90	TIMES FOR MAX.	- TD = 6.1200	TV = 5.6400	TA = 6.1000
PER = 1.95	TIMES FOR MAX.	- TD = 6.1200	TV = 5.6400	TA = 6.1000
PER = 2.00	TIMES FOR MAX.	- TD = 6.1400	TV = 5.6400	TA = 6.1000
PER = 2.05	TIMES FOR MAX.	- TD = 6.1400	TV = 5.6400	TA = 6.1200
PER = 2.10	TIMES FOR MAX.	- TD = 6.1400	TV = 5.6400	TA = 6.1200
PER = 2.15	TIMES FOR MAX.	- TD = 6.1400	TV = 5.6400	TA = 6.1200
PER = 2.20	TIMES FOR MAX.	- TD = 9.6400	TV = 5.6400	TA = 9.6200
PER = 2.25	TIMES FOR MAX.	- TD = 9.6800	TV = 5.6400	TA = 9.6400
PER = 2.30	TIMES FOR MAX.	- TD = 9.7000	TV = 5.6400	TA = 9.6600
PER = 2.35	TIMES FOR MAX.	- TD = 9.7400	TV = 5.6400	TA = 9.7000
PER = 2.40	TIMES FOR MAX.	- TD = 9.7800	TV = 5.6400	TA = 9.7400
PER = 2.50	TIMES FOR MAX.	- TD = 9.8400	TV = 5.6400	TA = 9.8000
PER = 2.60	TIMES FOR MAX.	- TD = 12.6400	TV = 5.6400	TA = 12.6000
PER = 2.70	TIMES FOR MAX.	- TD = 12.7200	TV = 5.8800	TA = 12.6800
PER = 2.80	TIMES FOR MAX.	- TD = 6.2000	TV = 5.8800	TA = 6.1600
PER = 2.90	TIMES FOR MAX.	- TD = 6.2200	TV = 5.8800	TA = 6.1600
PER = 3.00	TIMES FOR MAX.	- TD = 6.3800	TV = 5.8800	TA = 6.3400
PER = 3.10	TIMES FOR MAX.	- TD = 6.4000	TV = 5.8800	TA = 6.3600
PER = 3.20	TIMES FOR MAX.	- TD = 6.4000	TV = 5.8800	TA = 6.3600



Written by: T.H.H. Date: 96 / 03 / 19 Reviewed by: E.K. and N.M. Date: 96 / 03 / 21
YY MM DD YY MM DD

Client: FHWA Project: GEC-3 Project/Proposal No.: GE3686 Task No.: F

PER = 3.30	TIMES FOR MAX. -	TD = 5.5000	TV = 5.8800	TA = 5.4600
PER = 3.40	TIMES FOR MAX. -	TD = 5.5000	TV = 5.8800	TA = 5.4600
PER = 3.50	TIMES FOR MAX. -	TD = 5.5200	TV = 5.8800	TA = 5.4600
PER = 3.60	TIMES FOR MAX. -	TD = 5.5200	TV = 5.8800	TA = 5.4600
PER = 3.70	TIMES FOR MAX. -	TD = 5.5200	TV = 5.8800	TA = 5.4600
PER = 3.80	TIMES FOR MAX. -	TD = 5.5200	TV = 5.8800	TA = 5.4600
PER = 3.90	TIMES FOR MAX. -	TD = 5.5200	TV = 5.8800	TA = 5.4600
PER = 4.00	TIMES FOR MAX. -	TD = 5.5200	TV = 5.8800	TA = 5.4600
PER = 4.10	TIMES FOR MAX. -	TD = 11.9200	TV = 5.8800	TA = 11.8600
PER = 4.20	TIMES FOR MAX. -	TD = 11.9400	TV = 5.8800	TA = 11.8800
PER = 4.30	TIMES FOR MAX. -	TD = 11.9600	TV = 5.8800	TA = 11.9000
PER = 4.40	TIMES FOR MAX. -	TD = 11.9800	TV = 5.8800	TA = 11.9200
PER = 4.50	TIMES FOR MAX. -	TD = 9.8600	TV = 5.8800	TA = 9.7800
PER = 4.60	TIMES FOR MAX. -	TD = 9.8800	TV = 5.8800	TA = 9.7800
PER = 4.70	TIMES FOR MAX. -	TD = 9.9000	TV = 5.8800	TA = 9.8000
PER = 4.80	TIMES FOR MAX. -	TD = 9.9400	TV = 5.8800	TA = 9.8400
PER = 4.90	TIMES FOR MAX. -	TD = 10.2400	TV = 5.8800	TA = 10.2000
PER = 5.00	TIMES FOR MAX. -	TD = 10.2800	TV = 5.8800	TA = 10.2000
PER = 5.10	TIMES FOR MAX. -	TD = 10.5600	TV = 5.8800	TA = 10.5200
PER = 5.20	TIMES FOR MAX. -	TD = 10.6000	TV = 5.8800	TA = 10.5200
PER = 5.40	TIMES FOR MAX. -	TD = 10.7400	TV = 5.8800	TA = 10.7000
PER = 5.60	TIMES FOR MAX. -	TD = 10.7800	TV = 5.8800	TA = 10.7200
PER = 5.80	TIMES FOR MAX. -	TD = 10.8200	TV = 5.8800	TA = 10.7400
PER = 6.00	TIMES FOR MAX. -	TD = 10.8600	TV = 5.8800	TA = 10.7600
PER = 6.20	TIMES FOR MAX. -	TD = 11.0400	TV = 5.8800	TA = 10.8000
PER = 6.40	TIMES FOR MAX. -	TD = 11.0800	TV = 5.8800	TA = 11.0200
PER = 6.60	TIMES FOR MAX. -	TD = 11.1000	TV = 5.8800	TA = 11.0400
PER = 6.80	TIMES FOR MAX. -	TD = 11.1400	TV = 5.8800	TA = 11.0600
PER = 7.00	TIMES FOR MAX. -	TD = 11.3400	TV = 5.8800	TA = 11.0800
PER = 7.20	TIMES FOR MAX. -	TD = 18.8000	TV = 5.8800	TA = 18.7000
PER = 7.40	TIMES FOR MAX. -	TD = 15.8000	TV = 5.8800	TA = 15.6800
PER = 7.60	TIMES FOR MAX. -	TD = 16.0000	TV = 5.8800	TA = 15.9600
PER = 7.80	TIMES FOR MAX. -	TD = 16.0800	TV = 5.8800	TA = 15.9800
PER = 8.00	TIMES FOR MAX. -	TD = 16.2800	TV = 5.3400	TA = 16.2200
PER = 8.50	TIMES FOR MAX. -	TD = 16.4800	TV = 5.3400	TA = 16.2800
PER = 9.00	TIMES FOR MAX. -	TD = 12.7600	TV = 5.3400	TA = 12.6400
PER = 9.50	TIMES FOR MAX. -	TD = 9.1200	TV = 5.3400	TA = 8.6800

SPECTRAL VALUES --

[Acceleration of gravity used = 32.20]

Channel deposit

DAMPING RATIO = .05

NO.	PERIOD	REL.DISP.	REL.VEL.	PSU.REL.VEL.	ABS.ACC.	PSU.ABS.ACC.	FREQ.
1	.01	.00003	.00046	.02044	.39908	.39887	100.00
2	.03	.00030	.01027	.06226	.40595	.40497	33.33
3	.04	.00052	.01847	.08173	.39917	.39870	25.00
4	.05	.00081	.02559	.10145	.39709	.39591	20.00
5	.06	.00120	.04522	.12598	.40882	.40971	16.67
6	.07	.00164	.05642	.14726	.41139	.41050	14.29
7	.08	.00262	.08950	.20611	.50323	.50273	12.50
8	.09	.00345	.10164	.24073	.52235	.52193	11.11
9	.10	.00462	.15772	.29010	.57207	.56606	10.00
10	.11	.00615	.26615	.35140	.63195	.62335	9.09
11	.12	.01010	.37763	.52891	.86651	.86006	8.33
12	.13	.01022	.36754	.49392	.73485	.74138	7.69
13	.14	.00928	.33240	.41653	.59344	.58055	7.14
14	.15	.01189	.36002	.49805	.65094	.64790	6.67
15	.16	.01425	.42591	.55954	.67738	.68240	6.25
16	.17	.01900	.54535	.70222	.81595	.80603	5.88
17	.18	.02209	.66672	.77122	.83500	.83605	5.56
18	.19	.02231	.63587	.73766	.75761	.75757	5.26
19	.20	.02384	.68937	.74906	.73279	.73082	5.00



Written by: T.H.H. Date: 96 / 03 / 19 Reviewed by: E.K. and N.M. Date: 96 / 03 / 21
 YY MM DD YY MM DD

Client: FHWA Project: GEC-3 Project/Proposal No.: GE3686 Task No.: F

20	.21	.03245	.97318	.97098	.89860	.90223	4.76
21	.22	.04016	1.12919	1.14696	1.01850	1.01730	4.55
22	.23	.04893	1.34189	1.33681	1.13829	1.13413	4.35
23	.24	.05327	1.41448	1.39473	1.13022	1.13398	4.17
24	.25	.04816	1.19123	1.21031	.94875	.94467	4.00
25	.26	.04833	1.09688	1.16788	.88725	.87650	3.85
26	.27	.05457	1.12735	1.26998	.91243	.91782	3.70
27	.28	.05998	1.08096	1.34589	.93576	.93794	3.57
28	.29	.06573	1.20591	1.42409	.95755	.95821	3.45
29	.30	.07248	1.43049	1.51806	.98905	.98740	3.33
30	.31	.07869	1.49902	1.59491	.99943	1.00392	3.23
31	.32	.07603	1.52572	1.49289	.91779	.91033	3.13
32	.33	.08573	1.45130	1.63239	.95937	.96524	3.03
33	.34	.09293	1.58596	1.71735	.97889	.98561	2.94
34	.35	.08897	1.52094	1.59727	.89869	.89050	2.86
35	.36	.08518	1.45384	1.48672	.81032	.80584	2.78
36	.37	.08256	1.38740	1.40207	.74136	.73942	2.70
37	.38	.08057	1.38080	1.33224	.69048	.68410	2.63
38	.39	.08685	1.42869	1.39917	.69829	.70005	2.56
39	.40	.09506	1.45615	1.49319	.73210	.72841	2.50
40	.41	.10146	1.48890	1.55482	.73676	.73998	2.44
41	.42	.10170	1.50159	1.52137	.71580	.70682	2.38
42	.43	.10021	1.44514	1.46428	.66709	.66448	2.33
43	.44	.10779	1.42713	1.53923	.68129	.68261	2.27
44	.45	.11979	1.52055	1.67259	.73130	.72527	2.22
45	.46	.13195	1.60292	1.80228	.76705	.76452	2.17
46	.47	.14191	1.68114	1.89711	.79097	.78763	2.13
47	.48	.15144	1.70611	1.98230	.80937	.80585	2.08
48	.49	.15917	1.72732	2.04102	.81806	.81279	2.04
49	.50	.16681	1.72178	2.09625	.82019	.81808	2.00
50	.51	.17161	1.76990	2.11423	.81758	.80892	1.96
51	.52	.17727	1.82332	2.14200	.80362	.80379	1.92
52	.53	.17975	1.85917	2.13098	.79282	.78456	1.89
53	.54	.18304	1.89959	2.12978	.76951	.76960	1.85
54	.55	.18863	1.91174	2.15485	.76509	.76450	1.82
55	.56	.20404	2.05439	2.28929	.79816	.79769	1.79
56	.57	.21975	2.23594	2.42237	.83059	.82926	1.75
57	.58	.23475	2.39955	2.54306	.86037	.85556	1.72
58	.60	.26313	2.67290	2.75548	.89874	.89613	1.67
59	.62	.28459	2.83653	2.88412	.91214	.90771	1.61
60	.64	.29750	2.86089	2.92067	.89898	.89049	1.56
61	.66	.30479	2.76251	2.90162	.86215	.85787	1.52
62	.68	.30702	2.62209	2.83684	.81677	.81405	1.47
63	.70	.30669	2.45482	2.75283	.77387	.76737	1.43
64	.72	.30781	2.29779	2.68618	.72966	.72799	1.39
65	.74	.30475	2.25480	2.58759	.68812	.68232	1.35
66	.76	.30093	2.33112	2.48786	.64081	.63876	1.32
67	.78	.29415	2.35489	2.36949	.59603	.59277	1.28
68	.80	.28899	2.31478	2.26971	.55799	.55361	1.25
69	.82	.29072	2.29165	2.22763	.53167	.53009	1.22
70	.84	.29991	2.27060	2.24331	.52229	.52112	1.19
71	.86	.31341	2.25612	2.28980	.52080	.51955	1.16
72	.88	.32937	2.28778	2.35169	.52390	.52146	1.14
73	.90	.34723	2.36514	2.42414	.52790	.52558	1.11
74	.92	.36710	2.45947	2.50710	.53394	.53175	1.09
75	.94	.38744	2.55702	2.58975	.54118	.53759	1.06
76	.96	.41062	2.65669	2.68751	.54843	.54626	1.04
77	.98	.43341	2.75190	2.77878	.55693	.55329	1.02
78	1.00	.45545	2.83103	2.86170	.56130	.55840	1.00
79	1.05	.49637	2.93984	2.97028	.55560	.55199	.95
80	1.10	.50641	2.79994	2.89258	.51546	.51312	.91
81	1.15	.53286	2.85465	2.91137	.49652	.49400	.87
82	1.20	.55783	2.99701	2.92080	.47734	.47495	.83
83	1.25	.60256	3.05147	3.02879	.47561	.47281	.80



Written by: T.H.H. Date: 96 / 03 / 19 Reviewed by: E.K. and N.M. Date: 96 / 03 / 21
YY MM DD YY MM DD

Client: FHWA Project: GEC-3 Project/Proposal No.: GE3686 Task No.: F

84	1.30	.62708	3.17183	3.03080	.45676	.45492	.77
85	1.35	.63041	3.14471	2.93406	.42645	.42409	.74
86	1.40	.61428	2.97409	2.75690	.38654	.38425	.71
87	1.45	.59415	2.71080	2.57458	.34938	.34647	.69
88	1.50	.55837	2.56719	2.33889	.30599	.30426	.67
89	1.55	.50576	2.39877	2.05019	.25933	.25810	.65
90	1.60	.50700	2.30907	1.99098	.24426	.24281	.63
91	1.65	.51166	2.17438	1.94839	.23202	.23042	.61
92	1.70	.50999	2.13678	1.88492	.21821	.21636	.59
93	1.75	.50093	2.10896	1.79855	.20273	.20054	.57
94	1.80	.49143	2.07196	1.71542	.18751	.18596	.56
95	1.85	.48759	2.02636	1.65602	.17498	.17467	.54
96	1.90	.48361	1.97456	1.59927	.16503	.16425	.53
97	1.95	.47797	1.91994	1.54009	.15519	.15411	.51
98	2.00	.47086	1.86601	1.47926	.14555	.14432	.50
99	2.05	.46441	1.81579	1.42339	.13678	.13549	.49
100	2.10	.45839	1.77142	1.37150	.12889	.12744	.48
101	2.15	.45358	1.73412	1.32554	.12188	.12030	.47
102	2.20	.47526	1.70419	1.35733	.12115	.12039	.45
103	2.25	.49811	1.68116	1.39098	.12151	.12063	.44
104	2.30	.51470	1.66412	1.40606	.12006	.11929	.43
105	2.35	.52568	1.65180	1.40550	.11737	.11670	.43
106	2.40	.53012	1.64287	1.38784	.11365	.11284	.42
107	2.50	.51775	1.63002	1.30126	.10234	.10157	.40
108	2.60	.52509	1.61702	1.26894	.09573	.09523	.38
109	2.70	.49002	1.62714	1.14033	.08311	.08241	.37
110	2.80	.44091	1.63050	.98939	.07030	.06895	.36
111	2.90	.42646	1.62437	.92399	.06349	.06217	.34
112	3.00	.41493	1.60920	.86902	.05700	.05652	.33
113	3.10	.40391	1.58668	.81866	.05221	.05153	.32
114	3.20	.39115	1.55909	.76802	.04755	.04683	.31
115	3.30	.37886	1.52877	.72134	.04427	.04265	.30
116	3.40	.37878	1.49779	.69998	.04182	.04017	.29
117	3.50	.37704	1.46779	.67685	.03937	.03774	.29
118	3.60	.37414	1.43998	.65300	.03701	.03539	.28
119	3.70	.37037	1.41513	.62894	.03477	.03317	.27
120	3.80	.36620	1.39366	.60551	.03268	.03109	.26
121	3.90	.36207	1.37569	.58332	.03076	.02919	.26
122	4.00	.35830	1.36110	.56282	.02902	.02746	.25
123	4.10	.38420	1.34961	.58878	.02841	.02802	.24
124	4.20	.40691	1.34094	.60874	.02871	.02828	.24
125	4.30	.42513	1.33467	.62120	.02865	.02819	.23
126	4.40	.43841	1.33041	.62605	.02824	.02776	.23
127	4.50	.44777	1.32777	.62521	.02753	.02711	.22
128	4.60	.47135	1.32640	.64382	.02769	.02731	.22
129	4.70	.49334	1.32597	.65952	.02771	.02738	.21
130	4.80	.51388	1.32620	.67266	.02762	.02735	.21
131	4.90	.53276	1.32684	.68314	.02748	.02720	.20
132	5.00	.56267	1.32763	.70707	.02791	.02759	.20
133	5.10	.59540	1.32848	.73353	.02827	.02807	.20
134	5.20	.63441	1.32921	.76656	.02901	.02876	.19
135	5.40	.71325	1.32992	.82991	.03016	.02999	.19
136	5.60	.78412	1.32919	.87978	.03099	.03066	.18
137	5.80	.84196	1.32673	.91210	.03111	.03069	.17
138	6.00	.88577	1.32254	.92758	.03061	.03017	.17
139	6.20	.92380	1.31669	.93619	.02960	.02946	.16
140	6.40	.95385	1.30931	.93644	.02884	.02855	.16
141	6.60	.96846	1.30058	.92197	.02766	.02726	.15
142	6.80	.96842	1.29075	.89482	.02615	.02568	.15
143	7.00	.96416	1.28006	.86543	.02438	.02412	.14
144	7.20	.96031	1.26867	.83803	.02296	.02271	.14
145	7.40	1.00756	1.25675	.85550	.02273	.02256	.14
146	7.60	1.05649	1.24439	.87343	.02260	.02243	.13
147	7.80	1.08640	1.23191	.87513	.02220	.02189	.13



Written by: T.H.H. Date: 96 / 03 / 19 Reviewed by: E.K. and N.M. Date: 96 / 03 / 21
YY MM DD YY MM DD

Client: FHWA Project: GEC-3 Project/Proposal No.: GE3686 Task No.: F

148	8.00	1.10868	1.23626	.87076	.02146	.02124	.13
149	8.50	1.06940	1.26059	.79050	.01843	.01815	.12
150	9.00	1.04769	1.28333	.73142	.01618	.01586	.11
151	9.50	1.02550	1.30422	.67825	.01450	.01393	.11
152	10.00	.00000	.00000	.00000	.00000	.00000	.10

VALUES IN PERIOD RANGE .1 TO 2.5 SEC.

AREA OF ACC. RESPONSE SPECTRUM = 1.064
 AREA OF VEL. RESPONSE SPECTRUM = 5.052
 MAX. ACCELERATION RESPONSE VALUE = 1.138
 MAX. VELOCITY RESPONSE VALUE = 3.172



5.9 SUMMARY AND CONCLUSIONS

A cable-stayed bridge with an approach embankment that traverses liquefiable ground is to be constructed in a coastal city in the western United States. The project site is located in a broad coastal plain and lies in an area of high seismic exposure due to its proximity to three faults and a "blind" fold and thrust belt.

The soil stratigraphy beneath the embankment consists of 5 m of recent alluvium overlying up to 20 m of marine terrace deposits of silty sand, sandy silt, and silty clay. The channel is underlain by approximately 30 m of recent deposits of silts, clays, and sands.

The owner dictated that a two-level earthquake design criteria be used. The criteria called for design to resist the Operational Level Earthquake (OLE) (defined as the event with a PHGA that has a 50 percent probability of not being exceeded in a 50-year period) without loss of serviceability and to withstand the Contingency Level Earthquake (CLE) (defined as the event with a PHGA that has a 10 percent probability of not being exceeded in 50 years), with damage repairable in 2 to 4 weeks.

The probabilistic seismic hazard analysis resulted in a magnitude $M_w = 7$ event with a peak horizontal ground acceleration of 0.4 g for the CLE and a magnitude $M_w = 8$ event with a peak horizontal ground acceleration of 0.2 g for the OLE.

The liquefaction analyses indicated that liquefaction is likely to occur in the free-field during both the OLE and CLE events. The analyses showed that liquefaction is likely to occur both in the free-field and under the embankment during the CLE. Liquefaction is not anticipated under the embankment during the OLE. However, as factor of safety against liquefaction under the embankment is nearly one during the OLE, some embankment deformation was expected to occur in the OLE.

Consequently, to minimize the extent of lateral spreading in the design earthquakes, it was decided to densify the potentially liquefiable soil to reduce the risk of unacceptable performance. As the site was in an undeveloped area with no structures or utilities in the vicinity, dynamic compaction was recommended. The densification program was designed to provide normalized and standardized blow counts, $(N_1)_{60}$, equal to or greater than 25 at the site.

Post liquefaction stability analyses were carried out using residual shear strength parameters for the liquefied sand. Results of the analyses yielded a static factor of safety greater than 1.5, indicating the embankment would stabilize once the shaking stopped, even if the soil did liquefy. The estimated permanent seismic deformation of the embankment in the OLE was less than 0.15 m. The estimated permanent seismic deformation of the embankment in the CLE was calculated to be 0.36 m. These magnitudes of potential deformation were considered acceptable.

A site-specific response analysis was conducted to develop response spectra for the soil in the main channel for the OLE and CLE. Three time histories were selected for each level of loading. The response spectra were obtained using the computer program SHAKE (Schnabel et al., 1972; Idriss and Sun, 1992) and were provided to the structural engineer for use in design of the bridge structure.

REFERENCES

- AASHTO (1992), "Standard Specifications for Highway Bridges," 15th Edition, American Association of State Highway and Transportation Officials, Washington, District of Columbia.
- Abrahamson, N.A. and Silva, W.J. (1996), "Preliminary Attenuation Relations for Horizontal Response Spectra Including Data from the 1994 Northridge Earthquake," Draft Report to Brookhaven National Laboratory, New York.
- Algermissen, S.T., Perkins, D.M. (1976), "A Probabilistic Estimate of Maximum Acceleration in Rock in the Contiguous United States," U.S. Geological Survey Open File Report 76-416.
- Algermissen, S.T., Perkins, D.M., Thenhaus, P.C., Hanson, S.L. and Bender, B.L. (1991), "Probabilistic Earthquake Acceleration and Velocity Maps for the United States and Puerto Rico," U.S. Geological Survey, Miscellaneous Field Studies Map MF-2120.
- ASTM (1994), "Annual Book of ASTM Standards, Section 4, Construction," American Society for Testing and Materials, Philadelphia, Pennsylvania, 978 p.
- Campbell, K.W. (1993), "Empirical Prediction of Near Source Ground Motion from Large Earthquakes," Proc. International Workshop on Earthquake Hazard and Large Dams in the Himalayas, sponsored by the Indian National Trust of Art and Cultural Heritage (INTACH), New Delhi, India.
- Cheney, R.S. (1988), "Permanent Ground Anchors," Report FHWA-DP-68-1R, Federal Highway Administration, 136 p.
- Cornell, C.A. (1968), "Engineering Seismic Risk Analysis", Bulletin, Seismological Society of America, Vol. 58, No. 5.
- Dobry, R., Idriss, I.M. and Ng, E. (1978), "Duration Characteristics of Horizontal Components of Strong-Motion Earthquake Records," Bulletin of the Seismological Society of America, Vol. 68, No. 5, pp. 1487-1520.
- Gray, H. (1936), "Stress Distribution in Elastic Solids," Proc. 1st International Conference on Soil Mechanics and Foundation Engineering, Vol. 2, p. 157.
- Hynes, M.E. and Franklin, A.G. (1984), "Rationalizing the Seismic Coefficient Method," Miscellaneous Paper GL-84-13, U.S. Army Engineer Waterways Experiment Station, Vicksburg, Mississippi, 34 p.

Idriss, I.M. and Sun, J.I. (1992), "User's Manual for SHAKE 91," Center for Geotechnical Modeling, Department of Civil and Environmental Engineering, University of California, Davis, California, 13 p. (plus Appendices).

Imai, T. and Tonouchi, K. (1982), "Correlation of N-Value with S-Wave Velocity and Shear Modulus," Proc. 2nd European Symposium on Penetration Testing, Amsterdam, The Netherlands, pp. 67-72.

Johnston, A.C. and Nava, S.J. (1994), "Seismic Hazard Assessment in the Central United States," Proc. ATC-35 Seminar on New Developments in Earthquake Ground Motion Estimation and Implications for Engineering Design Practice, Applied Technology Council, ATC 35-1, Redwood City, California, pp. 2-1 - 2-12.

Lam, I.P., and Martin, G.R. (1986), "Seismic Design of Highway Bridge Foundations - Vol. II. Design Procedures and Guidelines," Report No. FHWA/RD-86-102, U.S. Department of Transportation, Federal Highway Administration, McLean, Virginia, 167 p.

Lovell, C.W., Sharma, S. and Carpenter, J.R. (1984), "Introduction to Slope Stability Analysis with STABL4," prepared for Federal Highway Administration, U.S. Department of Transportation 104 p.

McGuire, R.K. (1976), "FORTRAN Computer Program for Seismic Risk Analysis", U.S. Geological Survey Open-File Report 76-67.

NHI (1996), "Design and Construction of Driven Pile Foundations," National Highway Institute Workshop Manual, Volumes I and II, (Working Draft).

Nuttli, O.W. (1981), "Similarities and Differences Between Western and Eastern United States Earthquakes, and their Consequences for Earthquake Engineering," Earthquakes and Earthquake Engineering: The Eastern United States, Vol. 1, Assessing the Hazard - Evaluating the Risk, J.E. Beavers, Ed., Ann Arbor Science Publishers, Inc., Ann Arbor, Michigan, pp. 25-51.

Poe, K.M. (1992), "Seismic Mitigation of the Memphis Water System," Proc. Lifeline Earthquake Engineering in the Central and Eastern U.S., ASCE Monograph No. 5, pp. 16-28.

Poulos, N.G. and Davis, E.M. (1974), Elastic Solutions for Soil and Rock Mechanics, John Wiley and Sons, Inc., New York, 410 p. (Reprinted in 1991 by Centre for Geotechnical Research, University of Sydney, Australia).

Reese, L.C., Cooley, L.A., and Radhakrishnan, R. (1984), "Laterally Loaded Piles and Computer Program COM624G," Waterways Experiment Station, U.S. Army Engineers, Technical Report K-84-2.

Richards, R., Jr. and Elms, D.G. (1979), "Seismic Behavior of Gravity Retaining Walls" Journal of the Geotechnical Engineering Division, ASCE, Vol. 105, No. GT4, pp. 449-464.

Schnabel, P.B., Lysmer, J., and Seed, H.B. (1972), "SHAKE: A Computer Program for Earthquake Response Analysis of Horizontally Layered Sites," Report No. UCB/EERC-72-12, Earthquake Engineering Research Center, University of California, Berkeley, California, 102 p.

Seed, H.B. and Idriss, I.M. (1982), "Ground Motions and Soil Liquefaction During Earthquakes," Monograph No. 5, Earthquake Engineering Research Institute, Berkeley, California, 134 p.

Seed, H.B., Wong, R.T., Idriss, I.M. and Tokimatsu, K. (1984), "Moduli and Damping Factors for Dynamic Analyses of Cohesionless Soils," Report No. UCB/EERC-84/14, University of California, Berkeley, Earthquake Engineering Research Center, 37 p.

Trifunac, M.D. and Brady, A.G. (1975), "A Study of the Duration of Strong Earthquake Ground Motion," Bulletin of the Seismological Society of America. Vol. 65, pp. 581-626.

Vucetic, M. and Dobry, R. (1991), "Effect of Soil Plasticity on Cyclic Response," Journal of Geotechnical Engineering, ASCE Vol. 117, No. 1. pp. 89-107.

Wang, S.T. and Reese, L.C., (1991), "COM624P, Laterally Loaded Pile Analysis Program for the Microcomputer," Version 2.0, Report No. FHWA-SA-91-048, U.S. Department of Transportation, Federal Highway Administration, Office of Technology Applications, Washington District of Columbia, 504 p.

